The economics of climate change

On the role of risk and preferences

Olijslagers, S.W.J.

Publication date
2022

Document Version
Final published version

Climate change is one of the main risks that the economy will face in the upcoming decades. Climate scientists have improved our knowledge about climate change, but future impacts of climate change remain uncertain. This thesis focuses on estimating the social cost of carbon, which is the discounted value of all future damages caused by emitting one unit of carbon today, taking into account this uncertainty. Adding uncertainty increases the social cost of carbon, and thus the optimal carbon price, by a substantial amount. The policy implication is that the large amount of uncertainty around future climate damages should lead to more stringent carbon abatement policy. The focus should not only be on the expected impacts of climate change, but also on limiting the probability of a large irreversible impact.

Stan Olijslagers (1995) holds a BSc in Econometrics and Operations Research from Tilburg University. He obtained a Master's degree (Cum Laude) in Quantitative Finance and Actuarial Science from the same institution. After graduating from Tilburg University, he joined the Macro and International Economics department of the University of Amsterdam as a PhD candidate under the supervision of Prof. Sweder van Wijnbergen. He is currently working as a researcher at the CPB (Netherlands Bureau for Economic Policy Analysis).

The Economics of Climate Change: On the Role of Risk and Preferences Stan Olijslagers

791

tinbergen institute

The Economics of Climate Change: On the Role of Risk and Preferences

Stan Olijslagers

Universiteit van Amsterdam

THE ECONOMICS OF CLIMATE CHANGE: ON THE ROLE OF RISK AND PREFERENCES

ISBN: 978-90-361-0672-6

Cover: Francisco de Goya, *El Coloso*, Museo Nacional del Prado.

Cover design: *Crasborn Graphic Designers bno*, Valkenburg a.d. Geul

This book is no. **791** of the Tinbergen Institute Research Series, established through cooperation between Rozenberg Publishers and the Tinbergen Institute. A list of books which already appeared in the series can be found in the back.

THE ECONOMICS OF CLIMATE CHANGE: ON THE ROLE OF RISK AND PREFERENCES

ACADEMISCH PROEFSCHRIFT

ter verkrijging van de graad van doctor
aan de Universiteit van Amsterdam
op gezag van de Rector Magnificus
prof. dr. ir. K. I. J. Maex
ten overstaan van een door het College voor Promoties ingestelde
commissie, in het openbaar te verdedigen in de Agnietenkapel
op dinsdag 22 februari 2022, te 12.00 uur

door
Stan Wilhelmus Johannes Olijslagers

geboren te Sint-Michielsgestel

Promotiecommissie

Promotores:	prof. dr. S.J.G. van Wijnbergen	Universiteit van Amsterdam
	prof. dr. R.M.W.J. Beetsma	Universiteit van Amsterdam
Overige leden:	prof. dr. F. van der Ploeg	Universiteit van Amsterdam
	dr. T.R.G.R. Douenne	Universiteit van Amsterdam
	prof. dr. A.J. de Zeeuw	Tilburg University
	dr. G.C. van der Meijden	Vrije Universiteit Amsterdam
	dr. F. Venmans	London School of Economics
	prof. dr. R.J.A. Laeven	Universiteit van Amsterdam
	prof. dr. ir. M.H. Vellekoop	Universiteit van Amsterdam

Faculteit Economie en bedrijfskunde

Acknowledgements

I am very grateful for all the help, guidance, and support that I received of numerous people. My time at the UvA can be split into two parts: pre-corona and post-corona. Before the outbreak of the virus, I really enjoyed the discussions, coffee talks, lunches, lectures, and conversations with colleagues and other PhD students. Permanently working from home didn't make the task of writing my thesis easier. Luckily, all research and teaching tasks could continue digitally during the pandemic.

The first person that I would like to thank is Damiaan Chen. If I didn't meet Damiaan, I probably wouldn't have started a PhD at all. I worked together with Damiaan during my internship at the Dutch Central Bank, and Damiaan arranged a meeting between me and my promotor Sweder. Before that meeting I did not have concrete plans to start a PhD. After a few days of contemplating, I decided to take up the challenge and start the PhD adventure.

Second, I am very grateful for all the support that I received from my promotor Sweder van Wijnbergen. The discussions and feedback about my work were very useful. Sweder gave me enough freedom and responsibility, without giving too little guidance. I admire his creativity and focus on policy relevance. And I am happy that our discussions were broader than climate economics alone. I was trained as an econometrist, but the discussions about several economic topics helped me to develop my economic thinking.

Third, I would like to thank Rick van der Ploeg for the collaboration on the fifth chapter. The (mostly digital) meetings were always fruitful. There was never a lack of enthusiastic ideas, and I learned a lot from working together.

I really enjoyed my time at the office that I shared with Ioana, Daniel and Merve. Thanks for sharing research ideas, having drinks together, giving Sinterklaas presents, making eastern European jokes and talking about random things. I also enjoyed working together with the other MInt PhDs: Pim, Jante, Eva, Josha, Rui, Andras, Daniel, Stefan, and Konstantin.

I was happy about the good collaboration with Ward around the tutorials of Macro II. Additionally, I want to thank my MInt colleagues for the help and lunch talks: Roel, Franc, Massimo, Marcelo, Albert-Jan, Elisabeth, Christian, Dirk, Kees, Peter and Thomas. Also, the UvA staff was always very helpful.

And last but not least, I would like to thank my girlfriend Marieke, my parents and my sisters for their support. Although they were not able to help me content-wise, they were very valuable to me during my PhD. Especially during the pandemic and the search for a new job, they were always there to help me.

List of authors

Discounting the future: On climate change, ambiguity aversion and Epstein-Zin preferences
This chapter is joint work with prof. dr. Sweder van Wijnbergen. Stan has developed the research idea and the structure of the paper together with Sweder. Stan has developed the model and solved the model using numerical methods. Stan also wrote down the results and was involved in rewriting and editing the paper.

Solution methods for DSGE models in continuous time: Application to a climate-economy model
This chapter is single-authored.

The social cost of carbon: Optimal policy versus business-as-usual
This chapter is single-authored.

On current and future carbon prices in a risky world
This chapter is joint work with prof. dr. Sweder van Wijnbergen and prof. dr. Frederick van der Ploeg. Stan has developed the research idea and the structure of the paper together with Sweder and Rick. Stan has developed the model and solved the model using numerical methods. Stan also wrote down the results and was involved in rewriting and editing the paper.

The financial support of pension administrator and wealth manager MN services is gratefully acknowledged.

Contents

1 Introduction

"Global warming is the most significant of all environmental externalities. It menaces our planet and looms over our future like a Colossus (see Figure 1 from Goya). It is particularly pernicious because it involves so many activities of daily life, affects the entire planet, does so for decades and even centuries, and, most of all, because none of us acting individually can do anything to slow the changes."

W.D. Nordhaus (2019)
Climate change:
the ultimate challenge for economics

Nowadays, there is vast evidence of climate change and the threats to our planet (IPCC, 2013, 2021). But there is still much uncertainty about how the climate system will evolve over time and what the effects of climate change will be on the economy. This thesis puts the uncertainty around future climate damages at the center of the analysis. We develop integrated assessment models to estimate the social cost of carbon, which is the welfare loss of carbon emissions. We emphasize the effects of uncertainty and preferences towards risk and uncertainty.

Global warming is caused by anthropogenic carbon emissions and limiting warming requires substantial reductions in these emissions. Global warming will have serious consequences for economic growth, human live and the environment. A higher global mean temperature will affect food security and ecosystems, with the risk of triggering tipping points that will lead to irreversible changes in the ecosystem. It furthermore leads to higher sea levels with additional threats of flooding and more frequent extreme weather events such as natural disasters. Some areas will become unlivable which forces people to migrate to other areas. Figure 1.1 gives an overview of several projected impacts of climate change.

From an economic perspective, global warming is a typical example of a negative externality. Stern et al. (2006) even call it the biggest market failure the world has ever seen. Firms and households produce carbon emissions, but they do not pay for the negative consequences of these emissions. In the presence of a negative externality, some kind of regulation must be imposed to tackle the externality. One way to internalize the externality is to levy a tax on carbon emissions equal to the welfare loss of one unit of emissions. This is called the Pigouvian approach (Pigou, 1920). An alternative solution is to set up a trading system of carbon emission permits as proposed by Coase (1960). In this setting, firms also have an incentive to lower emissions because they can sell their permits on a market. The European Union for example adopted the Coasian approach with the EU Emissions Trading System.

One specific feature of the climate change externality is its global nature. Carbon emissions spread very fast and it does not matter where emissions take place. It is therefore a global problem that also needs a global policy response. No country or individual can solve the problem alone, collective action is necessary. The global nature of the problem makes the implementation of climate policy more complex. Local negative externalities

Figure 1.1: *Projected impacts of climate change.*

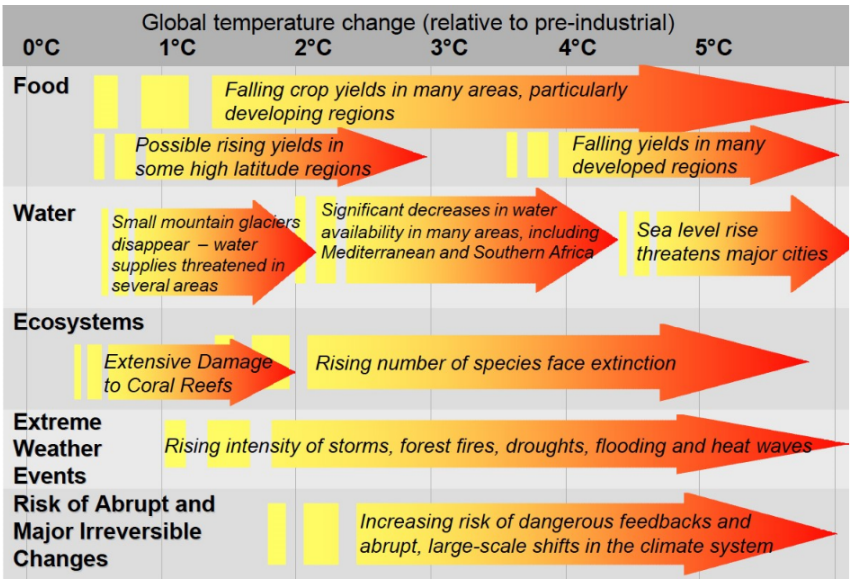

Source: Stern et al. (2006).

such as pollution can be solved on a national level, but the climate change externality requires international coordination.

In 2018, William Nordhaus was awarded the Sveriges Riksbank Prize in Economic Sciences in Memory of Alfred Nobel for his work on climate change economics. Nordhaus already started with climate change modeling in 1975, way before climate change became a mainstream topic. He started the literature on the so called integrated assessment models (IAMs): combined economic and climate models that are used to analyze climate change in an economic context. Nordhaus (2019)[1] started with a partial equilibrium setup with an energy model in which interest rates and discount rates were taken as given. Nordhaus (2019) then added a detailed model for the carbon concentration (as a function of carbon emissions) and looked at the costs of different constraints on the carbon concentration. Given a specific constraint, shadow prices for carbon emissions could be calculated. This type of analysis gives information about how costly it is to keep the carbon concentration below a certain level.

Almost two decades later, Nordhaus came up with a much improved version of his climate change model. Nordhaus (1992) was the first version of the nowadays well known DICE model: Dynamic Integrated model of Climate and the Economy. One of the main shortcomings of the initial model was that it did not say much about the benefits of carbon reduction, it was focused on the cost of carbon reduction. It was therefore not possible to look at optimal policy in such a framework. Another shortcoming of the initial model was that the model was a partial equilibrium model. Since climate change is analyzed at a global scale, a general equilibrium model is preferred. Additionally, discount rates are very important in climate economy models since the analysis takes place over a long time horizon. This is another reason to consider a general equilibrium model.

[1]This article was originally written in 1975 and came out as a working paper. In 2019 the American Economic Review published it.

The DICE model fixes these two issues. The base of the DICE model is a Ramsey-type optimal growth model. To keep the model tractable and solvable, Nordhaus (1992) scales down the carbon dioxide model to three equations and he adds two equations to model the global temperature anomaly in response to carbon dioxide concentrations. One key conceptual difference is that Nordhaus (1992) adds a damage function to the model: the global temperature anomaly is mapped into economic losses via a damage function. The model is therefore suitable to compare the costs and the benefits of reducing carbon emissions. The DICE model is updated frequently, the last iteration is the DICE-2016 model (Nordhaus, 2017). The model is still very similar to the earliest version, but the calibration is often updated due to new insights. Nordhaus (2018) gives an overview of the changes in the DICE model over the years.

One key concept that Nordhaus introduced is the social cost of carbon (SCC). The social cost of carbon is the present value of all damages caused by emitting one unit of carbon today. The social cost of carbon is a rich concept that incorporates the economic setup, the climate module, the damage function and the preference specification of a model. The SCC is also an important number for policymakers, since it represents the benefit of carbon abatement and can therefore be used in cost-benefit analysis. The DICE model is one of the three integrated assessment models that the US government uses for its estimate of the social cost of carbon.

This thesis builds upon Nordhaus's work and focuses on improving the integrated assessment models in two main areas. The main research question of this thesis is: what is the social cost of carbon?

First, the DICE model does not explicitly take into account uncertainty. Uncertainty is however a very important issue in climate change economics. It remains hard to predict how much warming a given amount of carbon emissions will exactly generate and it is even harder to predict how much damages there will be for a given temperature increase. The fact that we cannot exactly predict the impact of climate change is no reason to wait with policy. On the contrary, the uncertainty gives even more reason to stay on the safe side (the precautionary principle). This thesis formally introduces several types of uncertainty within IAMs. It is shown that uncertainty leads to a substantially larger estimate of the social cost of carbon.

Second, more realistic preference specifications are introduced within integrated assessment models. Next to the climate model and the damage specification, the SCC is also very sensitive to preferences about risk and consumption smoothing over time. The type of utility functions that are standard in the literature (logarithmic utility or power utility) are very tractable, but also have serious limitations. There is only one parameter that controls both the preferences for risk aversion and consumption smoothing over time. Mehra and Prescott (1985) show using financial data that the power utility specification is strongly rejected. This thesis explores the implications of more realistic preference specifications in an IAM.[2]

Chapter 2 of this thesis analyzes an IAM with both climate disaster risk and a more realistic preference specification. The purpose of the model is to estimate the 'negative value' of carbon emissions. We thus take an asset pricing perspective and opt for

[2]Several authors worked on more realistic preference specifications and uncertainty within integrated assessment models. The related literature in this thesis is discussed within each chapter.

an endowment economy (Lucas Jr, 1978). Furthermore, we analyze the problem under the business-as-usual scenario (BAU), in which no additional climate policies are implemented. The variable of interest is the social cost of carbon, which should be interpreted as the benefit of reducing one unit of carbon emissions today (given current climate policy). In this chapter we do not yet look at optimal climate policy, but we focus on the benefit side of the the cost-benefit analysis. This chapter makes several contributions. First, we consider a utility function that separates prefences for risk and consumption smoothing, in line with empirical evidence (Epstein & Zin, 1991). Second, we assume that both the size and timing of climate disasters are stochastic. Third, we differentiate between different layers of uncertainty. More specific, we distinguish between risk (known probabilities) and ambiguity (unknown probabilities). As in Ellsberg (1961), we assume that the representative agent is ambiguity averse. And fourth, we are able to derive closed form solutions up to solving an integral and the model is therefore very transparent. We show that taking into account risk and ambiguity leads to a substantially higher social cost of carbon. The fact that there is much uncertainty around climate change impacts gives the incentive to stay on the safe side and to pursue ambitious climate policies.

With some specific assumptions, we were able to solve the model in chapter 2 using numerical integration, which took only a couple of seconds to solve. However, when considering a richer model with optimal climate policy this is not possible anymore. Instead, more complex numerical methods are necessary to solve the models. In chapter 3 we develop and compare two types of solution methods. Climate economy models consist of both economic and climate variables. These type of models therefore often have several state variables. The time it takes to solve a model grows exponentially with the number of state variables, this is also known as the curse of dimensionality. The two methods that are discussed in chapter 3 (finite difference method on sparse grids and stochastic grid method) are especially suited to solve high dimensional problems. The finite difference method relies on sparse grids to alleviate the curse of dimensionality. The stochastic grid method is based on random grid points, which gives a similar level of accuracy with less grid points. Both methods are applied to an example climate economy model and the advantages and disadvantages of both methods are discussed. However, both methods outperform traditional standard solution methods in a high-dimensional setting.

We then apply the stochastic grid method to a fully stochastic integrated assessment model with a detailed climate model in chapter 4. The social cost of carbon is forward looking in the sense that it incorporates (expected) future damages caused by one unit of additional emissions today. The SCC is therefore also a function of future climate policy. Chapter 4 investigates how sensitive the SCC is to the climate policy scenario. Two often used scenarios are the business-as-usual (BAU) scenario and the optimal policy scenario. In the business-as-usual scenario the SCC can be interpreted as the benefit of reducing carbon emissions by one unit given the current situation. The SCC in the optimal scenario is the optimal Pigouvian tax that, when globally implemented, will achieve the socially optimal outcome. Both scenarios are used in the literature to calculate the SCC. We show that when damages are a convex function of temperature, the SCC in the BAU scenario is much larger compared to the optimal policy scenario. In this chapter we also illustrate the effects of uncertainty on optimal policy, the social cost of carbon and the climate state variables. Lastly, the implications of delay of climate policy are investigated.

In chapter 5 the focus is shifted to the time path of the social cost of carbon and optimal abatement policies. Most studies focus on the social cost of carbon today and sometimes the path of future carbon prices is delivered as a byproduct. This is also true for chapters 2 and 4. The path of carbon prices is however as important as the initial level, since firms that invest in carbon reduction make the trade-off between current costs and future prices. The focus in this chapter is thus on the time path of optimal carbon taxes and we therefore calculate the social cost of carbon using the optimal policy scenario. The SCC is thus equal to the optimal Pigouvian tax in this setting. We start with a very simple setting in which temperature is a linear function of cumulative carbon emissions, damages are proportional to the size of the economy and damages are a linear function of temperature. In this benchmark setting, we show that the social cost of carbon grows in expectation at the same rate as the economy. We then look at the following extensions: convex damages, resolution of uncertainty, learning-by-doing in abatement, two types of tipping points and a temperature cap. For each of these extensions we look at the effect on the growth rate of the SCC. We conclude that the optimal social cost of carbon should grow in expectation faster than the growth rate of the economy.

2 Discounting the future: On climate change, ambiguity aversion and Epstein-Zin preferences

2.1 Introduction

Climate change is one of the main risks the economy will face in the upcoming decades or possibly even centuries. However, there is still much uncertainty about climate change impacts. While (almost) all scientists agree on the fact that climate change will have possibly dramatic negative consequences for the environment and economic growth, we are still not able to accurately estimate the extent and timing of future damages induced by climate change. But one thing we do know is that such consequences will take place far in the future, while if they are to be avoided policies need to be implemented today. This has made the issue of discounting future uncertain costs of climate change back towards today arguably the most important element of the climate change debate and that is the subject of this paper.

Rather than arguing about specific numerical values for parameters such as time preference, we challenge the structure of preferences commonly assumed to derive the appropriate discounting procedures and discount rates.[3] Specifically, in this paper we model climate damages as disaster risk and assume that there is ambiguity about the arrival rate and size of future climate disasters. We show that implementing these extensions leads to estimates of the social cost of carbon that are substantially larger than have been derived so far using conventional approaches to time and risk discounting.

The impact of climate change on the economy is often modeled using combined climate economy models called Integrated Assessment Models (IAMs). IAMs integrate the knowledge of different domains into one model. In the case of climate change, IAMs combine an economic model with a climate model. Three well-known IAMs are DICE (Nordhaus, 2014a), PAGE (Hope, 2006) and FUND (Tol, 2002).[4] These models are, among others, used as policy tools for cost-benefit analyses. They provide a conceptual framework to better understand the complex problem of climate change by combining different fields and allowing for feedback effects between those fields.

But IAMs also have drawbacks. To quote Pindyck (2017): "*IAM-based analyses of climate policy create a perception of knowledge and precision that is illusory ... .*"(p.53). His critique is that the models are (1) sensitive to the choices of parameters and functional forms, especially the discount rate. Besides, we know very little about (2) climate sensitivity and (3) damage functions. Finally, (4) IAMs don't incorporate tail risk. He recommends simplifying the problem by focusing on the catastrophic outcomes of climate change, instead of modeling the underlying causes. In line with that view we focus on disaster risks and the associated ambiguities and risks.

The three main IAMs are deterministic, largely because stochastic models with many state variables are more difficult to solve than deterministic models. To nevertheless cap-

[3]For a very different (and strongly worded) view focusing on the social welfare aspects of the rate of time preference rather than on individual preferences, see Stern (2015) and Chichilnisky, Hammond, and Stern (2018) who look at a positive rate of time preference as discrimination between generations that happen to have been born at different moments in time.

[4]The references do not contain the most recent versions of the IAMs.

ture uncertainty, some authors perform a Monte Carlo-like approach by analyzing several deterministic runs with different parameter values and then taking a weighted average of all runs (Dietz, 2011; Nordhaus, 2014b). Such an analysis is useful if we are interested in the sensitivity of the models to different parameter values. However, it is conceptually different from explicitly using stochastic variables, since for each run all uncertainty is resolved at time 0. Crost and Traeger (2013) compare the Monte Carlo approach to a model that actually uses random variables and find that the Monte Carlo approach underestimates the impact of uncertainty. And as we will discuss below, particularly under the structure of preferences we are analyzing, the timing of the resolution of uncertainty matters a great deal.

We propose an analytically solvable IAM that addresses both the critiques of Pindyck (2017) and of Crost and Traeger (2013) on the use of deterministic IAMs. Since there is so little known about the damage functions, we investigate the impact of both attitudes towards well defined measurable risks and ambiguity aversion towards unmeasurable uncertainty on the willingness to pay for avoiding climate risk. Furthermore we model climate risk as disaster risk instead of assuming that temperature increases generate a known amount of damage every year. The model is transparent due to the closed form solutions for the social cost of carbon. Where stochastic numerical IAMs commonly take hours or more to be solved, solving this model only requires numerical integration and is therefore solved within seconds.

The economy is modeled as a pure exchange economy with exogenous but stochastic endowments. We extend the general equilibrium Consumption-based Capital Asset Pricing Model (CCAPM), also known as Lucas-tree model, developed in Lucas Jr (1978) in several directions. In the literature, this model is widely used in conjunction with a lognormal distribution.[5] The diffusion component of the endowment captures fluctuations in consumption. But we take into account that the nature of climate risk is different from 'normal' economic risk as captured by a diffusion term. Climate disasters are events that occur rarely and take place abruptly (Goosse, 2015). To model this feature, we add a jump process to the endowment consumption stream to capture the climate disaster risk.

The intensity of the disasters is temperature-dependent. We model emissions, atmospheric carbon concentration and the temperature anomaly. The arrival rate of climate disasters is increasing in temperature. Furthermore we explicitly take into account that it is hard to estimate the probability that a disaster occurs and its expected impact by assuming that the agent does not know the exact probability distributions of the arrival rate of climate disasters and the size of the disasters: there is so called ambiguity about the characteristics of the jump risk component. And the agent is assumed to be averse to this ambiguity or Knightian uncertainty. Finally we use the continuous time version of Epstein-Zin utility, also called stochastic differential utility (SDU), which allows us to separate the intertemporal elasticity of substitution from the degree of risk aversion. In the widely used power utility specification risk aversion and elasticity of intertemporal substitution (EIS) are captured by one parameter, they are equal to each other's inverse. There is strong empirical evidence placing the relative degree of risk aversion in the range of 5 - 10 (Cochrane, 2009). Using such estimates in combination with power utility then

[5]Although Lucas Jr (1978) doesn't assume a specific distribution for the endowment stream.

results in implied estimates for the EIS much lower than direct empirical estimates of the EIS suggest. But especially for long term problems such as climate change intertemporal choices play an important role and restricting parameters such as the EIS is a severe limitation. SDU preferences make it possible to separate risk aversion and the elasticity of intertemporal substitution. We can therefore disentangle risk aversion effects (known probabilities), ambiguity aversion effects (unknown probabilities) and substitution effects. The Epstein-Zin preferences also allow for the possibility that the agent has a preference for early resolution of risk, clearly of relevance in a discussion on climate risks. We show that the specification of the agent's preferences in combination with stochastic disaster risk has large effects on how much one is willing to pay to reduce climate risk.

In this chapter, we explicitly focus on the valuation of climate risk in the business-as-usual (BAU) scenario and we do not analyse optimal abatement policies. Optimal abatement policy is studied in later chapters. The idea is that an analysis of the environmental costs of current policies (not current plans...) is useful in the climate policy debate. A commonly used measure for the cost of carbon emissions is the social cost of carbon (SCC), the long term discounted damage in dollar terms of emitting one ton of carbon today. The BAU scenario is also the default scenario to calculate the social cost of carbon in Nordhaus (2014a). Note that the social cost of carbon in our model is not equal to the globally optimal Pigouvian carbon tax, since we do not consider abatement policy in this model. The social cost of carbon using a baseline scenario can be interpreted as the monetized welfare loss of emitting one additional unit of carbon today, given the current global carbon abatement policy scenario under the assumption that no measures will be taken in the future either. This seems to us an important first step to take for as long as effective international policies are not yet agreed upon and future agreement is not yet certain. The cost of doing nothing surely is an important input in the debate, but we elaborate on the differences between the SCC under the BAU scenario and the SCC assuming optimal abatement policies in chapter 4.

Our base calibration yields a sizable social cost of carbon. Similar to the numerical IAMs, the SCC in our model is very sensitive to the choice of the input parameters. But in addition we can easily explore the implications of ambiguity aversion, preferences for early resolution of uncertainty and (related to that) a higher EIS than implied by commonly accepted values for the degree of risk aversion. In spite of incorporating all these generalizations we can still derive analytic expressions for the SCC, up to an integral, in our core model setup, making it transparent how ambiguity aversion and Epstein-Zin preferences influence the SCC. Our numerical example using best estimates of the various parameters indicates that introducing ambiguity aversion yields a SCC that is between 28% and 36% higher depending on the structure of climate risk. Moreover we highlight that the social cost of carbon is also sensitive to choices about time discounting, either via the pure rate of time preference, risk aversion or the elasticity of intertemporal substitution, and that all these parameters interact with the cost of ambiguity aversion. But the overall conclusion remains: insufficient attention to risk pricing leads to substantial underestimation of the SCC.

2.2 Related literature

This paper is related to two strands of literature. First, our methodology is related to consumption based asset pricing models with disaster risk and/or non-expected utility. And second, the paper is related to research on the impact of climate change on the economy.

The model we develop is an extension of the Consumption based Capital Asset Pricing Model (CCAPM) by Lucas Jr (1978). Mehra and Prescott (1985) point out that for plausible parameter values, the CCAPM produces a way too low equity premium and correspondingly a too high risk-free rate. These puzzles are called respectively the Equity Premium Puzzle and the Risk-Free Rate Puzzle. Jump risk or disaster risk has been proposed as a possible solution of these puzzles (Barro, 2006; Rietz, 1988). Extensions to the early disaster/jump risk models are the use of Stochastic Differential Utility (SDU) instead of power utility, and the introduction of time-varying disaster probabilities and multi-period (i.e. persistent) disasters (Barro, 2009; Tsai & Wachter, 2015; Wachter, 2013). Climate change induced disasters fit in the rare disaster literature since climate change is increasingly thought to give rise to abrupt destructive changes in the Earth's environment (Goosse, 2015). We define disaster shocks as shocks whose occurrence has a small probability at any given moment of time but with possibly large and persistent negative effects on the economy once they do take place.

Ambiguity aversion, aversion of unmeasurable or Knightian uncertainty, is the second extension of the CCAPM we introduce to our climate model. Liu, Pan, and Wang (2004) consider a general equilibrium model with rare disasters and ambiguity aversion in their analysis of option pricing 'smirks'. Their agent is only concerned about misspecification of the jump process, a logical choice that we follow, since the probability distribution of rare events is by their very nature much harder to estimate than the diffusion component.

Risk aversion and ambiguity aversion are obviously important in a climate change setting, but since abrupt climate change is anticipated to take place far into the future, intertemporal choices play an important role as well. Power utility is therefore an unsatisfactory framework since with that structure of preferences, risk aversion and EIS cannot be varied independently. This is why we adopt the Stochastic Differential Utility framework introduced by Duffie and Epstein (1992b) since with SDU the risk aversion parameter and the elasticity of intertemporal substitution (EIS) are no longer restricted to be each other's inverse. We go beyond the setting of Tsai and Wachter (2015) who also use SDU to analyze the consequences of disaster risk for asset prices by in addition introducing ambiguity aversion. This extension is especially relevant in a climate disaster model since there is no clear history of events on which we can base our estimates of the damages.

The second strand in the literature our paper is obviously related to is the literature on climate change economics and especially to the part of that literature that considers climate disaster risk, non-expected utility and analytic approaches to solve their models. This paper is to the best of our knowledge the first paper to consider ambiguity aversion in a framework with climate disaster risk.

Barro (2015) extends his disaster risk model with environmental disasters and focuses on discount rates and optimal environmental investment. He does not incorporate a

climate model but rather assumes that the disaster probability is constant and that it can be reduced by environmental investment. Bansal, Kiku, and Ochoa (2016) propose a climate model based on the Long-Run-Risk (LRR) model of Bansal and Yaron (2004). In the LRR-model, the agent has Epstein-Zin preferences and consumption growth contains persistent shocks. Bansal et al. (2016) model climate disasters as a jump process that affects both consumption itself and the growth rate of consumption. They show that the outcomes of their model are very sensitive to choices of the EIS. Karydas and Xepapadeas (2019) consider a dynamic asset pricing framework with both macroeconomic disasters and climate change related disasters and analyze the implications for portfolio allocation. Our approach differs from these papers by including ambiguity aversion.

Furthermore, our paper is related to the literature on climate change economics that considers risk and non-expected utility. The most well-known integrated assessment model is the DICE model (Nordhaus, 2017). This model is deterministic and the representative agent is assumed to have power utility. Several papers have recently studied the impact of risk and more complex preference structures on the social cost of carbon. For instance Cai and Lontzek (2019), Hambel, Kraft, and Schwartz (2021) and Jensen and Traeger (2014) study integrated assessment models with Epstein-Zin preferences and different types of economic and climate risk. Epstein-Zin preferences can have a substantial effect on the discount rate, for obvious reasons a very important parameter in climate models.

Traeger (2014) studies the effect of ambiguity aversion on discount rates. Millner, Dietz, and Heal (2013) look at the effect of ambiguity about the climate sensitivity on optimal policy, where Lemoine and Traeger (2016) focus on ambiguity about tipping points that affect the climate dynamics. All three papers use the smooth ambiguity approach proposed by Klibanoff, Marinacci, and Mukerji (2005). In contrast, we consider the multiple priors approach to model ambiguity aversion, in which the worst case within a specified set of priors is chosen following Gilboa and Schmeidler (1989). Lastly, Barnett, Brock, and Hansen (2020) introduce ambiguity aversion into a climate-economy model, also based on the smooth ambiguity approach of Klibanoff et al. (2005). Barnett et al. (2020) consider even three different types of uncertainty: they distinguish between risk, ambiguity and model misspecification. Our key contribution to this literature is that (1) we study ambiguity aversion in a climate disaster risk framework, (2) we use a different ambiguity approach (the multiple priors approach), and (3) we provide a closed form expression for the social cost of carbon (up to solving an integral) which facilitates conceptual understanding of the results particularly where non-linear effects are at play.

The three IAMs that were mentioned in the introduction are all solved using numerical methods. However, since it has become clear that the choice of the input parameters has a large influence on the results, we think it is useful to know how these parameters exactly influence the outcomes and therefore opt for models allowing for analytical solutions. There are a few recent papers that also focused on obtaining analytic solutions. Golosov, Hassler, Krusell, and Tsyvinski (2014) were the first to obtain closed form solutions in an IAM. However, this required quite strict assumptions such as logarithmic utility and full depreciation of capital every decade. Bretscher and Vinogradova (2018) develop a stylized production-based model where the current carbon concentration directly enters the damage function and obtain closed form solutions for the optimal abatement policy. Van den Bremer and Van der Ploeg (2021) consider a rich stochastic production-based

model with Epstein-Zin preferences, convex damages, uncertainty in state variables, correlated risks and skewed distributions to capture climate feedbacks. Since the model is too complex to obtain exact analytic solutions, they obtain closed form approximate solutions using perturbation methods. Lastly, Traeger (2021) extends the model of Golosov et al. (2014). Where in other analytic other models the atmospheric carbon concentration often directly enters the damage function (Bretscher & Vinogradova, 2018; Golosov et al., 2014), Traeger (2021) explicitly models the carbon cycle and the temperature anomaly while damages are induced by an increasing temperature. Additionally Traeger (2021) considers the effect of stochastic state variables.

2.3 Model

In this section we first outline the setup for the economy, then extend that setup to incorporate a climate model and finally discuss the utility specification.

Since we do not consider mitigation policies in this paper, we opt for assuming a pure exchange economy, where agents are endowed with an exogenous stochastic income stream. Agents can buy risky stocks, which give a claim on the endowment. Consumption goods are perishable, transferring wealth to the future is only possible by buying stocks. The income stream can intuitively be seen as a tree that produces an uncertain amount of fruit every time period. All agents can buy stocks, which are shares in the tree. The fruit is non-storable, so it must be consumed at the period of the endowment. This implies that aggregate endowment equals aggregate consumption at every moment in time. It is assumed that all agents have identical preferences and endowments, so the separate agents can be replaced by one representative agent. We extend the standard pure exchange model by assuming that the stochastic endowment stream is subject to climate disasters, where the probability of a climate disaster depends on the temperature level.

2.3.1 Economy

The aggregate endowment process follows a geometric Brownian motion with an additional jump component that represents climate disasters. Suppose we have a probability space $(\Omega, \mathcal{F}, \mathbb{P})$ on which a standard Brownian motion Z_t, a Poisson process N_t with arrival rate λ_t and a random variable J_t are defined. The arrival rate of climate disasters is a function of the temperature level. The distribution of the size of disasters is assumed to be the same for any t. The three types of shocks, namely Brownian motions, Poisson arrivals and disaster sizes, are assumed to be independent. Assume there is a filtration $\mathbb{F} = \{\mathcal{F}_t : t \geq 0\}$. We will use the following notation throughout this chapter: $E_t[.] = E[.|\mathcal{F}_t]$. Consider the following process for aggregate endowments:

$$dC_t = \mu C_t dt + \sigma C_t dZ_t + J_t C_{t-} dN_t. \tag{2.1}$$

The endowment follows the usual geometric Brownian motion dynamics, with an additional jump process. C_{t-} denotes aggregate endowment just before a jump ($C_{t-} = \lim_{h \downarrow 0} C_{t-h}$). In equilibrium aggregate consumption must equal aggregate endowment and therefore the process is also referred to as the aggregate consumption process. The growth rate $\mu \geq 0$ and the volatility $\sigma > 0$ are constant. When a climate disaster arrives

at time t, the size of the disaster is controlled by the random variable J_t. We assume that J_t has the following density: $f(x) = \eta(1+x)^{\eta-1}$ where $-1 < x < 0$. J_t can thus be seen as the percentage loss of aggregate consumption after a disaster. The expected disaster size equals $E_t[J_t] = \frac{-1}{\eta+1}$ and the moments $E_t\Big[(1+J_t)^n\Big] = \frac{\eta}{\eta+n}$ can be easily calculated. In line with the subject of climate disasters, jumps can only be negative.

2.3.2 Climate model

The arrival rate of disasters is assumed to be temperature dependent. We assume that damages are linearly increasing in temperature: $\lambda_t = \lambda_T T_t$. However, our derivations remain valid for non-linear specifications of the arrival rate. We discuss this assumption in the calibration section. We make some simplifying assumptions to allow for an analytic solution of the model. The main requirement is that the state variables of the climate submodel are deterministic, an assumption we have relaxed in chapter 4.

Industrial emissions (from fossil fuel burning) are usually modeled as the product of the carbon intensity of aggregate output and aggregate output (or aggregate consumption) itself. In addition to industrial emissions, land-use change such as deforestation also causes carbon emissions.[6] We simplify the problem by modeling emissions as exogenous, which in the current setting is not all that important because output growth itself is not yet endogenized. Thus we directly model total emissions, which are the sum of industrial emissions and emissions caused by for example land-use change. This simplification is necessary to keep the state variables deterministic, which in turn is necessary for analytical solvability. If we would not make this assumption, emissions are stochastic and this would make it impossible to solve the model analytically. We therefore assume that emissions are growing at a rate $g_{E,t}$. The growth rate itself moves towards the long-run equilibrium $g_{E,\infty}$ at a rate δ_E. By assuming that $g_{E,\infty} < 0$, this specification allows us to have growing emissions today, but in the long run the growth rate will become negative and emissions will go to zero. This is a logical assumption since there is a point where the stock of fossil fuels will be depleted. This gives us the following process for emissions:

$$\begin{aligned} dE_t &= g_{E,t} E_t dt, \\ dg_{E,t} &= \delta_E(g_{E,\infty} - g_{E,t})dt. \end{aligned} \tag{2.2}$$

We calibrate exogenous emissions to match the baseline scenario in Nordhaus (2017). In our setup, it is not a great loss to lose the direct connection between the economy and the carbon emissions since we use a Lucas-tree model where the economy already has an exogenous growth rate. We do not analyse optimal policy and therefore the causes of economic growth and emissions are not of first order importance. What is important for the valuation of the risk is that the climate model is in line with reality.

Since we focus on disaster risks which through our climate model depend on cumulative emissions, not incorporating any short term correlation between economic growth and emissions has no major consequences for the answers to the questions addressed in this paper. In reality, emissions are low when the economy is in a recession and vice-versa, there

[6] For an extensive report on the relation between land-use change and emissions we refer to the special IPCC report (Noble, Bolin, Ravindranath, Verardo, & Dokken, 2000).

is a substantial correlation between economic growth and worldwide carbon emissions. However, due to thermal inertia it takes some time for temperature to react on emissions and the contemporaneous correlation between consumption and temperature will be lower. When climate risk is high in good states, one would be willing to pay less to reduce the risk. So the correlation between temperature and the consumption process does play a role in the valuation of damages. However, since the contemporaneous correlation between aggregate consumption and temperature is smaller compared to the correlation between aggregate consumption and emissions we expect that this does not play a large role given our focus on disaster risks.

We use the climate model (carbon cycle and temperature model) discussed in Mattauch et al. (2019), which they call the IPCC AR5 impulse-response model. This model is in line with recent insights from the climate literature and is also used in IPCC (2013). Specifically, this climate model incorporates the fact that thermal inertia play a smaller role than commonly assumed in the climate modules in economic models. Climate modules commonly used in economic models tend to overstate the time it takes for the earth to warm in response to carbon emissions (Dietz, Van der Ploeg, Rezai, & Venmans, 2020).

The first step is to model how the carbon concentration evolves over time given a path of carbon emissions. Define by M_t the atmospheric carbon concentration compared to the pre-industrial level M_{pre}. We then assume that the carbon concentration is the sum of four artificial carbon boxes: $M_t = \sum_{i=0}^{3} M_{i,t}$. This specification can capture that the decay of carbon has multiple time scales and that a fraction of emissions will stay in the atmosphere forever. The dynamics of carbon box i are given by:

$$dM_{i,t} = \nu_i \Big(E_t - \delta_{M,i} M_{i,t} \Big) dt. \tag{2.3}$$

ν_i is the fraction of emissions that ends up in carbon box i, which implies that $\sum_{i=0}^{3} \nu_i = 1$. $\delta_{M,i}$ controls the decay rate of carbon in box i. We assume that all carbon that ends up in box 0 will permanently stay in the atmosphere, such that $\delta_{M,0} = 0$. The other three boxes have a positive decay rate: $\delta_{M,i} > 0, i \in \{1, 2, 3\}$.

The next step is to model the impact of carbon concentration on temperature. This requires modeling what is called radiative forcing: radiative forcing is the difference between energy absorbed by the earth from sunlight and the energy that is radiated back to space. A higher atmospheric carbon concentration strengthens the greenhouse effect and therefore leads to higher radiative forcing. We propose a logarithmic relation between atmospheric carbon concentration and radiative forcing:

$$F_{M,t} = \alpha \frac{\upsilon}{\log(2)} \log \Big(\frac{M_t + M_{pre}}{M_{pre}} \Big). \tag{2.4}$$

α equals the climate sensitivity: the long-run change in temperature due to a doubling of the carbon concentration compared to the pre-industrial level. υ is a parameter that is also part of the temperature module and this parameter will be discussed later. We also include non-carbon related (exogenous) forcing $F_{E,t}$, which follows:

$$dF_{E,t} = \delta_F (F_{E,\infty} - F_{E,t}) dt. \tag{2.5}$$

Total radiative forcing is the sum of carbon-related radiative forcing and exogenous forcing: $F_t = F_{M,t} + F_{E,t}$.

The final step moves from F_t to the actual surface temperature T_t. T_t is the difference between the actual temperature compared to the pre-industrial temperature level. The change in surface temperature is a delayed response to radiative forcing. Call the heat capacity of the surface and the upper layers of the ocean τ while τ_{oc} equals the heat capacity of the deeper layers of the ocean. The parameter κ captures the speed of temperature transfer between the upper layers and the deep layers of the ocean. The dynamics of temperature are then given by:

$$\begin{aligned} dT_t &= \frac{1}{\tau}\Big(F_t - \upsilon T_t - \kappa(T_t - T_t^{oc})\Big)dt, \\ dT_t^{oc} &= \frac{\kappa}{\tau_{oc}}(T_t - T_t^{oc})dt. \end{aligned} \tag{2.6}$$

From this equation, one can verify that the long run equilibrium temperature for a given level of radiative forcing equals: $T_t^{eq} = \frac{F_t}{\upsilon}$. The parameter υ therefore controls the equilibrium temperature response to a given level of forcing. Note that when $M_t = 2M_{pre}$, we obtain that $F_t = \alpha\upsilon + F_t^E$ and $T_t^{eq} = \alpha + \frac{F_t^E}{\upsilon}$. Therefore the parameter α can indeed be interpreted as the equilibrium temperature response to a doubling of the carbon concentration. We can rewrite the first equation to:

$$dT_t = \frac{1}{\tau}\Big(\upsilon(T_t^{eq} - T_t) - \kappa(T_t - T_t^{oc})\Big). \tag{2.7}$$

This equation is more intuitive, since it captures the fact that the temperature moves towards its equilibrium level at a rate proportional to $T_t^{eq} - T_t$. The second part shows that the oceans are delaying this convergence. It takes time for T_t^{oc} to adjust towards T_t and this will also delay the convergence of T_t towards the equilibrium level T_t^{eq}. As specified earlier, the arrival rate of climate disasters is a linear function of temperature T_t.

2.3.3 Utility specification

The representative agent maximizes his utility of consumption over an infinite planning horizon. We consider the continuous time version of Epstein-Zin preferences (Epstein & Zin, 1989), called stochastic differential utility (SDU) (Duffie & Epstein, 1992b). Epstein and Zin (1989) consider the following class of preferences in discrete time: $V_t = [(1-\beta)C_t^{1-1/\epsilon} + \beta ce_t(V_{t+1})^{1-1/\epsilon}]^{\frac{1}{1-1/\epsilon}}$ where $\epsilon = EIS$, β is the time preference parameter and $ce_t(.)$ is a certainty equivalent function. When considering a deterministic consumption program, V_t is a constant elasticity of substitution (CES) utility function. In the other limiting case where only a static gamble is considered, there are no intertemporal choices and the utility is entirely determined by the certainty equivalent function $ce_t(.)$. The certainty equivalent function (or risk aggregator) that is widely used throughout the literature is $ce_t(V_{t+1}) = E_t(V_{t+1}^{1-\gamma})^{\frac{1}{1-\gamma}}$ where γ is the coefficient of relative risk-aversion, which we assume to be constant. This specification of $ce_t(.)$ yields a special case of the preferences studied by Kreps and Porteus (1978) and is therefore also called Kreps-Porteus utility. Static gambles are evaluated as if the agent has power utility, but in a

dynamic stochastic setting EIS and risk aversion are decoupled: this specification allows to separate risk aversion γ from the elasticity of intertemporal substitution ϵ. An important property of this utility specification is that the agent has preferences for early resolution of uncertainty if $\epsilon > \frac{1}{\gamma}$ and for late resolution if $\epsilon < \frac{1}{\gamma}$.

We consider a special case of SDU, the continuous time equivalent of Kreps-Porteus utility, or rather an ordinally equivalent utility process. Similar to the discrete time case, SDU can be represented by a combination of an aggregator f that determines the degree of intertemporal substitution and a certainty equivalent operator ce. In the case of Kreps-Porteus utility, $f(C,V) = \frac{\beta}{1-1/\epsilon}\frac{C^{1-1/\epsilon}-V^{1-1/\epsilon}}{V^{-1/\epsilon}}$ and $ce(\sim V) = [E(V^{1-\gamma})]^{\frac{1}{1-\gamma}}$. In this case the drift of the value function consists of the aggregator $f(C,V)$ and a variance multiplier A that belongs to ce. Duffie and Epstein (1992b) show that there exists an ordinally equivalent utility process with aggregator f as in (2.8). In this case $ce(\sim V) = E(V)$ and the variance multiplier A that belongs to c is zero. The agent's utility or value function then becomes:

$$V_t = E_t\Big[\int_t^\infty f(C_s, V_s)ds\Big]$$

where

$$f(C,V) = \frac{\beta}{1-1/\epsilon}\frac{C^{1-1/\epsilon} - \big((1-\gamma)V\big)^{\frac{1}{\zeta}}}{\big((1-\gamma)V\big)^{\frac{1}{\zeta}-1}} \quad \text{for } \epsilon \neq 1 \tag{2.8}$$

$$\text{with } \zeta = \frac{1-\gamma}{1-1/\epsilon}.$$

Throughout this paper, we refer to this utility specification as stochastic differential utility (SDU) although Duffie and Epstein (1992b) actually consider a more general class of utilities under that label. Similar to the discrete time counterpart, γ denotes risk-aversion, ϵ is the elasticity of intertemporal substitution and β equals the time preference parameter. We will focus on the case where $\epsilon \neq 1$ and therefore will derive our results only for this case. For the case $\epsilon = 1$ we can take the limit $\epsilon \to 1$ or follow the same derivation but with $f(C,V) = \beta(1-\gamma)V\Big(\log C - \frac{1}{1-\gamma}\log\big((1-\gamma)V\big)\Big)$. If $\gamma = \frac{1}{\epsilon}$, the utility specification reduces to standard power utility.

2.3.4 Ambiguity

There is much uncertainty regarding the arrival rate and magnitude of climate disasters. And, as stressed by Pindyck (2017), we know very little about the damage functions. Where consumption growth and volatility can be estimated more accurately from historical data, the estimation of the climate disaster parameters will be much harder since climate disasters do not happen that often. It is fair to state that we simply do not know the exact distribution of climate damages. We consider it therefore desirable to account for the possibility that the 'best estimate' model is not the true model: there is ambiguity. We assume that the representative agent is ambiguity averse.

It is important to stress the difference between risk and ambiguity. When we are talking about risk, an agent knows the probabilities and possible outcomes of all events.

When the agent has to deal with ambiguity, the probabilities attached to particular events are unknown. The distinction between risk and ambiguity is already extensively discussed in Knight (1921), which is why ambiguity is often referred to as Knightian uncertainty. Ellsberg (1961) shows using the Ellsberg Paradox that people are ambiguity averse, i.e. they prefer known probabilities over unknown probabilities.

We use the *recursive multiple priors utility* developed in continuous time by Chen and Epstein (2002) to model ambiguity. For an overview of different methods to model ambiguity we refer to appendix 2.A. An advantage of this method compared to other methods is that it preserves the homotheticity of the value function.

To apply the approach of Chen and Epstein (2002) to model ambiguity, we begin by defining the 'best estimate' model or reference model as the agent's most reliable model with probability measure $\mathbb{P}$. But the agent also takes into account other, alternative models. The alternative models have measure $\mathbb{Q}^{a,b}$; the jump arrival rate becomes $\lambda_t^{\mathbb{Q}} = a_t\lambda_t$ and the jump size parameter becomes $\eta_t^{\mathbb{Q}} = b_t\eta$. Remember that the expected jump size equals $\frac{-1}{\eta+1}$, which implies that a low b_t leads to a more negative jump size. The agent takes into account that his reference model is not the true model and he therefore specifies a set of models that he considers possible. Given the set of models, he then considers the worst case (Chen & Epstein, 2002; Gilboa & Schmeidler, 1989).

The size of the set of models is assumed to depend on the ambiguity aversion parameter θ. All models with a distance smaller than θ are allowed in the set of admissible models. The distance between the reference model $\mathbb{P}$ and an alternative model $\mathbb{Q}^{a,b}$ is measured using the concept of *relative entropy*, a common metric for the distance between two probability measure (see for example Hansen and Sargent (2008)). The distance or *relative entropy* between the reference and alternative model depends on the parameters a_t and b_t and can therefore be written as $RE(a_t, b_t)$. The relative entropy metric satisfies $RE(a_t, b_t) \geq 0 \ \forall(a_t, b_t)$ and $RE(1, 1) = 0$: the distance of the reference model to itself is by definition equal to 0. If θ is large, the agent is very ambiguity averse and thus considers a large set of models. The preferences of the agent then become:

$$\begin{aligned} &V_t = \min_{\mathbb{Q}\in\mathcal{P}^\theta} V_t^{\mathbb{Q}} \\ &\text{where} \ \ V_t^{\mathbb{Q}} = E_t^{\mathbb{Q}}\Big[\int_t^\infty f(C_s, V_s^{\mathbb{Q}})ds\Big] \\ &\text{and} \ \ \mathcal{P}^\theta = \{\mathbb{Q}^{a,b} : RE(a_t, b_t) \leq \theta \ \forall t\}. \end{aligned} \tag{2.9}$$

Here $V_t^{\mathbb{Q}}$ is the SDU utility process given the measure $\mathbb{Q}$. $\theta = 0$ implies that $\mathcal{P}^\theta = \{\mathbb{P}\}$ and the agent only considers one measure, namely the reference measure. Thus there is no ambiguity aversion when $\theta = 0$. Where the risk aversion parameter γ can be seen a parameter that is relevant for any risky bet, the parameter θ captures intrinsic ambiguity aversion (one person might be more ambiguity averse than another), but it is also source dependent. If there is a lot of information and data available about a process, the set of admissible priors will be smaller compared to a process about which not much is known.

It is not necessary to have a constant θ, one could for example incorporate learning by assuming that θ_t is a decreasing function over time as the actual stochastic processes unfold. The agent then obtains more information about a process over time and therefore one could argue it is plausible that the set of priors will be shrinking over time. However,

Figure 2.1: *Relative entropy for different values of a_t and b_t. Results are given for $\lambda_t = 0.1$.*

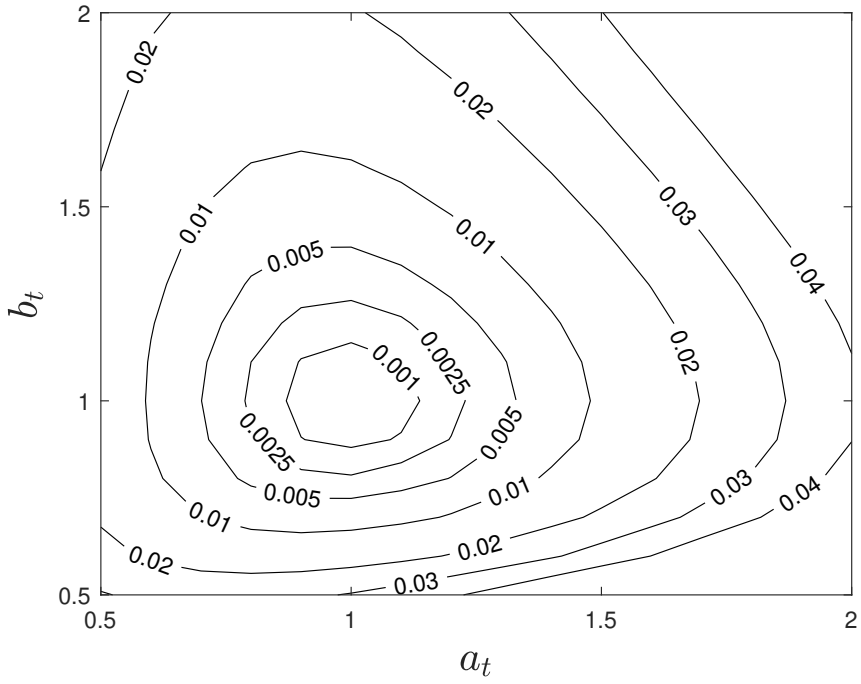

there does not (yet) seem to exist a generally accepted framework to determine how the set of priors should shrink over time based on new observations. In particular the multiple prior approach does not lend itself to Bayesian updating since we do not define model probabilities in this approach. Similar to Chen and Epstein (2002) we will therefore focus on the case with a constant θ.

In appendix 2.B we derive that relative entropy equals:

$$RE(a_t, b_t) = (1 - a_t)\lambda_t + a_t\lambda_t\Big(\log(a_t b_t) + \frac{1}{b_t} - 1\Big). \tag{2.10}$$

If we take a look at this expression for the relative entropy, it is clear that for $(a_t, b_t) = (1, 1)$, the relative entropy equals zero. When one or both of the two variables deviate from the reference model, the relative entropy increases. Every contour in figure 2.1 gives a set of combinations (a_t, b_t) that yields the same relative entropy. If for example $\theta = 0.01$, then all (a_t, b_t) combinations within that contour line are included in the set of admissible priors. The worst case probability measure will be the probability measure for which either a_t is large (high arrival rate) and/or b_t is small, since the expectation of the jump size under the alternative measure is inversely related to b_t: $E_t^{\mathbb{Q}}[J_t] = \frac{-1}{b_t\eta+1}$.

From the current setup, it is hard to argue what a reasonable value for ambiguity aversion θ would be. In order to give more guidance about reasonable values for θ, we use the concept of *detection error probabilities* introduced by Anderson, Hansen, and Sargent (2003).[7] Consider the following thought experiment. Assume that the representative agent would be able to observe the process of consumption over the next N years, and

[7]See for example Maenhout (2006) for another application of detection error probabilities.

after observing the process the agent has to choose which of the two models (the reference model or the worst-case model) is most likely. There are two types of errors in this case. The agent could choose the reference model while the process was actually generated by the worst-case model and he could also make the opposite error. The detection error probability is defined as the average of the probability of the two errors. Appendix 2.C describes how the detection error probability is calculated.

The detection error probability depends on N, since when the agent observes the process for a longer period, the probability of a mistake will be smaller. The detection error probability also depends on the ambiguity aversion parameter. When θ is small, the reference and worst-case model are similar to each other and the probability of a mistake is large. On the other hand, when the agent is extremely ambiguity averse the reference and worst-case models are very different and the detection error probability becomes small. The representative agent wants to make the set of models sufficiently large to make a robust decision, but on the other hand does not want to take into account implausible models. Since the detection error also depends on the other parameters of the model, we come back to the issue of calibrating the ambiguity aversion parameter in the calibration section.

2.4 Solving the model

We first derive for each alternative probability measure $\mathbb{Q}^{a,b}$ the corresponding Hamilton-Jacobi-Bellman (HJB) equation and find an expression for the value function $V_t^{\mathbb{Q}}$. Then we derive the HJB-equation for $V_t = \min_{\mathbb{Q}\in\mathcal{P}^\theta} V_t^{\mathbb{Q}}$. At the end of the section we discuss our solution method.

2.4.1 HJB-equation

The value function is a function of aggregate consumption and all the climate state variables. Let $V_C^{\mathbb{Q}}$ denote the first derivative of the value function with respect to aggregate consumption, similar notation is used for the second derivative. For notational purposes, define the vector of climate state variables:

$$X_t = [g_{E,t}\ E_t\ M_{0,t}\ M_{1,t}\ M_{2,t}\ M_{3,t}\ F_{E,t}\ T_t\ T_t^{oc}]'. \tag{2.11}$$

The vector of state variables then follows: $dX_t = \mu_X(X_t)dt$. Denote by $V_X^{\mathbb{Q}}$ the row vector of partial derivatives of the value function $V_t^{\mathbb{Q}}$ with respect to the vector of state variables X_t: $V_X^{\mathbb{Q}} = \left[\frac{\partial V^{\mathbb{Q}}(C_t,X_t)}{\partial g_{E,t}} \quad ... \quad \frac{\partial V^{\mathbb{Q}}(C_t,X_t)}{\partial T_t^{oc}}\right]$.

We show in appendix 2.D that under the measure $\mathbb{Q}^{a,b}$, the value function $V_t^{\mathbb{Q}}$ satisfies the following Hamilton-Jacobi-Bellman equation:

$$\begin{aligned} 0 = {} & f(C_t, V_t^{\mathbb{Q}}) + V_C^{\mathbb{Q}}\mu C_t dt + \frac{1}{2}V_{CC}^{\mathbb{Q}}\sigma^2 C_t^2 + V_X^{\mathbb{Q}}\mu_X(X_t) \\ & + \lambda_t^{\mathbb{Q}} E_t^{\mathbb{Q}}\big[V^{\mathbb{Q}}\big((1+J_t)C_{t-}, X_t\big) - V^{\mathbb{Q}}(C_{t-}, X_t)\big]. \end{aligned} \tag{2.12}$$

The HJB-equation is a partial differential equation. We conjecture and verify that the

value function under the measure $\mathbb{Q}^{a,b}$ is of the following form:

$$V^{\mathbb{Q}}(C_t) = g^{\mathbb{Q}}(X_t)\frac{C_t^{1-\gamma}}{1-\gamma}, \tag{2.13}$$

where $g^{\mathbb{Q}}(X_t)$ is some function of X_t. Substituting this form of the value function into the HJB-equation and calculating the expectation gives the following reduced HJB-equation (see appendix 2.E):

$$\begin{aligned} 0 = &\frac{\beta}{1-1/\epsilon}\Big(g^{\mathbb{Q}}(X_t)^{-\frac{1}{\zeta}} - 1\Big) + \mu - \frac{\gamma}{2}\sigma^2 + \frac{g_X^{\mathbb{Q}}(X_t)}{g^{\mathbb{Q}}(X_t)(1-\gamma)}\mu_X(X_t) \\ &+ a_t\lambda_t\frac{-1}{b_t\eta + 1 - \gamma}. \end{aligned} \tag{2.14}$$

Given a probability measure $\mathbb{Q}^{a,b}$, we could solve this equation to find $g^{\mathbb{Q}}(X_t)$. Now let us return to the problem with ambiguity. We are not interested in the solution for every single measure $\mathbb{Q}^{a,b}$, but we want to find the solution to $V_t = \min_{\mathbb{Q}\in\mathcal{P}^\theta} V_t^{\mathbb{Q}}$. We can replace the global minimization problem of equation (2.9) by an instantaneous optimization problem at every time period t, since relative entropy is a function of a_t, b_t and λ_t, which are all three known at time t. The HJB-equation of the problem with ambiguity then becomes:

$$\begin{aligned} 0 = \min_{(a_t,b_t)\ s.t.\ RE(a_t,b_t)\le\theta} &\Big\{\frac{\beta}{1-1/\epsilon}\Big(g^{\mathbb{Q}}(X_t)^{-\frac{1}{\zeta}} - 1\Big) + \mu - \frac{\gamma}{2}\sigma^2 \\ &+ \frac{g_X^{\mathbb{Q}}(X_t)}{g^{\mathbb{Q}}(X_t)(1-\gamma)}\mu_X(X_t) + a_t\lambda_t\frac{-1}{b_t\eta + 1 - \gamma}\Big\}. \end{aligned} \tag{2.15}$$

2.4.2 Optimal control variables

From the HJB-equation we can then calculate the optimal control variables a_t^* and b_t^*. This is a constrained optimization problem with Lagrangian:

$$L(a_t, b_t, l_t) = a_t\lambda_t\frac{-1}{b_t\eta + 1 - \gamma} - l_t\Big(RE(a_t, b_t) - \theta\Big). \tag{2.16}$$

Here l_t is the Lagrange multiplier. a_t^* and b_t^* and the Lagrange-multiplier l_t are the solutions to the following first order conditions:

$$\begin{aligned} \frac{\partial}{\partial a_t}L(a_t, b_t, l_t) &= \lambda_t\frac{-1}{b_t\eta + 1 - \gamma} - l_t\lambda_t\Big(\log(a_tb_t) + \frac{1}{b_t} - 1\Big) = 0, \\ \frac{\partial}{\partial b_t}L(a_t, b_t, l_t) &= a_t\lambda_t\frac{\eta}{(b_t\eta + 1 - \gamma)^2} - l_ta_t\lambda_t\frac{b-1}{b^2} = 0, \\ \frac{\partial}{\partial l_t}L(a_t, b_t, l_t) &= \theta - (1-a_t)\lambda_t - a_t\lambda_t\Big(\log(a_tb_t) + \frac{1}{b_t} - 1\Big) = 0. \end{aligned} \tag{2.17}$$

Figure 2.2 illustrates the optimization problem. Given an entropy budget θ and the arrival rate λ_t, one can determine the feasible set of (a_t, b_t). Figure 2.1 shows the feasible sets for several budgets. A contour plot of the objective function for several (a_t, b_t) combinations is given in subfigure 2.2a. Clearly combinations in the bottom right corner

Figure 2.2: *Selection of the optimal a and b.*

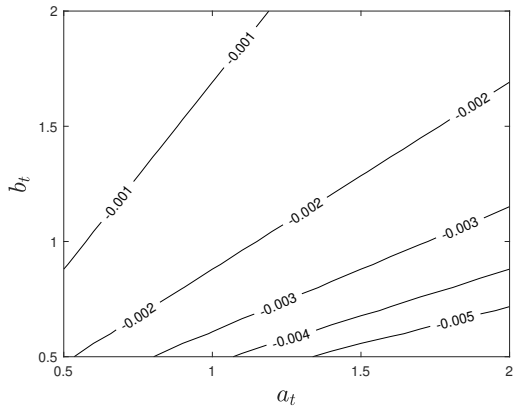

(a) Contour plot of the objective function of the constrained minimization problem for different values of a_t and b_t.

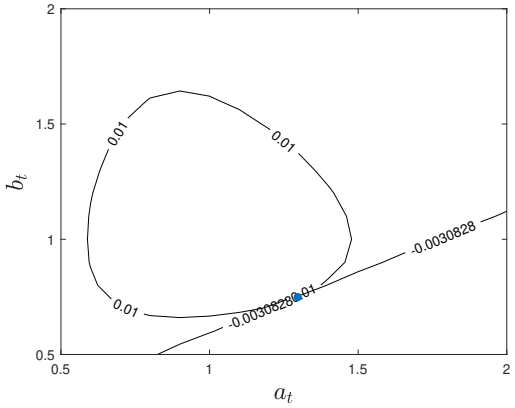

(b) Illustration of selection of optimal (a_t, b_t). The oval area shows all admissible values for a_t and b_t that are within the relative entropy budget of 0.01. The straight line is the objective function.

(high a_t, low b_t) give the lowest objective function. The goal is to minimize this function, given the relative entropy constraint. Subfigure 2.2b shows how the optimal combination (a_t^*, b_t^*) is determined. The point where objective function touches the feasible region is the optimal solution. From now on we use the following notation for the optimal arrival rate and jump size: $\lambda_t^* = a_t^* \lambda_t$ and $\eta_t^* = b_t^* \eta$. Since a_t^* and b_t^* are a function of λ_t, they are implicitly a function of temperature T_t as well. Furthermore we define by $g(X_t)$ the function that solves that HJB-equation with parameters a_t^* and b_t^*.

Figure 2.3 shows the optimal a_t^* and b_t^* as a function of λ_t. For each λ_t one finds the corresponding a_t^* and b_t^* by solving the first order conditions. A constant relative entropy budget implies that a_t is decreasing in λ_t and b_t is increasing in λ_t. The idea behind the time-varying parameters is illustrated in the following example. Assume $\theta = 0.01$. At time t, the arrival rate equals 0.05 and at time t' the arrival rate equals 0.1. At every time point the following equality must hold at the optimum: $RE(a_t, b_t, \lambda_t) = \theta$. For $\lambda_t = 0.05$ the optimal parameters are $(a_t^*, b_t^*) = (1.41, 0.68)$ and $RE(1.41, 0.68, 0.05) = 0.01$. Now consider time t' with arrival rate 0.1. If we would use the same optimal parameters as at time t, the relative entropy exceeds the budget: $RE(1.41, 0.68, 0.1) > 0.01$. The distance or relative entropy between the reference model and the worst-case model is increasing in the arrival rate λ_t. For a larger arrival rate, an x% increase in the arrival rate generates a larger 'distance' between the two measures. Intuitively, when the arrival rate is larger, more disasters are observed. With the same a_t^* and b_t^*, detecting which probability distribution is the true distribution is easier when disasters occur frequently. Therefore the optimal a_t and b_t must adjust to make sure that the relative entropy remains within the constant budget. At time t', the optimal parameters become: $(a_t^*, b_t^*) = (1.30, 0.75)$.

2.4.3 Solution method

It is typically not possible to solve the partial differential equation of the problem with climate state variables (except when the highly restrictive assumption of a unit EIS is

Figure 2.3: *Optimal parameters a_t and b_t as a function of the arrival rate λ_t with constant ambiguity aversion parameter θ. Input parameters: $\theta = 0.01$, $\eta = 61.5$, $\gamma = 5$.*

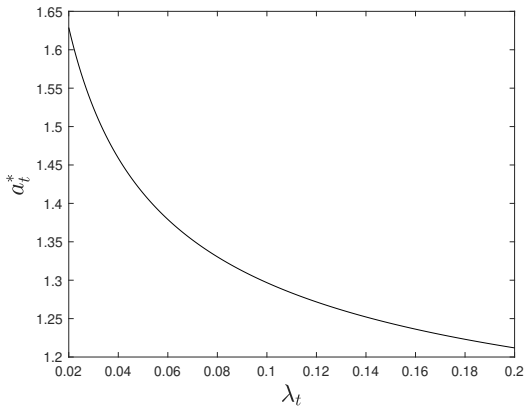

(a) Optimal a_t as function of λ_t.

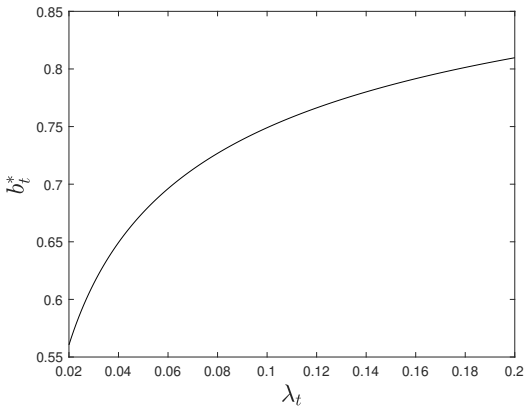

(b) Optimal b_t as function of λ_t.

made). However we are able to obtain exact solutions for the value function and the consumption-to-wealth ratio without making restrictive assumptions like $EIS = 1$, and the consumption-to-wealth ratio is what we need for assessing the SCC. We will now sketch our approach.

Duffie and Epstein (1992a) derive that the stochastic discount factor (or pricing kernel) with stochastic differential utility equals $\pi_t = \exp\Big\{\int_0^t f_V(C_s, V_s)ds\Big\} f_C(C_t, V_t)$. However, the stochastic discount factor has to be adjusted for the ambiguity aversion preferences. Chen and Epstein (2002) show that the stochastic discount factor in the ambiguity setting should be multiplied by the Radon-Nikodym derivative $\xi_t^{a^*,b^*}$ of the measure corresponding to the optimal a^* and b^*. $\xi_t^{a,b}$ is defined in (2.36). When calculating the stochastic discount factor, we obtain an expression that depends on the unknown function $g(X_t)$. But by substituting the HJB-equation into the stochastic discount factor we obtain an expression that only depends on known parameters.

As an intermediate step it is helpful to introduce the concept of consumption strips. A consumption strip is an asset that pays a unit of aggregate consumption C_s at time time $s > t$. Call its price at time t: $H(C_t, X_t, u)$, where u denotes the time to maturity; $u = s - t$. The price of a consumption strip paying out at time $s > t$ equals:

$$\begin{aligned} H_t &= H(C_t, X_t, u) \\ &= E_t\Big[\frac{\pi_s}{\pi_t} C_s\Big] = \exp\Big\{-\int_t^{t+u} CDR_s ds\Big\} C_t. \end{aligned} \tag{2.18}$$

We will refer to CDR_t as the consumption discount rate. We can use the fact that every asset multiplied by the stochastic discount factor must be a martingale to calculate the value of such an asset.

Furthermore, we can define a stock S_t that gives a claim to the Lucas-tree and therefore it pays a continuous stream of dividends C_t. The value of such a stock then obviously

becomes:

$$S_t = \int_0^\infty H(C_t, X_t, u)du. \tag{2.19}$$

In equilibrium aggregate wealth must be equal to the value of the stock. The state-dependent consumption-wealth ratio therefore equals:

$$k(X_t) = \frac{C_t}{S_t} = \frac{C_t}{\int_0^\infty H(C_t, X_t, u)du} = \left(\int_0^\infty \exp\Big\{ - \int_t^{t+u} CDR_s ds \Big\} du \right)^{-1}. \tag{2.20}$$

Using the expression for the consumption-wealth ratio, we can calculate the value function. At the optimum (see for example Munk (2015), Ch. 17), we have the envelope condition that $f_C = V_S$. Furthermore, we derived that $V(C_t, X_t) = \frac{g(X_t)C_t^{1-\gamma}}{1-\gamma}$. Using the chain rule we get:

$$V_S = V_C \frac{\partial C}{\partial S} = V_C k(X_t) = g(X_t) C_t^{-\gamma} k(X_t). \tag{2.21}$$

Also we have for the intertemporal aggregator:

$$f_C = \beta g(X_t)^{\frac{1/\epsilon - \gamma}{1-\gamma}} C_t^{-\gamma}. \tag{2.22}$$

Together this gives us:

$$g(X_t) = \Big(\frac{k(X_t)}{\beta} \Big)^{-\frac{1-\gamma}{1-1/\epsilon}}. \tag{2.23}$$

We can now derive an expression for the stochastic discount factor in terms of known parameters and using this stochastic discount factor, we can calculate the price of a consumption strip. We will analyse the consumption strips in detail in the next section. Integrating over the maturities of consumption strips with different maturities gives us the value of the stock, which in turn enables us to calculate the consumption-wealth ratio. Lastly, we can link $g(X_t)$ to the consumption-wealth ratio, which then allows us to derive an expression for the value function.

2.5 Asset prices and discounting

2.5.1 Asset market

Before going to the main part of this paper, the analysis of the social cost of carbon, we first calculate the risk-free rate and the risk premium as an input in the analysis of the SCC. Assume that the representative agent has the possibility to invest in two assets, namely a risk-free asset and a risky stock. The risk-free asset with price B_t pays a continuously compounded interest rate r_t. The stock pays continuous dividends at a rate C_t and has ex-dividend price S_t. We denote the cum-dividend stock price by S_t^d. Using equation (2.20) we can write $S_t = \frac{C_t}{k(X_t)}$. The assets have the following processes:

$$dB_t = r_t dt, \tag{2.24}$$

$$
\begin{aligned}
dS_t^d &= dS_t + C_t dt = \frac{1}{k(X_t)} dC_t - \frac{C_t}{k(X_t)^2} dk(X_t) + k(X_t) S_t dt \\
&= \Big(\mu - \frac{k_X(X_t)}{k(X_t)} \mu_X(X_t) + k(X_t)\Big) S_t dt + \sigma S_t dZ_t + J_t S_{t-} dN_t.
\end{aligned}
\tag{2.25}
$$

Chen and Epstein (2002) show that the stochastic discount factor with ambiguity and stochastic differential utility equals $\pi_t = \xi_t^{a^*,b^*} \exp\Big\{ \int_0^t f_V(C_s, V_s) ds \Big\} f_C(C_t, V_t)$. This allows us to derive an explicit stochastic differential equation for the stochastic discount factor. Using this stochastic discount factor, we can calculate the endogenous risk-free rate and the endogenous risk premium of the stock.[8] The interest rate r_t equals:

$$
\begin{aligned}
r_t = \beta + \frac{\mu}{\epsilon} - \Big(1 + \frac{1}{\epsilon}\Big)\frac{\gamma}{2}\sigma^2 - \Big(\gamma - \frac{1}{\epsilon}\Big) a_t^* \lambda_t \frac{-1}{b_t^* \eta + 1 - \gamma} \\
- a_t^* \lambda_t \Big(\frac{b_t^* \eta}{b_t^* \eta - \gamma} - 1 \Big).
\end{aligned}
\tag{2.26}
$$

The risk premium of the dividend paying stock (the expected excess return of that asset compared to investing in the risk-free asset) then equals:

$$
rp_t = \gamma \sigma^2 + a_t^* \lambda_t \Big(\frac{-1}{b_t^* \eta + 1} - \frac{b_t^* \eta}{b_t^* \eta + 1 - \gamma} + \frac{b_t^* \eta}{b_t^* \eta - \gamma} \Big). \tag{2.27}
$$

2.5.2 Consumption discount rate

As shown in appendix 2.F, the price of a consumption strip at time t that pays aggregate consumption C_s and has time to maturity $u = s - t$ equals:

$$
\begin{aligned}
H_t &= \exp\Big\{ - \int_t^{t+u} CDR_s ds \Big\} C_t, \quad \text{where} \\
CDR_t &= \underbrace{r_t}_{A} + \underbrace{rp_t}_{B} - \underbrace{\Big(\mu + a_t^* \lambda_t \frac{-1}{b_t^* \eta + 1}\Big)}_{C} \\
&= \beta + (1/\epsilon - 1)\Big(\mu - \frac{\gamma}{2}\sigma^2 + a_t^* \lambda_t \frac{-1}{b_t^* \eta + 1 - \gamma}\Big).
\end{aligned}
\tag{2.28}
$$

We discuss the consumption discount rate CDR_t in detail, since it is also an essential component of the social cost of carbon. The effective discount rate on a consumption strip consists of three terms, labeled A, B and C. Part A is the risk-free rate, which is used to discount a risk-free cashflow. The consumption strip is a risky asset and therefore the risk-free rate is increased with a risk-premium, part B. Lastly, the discount rate should be corrected for the growth of the aggregate consumption process. On average, consumption grows at a rate $\mu + a_t^* \lambda_t \frac{-1}{b_t^* \eta + 1}$. Note that the average growth rate is smaller than μ since climate disasters have a negative impact on consumption.

Consider first the most simple case without climate disasters and risk, i.e. the case with $(\sigma, \lambda_T) = (0, 0)$; then consumption strips are not risky anymore so the risk premium

[8] The derivations are given in appendix 2.F.

is zero. The interest rate reduces to the well-known Ramsey rule for the interest rate (Ramsey, 1928):

$$r_t = \beta + \frac{\mu}{\epsilon}, \tag{2.28a}$$

which implies a growth corrected discount rate $r_{n,t}$ for the case of $(\sigma, \lambda_T) = (0, 0)$ equal to:

$$r_{n,t} = \beta + (1/\epsilon - 1)\mu. \tag{2.28b}$$

Now add just diffusion risk: $\sigma > 0, \lambda_T = 0$. In a general equilibrium setting this will both affect the interest rate (due to a flight to safety) and the risk premium, in this case $\gamma\sigma^2$:

$$r_t = \beta + \frac{\mu}{\epsilon} - (1 + 1/\epsilon)\frac{\gamma}{2}\sigma^2, \tag{2.28c}$$

$$rp_t = \gamma\sigma^2. \tag{2.28d}$$

Adding the risk premium to the risk-free rate but correcting for the growth rate once again gives the growth-adjusted discount rate, now for $\sigma > 0, \lambda_T = 0$:

$$r_{n,t} = \beta + (1/\epsilon - 1)\Big(\mu - \frac{\gamma}{2}\sigma^2\Big). \tag{2.28e}$$

One would intuitively expect that adding risk to the consumption stream and the associated risk premium $\gamma\sigma^2$ to the interest rate would lead to a higher risk-adjusted discount rate. However, due to the flight to safety effect the risk-free rate decreases which in itself lowers the discount rate. Which of the two effects dominates depends on the elasticity of intertemporal substitution.

- When $\epsilon = 1$, both the interest rate and risk premium effect cancel out and the discount rate simply becomes β.
- When $\epsilon < 1$, the discount rate in the presence of risk ($\sigma > 0$) is actually smaller than the discount rate in the absence of risk ($\sigma = 0$). This implies that for $\epsilon < 1$ adding risk to the consumption stream increases the value of the consumption strip.
- When $\epsilon > 1$ we get the more intuitive outcome. In that case the risk premium effect dominates and the discount rate in the presence of risk is larger than the discount rate in the absence of risk.

Taking the impact of growth and risk both into account, and reasonably assuming $\mu - \frac{\gamma}{2}\sigma^2 > 0$, it becomes clear from (2.28) that the overall effect of a higher value for ϵ implies a lower growth adjusted discount rate.

Where ϵ determines the relative importance of the interest rate and risk premium effects, risk aversion γ determines the magnitude. A large risk aversion amplifies the effect of risk on the discount rate. When the agent is risk neutral ($\gamma = 0$), risk has no effect on the discount rate. The preceding discussion makes abundantly clear that using a General Equilibrium framework endogenizing the risk-free rate is essential in this context.

Assume now that additionally climate disasters also play a role: $\sigma > 0, \lambda_T > 0$; the discount rate of the consumption strip then becomes state dependent.

First assume that there is no ambiguity aversion ($\theta = 0$). Once again, adding climate disaster risk has an effect on both the interest rate and the risk premium. And similarly to the changes in the σ case, when $\epsilon < 1$ the interest rate effect dominates so that in that case adding disasters leads to a lower discount rate. But when $\epsilon > 1$, the risk premium effect dominates and adding climate disasters actually leads to higher discount rates.

Equation (2.28) indicates that the climate-risk related term in the discount rate for the reference case $a_t^* = 1, b_t^* = 1$ equals $\lambda_t \frac{-1}{\eta+1-\gamma}$. The term scales with the arrival rate λ_t: more frequent disasters have a larger effect on discount rates. The term $\frac{-1}{\eta+1-\gamma}$ can be interpreted as the certainty equivalent of the climate shock. When $\gamma = 0$, the certainty equivalent is equal to $E_t[J_t] = \frac{-1}{\eta+1}$.

Including ambiguity aversion leads to a larger worst case arrival rate: $a_t^* > 1 \Rightarrow a_t^* \lambda_t > \lambda_t$ and a more negative certainty equivalent term since $b_t^* < b_t$. Therefore we can unambiguously conclude that ambiguity aversion amplifies the effect of climate risk on discounting. And once again assuming a reasonable parameterization,[9] increasing ϵ still leads to a lower discount rate.

2.6 Social cost of carbon

Given the value function, we can calculate the Social cost of carbon (SCC), which we define as the marginal cost (in terms of reduced welfare) of increasing carbon emissions by one ton carbon scaled by the marginal welfare effect of one additional unit of consumption to obtain the social cost of carbon in terms of the price of time t consumption units (to which we refer as 'in dollar terms', for brevity's sake). With a single carbon box, the marginal cost of increasing carbon emissions by one unit is the derivative of the value function with respect to the carbon concentration M_t: $\frac{\partial V_t}{\partial M_t}$. However, with multiple carbon boxes, emitting one unit of carbon leads to an increase of ν_i units in box i, $i \in \{0, 1, 2, 3\}$. We slightly abuse notation and define $\frac{\partial}{\partial M_t} \equiv \nu_0 \frac{\partial}{\partial M_{0,t}} + \nu_1 \frac{\partial}{\partial M_{1,t}} + \nu_2 \frac{\partial}{\partial M_{2,t}} + \nu_3 \frac{\partial}{\partial M_{3,t}}$. Differentiation of the value function gives:

$$
\begin{aligned}
SCC_t &= -\frac{\partial V_t / \partial M_t}{f_C(C_t, V_t)} = -\frac{\frac{\partial}{\partial M_t} g(X_t)}{(1-\gamma) g(X_t) k(X_t)} C_t = -\frac{\frac{\partial}{\partial M_t} \left(\frac{k(X_t)}{\beta}\right)^{-\frac{1-\gamma}{1-1/\epsilon}}}{(1-\gamma)\left(\frac{k(X_t)}{\beta}\right)^{-\frac{1-\gamma}{1-1/\epsilon}} k(X_t)} C_t \\
&= -\frac{C_t}{1/\epsilon - 1} \frac{\frac{\partial}{\partial M_t} k(X_t)}{k(X_t)^2} = \frac{C_t}{1/\epsilon - 1} \frac{\partial}{\partial M_t} \int_t^\infty \exp\Big\{ - \int_t^{t+u} CDR_s ds \Big\} du \qquad (2.29) \\
&= C_t \int_t^\infty \underbrace{\exp\Big\{ - \int_t^{t+u} CDR_s ds \Big\}}_{\text{A}} \int_t^{t+u} \frac{\partial}{\partial M_t} \Big(\underbrace{a_s^* \lambda_s}_{B} \underbrace{\frac{1}{b_s^* \eta + 1 - \gamma}}_{C} \Big) ds du.
\end{aligned}
$$

We will first discuss the general formula and then the implications of different preferences.

Equation (2.29) shows that the social cost of carbon is proportional to C_t, the aggregate consumption level: when the current aggregate consumption level doubles, the SCC

[9] Specifically, we assume throughout the rest of the analysis that $\mu - \frac{\gamma}{2}\sigma^2 + a_t^* \lambda_t \frac{-1}{b_t^* \eta + 1 - \gamma} > 0 \ \ \forall t$.

doubles as well. For a given consumption level, the SCC depends on three terms, labeled A, B and C respectively. The social cost of carbon measures the marginal welfare loss of emitting an additional unit of carbon today. It is, in discrete time terms, the discounted sum of all future damages done by emitting one ton of carbon today. The outer integral indicates that all future marginal damages are included in the SCC. Future damages are discounted with the consumption discount rate (term A). The integral over the terms B and C captures the marginal damage for a given maturity u. What matters is the cumulative effect of a unit of carbon emissions at time t on the terms B and C over the time period t to $t+u$. Not only the impact of M_t on T_{t+u} plays a role, but the whole path of the temperature between t and $t+u$, since any climate damages that occur within this period have an effect on consumption at time $t+u$.

Without ambiguity aversion ($\theta = 0$) the marginal effect of M_t on terms B and C has a simple expression. Term C is independent of M_t and $\frac{\partial}{\partial M_t}\lambda_s = \lambda_T \frac{\partial}{\partial M_t} T_s$. If we now consider the marginal damages, λ_T captures the increase in the arrival rate when temperature increases by one degree. $\frac{\partial}{\partial M_t} T_s$ gives the marginal increase of temperature at time s due to an increase of atmospheric carbon concentration at time t. In the case without ambiguity, term C equals $\frac{1}{\eta+1-\gamma}$. Without risk aversion, this is equal to the expected value of a climate disaster.

Consider first the impact of γ and ϵ. When the agent is risk averse, term C can be interpreted as the certainty equivalent of the loss after a disaster. The certainty equivalent is clearly increasing in risk aversion. But risk aversion also has an effect on the discount rate CDR_t. As discussed before, increasing risk aversion increases the discount rate when $\epsilon > 1$. In this case the discounting effect works in opposite direction of the effect on the certainty equivalent: for $\epsilon > 1$ the impact of γ on the SCC is therefore ambiguous. But for $\epsilon < 1$ the two effects reinforce each other and the SCC is then an increasing function of γ. Consider next the impact of ϵ. The elasticity of intertemporal substitution ϵ only plays a role in the discount rate. When ϵ increases, the willingness to substitute over time increases which leads to lower discount rates. So a higher ϵ unambiguously leads to a higher SCC.

When ambiguity aversion is present, i.e. $\theta > 0$, we obtain that $a_s^* > 1$ (higher worst-case arrival rate) and $b_s^* < 1$ (higher worst-case jump size). The ambiguity aversion parameter θ does not directly show up in the formula, but its effect works via a_s^* and b_s^*. With $\theta > 0$ both the arrival rate of disasters in the expression is higher (so term B is larger) and the certainty equivalent, which with ambiguity aversion becomes $\frac{1}{b_s^*\eta+1-\gamma}$, is also higher. Through these two channels ambiguity aversion leads to a higher social cost of carbon. But similar to risk aversion, ambiguity aversion also affects discount rates and the sign again depends on the elasticity of intertemporal subtitution ϵ. When $\epsilon < 1$, ambiguity aversion additionally leads to a lower discount rate and thus an even higher SCC. When $\epsilon = 1$, the discount rate is simply β and ambiguity has no effect on the discount rate. Lastly, when $\epsilon > 1$, increasing θ leads to higher discount rates. Therefore increasing ambiguity aversion has two offsetting effects in this case. We will focus in the numerical section on the empirically supported case where $\epsilon > 1$.

Summarizing, when considering the effect of ambiguity aversion on the social cost of carbon we can identify two effects. First, including ambiguity aversion leads to a higher arrival rate and a larger certainty equivalent, which pushes the social cost of carbon up.

Table 2.1: *Parameters for the economic model.*

Par.	Description	Value
C_t	Initial consumption level (PPP, in trillion 2015 $)	83.07
λ_T	Arrival rate parameter	0.02 / 0.04
η	Disaster size parameter	30.25 / 61.5
$E[J]$	Expected disaster size	-0.032 / -0.016
γ	Risk aversion	5
θ	Ambiguity aversion	0.01
ϵ	Elasticity of substitution	1.5
CDR_0	Consumption discount rate	1.5%

We call this effect the direct effect of ambiguity aversion. Second, there is a more indirect general equilibrium effect through the impact of ambiguity aversion on discount rates. We call this the discounting effect. The discount rate that should be used to discount future climate disasters is the consumption discount rate, and when the elasticity of substitution is larger than 1, ambiguity aversion leads to a higher consumption discount rate. This is an intuitive result: if the representative agent is very ambiguity averse about climate disasters, he would rather like to consume today than to postpone consumption since the future consumption level is uncertain. Ambiguity aversion therefore increases the consumption discount rate and decreases the price of a future consumption strip. Thus for $\epsilon > 1$ it is ultimately a numerical issue which of the two effects will dominate. We will highlight both effects separately in the numerical section and show that for our calibration, the first effect dominates. In our numerical analysis the net impact is positive: more ambiguity aversion leads to a higher SCC. We turn to that numerical analysis in the next section.

2.7 Climate change and the social cost of carbon: numerical results

2.7.1 Calibration

Appendix 2.G gives the full details of the calibration of the climate model. Parameters for the growth rate of emissions and the initial level are chosen to match the baseline scenario of the DICE-2016 calibration (Nordhaus, 2017). The parameters of the carbon cycle and temperature model are taken from Mattauch et al. (2019). In addition, and different from Mattauch et al. (2019), we also include a base level of non-carbon related radiative forcing and calibrate it to match exogenous forcing in DICE-2016. Figure 2.4 shows the future path of the climate state variables using our emissions path and climate model. Under the business-as-usual scenario, emissions are projected to peak at the end of the century, and decline from then on. The surface temperature will then rise by almost 4 degrees in 2100.

The calibration of the economic parameters is given in table 2.1. Since we consider an exogenous endowment economy, output and consumption are the same thing in our model. That leaves the question open whether we should calibrate the endowment to output or

Figure 2.4: *Future path of climate variables.*

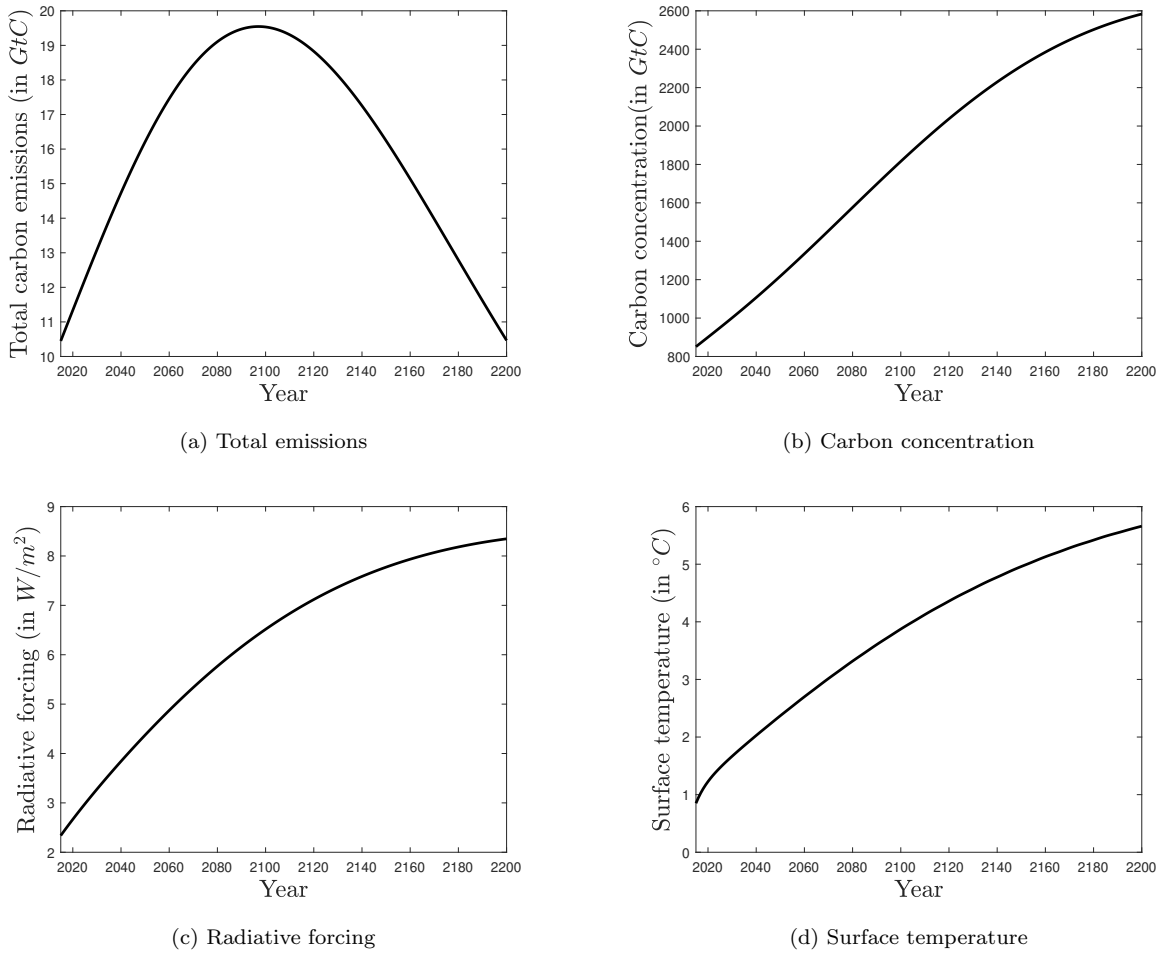

(a) Total emissions

(b) Carbon concentration

(c) Radiative forcing

(d) Surface temperature

to consumption data. The focus of the paper is on the social cost of carbon. What ultimately matters for the social cost of carbon is consumption, since utility depends on consumption and not on output. To make our results more comparable to other models, we therefore calibrate endowment to consumption data. The next choice to be made is whether one should aggregate output or consumption data using market exchange rates or using purchasing power parities (PPP). In line with the DICE-2016 model we use purchasing power parity exchange rates. Consumption data is not directly available in PPP. To obtain a proxy for world consumption in PPP we first obtain output data in PPP. Then we determine the world consumption ratio using market exchange rates. Our proxy for world consumption in PPP is then output in PPP multiplied by the world consumption ratio. Real world GDP (PPP) in 2015 equals 114.137 trillion 2015 $ (IMF World Economic Outlook October 2016). World consumption in 2015 using market exchange rates equals 55.167 (in trillion 2010 $), while world GDP using market exchange rates equals 75.803 (in trillion 2010 $) (Worldbank Database). This yields a consumption-output ratio of 72.78%. Applying this ratio to World GDP (PPP) then gives 83.065 (in trillion 2015 $) for aggregate consumption in PPP terms.

The next step is to calibrate the climate disaster distribution, and in particular the parameters λ_T and η. Our setup does allow for an arrival rate that is convex in temperature, but we do not consider this extension since it would give another free parameter to calibrate. Karydas and Xepapadeas (2019) also consider climate disasters and assume, based on natural disaster data, that for every degree warming the arrival rate increases by 6%. The disaster size is calibrated to 1.6%. This implies that the expected growth loss due to climate change would be $6\% \times 1.6\% = 0.096\%$ per degree global warming. Nordhaus (2017) models the economic impact of climate change as the percentage loss of output as a function of temperature (level impact). Hambel et al. (2021) consider both a level and a growth impact of climate damages. They find that a loss of 0.026% per degree warming gives the same GDP loss in the year 2100 as the level impact of Nordhaus (2017). Setting the disaster size to 1.6% and calibrating λ_T such that on average climate disasters lead to a loss of 0.026% gives $\lambda_T = 1.63\%$, much lower than the arrival rate assumed in Karydas and Xepapadeas (2019). The calibration of Karydas and Xepapadeas (2019) obviously gets much higher expected damages than the calibration of Nordhaus (2014a) yields.

We decide to choose $\lambda_T = 4\%$, which is in between these two calibrations and set $\eta = 61.5$ which yields $E_t[J_t] = -1.6\%$, in line with Karydas and Xepapadeas (2019). Additionally, we consider a variant with less frequent but on average larger disasters: $\lambda_T = 2\%$, and a disaster size parameter $\eta = 30.25$ which gives $E_t[J_t] = -3.2\%$. While both calibrations have on average the same impact, their impact on risk premia is very different.

We now turn to the calibration of risk aversion and ambiguity aversion. We set risk aversion equal to 5. This level of risk aversion can be seen as conservative if we compare it to common values in the asset pricing literature.[10]

The level of ambiguity aversion is harder to calibrate. To get a feeling for reasonable values of ambiguity aversion, we use the concept of detection error probabilities. The ambiguity aversion parameter θ pins down the arrival rate and the expected jump size in the worst-case scenario. A higher θ leads to a higher worst-case arrival rate and a more negative worst-case expected jump size. The detection error probability is the probability of choosing the wrong model (so choosing the reference model $\mathbb{P}$ when the worst-case $\mathbb{Q}$ is true and vice-versa). When θ is higher, the two models are more different and the probability of making a mistake is therefore lower. When the detection error probability is close to 50%, the two models are very similar. This is an indication of a low ambiguity aversion parameter. On the other hand, when the detection error probability is close to 0, it is easy to distinguish the worst-case model from the reference model. This indicates that the worst-case model is extreme and the ambiguity aversion parameter very high.

We calculate the detection error probability assuming that the consumption process can be observed over a period of 100 years. The ambiguity aversion parameter θ is varied between 0 and 0.02. The results are given in figure 2.5. Detection error probabilities are decreasing in θ and are higher for a lower λ_T. This is intuitive, since a lower λ_T implies that there are less disasters over the observed time period and the probability of choosing the wrong model is therefore larger. We choose to set $\theta = 0.01$ in the base calibration,

[10] A coefficient of relative risk aversion between 5 and 10 is common in the asset pricing literature according to Cochrane (2009).

Figure 2.5: *Detection error probabilities as a function of θ.*

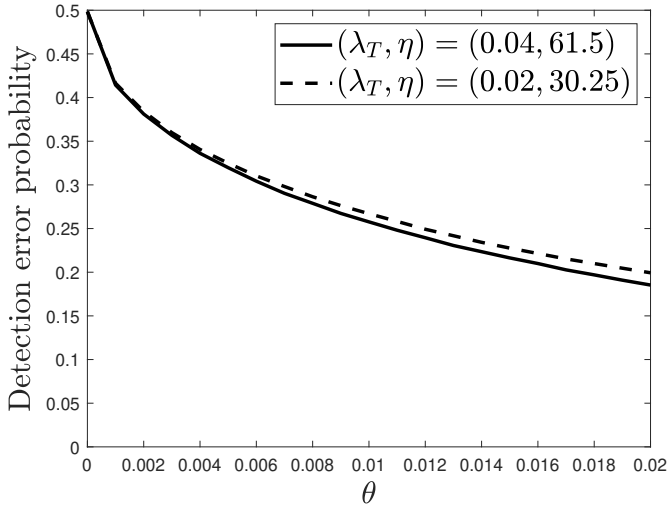

which gives a detection error probability of 26.7% for $(\lambda_T, \eta) = (0.02, 30.25)$ and 25.8% for $(\lambda_T, \eta) = (0.04, 61.5)$ (cf figure 2.5). This level of ambiguity aversion balances the trade-off between wanting to make a robust decision, but not taking into account too extreme models. The detection error probabilities for $\theta = 0.01$ are sufficiently far away from 50%, which implies the two models are not too close to each other. On the other hand, the detection error probabilities are also not close to 0, which would indicate an extreme amount of ambiguity aversion. However, since this parameter remains hard to calibrate we do vary θ in robustness checks. Figure 2.6 shows the resulting arrival rate and expected disaster size with ambiguity aversion ($\theta = 0.01$) and without ambiguity aversion ($\theta = 0$) in both cases.

The parameters that still have to be calibrated affect the social cost of carbon only indirectly, via the discount rate. Equation (2.28) shows that one can separate the expression for the consumption discount rate (the relevant discount rate for the social cost of carbon) CDR_t in a time-independent part CDR_0 and a part that does depend on time:

$$\begin{aligned} CDR_t &= CDR_0 + (1/\epsilon - 1)a_t^* \lambda_t \frac{-1}{b_t^* \eta + 1 - \gamma}, \\ CDR_0 &= \beta + (1/\epsilon - 1)\Big(\mu - \frac{\gamma}{2}\sigma^2\Big). \end{aligned} \tag{2.30}$$

CDR_0 is the consumption discount rate in the absence of climate disasters. First, the value of the elasticity of intertemporal substitution ϵ determines whether additional risk increases or decreases the discount rate. Generally, there is strong empirical evidence of an EIS larger than one (Van Binsbergen, Fernández-Villaverde, Koijen, & Rubio-Ramírez, 2012; Vissing-Jørgensen & Attanasio, 2003). When $\epsilon > 1$, we are in the realistic situation that additional risk decreases asset prices. We choose $\epsilon = 1.5$, which is a common value in the literature on Epstein-Zin preferences. The growth rate μ, the volatility σ and the pure rate of time preference β only affect the social cost of carbon via CDR_0. The calibration of β has been widely discussed in the climate change literature. Additionally, we could

Figure 2.6: *Arrival rate and expected disaster size over time with and without ambiguity aversion.*

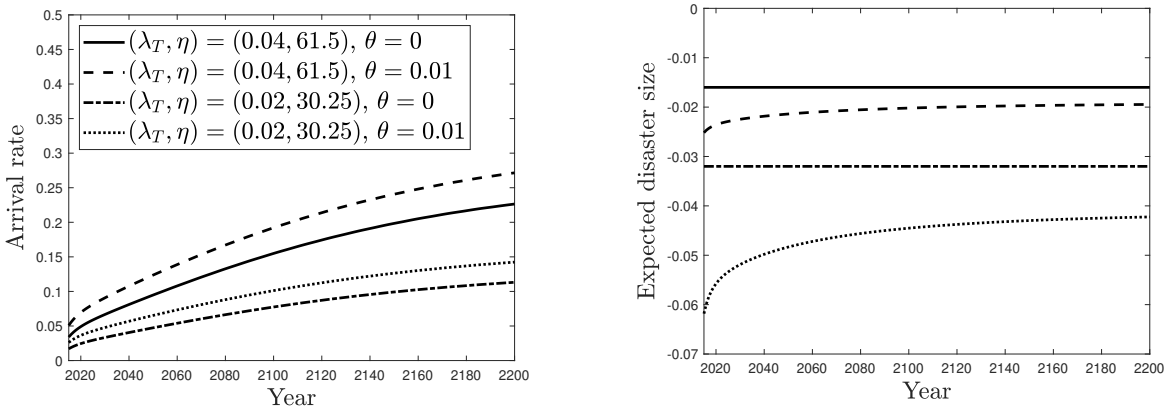

(a) Arrival rate λ_t^*

(b) Expected disaster size $\frac{-1}{b_t^* \eta + 1}$

calibrate σ from observed consumption volatility. However, as Mehra and Prescott (1985) point out, the model in that case would generate a way too low risk premium (the equity premium puzzle). A way to circumvent this is to calibrate σ to the volatility of stock prices, but this solution is also not very satisfactory. There have been several (partial) solutions proposed to the equity premium puzzle, for example including economic disaster risk. Solving the equity premium puzzle goes beyond the scope of this paper. Since both β and σ only affect the SCC via CDR_0, we choose to directly calibrate the consumption discount rate in the absence of climate risk. In our base calibration, we choose $CDR_0 = 1.5\%$, but we show our results for values of CDR_0 between 0.5% and 2.5%. The parameter combinations $(\beta, \mu, \sigma) = (2.25\%, 2.5\%, 3\%)$ and $(\beta, \mu, \sigma) = (1.5\%, 2.5\%, 10\%)$ for example yield a consumption discount rate $CDR_0 = 1.5\%$. Note that the actual consumption discount rate CDR_t is higher because of the impact of climate disasters on discounting.

2.7.2 Social cost of carbon

Ambiguity aversion and the SCC

Figure 2.7 shows for each of the two sets of assumptions on the disaster risk parameters the social cost of carbon for different values of θ. Ambiguity aversion clearly leads to a substantially higher social cost of carbon. For the $(\lambda_T, \eta) = (0.04, 61.5)$ case, the SCC is 28% higher with $\theta = 0.01$ compared to the case without ambiguity aversion. The relative increase is even larger when we consider the $(\lambda_T, \eta) = (0.02, 30.25)$ case: the SCC is then 36% higher with ambiguity aversion. The intuition behind this difference is that the relative entropy between the reference model and the worst-case model is increasing in λ_t. When the arrival rate is smaller, disasters happen less frequently and the two probability distributions are harder to distinguish. With the same ambiguity aversion level θ, this then implies that a_t^* is larger for $\lambda_T = 0.02$ compared to the a_t^* for $\lambda_T = 0.04$ and also that b_t^* is lower for $\lambda_T = 0.02$ compared to $\lambda_T = 0.04$. Therefore the relative increase in the SCC due to ambiguity aversion is larger with $\lambda_T = 0.02$ than it is with $\lambda_T = 0.04$.

Figure 2.7: *Social cost of carbon as a function of θ.*

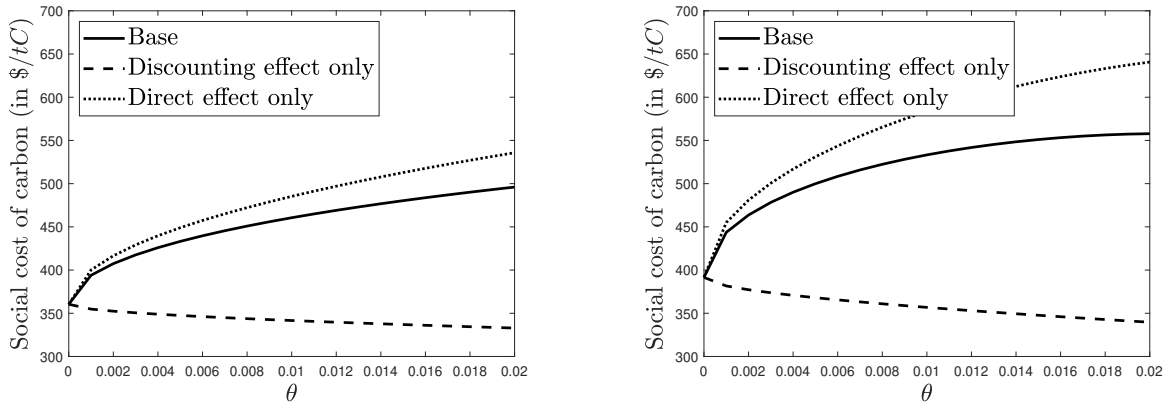

(a) $(\lambda_T, \eta) = (0.04, 61.5)$ (b) $(\lambda_T, \eta) = (0.02, 30.25)$

This figure shows the social cost of carbon as a function of the ambiguity aversion parameter θ. The total effect of ambiguity aversion on the SCC is given by the solid line *(base)*. We additionally distinguish two special cases. In the *discounting effect only* case (dashed line) we assume that increasing θ does lead to an increase in the discount rate, but does not change the arrival rate and the certainty equivalent in the SCC formula. In the *direct effect only* case (dotted line) we look at the opposite case, where increasing θ is assumed to have an effect on the arrival rate and the certainty equivalent, but not on the consumption discount rate CDR_t.

From equation (2.30) it is clear that ambiguity aversion does not only affect the arrival rate and certainty equivalent of climate disasters, but also the discount rate: in our calibration with $\epsilon = 1.5$, more ambiguity aversion leads to a higher discount rate. We disentangle the two effects on the SCC by first considering the *discounting only* effect, in which we assume ambiguity aversion only affects the discount rate CDR_t, but we leave the arrival rate and the certainty equivalent in the SCC formula unaffected by ambiguity aversion (the line with label *discounting only* in figure 2.7). And second we consider the opposite case, where we leave the consumption discount rate CDR_t unchanged, but we do take into account the direct effect of ambiguity aversion on the arrival rate and certainty equivalent of the climate disasters, with the label *direct only* in figure 2.7. The two effects are combined in the base case where both the direct effect and the impact via the discount rate are incorporated (labeled *base* in figure 2.7). Figure 2.7 clearly indicates that ambiguity aversion increases the discount rate and therefore the SCC is decreasing in θ when only the discounting effect of ambiguity aversion is considered. This also implies that when we look at the direct only effect, the SCC is above the base case SCC since the negative impact of discounting is left out. Overall we can conclude that ambiguity aversion does indeed lead to a higher discount rate, but that the direct effect on the SCC dominates and that ambiguity aversion therefore leads to a higher social cost of carbon, and in our calibration substantially so.

The elasticity of intertemporal substitution ϵ and the SCC

The sign of the discounting effect depends on the choice of ϵ. When $\epsilon < 1$, additional risk, more risk aversion or more ambiguity aversion would lower discount rates and both the discounting effect and the direct effect of ambiguity aversion would have the same sign. However, this would lead to counter-intuitive effects. For example $\epsilon < 1$ implies that the

Table 2.2: *Social cost of carbon as function of risk aversion and ambiguity aversion.*

Social Cost of Carbon	$(\lambda_T, \eta) = (0.04, 61.5)$	$(\lambda_T, \eta) = (0.02, 30.25)$
$\gamma = 0$, $\theta = 0$	363	363
$\gamma = 5$, $\theta = 0$	360	392
$\gamma = 5$, $\theta = 0.01$	461	533

price of a consumption strip increases when the volatility of consumption increases. For $\epsilon = 1$, the consumption discount rate CDR_t simply equals β and risk, risk aversion and ambiguity aversion do not affect discount rates.

Risk aversion, ambiguity aversion and the SCC

In table 2.2 we compare the effect of risk aversion and of ambiguity aversion. By definition, the SCC is the same for both calibrations when risk aversion γ and ambiguity aversion θ are both 0. In that case the expected value of both calibrations is the same and since risk is then not priced, the SCC is the same for both calibrations. Introducing risk aversion has a negligible effect on the SCC for the frequent disasters with low disaster size: for $(\lambda_T, \eta) = (0.04, 62.5)$ the direct impact of risk aversion on the certainty equivalent is small and is canceled out by the *discounting* effect: for this configuration the SCC is even slightly lower than what it is without risk aversion. This changes when damages are more infrequent but larger. In the alternative calibration with $(\lambda_T, \eta) = (0.02, 30.25)$, risk aversion does increase the social cost of carbon from 363\$ to 392\$. This increase is still modest compared to the effect of ambiguity aversion. In both cases, introducing ambiguity aversion leads to a significantly higher value of the social cost of carbon. The table shows the very different implications that risk aversion and ambiguity aversion have for the valuation of climate risk.

Discount rates and the SCC

Figure 2.8 shows the dependence of the SCC on the time-independent part of the consumption discount rate CDR_0, the core discount rate. Note that the actual discount rate that is used to discount future damages (CDR_t) is higher than CDR_0 due to the effect of climate disasters itself on discounting. When core discount rates are close to zero, the social cost of carbon becomes very high. With $CDR_0 = 0.5\%$, the SCC is even above 2000\$ in both cases, around four times higher than in the base calibration. On the other hand, setting $CDR_0 = 2.5\%$ gives a social cost of carbon that is less than half the value in the base calibration. This figure highlights the importance of the discount rate when analyzing climate change and in particular its impact on the social cost of carbon.

2.8 Conclusion

Climate change will beyond reasonable doubt have a large impact on economic growth in the future. However, because of the complex nature of the problem and the lack of data, it is not possible to accurately estimate the timing and extent of its impact. But one thing we do know is that potentially large and irreversible consequences are likely to take place unless mitigating policies are implemented. But these changes will happen

Figure 2.8: *Social cost of carbon as a function of* CDR_0.

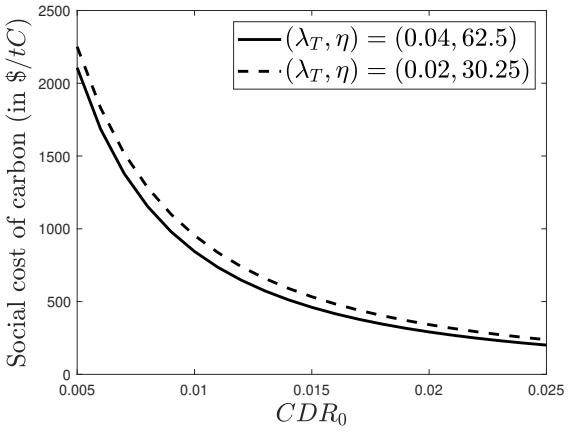

far into the future, while mitigating policies are (or should be) under consideration right now. That discrepancy puts the discussion on discounting at the center of the debate about the social cost of carbon and what we should do about climate change: to compare uncertain future damages with costs today, those future damages need to be discounted back towards today. The debate in the literature has largely zeroed in on the rate of time preference; the problem there is that to be consistent with capital market data, discount rates must be relatively high which in turn does not leave much once climate change consequences a century out are discounted back towards today (cf Weitzman (2007) for a very lucid overview of this debate). In this paper we squarely focus on the discounting question, but we take a different approach. Rather than discussing numerical values of certain parameters, we explore alternative specifications of preferences, and show the implications for the social cost of carbon.

We focus on the effect of Epstein-Zin recursive preferences on outcomes of the model, on the impact of unmeasurable risk (ambiguity) and the interaction between those two. Both breaking the link between γ and the EIS (by introducing stochastic differential utility, the continuous time implementation of Epstein-Zin preferences) and introducing ambiguity aversion are conceptually relevant in the climate change setting. The first extension is relevant because climate change problems have a very long horizon and therefore the elasticity of intertemporal substitution (EIS) unavoidably plays an important role. Arbitrarily restricting its value to $1/\gamma$ is then surely unsatisfactory. Second, conceptually ambiguity aversion is a logical extension, since we have no accurate estimation of climate damages nor in particular of their probability density function in the future. The assumption of unmeasurable risk ('Knightian uncertainty') then is a natural framework to use. Finally we highlight the sometimes complicated interactions between ambiguity aversion and intertemporal substitution elasticities for the value of the social cost of carbon.

To do all this we set up an analytic IAM by extending a disaster risk model with a climate change model and a temperature dependent arrival rate. Furthermore, we model climate risk as tail risk instead of assuming that temperature increases generate a certain amount of damage every year. The model is transparent because we manage to derive closed form solutions for the social cost of carbon. Where stochastic numerical IAMs

can take hours to be solved, solving our model only requires numerical integration and is therefore solved within seconds.

Our base calibration generates a substantial social cost of carbon which is between 461$ and 533$ per ton of carbon. This is both much higher than for example the estimate of 114$ that is obtained using the DICE-2016R model (Nordhaus, 2017), and also much higher than current market prices in for example the European Emissions Trading System.[11] Moreover we use our model to highlight how ambiguity aversion changes the social cost of carbon.

Analysing the effect of ambiguity aversion on the SCC is a complicated exercise since multiple potentially offsetting effects play a role: ambiguity aversion has both an effect on the arrival rate and certainty equivalent of disasters for given discount rates (more ambiguity aversion leads to a higher certainty equivalent) and on the discounting component. The effect of ambiguity aversion on discounting depends on the EIS. When $EIS < 1$, increasing ambiguity aversion leads to a smaller effective discount rate on climate damages. For the more interesting (because empirically supported) case $EIS > 1$, the opposite is true, in which case increasing ambiguity aversion has two offsetting effects on the SCC. However, we show that the direct effect dominates and therefore that the presence of ambiguity aversion leads to a (substantially) higher social cost of carbon.

Lastly, we also show the importance of the consumption discount rate on the social cost of carbon. It is of course well known that the social cost of carbon is very sensitive to changes in the discount rate. However, we stress that analyzing the discount rate impact of climate change involves more than a discussion of the pure rate of time preference on the discount rate; a low discount rate can also be caused by a high elasticity of intertemporal substitution, and additionally the discount rate depends in elaborate ways on the growth rate of the economy, volatility, risk aversion, climate disaster risk and ambiguity aversion. Disentangling these various effects and their interactions is the key contribution of this paper. One major theme emerges: proper risk pricing and incorporating ambiguity aversion leads to much higher estimates of the social cost of carbon. These findings are surely of more than just academic interest.

[11] These prices are usually quoted per ton of carbon dioxide, which involves a conversion factor of 3.67.

2.A Overview of methods to model ambiguity

There are several different approaches that are commonly used in the literature to model ambiguity about parameters. A widely used approach in the static setting is the maxmin approach of Gilboa and Schmeidler (1989). Assume the agent does not know the distribution of a random variable. The idea is to first specify a set of reasonable probability measures $\mathbb{Q}$. The agent is ambiguity averse and given this set of measures he considers the worst case measure. Utility is then of the form $V_t = \min_{\mathbb{Q}\in\mathcal{P}} E_{\mathbb{Q}}[U(C_t)]$ for some utility specification $U(.)$.

It is not straightforward to extend the Gilboa-Schmeidler maxmin preferences to a dynamic setting. We will discuss two approaches that have been proposed by Chen and Epstein (2002) and by Hansen, Sargent, Turmuhambetova, and Williams (2001) in the setting of our model.

Consider the agent's problem. In the setting without ambiguity, the value function is given by:

$$V_t = E_t\Big[\int_t^\infty f(C_s, V_s)ds\Big]. \tag{2.31}$$

However, in the model with ambiguity the agent takes into account the fact that he is not certain about the true value of the arrival rate λ_t and the jump size parameter η.

Hansen et al. (2001) propose two approaches to model ambiguity: the *multiplier* approach and the *constraint* approach. We first consider the *multiplier* approach. The 'best estimate' model or reference model is the agent's most reliable model with measure $\mathbb{P}$, but he also takes into account other, alternative models. The alternative models have measure $\mathbb{Q}^{a,b}$, the jump arrival rate becomes $\lambda_t^{\mathbb{Q}} = a_t\lambda_t$ and the jump size parameter becomes $\eta_t^{\mathbb{Q}} = b_t\eta$. Deviating from the reference model is penalized since the agent does not choose the 'best estimate' model. The size of the penalty is proportional to $d(a_t, b_t)$, which represents the distance between the alternative model and the reference model. An alternative model that has a large distance to the reference model is considered less likely to be true and therefore using it receives a larger penalty. The distance function should satisfy $d(a_t, b_t) \geq 0\ \forall(a_t, b_t)$ and $d(1, 1) = 0$. Therefore using the reference model carries a zero penalty. The penalty is scaled by θ, which is the ambiguity aversion parameter. This parameter controls the importance of the penalty term. Then the agent solves the following problem:

$$V_t = \min_{\{a_s,b_s\}_{s\geq t}} E_t^{\mathbb{Q}}\Big[\int_t^\infty \Big(f(C_s, V_s) + e^{-\beta(s-t)}\theta d(a_s, b_s)\Big)ds\Big]. \tag{2.32}$$

$E_t^{\mathbb{Q}}$ denotes the expectation under the alternative model with parameters $\lambda_t^{\mathbb{Q}}$ and $\eta_t^{\mathbb{Q}}$. The expected utility of consumption is lower for high a_t and low b_t. We see that the agent faces a trade-off between how likely a combination of (a_s, b_s) is in terms of distance to the reference model and how bad it is in terms of expected utility. This trade-off results in optimal values of a_s and b_s.

The *constraint* approach is closely related to the *multiplier* approach. Instead of adding a penalty function, the agent can put a constraint on the distance function $d(a_t, b_t)$.

Then the problem becomes:

$$\begin{aligned} V_t &= \min_{\{a_s,b_s\}_{s\geq t}} E_t^{\mathbb{Q}}\Big[\int_t^\infty f(C_s,V_s)ds\Big], \\ &\text{s.t. } \int_t^\infty e^{-\beta(s-t)}d(a_s,b_s)ds \leq \phi. \end{aligned} \tag{2.33}$$

So in this approach, ϕ to controls the size of the set of alternative models that seem reasonable to him. ϕ can again be seen as an ambiguity aversion parameter. A high ϕ implies a large set of priors and therefore corresponds to high ambiguity aversion. Given the constraint the worst-case model is chosen. This approach is very similar to the penalty approach and the two problems are related via Lagrangian optimization where θ can be seen as the Lagrange multiplier.

Hansen and Sargent (2001) consider how the penalty and constraint approaches are related. They show that when the consumption process follows a pure geometric Brownian motion (i.e. no jumps), there exists a ϕ for the constraint approach and a θ for the multiplier approach such that both problems yield the same optimal outcome. The constraint approach is directly motivated from the Gilboa-Schmeidler maxmin utility. Since the multiplier approach is weakly related to the constraint approach, these approaches are indirectly also motivated by the static maxmin utility specification. Furthermore, the multiplier utility is axiomatized by Strzalecki (2011).

A disadvantage of both these approaches is that utility is not homothetic. Maenhout (2004) proposes to use a state-dependent Lagrange-multiplier $\theta(V_t)$ in the framework of the multiplier approach to obtain homothetic utility. This approach is also adopted by Liu et al. (2004). However, by assuming that the ambiguity aversion parameter θ can be state dependent, the relation with the constraint preferences is lost. Pathak (2002) extensively discusses this issue. He argues that the main motivation of the multiplier approach by Hansen et al. (2001) is through the constraint approach. But with the state-dependent ambiguity aversion parameter this new utility specification cannot be seen anymore as a dynamic extension of the Gilboa-Schmeidler utility. Furthermore, the axiomatic foundation is not valid anymore. Pathak (2002) proposes an alternative method to model ambiguity: *recursive multiple priors utility* developed in continuous time by Chen and Epstein (2002).

We follow the advise of Pathak (2002) and in contrast to Liu et al. (2004) we choose to use the approach of Chen and Epstein (2002). The approach is closely related to the constraint approach of Hansen et al. (2001), but does preserve the homotheticity of the preferences. Consider the following problem:

$$\begin{aligned} V_t &= \min_{\{a_s,b_s\}_{s\geq t}} E_t^{\mathbb{Q}}\Big[\int_t^\infty f(C_s,V_s)ds\Big], \\ &\text{s.t. } d(a_t,b_t) \leq \theta \quad \forall t. \end{aligned} \tag{2.34}$$

The main difference with the constraint approach of Hansen et al. (2001) is that not the lifetime distance between the reference measure and the alternative measure is bounded, but at every time period t the distance between the measures is bounded. This approach leads to more tractable solutions. The recursive multiple priors utility is axiomatized by Epstein and Schneider (2003).

Lastly we will briefly discuss the *smooth ambiguity* model, since it is often used in the literature as well. Assume that the agent does not know the true values of λ and η. In this approach the agent first constructs a probability distribution that reflects his beliefs on λ and η. Define $p(x,y) = P(\lambda = x, \eta = y)$. To incorporate ambiguity aversion, he then transforms this distribution to put more weight on the events that give him low utility and less weight on the events that give high utility. This results in the following problem:

$$V_t = \int_0^\infty \int_0^\infty \Big(p(x,y)\phi\Big(E_t\Big[\int_t^\infty f(C_s,V_s)ds\Big|\lambda = x, \eta = y\Big]\Big)\Big)dxdy. \tag{2.35}$$

Here the function ϕ controls the ambiguity aversion of the agent. When ϕ is a concave function, the agent is ambiguity averse. This approach was introduced by Klibanoff et al. (2005). This may be a matter of taste, but we think that the assumption of probabilities attached to the different priors is in fact at variance with the basic assumption that ambiguity is about unmeasurable processes, i.e. we cannot map events to probability densities, or in this case priors to model probabilities. And since the recursive multiple priors utility is intuitive and leads to tractable results, we chose not to move in the direction of the smooth ambiguity model.

2.B Derivation of relative entropy

For each $a = (a_s)_{s\geq t}$ and $b = (b_s)_{s\geq t}$ we define the measure $\mathbb{Q}^{a,b}$ which is equivalent to $\mathbb{P}$ and has Radon-Nikodym derivative $\frac{d\mathbb{Q}^{a,b}}{d\mathbb{P}}|_{\mathcal{F}_t} = \xi_t^{a,b}$ where $\xi_t^{a,b}$ follows:

$$d\xi_t^{a,b} = (\lambda_t - \lambda_t^{\mathbb{Q}})\xi_t^{a,b}dt + \Big(\frac{\lambda_t^{\mathbb{Q}} f^{\mathbb{Q}}(J_t)}{\lambda_t f(J_t)} - 1\Big)\xi_{t-}^{a,b}dN_t. \tag{2.36}$$

and $\xi_0^{a,b} = 1$. $\xi_t^{a,b}$ is chosen such that the jump distribution under $\mathbb{Q}^{a,b}$ has arrival rate $\lambda_t^{\mathbb{Q}}$ and such that the probability density function of the jump distribution equals $f^{\mathbb{Q}}(x)$. Specifically we assume that $\lambda_t^{\mathbb{Q}} = a_t\lambda_t$ and $\eta_t^{\mathbb{Q}} = b_t\eta$. We can calculate in this case the fraction of the two probability distributions: $\frac{f^{\mathbb{Q}}(x)}{f(x)} = \frac{\eta_t^{\mathbb{Q}}(1+x)^{\eta_t^{\mathbb{Q}}-1}}{\eta(1+x)^{\eta-1}} = b_t(1+x)^{(b_t-1)\eta}$. Substituting this into (2.36) gives:

$$d\xi_t^{a,b} = (1-a_t)\lambda_t\xi_t^{a,b}dt + \Big(a_tb_t(1+J_t)^{(b_t-1)\eta} - 1\Big)\xi_{t-}^{a,b}dN_t. \tag{2.37}$$

The Radon-Nikodym derivative $\xi_t^{a,b}$ that we have specified is the ratio between the alternative measure $\mathbb{Q}^{a,b}$ and the reference measure $\mathbb{P}$. We can use it to determine the relative entropy between the two measures. The relative entropy between $\mathbb{Q}^{a,b}$ and $\mathbb{P}$ over time unit Δ is defined as $E_t^{\mathbb{Q}}\Big[\log(\frac{\xi_{t+\Delta}^{a,b}}{\xi_t^{a,b}})\Big]$. Here $E_t^{\mathbb{Q}}$ denotes the expectation with respect to the alternative measure $\mathbb{Q}^{a,b}$. Then divide by Δ and let $\Delta \to 0$ to obtain the instantaneous relative entropy: $RE(a_t,b_t) = \lim_{\Delta\to 0}\frac{1}{\Delta}E_t^{\mathbb{Q}}\Big[\log\Big(\frac{\xi_{t+\Delta}^{a,b}}{\xi_t^{a,b}}\Big)\Big]$.

Applying Itô's lemma for jump processes to $\xi_t^{a,b}$, we obtain the following dynamics for $\log(\xi_t^{a,b})$:

$$d\log(\xi_t^{a,b}) = (1-a_t)\lambda_t dt + \Big(\log(a_tb_t) + (b_t-1)\eta\log(1+J_t)\Big)dN_t. \tag{2.38}$$

Using integration by parts we can calculate that $E_t^{\mathbb{Q}}[\log(1+J_t)] = -\frac{1}{\eta_t^{\mathbb{Q}}}$. Therefore the (instantaneous) relative entropy at time t equals:

$$\begin{aligned} RE(a_t,b_t) = \lim_{\Delta\to 0}\frac{1}{\Delta}E_t^{\mathbb{Q}}\Big[\log\Big(\frac{\xi_{t+\Delta}^{a,b}}{\xi_t^{a,b}}\Big)\Big] = \\ (1-a_t)\lambda_t + a_t\lambda_t\Big(\log(a_tb_t)+\frac{1}{b_t}-1\Big). \end{aligned} \tag{2.39}$$

2.C Calculating the detection error probability

After observing the process of consumption over a period N years, what is the probability of choosing the wrong model? Let us start with the case that the reference model $\mathbb{P}$ is the true model and the agent considers the alternative model $\mathbb{Q}^{a,b}$. Note that the Radon-Nikodym derivative informs us about the likelihood ratio of both models. When this derivative is larger than one after N years, the worst-case model $\mathbb{Q}^{a,b}$ is the most likely and the agent will choose the wrong model. The probability of making this error is equal to (see for example Maenhout (2006)):

$$P\Big(\xi_N^{a,b}>1|\mathbb{P}\Big) = P\Big(\log(\xi_N^{a,b})>0|\mathbb{P}\Big). \tag{2.40}$$

We calculate this probability by simulating the process of $\log(\xi_t^{a,b})$ forward. Simulation is done via a standard Euler method. Similarly, we can define the opposite mistake where the alternative model is actually true and the agent chooses the reference model. We now define the inverse Radon-Nikodym derivative: $\frac{d\mathbb{P}}{d\mathbb{Q}^{a,b}}|_{\mathcal{F}_t} = \tilde{\xi}_t^{\,a,b}$ where $\tilde{\xi}_t^{\,a,b}$ follows:

$$d\tilde{\xi}_t^{\,a,b} = (a_t-1)\lambda_t\tilde{\xi}_t^{\,a,b}dt + \Big(\frac{1}{a_tb_t}(1+J_t)^{(1-b_t)\eta}-1\Big)\tilde{\xi}_{t-}^{\,a,b}dN_t. \tag{2.41}$$

Applying Itô's lemma gives:

$$d\log(\tilde{\xi}_t^{a,b}) = (a_t-1)\lambda_t dt + \Big(-\log(a_tb_t)+(1-b_t)\eta\log(1+J_t)\Big)dN_t. \tag{2.42}$$

The probability of choosing the wrong model when actually the alternative model $\mathbb{Q}^{a,b}$ is true equals:

$$P\Big(\tilde{\xi_N}^{\,a,b}>1|\mathbb{Q}\Big) = P\Big(\log(\tilde{\xi_N}^{\,a,b})>0|\mathbb{Q}\Big). \tag{2.43}$$

Again this probability can be calculated by simulating the process $\log(\tilde{\xi}_t)$ forward. The detection error probability is then defined as:

$$\frac{1}{2}P\Big(\log(\xi_N^{a,b})>0|\mathbb{P}\Big)+\frac{1}{2}P\Big(\log(\tilde{\xi_N}^{\,a,b})>0|\mathbb{Q}\Big). \tag{2.44}$$

2.D Hamilton-Jacobi-Bellman equation

We will first derive the Hamilton-Jacobi-Bellman equation for every measure $\mathbb{Q}^{a,b}$. Duffie and Epstein (1992b) show that the HJB-equation for stochastic differential utility equals:

$$0 = f(C_t,V_t^{\mathbb{Q}})+\mathcal{D}\mathcal{V}^{\mathbb{Q}}. \tag{2.45}$$

Here $\mathcal{DV}^{\mathbb{Q}}$ is the drift of the value function. In order to calculate the drift of the value function, we will apply Itô's lemma. By Itô's lemma for jump processes we have:

$$\begin{aligned} dV_t^{\mathbb{Q}} &= V_C^{\mathbb{Q}}\Big(\mu C_t dt + \sigma C_t dZ_t^{\mathbb{Q}}\Big) + V_X^{\mathbb{Q}}\mu_X(X_t)dt + \frac{1}{2}V_{CC}^{\mathbb{Q}}\sigma^2 C_t^2 dt \\ &\quad + \Big(V^{\mathbb{Q}}\big((1+J_t)C_{t-}, X_t\big) - V^{\mathbb{Q}}(C_{t-}, X_t)\Big)dN_t. \end{aligned} \tag{2.46}$$

Then the drift under $\mathbb{Q}^{a,b}$ equals:

$$\begin{aligned} \mathcal{DV}^{\mathbb{Q}} &= V_C^{\mathbb{Q}}\mu C_t + V_X^{\mathbb{Q}}\mu_X(X_t) + \frac{1}{2}V_{CC}^{\mathbb{Q}}\sigma^2 C_t^2 \\ &\quad + \lambda_t^{\mathbb{Q}} E_t^{\mathbb{Q}}\big[V^{\mathbb{Q}}\big((1+J_t)C_{t-}, X_t\big) - V^{\mathbb{Q}}(C_{t-}, X_t)\big]. \end{aligned} \tag{2.47}$$

This gives the following Hamilton-Jacobi-Bellman equation:

$$\begin{aligned} 0 &= f(C_t, V_t^{\mathbb{Q}}) + V_C^{\mathbb{Q}}\mu C_t + V_X^{\mathbb{Q}}\mu_X(X_t) + \frac{1}{2}V_{CC}^{\mathbb{Q}}\sigma^2 C_t^2 \\ &\quad + \lambda_t^{\mathbb{Q}} E_t^{\mathbb{Q}}\big[V^{\mathbb{Q}}\big((1+J_t)C_{t-}, X_t\big) - V^{\mathbb{Q}}(C_{t-}, X_t)\big]. \end{aligned} \tag{2.48}$$

2.E Reduced HJB-equation

Substituting our conjecture $V^{\mathbb{Q}}(C_t, X_t) = \frac{g^{\mathbb{Q}}(X_t)C_t^{1-\gamma}}{1-\gamma}$ into $f(C_t, V_t)$ gives:

$$\begin{aligned} f(C_t, V^{\mathbb{Q}}(C_t, X_t)) &= \frac{\beta}{1-1/\epsilon}\frac{C_t^{1-1/\epsilon} - \Big(g^{\mathbb{Q}}(X_t)C_t^{1-\gamma}\Big)^{\frac{1}{\zeta}}}{\Big(g^{\mathbb{Q}}(X_t)C_t^{1-\gamma}\Big)^{\frac{1}{\zeta}-1}} \\ &= \frac{\beta}{1-1/\epsilon}\Big(g^{\mathbb{Q}}(X_t)^{1-\frac{1}{\zeta}}C_t^{1-\gamma} - g^{\mathbb{Q}}(X_t)C_t^{1-\gamma}\Big) \\ &= \beta\zeta\Big(g^{\mathbb{Q}}(X_t)^{-\frac{1}{\zeta}} - 1\Big)V^{\mathbb{Q}}(C_t, X_t). \end{aligned} \tag{2.49}$$

The partial derivatives of V are given by:

$$\begin{aligned} &V_C^{\mathbb{Q}} = g^{\mathbb{Q}}(X_t)C_t^{-\gamma}, \qquad V_{CC}^{\mathbb{Q}} = -\gamma g^{\mathbb{Q}}(X_t)C_t^{-\gamma-1}, \\ &V_X^{\mathbb{Q}} = \frac{g_X^{\mathbb{Q}}(X_t)C_t^{1-\gamma}}{1-\gamma}. \end{aligned} \tag{2.50}$$

Here $g_X^{\mathbb{Q}}$ denotes the row vector with partial derivatives to each of the state variables, similar to $V_X^{\mathbb{Q}}$. Additionally we can calculate the expectation:

$$\begin{aligned} &E_t^{\mathbb{Q}}\big[V^{\mathbb{Q}}\big((1+J_t)C_{t-}, X_t\big) - V^{\mathbb{Q}}(C_{t-}, X_t)\big] = \frac{E_t^{\mathbb{Q}}\big[(1+J_t)^{1-\gamma}\big] - 1}{1-\gamma}g^{\mathbb{Q}}(X_t)C_t^{1-\gamma} \\ &= \frac{\frac{b_t\eta}{b_t\eta+1-\gamma} - 1}{1-\gamma}g^{\mathbb{Q}}(X_t)C_t^{1-\gamma} = \frac{-1}{b_t\eta+1-\gamma}g^{\mathbb{Q}}(X_t)C_t^{1-\gamma}. \end{aligned} \tag{2.51}$$

Substituting $f(C_t, V^{\mathbb{Q}}(C_t, X_t))$ together with the partial derivatives of $V_t^{\mathbb{Q}}$ and the expectation into (2.12) yields the following equation:

$$\begin{aligned} 0 = &\frac{\beta}{1-1/\epsilon}\Big(g^{\mathbb{Q}}(X_t)^{-\frac{1}{\zeta}} - 1\Big)g^{\mathbb{Q}}(X_t)C_t^{1-\gamma} + \mu g^{\mathbb{Q}}(X_t)C_t^{1-\gamma} \\ &- \frac{\gamma}{2}\sigma^2 g^{\mathbb{Q}}(X_t)C_t^{1-\gamma} + \frac{g_X^{\mathbb{Q}}(X_t)C_t^{1-\gamma}}{1-\gamma}\mu_X(X_t) + a_t\lambda_t\frac{-1}{b_t\eta + 1 - \gamma}g^{\mathbb{Q}}(X_t)C_t^{1-\gamma}. \end{aligned} \tag{2.52}$$

Dividing by $g^{\mathbb{Q}}(X_t)C_t^{1-\gamma}$ gives:

$$\begin{aligned} 0 = &\frac{\beta}{1-1/\epsilon}\Big(g^{\mathbb{Q}}(X_t)^{-\frac{1}{\zeta}} - 1\Big) + \mu - \frac{\gamma}{2}\sigma^2 + \frac{g_X^{\mathbb{Q}}(X_t)}{g^{\mathbb{Q}}(X_t)(1-\gamma)}\mu_X(X_t) \\ &+ a_t\lambda_t\frac{-1}{b_t\eta + 1 - \gamma}. \end{aligned} \tag{2.53}$$

2.F Asset prices

2.F.1 Stochastic discount factor

Duffie and Epstein (1992a) derive that the stochastic discount factor with stochastic differential utility equals $\pi_t = \exp\Big\{\int_0^t f_V(C_s, V_s)ds\Big\}f_C(C_t, V_t)$. However, the stochastic discount factor has to be adjusted for the ambiguity aversion preferences. Chen and Epstein (2002) show that the stochastic discount factor in the ambiguity setting should be multiplied by the Radon-Nikodym derivative $\xi_t^{a^*,b^*}$ of the measure corresponding to the optimal a^* and b^*. $\xi_t^{a,b}$ is defined in (2.36).

We will start with deriving the explicit stochastic differential equation of the stochastic discount factor. First we calculate the derivatives of $f(C_t, V_t)$ with respect to C_t and V_t:

$$\begin{aligned} f_C(C,V) &= \frac{\beta C^{-1/\epsilon}}{\big((1-\gamma)V\big)^{\frac{1}{\zeta}-1}}, \\ f_V(C,V) &= \beta\zeta\Big(\Big(1-\frac{1}{\zeta}\Big)\Big((1-\gamma)V\Big)^{-\frac{1}{\zeta}}C^{1-1/\epsilon} - 1\Big). \end{aligned} \tag{2.54}$$

Substituting $V_t = g(X_t)\frac{C_t^{1-\gamma}}{1-\gamma}$ into $f_C(C_t, V_t)$ and $f_V(C_t, V_t)$ we obtain:

$$\begin{aligned} f_C(C_t, V_t) &= \beta g(X_t)^{1-\frac{1}{\zeta}}C_t^{-\gamma}, \\ f_V(C_t, V_t) &= \beta\zeta\Big\{g(X_t)^{-\frac{1}{\zeta}}\Big(1-\frac{1}{\zeta}\Big) - 1\Big\}. \end{aligned} \tag{2.55}$$

This gives:

$$\pi_t = \xi_t^{a^*,b^*}\exp\left(\int_0^t \beta\zeta\Big(g(X_s)^{-\frac{1}{\zeta}}\big(1-\frac{1}{\zeta}\big) - 1\Big)ds\right)\beta g(X_t)^{1-\frac{1}{\zeta}}C_t^{-\gamma}. \tag{2.56}$$

Take the logarithm and write as a differential equation:

$$\begin{aligned} d\log(\pi_t) = \beta\zeta\Big(g(X_t)^{-\frac{1}{\zeta}}\big(1-\frac{1}{\zeta}\big)-1\Big)dt - \gamma d\log(C_t) + d\log(\xi_t^{a^*,b^*}) \\ + (1-\frac{1}{\zeta})d\log\big(g(X_t)\big). \end{aligned} \tag{2.57}$$

Apply Itô's lemma to $\log(C_t)$, $\log(\xi_t^{a^*,b^*})$ and $\log\big(g(X_t)\big)$ and substitute the results; this leads to the following differential equation:

$$\begin{aligned} d\log(\pi_t) =& \Big\{\beta\zeta\Big(g(X_t)^{-\frac{1}{\zeta}}\big(1-\frac{1}{\zeta}\big)-1\Big) - \gamma\big(\mu-\frac{\sigma^2}{2}\big) + \lambda_t(1-a_t^*) \\ &+ (1/\epsilon-\gamma)\frac{g_X(X_t)}{g(X_t)(1-\gamma)}\mu_X(X_t)\Big\}dt \\ &- \gamma\sigma dZ_t + \Big(\log(a_t^*b_t^*) + \big((b_t^*-1)\eta-\gamma\big)\log(1+J_t)\Big)dN_t. \end{aligned} \tag{2.58}$$

After applying Itô's lemma to $\log(\pi_t)$ we find:

$$\begin{aligned} d\pi_t =& \Big\{\beta\zeta\Big(g(X_t)^{-\frac{1}{\zeta}}\big(1-\frac{1}{\zeta}\big)-1\Big) - \gamma\big(\mu-(\gamma+1)\frac{\sigma^2}{2}\big) + \lambda_t(1-a_t^*) \\ &+ (1/\epsilon-\gamma)\frac{g_X(X_t)}{g(X_t)(1-\gamma)}\mu_X(X_t)\Big\}\pi_t dt - \gamma\sigma\pi_t dZ_t \\ &+ \Big(a_t^*b_t^*(1+J_t)^{(b_t^*-1)\eta-\gamma}-1\Big)\pi_{t-}dN_t. \end{aligned} \tag{2.59}$$

We can now substitute the HJB-equation (2.53) into the stochastic discount factor. Several terms cancel out and we are left with:

$$\begin{aligned} d\pi_t =& \Big\{ -\beta - \frac{\mu}{\epsilon} + \Big(1+\frac{1}{\epsilon}\Big)\frac{\gamma}{2}\sigma^2 + \Big(\gamma-\frac{1}{\epsilon}\Big)\lambda_t^*\frac{-1}{b_t^*\eta+1-\gamma} \\ &+ \lambda_t(1-a_t^*)\Big\}\pi_t dt - \gamma\sigma\pi_t dZ_t \\ &+ \Big(a_t^*b_t^*(1+J_t)^{(b_t^*-1)\eta-\gamma}-1\Big)\pi_{t-}dN_t. \end{aligned} \tag{2.60}$$

2.F.2 Interest rate

By the no-arbitrage argument, r_t should be such that $\pi_t B_t$ is a martingale, where B_t is the price of the risk-free asset. Now write $d\pi_t = \mu_{\pi,t}\pi_t dt + \sigma_\pi\pi_t dZ_t + J_{\pi,t}\pi_{t-}dN_t$. The product with B_t then follows:

$$d\pi_t B_t = (r_t+\mu_{\pi,t})\pi_t B_t dt + \sigma_\pi\pi_t B_t dZ_t + J_{\pi,t}\pi_{t-}B_t dN_t. \tag{2.61}$$

This is a martingale if $r_t + \mu_\pi + \lambda_t E_t[J_{\pi,t}] = r_t + \mu_\pi + \lambda_t\Big(a_t^* \frac{b_t^*\eta}{b_t^*\eta-\gamma} - 1\Big) = 0$. Therefore the interest rate equals:

$$\begin{aligned} r_t =& -\mu_\pi - \lambda_t\Big(a_t^*\frac{b_t^*\eta}{b_t^*\eta-\gamma} - 1\Big) \\ &= \beta + \frac{\mu}{\epsilon} - \Big(1+\frac{1}{\epsilon}\Big)\frac{\gamma}{2}\sigma^2 - \Big(\gamma - \frac{1}{\epsilon}\Big)a_t^*\lambda_t\frac{-1}{b_t^*\eta+1-\gamma} \\ &- a_t^*\lambda_t\Big(\frac{b_t^*\eta}{b_t^*\eta-\gamma} - 1\Big). \end{aligned} \tag{2.62}$$

Substituting r_t into the stochastic discount factor gives:

$$\begin{aligned} d\pi_t =& \Big\{ -r_t - \lambda_t\Big(a_t^*\frac{b_t^*\eta}{b_t^*\eta-\gamma} - 1\Big)\Big\}\pi_t dt - \gamma\sigma\pi_t dZ_t \\ &+ \Big(a_t^* b_t^* (1+J_t)^{(b_t^*-1)\eta-\gamma} - 1\Big)\pi_{t-}dN_t. \end{aligned} \tag{2.63}$$

2.F.3 Equity premium

Using equation (2.25), we know that the drift of the stock equals $\mu_{S,t} = \mu - \frac{k_X(X_t)}{k(X_t)}\mu_X(X_t) + k(X_t)$. From (2.23) we have: $k(X_t) = \beta g(X_t)^{-\frac{1-1/\epsilon}{1-\gamma}}$. This gives: $\frac{k_X(X_t)}{k(X_t)} = -\frac{1-1/\epsilon}{1-\gamma}\frac{g_X(X_t)}{g(X_t)}$. Rewriting the HJB-equation (2.53) gives:

$$\begin{aligned} \frac{1-1/\epsilon}{1-\gamma}\frac{g_X(X_t)}{g(X_t)}\mu_X(X_t) + k(X_t) = \beta + (1/\epsilon - 1)\Big(\mu - \frac{\gamma}{2}\sigma^2 \\ + a_t^*\lambda_t\frac{-1}{b_t^*\eta+1-\gamma}\Big). \end{aligned} \tag{2.64}$$

Substituting this into $\mu_{S,t}$ gives:

$$\begin{aligned} \mu_{S,t} &= \mu - \frac{k_X(X_t)}{k(X_t)}\mu_X(X_t) + k(X_t) \\ &= \mu + \beta + (1/\epsilon - 1)\Big(\mu - \frac{\gamma}{2}\sigma^2 + a_t^*\lambda_t\frac{-1}{b_t^*\eta+1-\gamma}\Big). \end{aligned} \tag{2.65}$$

The risk premium is then equal to the excess return of the stock over the interest rate:

$$\begin{aligned} rp_t &= \mu_{S,t} + a_t^*\lambda_t\frac{-1}{b_t^*\eta+1} - r_t \\ &= \gamma\sigma^2 + a_t^*\lambda_t\Big(\frac{-1}{b_t^*\eta+1} - \frac{b_t^*\eta}{b_t^*\eta+1-\gamma} + \frac{b_t^*\eta}{b_t^*\eta-\gamma}\Big). \end{aligned} \tag{2.66}$$

2.F.4 Consumption strips

Let $H_t = H(C_t, X_t, s-t) = E_t\Big[\frac{\pi_s}{\pi_t}C_s\Big]$ be the price of an asset that pays out the aggregate consumption at time s. H_t is also called a consumption strip. Conjecture that

$H(C_t, X_t, u) = \exp\Big\{-\int_t^{t+u} CDR_s ds\Big\} C_t$. u denotes the time to maturity of the consumption strip. Clearly, $H(C_t, X_t, 0) = C_t$. Applying Itô's lemma to H_t gives:

$$\begin{aligned} dH_t &= H_C dC_t + H_X dX_t - \frac{\partial H_t}{\partial u} dt = \frac{1}{C_t} H_t dC_t \\ &- \frac{\partial}{\partial X_t}\Big(\int_t^{t+u} CDR_s ds\Big)\mu_X(X_t) H_t dt \\ &+ \frac{\partial}{\partial u}\Big(\int_t^{t+u} CDR_s ds\Big) H_t dt. \end{aligned} \tag{2.67}$$

We can calculate both derivatives:

$$\begin{aligned} &\frac{\partial}{\partial X_t}\Big(\int_t^{t+u} CDR_s ds\Big)\mu_X(X_t) = \frac{\partial}{\partial t}\Big(\int_t^{t+u} CDR_s ds\Big)\frac{\partial t}{\partial X_t}\mu_X(X_t) \\ &= \frac{\partial}{\partial t}\Big(\int_t^{t+u} CDR_s ds\Big) = CDR_{t+u} - CDR_t, \end{aligned} \tag{2.68}$$

$$\frac{\partial}{\partial u}\Big(\int_t^{t+u} CDR_s ds\Big) = CDR_{t+u}. \tag{2.69}$$

Therefore dH_t becomes:

$$dH_t = \Big(\mu + CDR_t\Big) H_t dt + \sigma H_t dZ_t + J_t H_{t-} dN_t. \tag{2.70}$$

Now define $dH_t = \mu_{H,t} H_t dt + \sigma H_t dZ_t + J_t H_{t-} dN_t$. By the no arbitrage condition, $\pi_t H_t$ must be a martingale:

$$\begin{aligned} d\pi_t H_t &= (\mu_{\pi,t} + \mu_H + \sigma\sigma_\pi)\pi_t H_t dt + (\sigma + \sigma_\pi)\pi_t H_t dZ_t \\ &+ \Big((1 + J_t)(1 + J_{\pi,t}) - 1\Big)\pi_{t-} H_{t-} dN_t. \end{aligned} \tag{2.71}$$

We can calculate the expectation of the jump term:

$$\begin{aligned} &E_t[(1 + J_t)(1 + J_{\pi,t}) - 1] = E_t[a_t^* b_t^* (1 + J_t)^{(b_t^* - 1)\eta + 1 - \gamma} - 1] \\ &= a_t^* \frac{b_t^* \eta}{b_t^* \eta + 1 - \gamma} - 1. \end{aligned} \tag{2.72}$$

Therefore $\pi_t H_t$ is a martingale if:

$$0 = \mu_\pi + \mu_H + \sigma\sigma_\pi + \lambda_t\Big(a_t^* \frac{b_t^* \eta}{b_t^* \eta + 1 - \gamma} - 1\Big). \tag{2.73}$$

Substituting μ_π, μ_H and $\sigma\sigma_\pi = -\gamma\sigma^2$ gives:

$$\begin{aligned} 0 &= \mu + CDR_t - r_t - \lambda_t\Big(a_t^* \frac{b_t^* \eta}{b_t^* \eta - \gamma} - 1\Big) - \gamma\sigma^2 \\ &+ \lambda_t\Big(a_t^* \frac{b_t^* \eta}{b_t^* \eta + 1 - \gamma} - 1\Big). \end{aligned} \tag{2.74}$$

Note that this implies that: $CDR_t = r_t + rp_t - (\mu + a_t^* \lambda_t \frac{-1}{b_t^* \eta + 1})$. Lastly, we can substitute r_t and rp_t, which yields:

$$CDR_t = \beta + (1/\epsilon - 1)\Big(\mu - \frac{\gamma}{2}\sigma^2 + a_t^* \lambda_t \frac{-1}{b_t^* \eta + 1 - \gamma}\Big). \tag{2.75}$$

2.G Calibration of climate model

Table 2.3: *Parameters for the climate model.*

Par.	Description	Value
E_0	Initial level of total emissions (in GtC, 2015)	10.45
g_0^E	Initial growth rate of emissions (2015)	0.017
g_∞^E	Long-run growth rate of emissions	-0.02
δ_{g^E}	Speed of convergence of growth rate of emissions	0.0075
M_0	Initial carbon concentration compared to pre-industrial (in GtC, 2015)	263
M_{pre}	Pre-industrial atmospheric carbon concentration (in GtC)	588
$M_{0,0}$	Initial carbon concentration box 0 (in GtC, 2015)	139
$M_{1,0}$	Initial carbon concentration box 1 (in GtC, 2015)	90
$M_{2,0}$	Initial carbon concentration box 2 (in GtC, 2015)	29
$M_{3,0}$	Initial carbon concentration box 3 (in GtC, 2015)	4
$\delta_{M,0}$	Decay rate of carbon box 0	0
$\delta_{M,1}$	Decay rate of carbon box 1	0.0025
$\delta_{M,2}$	Decay rate of carbon box 2	0.027
$\delta_{M,3}$	Decay rate of carbon box 3	0.23
ν_0	Fraction of emissions carbon box 0	0.217
ν_1	Fraction of emissions carbon box 1	0.224
ν_2	Fraction of emissions carbon box 2	0.282
ν_3	Fraction of emissions carbon box 3	0.276
F_0^E	Initial level of exogenous forcing (in W/m^2, 2015)	0.5
F_∞^E	Long-run level of exogenous forcing (in W/m^2)	1
δ_F	Speed of convergence exogenous forcing	0.02
T_0	Initial surface temperature compared to pre-industrial (in $°C$, 2015)	0.85
T_0^{oc}	Initial ocean temperature compared to pre-industrial (in $°C$, 2015)	0.0068
κ	Speed of temperature transfer between upper and deep ocean	0.73
υ	Equilibrium temperature response to radiative forcing	1.13
α	Equilibrium temperature impact of CO_2 doubling (in $°C$)	3.05
τ	Heat capacity of the surface	7.34
τ_{oc}	Heat capacity of the oceans	105.5

3 Solution methods for DSGE models in continuous time: Application to a climate-economy model

3.1 Introduction

This chapter considers two solution methods to solve multi-dimensional continuous-time DSGE models. The setting that we study is a stochastic endowment economy with disaster risk, in which the representative agent has Epstein-Zin preferences. We also show how to calculate the equilibrium asset prices in this setting. Specifically, we derive the endogenous risk-free rate, risk-premium and consumption-wealth ratios of the asset pricing model. We use this specific setting as an illustration for our solution methods, but the solution methods are applicable to a more general class of models.

The numerical example that we consider is a stochastic climate model in which the economy is subject to climate disasters. Outcome variables of interest are optimal carbon abatement policy, expected trajectories of the climate variables over time and the social cost of carbon (the monetized welfare loss of emitting one ton of carbon emissions).

The first method that we consider is the finite difference method using the sparse grid combination technique. Finite difference methods have recently been a popular method to solve continuous-time DSGE models. The value function of the model must satisfy the Hamilton-Jacobi-Bellman (HJB) equation. This equation is a controlled partial differential equation. The finite difference method is a standard method to solve partial differential equations. One of the first applications in economics is Candler (1999). More recently, Achdou, Han, Lasry, Lions, and Moll (2021) use the finite difference method to solve a heterogeneous agent model and to back out the wealth distribution. Barnett et al. (2020) solve a climate-economy model with ambiguity aversion using a finite difference scheme.

One extension to the standard finite difference method is the use of sparse grids. A good overview of different sparse grid solution methods is Pflüger (2010). Griebel (1998) proposes a finite difference algorithm with adaptive sparse grids. Ruttscheidt (2018) uses a similar algorithm to solve heterogeneous agent models. Brumm and Scheidegger (2017) apply adaptive sparse grid methods to discrete time problems using value function iteration. We do not consider adaptive sparse grids, but rather apply the sparse grid combination technique (Griebel, Schneider, & Zenger, 1990). The idea behind the combination technique is to solve the problem using several smaller regular grids, and combine the solutions of the smaller grids to obtain a single solution on a sparse grid. The main advantage of this technique compared to adaptive sparse grids is its simple implementation. Furthermore, the sub-problems can easily be solved in parallel which speeds up the computation time. The sparse grid combination method has to our knowledge not been applied to macro models yet. Another extension of this paper is that we show that the finite difference method is also applicable to the more general Epstein-Zin setting.

In addition to the finite difference method, we also consider the stochastic grid method (SGM), which is a regression-based method. Regression-based methods were originally proposed to calculate the price of american options (Longstaff & Schwartz, 2001; Tsitsiklis & Van Roy, 2001). The idea is that in a dynamic programming setting, the conditional expectation can be approximated using a regression. In the initial algorithms, the condi-

tional expectation $E_t[V_{t+\delta_t}]$ is approximated by regressing the value function at time $t+\delta_t$ on basis functions of the state variables at time t. The approach that we use is the regress later approach. The idea is to regress the value function at time t on basis functions of the state variables at time t, and then use (closed-form) conditional expectations of the basis functions to obtain an approximation of the conditional expectation of the value function. This method is used by Jain and Oosterlee (2012) to price options.

Several methods designed to value american options rely on forward simulation and then solve the recursive programming problem backwards. If we consider an optimal control problem, forward simulation is not possible, since the control is unknown. One way to solve this problem is to use a random control variable in the simulation stage, and then optimize over the control variable when solving the model backwards. This is for example applied in Andreasson and Shevchenko (2019). However, it is not necessary for the approximation of the conditional expectations to actually simulate the process of the state variables forward. It is more efficient to specify at every time point a support region for the state variables and draw random state variables from this support region. This idea is also used in Balata and Palczewski (2017) and Ikefuji, Laeven, Magnus, and Muris (2020). Different from pricing american options, in our setting each period the optimal contral variable has to be calculated. A key new insight of this paper is that in continuous time, one can directly use the first order conditions from the HJB-equation to find the optimal policy, which is faster than performing grid search or some other maximization algorithm. Furthermore, we show how to apply the stochastic grid method to recursive Epstein-Zin preferences.

Regression-based solution methods are widely used in derivative pricing, but are not often used to solve macro-models. A literature where these methods are used more often including an optimal control setting are portfolio choice models (Brandt, Goyal, Santa-Clara, & Stroud, 2005; Koijen, Nijman, & Werker, 2010). One closely related example of an application in a macro model is Ikefuji et al. (2020), who look at a stochastic climate-economy model and solve the model using a simulation and regression method.

3.2 General problem

We first specify a general problem, then the solution methods are discussed. After that we look at the accuracy and performance of the solution methods for several numerical examples.

The general setting that we consider in this paper is the setting of a stochastic Lucas-tree economy with disasters in continuous time. There is a single representative agent that maximizes utility of consumption. The agent receives a stochastic exogenous endowment

stream. We assume that the representative agent has Epstein-Zin utility:[12]

$$V_t = \max_{\{u_s\}_{s\geq t}} E_t\Big[\int_t^\infty f(C_s, V_s)ds\Big]$$

where

$$f(C,V) = \frac{\beta}{1-1/\epsilon}\frac{C^{1-1/\epsilon} - \big((1-\gamma)V\big)^{\frac{1}{\zeta}}}{\big((1-\gamma)V\big)^{\frac{1}{\zeta}-1}} \quad \text{for } \epsilon \neq 1 \tag{3.1}$$

$$\text{with } \zeta = \frac{1-\gamma}{1-1/\epsilon}.$$

Define X_t as the d_X-dimensional vector with state variables: $X_t = [X_{1,t} \ \ ... \ \ X_{d_X,t}]'$. u_t is the d_u-dimensional vector of control variables: $u_t = [u_{1,t} \ \ ... \ \ u_{d_u,t}]'$. Endowment Y_t follows a geometric Brownian motion with additional jump processes. The drift, volatility and arrival rate distributions can depend on the state variables X_t and the controls u_t:

$$dY_t = \mu(X_t, u_t, t)Y_t dt + \sigma(X_t, u_t, t)Y_t dZ_t^Y + \sum_{m=1}^{M} J_{m,t}Y_{t-}dN_{m,t}. \tag{3.2}$$

Z_t^Y is a standard Brownian motion. $N_{m,t}$ is a Poisson process with a state- and control-dependent arrival rate $\lambda_{m,t} = \lambda_m(X_t, u_t, t)$. The multiple Poisson processes are assumed to be independent. Y_{t-} denotes aggregate endowment just before a jump ($Y_{t-} = \lim_{h\downarrow 0} Y_{t-h}$). When a jump of Poisson process $N_{m,t}$ arrives at time t, the jump size is controlled by the random variable $J_{m,t}$. $J_{m,t}$ can be seen as the percentage change of Y_t after a jump. We assume that the distributions of the jump sizes are time invariant, so we drop the time-index of J_m from now on. The dynamics of the vector of state variables is given by:

$$dX_t = \mu_X(X_t, u_t, t)dt + \sigma_X(X_t, u_t, t)dZ_t^X. \tag{3.3}$$

Here Z_t^X is a d_X-dimensional standard Brownian motion, $\mu_X(X_t, u_t, t)$ is a d_X-dimensional drift vector and $\sigma_X(X_t, u_t, t)$ is a $d_X \times d_X$ matrix of volatilities. We assume that σ_X is a diagonal matrix, i.e. we assume that the Brownian motions of the different state variables are not correlated.

A fraction of the endowment can be spent on costly control variables. The cost function can be time- and state-dependent. Consumption is then equal to endowment net of the cost function: $C_t = Y_t(1 - c(X_t, u_t, t))$. Define the consumption-endowment ratio by $\xi_t = \xi(X_t, u_t, t) = 1 - c(X_t, u_t, t)$. One can for example consider that it is possible to invest part of the endowment to increase the drift of the endowment or decrease the volatility of the endowment. Another example is investing part of the endowment to avert catostrophes. Martin and Pindyck (2015) consider a model with multiple catastrophes and look at optimal investment to reduce the disaster probabilities. Barro (2015) considers a model with climate disasters with a constant probability and environmental investment

[12]Note that V_t is not directly the continuous time counterpart of the Epstein-Zin preferences, but a transformed ordinally equivalent utility process. This transformation is performed to make sure that the variance multiplier that belongs to f is 0. This transformation makes the utility function more tractable. For more details, see chapter 2 or Duffie and Epstein (1992b).

to decrease the probability of a climate disaster. The setting that we will consider as a numerical example is the setting of climate disasters where the arrival rate of climate disasters is a function of temperature. The control variable in this case is carbon emissions abatement.

We use this specific model to illustrate the solution methods. However, the solution methods are also applicable to several extensions. It is possible to also allow for jumps in the state variables. Furthermore, correlation between Brownian motions can be introduced. For the stochastic grid method, this is straightforward to implement. For the finite difference method, this is slightly more involved. We will come back to this point later. Another possible extension is to step away from the Lucas-tree model and to consider a capital and/or labour based model with a production function and investment.

3.2.1 HJB-equation

To keep notation simple, we often drop the explicit dependence of variables on the state and control variables. For example, we use μ_t instead of $\mu(X_t, u_t, t)$. We use notation V_X, V_{XX} for the derivatives of the value function with respect to the vector of state-variables: $V_X = \left[\frac{\partial V_t}{\partial X_{1,t}} \quad ... \quad \frac{\partial V_t}{\partial X_{d_X,t}}\right]$ and

$$V_{XX} = \begin{bmatrix} \frac{\partial^2 V_t}{(\partial X_{1,t})^2} & \cdots & \frac{\partial^2 V_t}{\partial X_{d_X,t}\partial X_{1,t}} \\ \vdots & \ddots & \vdots \\ \frac{\partial^2 V_t}{\partial X_{1,t}\partial X_{d_X,t}} & \cdots & \frac{\partial^2 V_t}{(\partial X_{d_X,t})^2} \end{bmatrix}. \tag{3.4}$$

We obtain the following HJB-equation that the value function $V(Y_t, X_t, t)$ must satisfy:

$$\begin{aligned} 0 = \max_{u_t} \Big\{ & f(C_t, V_t) + V_Y \mu_t Y_t + \frac{1}{2} V_{YY} \sigma_t^2 Y_t^2 + \frac{\partial V_t}{\partial t} + V_X \mu_X \\ & + \frac{1}{2} tr(V_{XX} \sigma_X \sigma_X') + \sum_{m=1}^{M} \lambda_{m,t} E\Big[V\Big(Y_{t-}(1+J_m), X_t, t\Big) - V(Y_{t-}, X_t, t)\Big]\Big\}. \end{aligned} \tag{3.5}$$

Now conjecture: $V(Y_t, X_t, t) = \frac{g(X_t,t) Y_t^{1-\gamma}}{1-\gamma}$. We can calculate the derivatives and we can substitute the conjecture of V_t into $f(C, V)$. Substituting our conjecture into $f(C, V)$ gives:

$$\begin{aligned} f(C_t, V_t) &= \frac{\beta}{1 - 1/\epsilon} \frac{\Big(Y_t \xi_t\Big)^{1-1/\epsilon} - \Big(g_t Y_t^{1-\gamma}\Big)^{\frac{1}{\zeta}}}{\Big(g_t Y_t^{1-\gamma}\Big)^{\frac{1}{\zeta}-1}} \\ &= \frac{\beta}{1 - 1/\epsilon} \Big(g_t^{1-\frac{1}{\zeta}} \xi_t^{1-1/\epsilon} Y_t^{1-\gamma} - g_t Y_t^{1-\gamma}\Big) \\ &= \beta\zeta \Big(g_t^{-\frac{1}{\zeta}} \xi_t^{1-1/\epsilon} - 1\Big) V_t. \end{aligned} \tag{3.6}$$

The partial derivatives of V_t are given by:

$$\begin{aligned} V_Y &= g_t Y_t^{-\gamma}, \quad V_{YY} = -\gamma g_t Y_t^{-\gamma-1}, \\ V_X &= \frac{g_X Y_t^{1-\gamma}}{1-\gamma}, \quad V_{XX} = \frac{g_{XX} Y_t^{1-\gamma}}{1-\gamma}, \\ \frac{\partial V_t}{\partial t} &= \frac{\frac{\partial g_t}{\partial t} Y_t^{1-\gamma}}{1-\gamma}. \end{aligned} \tag{3.7}$$

Here g_X denotes the row vector with partial derivatives to each of the state variables, similar to V_X and g_{XX} the matrix of second derivatives, similar to V_{XX}. Note that for $\gamma > 1$ (which we will assume throughout this chapter), V_t is negative. Substituting the derivatives and dividing by V_t gives the reduced HJB-equation:

$$\begin{aligned} 0 = \min_{u_t} \Bigg\{ \Bigg(& \beta\zeta\Big(g_t^{-1/\zeta}\xi_t^{1-1/\epsilon} - 1\Big) + (1-\gamma)\Big(\mu_t - \frac{1}{2}\gamma\sigma_t^2 + \\ & \sum_{m=1}^{M} \lambda_{m,t} E\Big[\frac{(1+J_m)^{1-\gamma}-1}{1-\gamma}\Big]\Big)\Bigg) g_t + \frac{\partial g_t}{\partial t} + g_X\mu_X + \frac{1}{2}tr\Big(g_{XX}\sigma_X\sigma_X'\Big)\Bigg\}. \end{aligned} \tag{3.8}$$

Note that since we assume that V_t is negative, dividing by V_t implies that the maximization problem becomes a minimization problem. Our goal is to find the function g_t that solves this partial differential equation. Given g_t, the optimal policy can be obtained using the first order condition(s). Denote the optimal policy by u_t^*. In special cases, it is possible to find a closed form expression for u_t^* as a function of g_t, g_X, g_{XX} and X_t. Otherwise, u_t^* is implicitly defined by the first order condition(s).

3.2.2 Asset prices

Once we know the function g_t, it is possible to derive the endogenous risk-free rate, risk premium and wealth-consumption ratio. Let π_t be the stochastic discount factor of the economy. First, define by B_t the risk free asset that pays continuous interest r_t. Furthermore, let S_t be the price of the asset that gives a claim on the consumption stream. It therefore pays continuous dividends equal to C_t. More formally: $S_t = E_t\Big[\int_t^\infty \frac{\pi_s}{\pi_t} C_s ds\Big]$. The risk premium is defined by the difference between the return on S_t (including dividend payments) and the return on the risk-free asset. The consumption-wealth ratio k_t in the model is equal to $\frac{C_t}{S_t}$. The interest rate r_t, risk premium rp_t and consumption-wealth ratio k_t can be expressed as a function of the parameters, g_t and the consumption-endowment

ratio ξ_t:

$$
\begin{aligned}
r_t = & \underbrace{\beta + \frac{\mu_t}{\epsilon} - \Big(1+\frac{1}{\epsilon}\Big)\frac{\gamma}{2}\sigma_t^2}_{\text{Standard interest rate}} - \underbrace{\frac{1}{2}\frac{1}{\zeta}(1/\zeta - 1)tr\Big(\frac{g_X' g_X}{g_t^2}\sigma_X\sigma_X'\Big)}_{\text{Diffusion risk of the state variables}} \\
& + \underbrace{1/\epsilon\Big(\mu_\xi - \frac{1}{2}(1+1/\epsilon)tr\Big(\frac{\xi_X'\xi_X}{\xi_t^2}\sigma_X\sigma_X'\Big)\Big) - 1/\epsilon(1/\zeta-1)tr\Big(\frac{g_X'\xi_X}{g_t\xi_t}\sigma_X\sigma_X'\Big)}_{\text{Drift and diffusion risk of the consumption-endowment ratio}} \\
& - \underbrace{\Big(\gamma - \frac{1}{\epsilon}\Big)\sum_{m=1}^{M}\lambda_{m,t}E\Big[\frac{(1+J_m)^{1-\gamma}-1}{1-\gamma}\Big] - \sum_{m=1}^{M}\lambda_{m,t}E\Big[(1+J_m)^{-\gamma}-1\Big]}_{\text{Jump risk}}, \\
rp_t = & \underbrace{\gamma\sigma_t^2}_{\text{Standard diffusion risk}} + \underbrace{\sum_{m=1}^{M}\lambda_{m,t}E\Big[J_m + (1+J_m)^{-\gamma} - (1+J_m)^{1-\gamma}\Big]}_{\text{Jump risk}} \\
& + \underbrace{\frac{1}{\zeta}(1/\zeta-1)tr\Big(\frac{g_X' g_X}{g_t^2}\sigma_X\sigma_X'\Big)}_{\text{Diffusion risk of the state variables.}} + \underbrace{\frac{1}{\epsilon^2}tr\Big(\frac{\xi_X'\xi_X}{\xi_t^2}\sigma_X\sigma_X'\Big) + \frac{1}{\epsilon}\Big(\frac{2}{\zeta}-1\Big)tr\Big(\frac{g_X'\xi_X}{g_t\xi_t}\sigma_X\sigma_X'\Big)}_{\text{Diffusion risk of the consumption-endowment ratio}}, \\
k_t = & \beta g_t^{-\frac{1}{\zeta}}\xi_t^{1-1/\epsilon}.
\end{aligned}
\tag{3.9}
$$

The derivations are given in appendix 3.A.

3.3 Solution method 1: Finite difference

The reduced HJB-equation is a partial differential equation. The finite difference method numerically solves this partial differential equation. We refer to Lapeyre, Sulem, and Talay (2005), chapter 7 and 8 or Thomas (2013), for proofs and more details on finite difference methods. First, we specify a bounded domain on which g_t is defined. Even though several state variables might have an unbounded domain, we still have to cut off the domain at some point. The cut off point should be far enough away of the area of interest. Let $\underline{X} = [\underline{X_1} \;\; ... \;\; \underline{X_{d_X}}]'$ and $\overline{X} = [\overline{X_1} \;\; ... \;\; \overline{X_{d_X}}]'$ be respectively the vector with minimum and maximum values for each of the state variables. We also cut off the time dimension at a point T far enough in the future. We can write the reduced HJB-equation as follows:

$$
\begin{aligned}
& 0 = \min_{u_t}\Big\{R(X_t, g_t, u_t, t)g_t + \frac{\partial g_t}{\partial t} + D_t g_t\Big\} \\
& \text{where} \;\; D_t g_t = \sum_{d=1}^{d_X}(\mu_X)_d\frac{\partial g_t}{\partial X_{d,t}} + \frac{1}{2}\sum_{d=1}^{d_X}(\sigma_X\sigma_X')_{d,d}\frac{\partial^2 g_t}{(\partial X_{d,t})^2} \\
& \text{and} \;\; R(X_t, g_t, u_t, t) = \beta\zeta\Big(g_t^{-1/\zeta}\xi_t^{1-1/\epsilon} - 1\Big) \\
& \quad + (1-\gamma)\Big(\mu_t - \frac{1}{2}\gamma\sigma_t^2 + \sum_{m=1}^{M}\lambda_{m,t}E\Big[\frac{(1+J_m)^{1-\gamma}-1}{1-\gamma}\Big]\Big).
\end{aligned}
\tag{3.10}
$$

D_t is a difference operator that depends on X_t, u_t and t. Here $(\mu_X)_d$ denotes the d-th element of the vector μ_X. Similar notation is used for the volatility matrix. Denote by e_d a d_X dimensional vector with zeros except for the d-th element, which is a one. A natural way to approximate the first and second derivative with respect to $X_{d,t}$ is to use the central finite difference approximations. Let δ_d be the finite difference step in dimension d. The derivatives can then be approximated by:

$$\begin{aligned}\frac{\partial g_t}{\partial X_{d,t}} &\approx \frac{g(X_t + \delta_d e_d, t) - g(X_t - \delta_d e_d, t)}{2\delta_d} \equiv \partial_d g(X_t, t), \\ \frac{\partial^2 g_t}{(\partial X_{d,t})^2} &\approx \frac{g(X_t + \delta_d e_d, t) - 2g(X_t) + g(X_t - \delta_d e_d, t)}{\delta_d^2} \equiv \partial_{dd} g(X_t, t).\end{aligned} \tag{3.11}$$

Finite difference schemes are unfortunately not always stable and might therefore not converge to the right solution. A textbook example is the one-dimensional advection equation $\frac{\partial g(x,t)}{\partial t} + a\frac{\partial g(x,t)}{\partial x} = 0$ where $a > 0$ with $g(x, 0)$ given. The finite difference approximation of $a\frac{\partial g(x,t)}{\partial x}$ with a central scheme with step size δ can then be written as:

$$a\frac{\partial g(x,t)}{\partial x} \approx \frac{a}{2\delta} g(x + \delta, t) - \frac{a}{2\delta} g(x - \delta, t). \tag{3.12}$$

This scheme turns out to be unstable when central differences are used. To obtain a stable scheme, the scheme must be monotonically decreasing in both $g(x + \delta, t)$ and $g(x - \delta, t)$. The coefficients of $g(x + \delta, t)$ and $g(x - \delta, t)$ must therefore both be non-positive. This is the case when a backward-difference approximation is used. More details on stability of finite difference schemes will be discussed later.

In our setting, the coefficient on the derivative $\frac{\partial g_t}{\partial X_{d,t}}$ is the drift of the state variable: $(\mu_X)_d$. The drift can be both positive and negative. In order to obtain a stable scheme, one can use the so-called upwind method. The upwind scheme either uses a forward or backward first difference approximation, depending on whether the drift is positive or negative. Formally, we define the upwind differential operator ∂_d^u as follows:[13]

$$\begin{aligned}\partial_d^+ g(X_t, t) &\equiv \frac{g(X_t + \delta_d e_d, t) - g(X_t, t)}{\delta_d}, \\ \partial_d^- g(X_t, t) &\equiv \frac{g(X_t, t) - g(X_t - \delta_d e_d, t)}{\delta_d}, \\ \frac{\partial g_t}{\partial X_{d,t}} &\approx \partial_d^+ g(X_t, t)\mathbb{1}_{(\mu_X)_d \geq 0} + \partial_d^- g(X_t, t)\mathbb{1}_{(\mu_X)_d < 0} \equiv \partial_d^u g(X_t, t).\end{aligned} \tag{3.13}$$

For the second derivative approximation, we can use the central difference scheme. The second central derivative scheme is monotone since the volatility is always non-negative: $(\sigma_X \sigma_X')_{d,d} \geq 0$. Due to the assumption that covariances between state variables are zero,

[13]Note that in the example of the advection equation, the backward difference approximation is stable when the drift a is positive. In our definition of the upwind scheme, we use a forward difference approximation when the drift is positive. The reason for this difference is that HJB-equations are solved backwards in time given a terminal condition, where the advection equation is solved forward in time given an initial condition.

we only have to consider $\frac{\partial^2 g_t}{(\partial X_{d,t})^2}$. If we would consider non-zero covariances between different Brownian motions, we would have to calculate $\frac{\partial^2 g_t}{\partial X_{i,t} \partial X_{j,t}}$ as well. The covariances can be negative and therefore it is not straightforward to obtain a monotone scheme. A way to deal with negative covariances is described in Ma and Forsyth (2017). We do not consider this extension.

Let us now define an operator $D_{i,j,t}$ on the grid points, that approximates the exact operator D_t. To keep the notation clear, we consider for now a 2-dimensional problem. The extension to a d_X dimensional problem is straightforward. Assume that the number of grid points per dimension equals N_d. This gives $\delta_d = \frac{\overline{X_d} - \underline{X_d}}{N_d - 1}$. Then we obtain the following grid points:

$$\begin{aligned} x_i^1 &= \underline{X_1} + \delta_1(i-1), \quad i \in \{1, ..., N_1\}, \\ x_j^2 &= \underline{X_2} + \delta_2(j-1), \quad j \in \{1, ..., N_2\}. \end{aligned} \tag{3.14}$$

Define for each grid point the following functions:

$$\begin{aligned} &g_{i,j,t} \equiv g(x_i^1, x_j^2, t), \quad u^*_{i,j,t} = u^*(x_i^1, x_j^2, g_{i,j,t}, t), \\ &\mu_{Xi,j,t} = \mu_X(x_i^1, x_j^2, u^*_{i,j,t}, t), \quad \mu^+_{Xi,j,t} = \max\Big(0, \mu_{Xi,j,t}\Big), \\ &\mu^-_{Xi,j,t} = -\min\Big(0, \mu_{Xi,j,t}\Big), \quad \sigma_{Xi,j,t} = \sigma_X(x_i^1, x_j^2, u^*_{i,j,t}, t). \end{aligned} \tag{3.15}$$

Using an upwind approximation for the first derivative and a central approximation for the second derivative we obtain for the interior points of the grid the following operator $D_{i,j,t}$:

$$\begin{aligned} D_{i,j,t} g_{i,j,t} = &\left(-\sum_{d=1}^{2} \frac{|(\mu_{Xi,j,t})_d|}{\delta_d} - \sum_{d=1}^{2} \frac{\Big(\sigma_{Xi,j,t}\sigma'_{Xi,j,t}\Big)_{d,d}}{\delta_d^2} \right) g_{i,j,t} \\ &+ \left(\frac{(\mu^-_{Xi,j,t})_1}{\delta_1} + \frac{1}{2} \frac{\Big(\sigma_{Xi,j,t}\sigma'_{Xi,j,t}\Big)_{1,1}}{\delta_1^2} \right) g_{i-1,j,t} \\ &+ \left(\frac{(\mu^-_{Xi,j,t})_2}{\delta_2} + \frac{1}{2} \frac{\Big(\sigma_{Xi,j,t}\sigma'_{Xi,j,t}\Big)_{2,2}}{\delta_2^2} \right) g_{i,j-1,t} \\ &+ \left(\frac{(\mu^+_{Xi,j,t})_1}{\delta_1} + \frac{1}{2} \frac{\Big(\sigma_{Xi,j,t}\sigma'_{Xi,j,t}\Big)_{1,1}}{\delta_1^2} \right) g_{i+1,j,t} \\ &+ \left(\frac{(\mu^+_{Xi,j,t})_2}{\delta_2} + \frac{1}{2} \frac{\Big(\sigma_{Xi,j,t}\sigma'_{Xi,j,t}\Big)_{2,2}}{\delta_2^2} \right) g_{i,j+1,t}. \end{aligned} \tag{3.16}$$

3.3.1 Boundary conditions

At the boundaries of the grid it is not possible to apply the central scheme for the second derivative since there is only one neighbour point available. Furthermore, the backward (forward) differences at the left (right) boundaries are also not possible anymore. We have

to specify some kind of boundary condition such that we are able to deal with these issues. It is often the case that the state variables are somehow mean-reverting. When this is the case, the drift of the state variable will be positive at the left boundary and negative at the right boundary if the boundaries are chosen far enough to the left and right. The upwind scheme will then use the forward (backward) difference at the left (right) boundary and therefore there are no problems with the first difference at the boundaries. In this case, we can assume as a boundary condition that the second derivative vanishes at the boundary to handle the problem with the central difference scheme for the second derivative. Every boundary condition will introduce an error at the boundary, but this error will be small for points far enough away from the boundaries.

One way to implement the boundary conditions is to introduce so called 'ghost' points. Consider the point at the boundary $g_{1,j,t}$ where $j \in \{2, .., N_2 - 1\}$, i.e. x_j^2 is not a boundary point but x_1^1 is at the boundary. In this case we can define the 'ghost' point $g_{0,j,t}$. The second difference approximation in dimension 1 becomes:

$$\partial_{11} g_{1,j,t} = \frac{1}{2} \frac{\left(\sigma_{X1,j,t} \sigma'_{X1,j,t}\right)_{1,1}}{\delta_1^2} \Big(g_{0,j,t} - 2g_{1,j,t} + g_{2,j,t} \Big). \tag{3.17}$$

Setting the second derivative equal to 0 implies that $g_{0,j,t} = 2g_{1,j,t} - g_{2,j,t}$. Given $g_{0,j,t}$, we can simply apply (3.16). For different boundary points, we can construct 'ghost' points in a similar way.

When the state variables are not mean-reverting and the upwind scheme might use the backward (forward) difference at the left (right) boundary, the boundary conditions specified above might not be stable. One can instead assume that the first derivative vanishes at the boundary. Again, a 'ghost' point can be introduced. For the point $g_{1,j,t}$ we will now obtain the 'ghost' point $g_{0,j,t} = g_{1,j,t}$. The reason that we do not always use the condition on the first derivative, is because the condition specified on the second derivative will lead to a smaller error.

3.3.2 Setting up the scheme

It is possible to perform all the operations directly for an entire vector of grid points. Define $R_{i,j,t} = R(x_i^1, x_j^2, g_{i,j,t}, u^*_{i,j,t}, t)$. We define the vector g_t^δ and the vector R_t^δ:

$$g_t^\delta \equiv \begin{bmatrix} g_{1,1,t} \\ g_{2,1,t} \\ \vdots \\ g_{N_1,1,t} \\ g_{1,2,t} \\ \vdots \\ g_{N_1,N_2,t} \end{bmatrix}, \quad R_t^\delta \equiv \begin{bmatrix} R_{1,1,t} \\ R_{2,1,t} \\ \vdots \\ R_{N_1,1,t} \\ R_{1,2,t} \\ \vdots \\ R_{N_1,N_2,t} \end{bmatrix}. \tag{3.18}$$

So these two vectors evaluate the functions $g(X_t, t)$ and $R(X_t, g_t, u_t^*, t)$ at all grid points of the state variables. The superscript δ on g_t^δ and R_t^δ indicates that these are vectors of the functions g_t and R_t evaluated at the different grid points. Using this notation we can

distinguish the vectors from the original functions $g_t = g(X_t, t)$ and $R_t = R(X_t, g_t, u_t^*, t)$. g_t^δ and R_t^δ are column vectors of length $N_1 N_2$.

Note that equation (3.16) describes the finite difference operation $D_{i,j,t}$ for a single point $g_{i,j,t}$. It is now possible to construct a matrix D_t^δ such that $D_t^\delta g_t^\delta$ performs the finite difference operation directly for the entire vector g_t^δ. The definition of the $N_1 N_2 \times N_1 N_2$ matrix D_t^δ is given in appendix 3.B. Note that D_t^δ is a very sparse matrix. Lastly, denote by $I_{N_1 N_2}$ the $N_1 N_2 \times N_1 N_2$ identity matrix. Similar to our state space, we also discretize the time-space. Assume the time step equals δ_t, this gives the grid of time points: $[t_0 = 0, t_1 = \delta_t, ..., t_{N_t} = T]$.

We will now propose two finite difference schemes: the explicit and the semi-implicit scheme. Let us start with the explicit scheme. A possible discrete approximation of the reduced HJB-equation (3.10) at time t_{i+1}, $i \in \{0, ..., N_t - 1\}$ is the following:

$$0 = \frac{g_{t_{i+1}}^\delta - g_{t_i}^\delta}{\delta_t} + \Big(D_{t_{i+1}}^\delta + diag(R_{t_{i+1}}^\delta)\Big) g_{t_{i+1}}^\delta. \tag{3.19}$$

Here $\frac{g_{t_{i+1}}^\delta - g_{t_i}^\delta}{\delta_t}$ is a backward approximation of the time derivative for the vector $g_{t_{i+1}}^\delta$. $D_{t_{i+1}}^\delta g_{t_{i+1}}^\delta$ equals a vector that approximates the true difference operator $D_{t_{i+1}} g_{t_{i+1}}$. Lastly, $diag(R_{t_{i+1}}^\delta) g_{t_{i+1}}^\delta$is the matrix-vector multiplication that calculates $R_t g_t$ at every grid point. Rewriting this equation gives the explicit scheme:

$$\begin{aligned} g_{t_i}^\delta &= A_{t_{i+1}}^E g_{t_{i+1}}^\delta, \\ A_{t_{i+1}}^E &\equiv I_{N_1 N_2} + \delta_t \Big(D_{t_{i+1}}^\delta + diag(R_{t_{i+1}}^\delta)\Big). \end{aligned} \tag{3.20}$$

Similarly, we can define the semi-implicit scheme as:

$$\begin{aligned} 0 &= \frac{g_{t_{i+1}}^\delta - g_{t_i}^\delta}{\delta_t} + \Big(D_{t_{i+1}}^\delta + diag(R_{t_{i+1}}^\delta)\Big) g_{t_i}^\delta, \\ \implies g_{t_i}^\delta &= A_{t_{i+1}}^I g_{t_{i+1}}^\delta, \\ A_{t_{i+1}}^I &\equiv \left(I_{N_1 N_2} - \delta_t \Big(D_{t_{i+1}}^\delta + diag(R_{t_{i+1}}^\delta)\Big) \right)^{-1}. \end{aligned} \tag{3.21}$$

The explicit scheme is the most straightforward scheme, but has the issue that the stability of the scheme depends on the time step. In some cases, a very small time step is required to obtain a stable solution. The semi-implicit scheme is generally more stable but either requires to invert a matrix or solve a linear system, where the explicit scheme merely requires a matrix vector multiplication. Note that the scheme is called semi-implicit since the vector $R_{t_{i+1}}^\delta$ still depends on $g_{t_{i+1}}^\delta$. A fully implicit scheme would solve the following equation for $g_{t_i}^\delta$:

$$0 = \frac{g_{t_{i+1}}^\delta - g_{t_i}^\delta}{\delta_t} + \Big(D_{t_i}^\delta + diag(R_{t_i}^\delta)\Big) g_{t_i}^\delta. \tag{3.22}$$

A fully implicit scheme is unconditionally stable. This implies that the stability conditions are met for an arbitrarily large time step. We will discuss stability later in more

detail. Since R_t^δ depends on the unknown function g_t^δ in a non-linear way, a non-linear solver must be used to obtain g_t^δ. However, this is inefficient. This is the reason why we do not consider the fully implicit scheme. Let us now describe the full algorithm.

The algorithm
Step 1: Start with an initial guess for g_T^δ .
Start one step before terminal time t_{N_t-1}. Backwards in time, for every time step t_i, $i = N_t - 1, ..., 1$, perform the following steps.
Step 2: $g_{t_{i+1}}^\delta$ is obtained from the previous iteration. Calculate the optimal policy $u_{t_{i+1}}^*$ using either a closed form or implicit expression that follows from the first order conditions. This requires as input $g_{t_{i+1}}^\delta$ and its derivatives. The derivatives can be calculated using central finite differences.
Step 3: Use $u_{t_{i+1}}^*$ to calculate $\mu_{Xt_{i+1}}$ and $\sigma_{Xt_{i+1}}$.
Step 4: Construct $D_{t_{i+1}}^\delta$ (see appendix 3.B).
Step 5: Use $g_{t_{i+1}}^\delta$ and $u_{t_{i+1}}^*$ to calculate $R_{t_{i+1}}^\delta$.
Step 6: Given $g_{t_{i+1}}^\delta$, $D_{t_{i+1}}^\delta$ and $R_{t_{i+1}}^\delta$, we can calculate A_t and either use the explicit scheme (3.20) or the semi-implicit scheme (3.21) to obtain $g_{t_i}^\delta$.
Optional: Step 7. To obtain the risk-free rate and the risk premium at period t_i, ξ_{t_i} and its derivatives can be calculated using (central) finite differences.
Repeat steps 2-7 until g_0^δ is obtained. Given g_0^δ, calculate the optimal policy u_0^* once more.

The matrix A_t (both in the explicit and implicit case) is a large sparse matrix. Several programming languages (e.g. Matlab and Python) have efficient procedures to set up the matrix A_t, by using the fact that only a few diagonal arrays are non-zero. In the case of the explicit scheme, the sparsity of the matrix speeds up the matrix-vector multiplication $A_t^E g_t^\delta$. In the case of the semi-implicit scheme, calculating the matrix A_t^I requires a matrix inversion. Actually inverting the matrix every time step is inefficient. Instead, one can find $g_{t_i}^\delta$ by solving the following linear system:

$$\left(I_{N_1 N_2} - \delta_t \Big(D_{t_{i+1}}^\delta + diag(R_{t_{i+1}}^\delta) \Big) \right) g_{t_i}^\delta = g_{t_{i+1}}^\delta. \tag{3.23}$$

There are several efficient routines to efficiently solve this linear system. We use the biconjugate gradient stabilized method, which is especially convenient to solve a linear system with a large and sparse matrix.

If the optimal policy u_t^* has a closed form expression, one can easily calculate the optimal policy given g_t and its derivatives. If this is not the case, a non-linear equation has to be solved. Solving such an equation can be slow. To speed up the computation, it is important to start with a good initial guess. A good guess is the optimal policy in the previous period. So the guess for $u_{t_i}^*$ is $u_{t_{i+1}}^*$. Furthermore, it pays off to supply the analytical Jacobian of the first order conditions to the solver. We use a trust-region algorithm with analytical Jacobian to calculate the optimal policy function.

As mentioned before, finite difference schemes can be unstable. Furthermore, oscillations might occur, which especially in the Epstein-Zin setting can cause problems since

it may lead to complex numbers. Consistency, convergence and stability are discussed in more detail in appendix 3.C.

Until now we have assumed that the time derivative $\frac{\partial g_t}{\partial t} \neq 0$. In the case of an infinite horizon problem the time derivative in not equal to zero when there is explicit time dependence. Also in finite horizon problems the time derivative is non-zero. However, many economic models have an infinite time horizon and do not have explicit time dependence. In this case $\frac{\partial g_t}{\partial t} = 0$. In a discrete time framework, one can then solve for the value function by starting with an initial guess and iterating over the Bellman equation until the value function converges. We can use a similar algorithm for the finite difference approach. This approach is described in appendix 3.D and turns out to be very similar to the finite difference scheme that we already proposed.

3.3.3 Sparse grids: Combination method

A problem with the finite difference approach is that it suffers from the curse of dimensionality. The size of the matrix A_t and of the vector g_t^δ grows exponentially with the number of dimensions. One solution to make sure the computational effort grows less fast with the number of dimensions is to use sparse grids. For a full grid with equal amount of points in each dimension, the total number of points on the d-dimensional grid equals N^d. So doubling the number of points in each dimension leads to 2^d times as much points. For a sparse grid with N points at the boundary in each dimension, the total number of points is of the order $\mathcal{O}(N(\log N)^{d-1})$. As an example, doubling the number of points at the boundary of a sparse grid in 3 dimensions from 128 to 256 leads to 2.3 times as many points, instead of 8 times as many points for the full grid. Of course, less points on the grid also implies that the approximation will be less accurate. The accuracy of the solution depends on the smoothness of the function that is approximated, together with the task (e.g. interpolation, finite difference). Overall it turns out that sparse grids do not give up too much accuracy, while they are not subject to the curse of dimensionality.

A possible extension of regular sparse grids are spatially adaptive sparse grids. Based on some condition, an algorithm puts more grid points at the places where the error of the approximation is the largest. This is useful if the function that is approximated is very non-linear in some area's. However, there are computational costs related to the adaptivity. Griebel (1998) proposes an algorithm to apply finite differences on adaptive sparse grids. For more details on (adaptive) sparse grids, see for example Pflüger (2010) or Zumbusch (2000).

We choose to apply the so called combination method (Griebel et al., 1990). Instead of directly solving the problem on a sparse grid, one can combine solutions on smaller full grids to generate a sparse grid solution. For linear interpolation tasks, it turns out that using the combination method or a direct sparse grid method give equivalent results. For non-linear tasks like solving a partial differential equation, combining full grids might not lead to exactly the same answer as solving the equation on the corresponding sparse grid. Nevertheless, the combination method has been widely applied. The first advantage is that one still solves full-grid problems. Finite difference operations on full grid problems are more straightforward to implement and can also be coded more efficient. Second, solving several sub-problems and combining them later is ideal for parallelization. Compared to

Figure 3.1: *Full grids for several level combinations in two dimensions.*

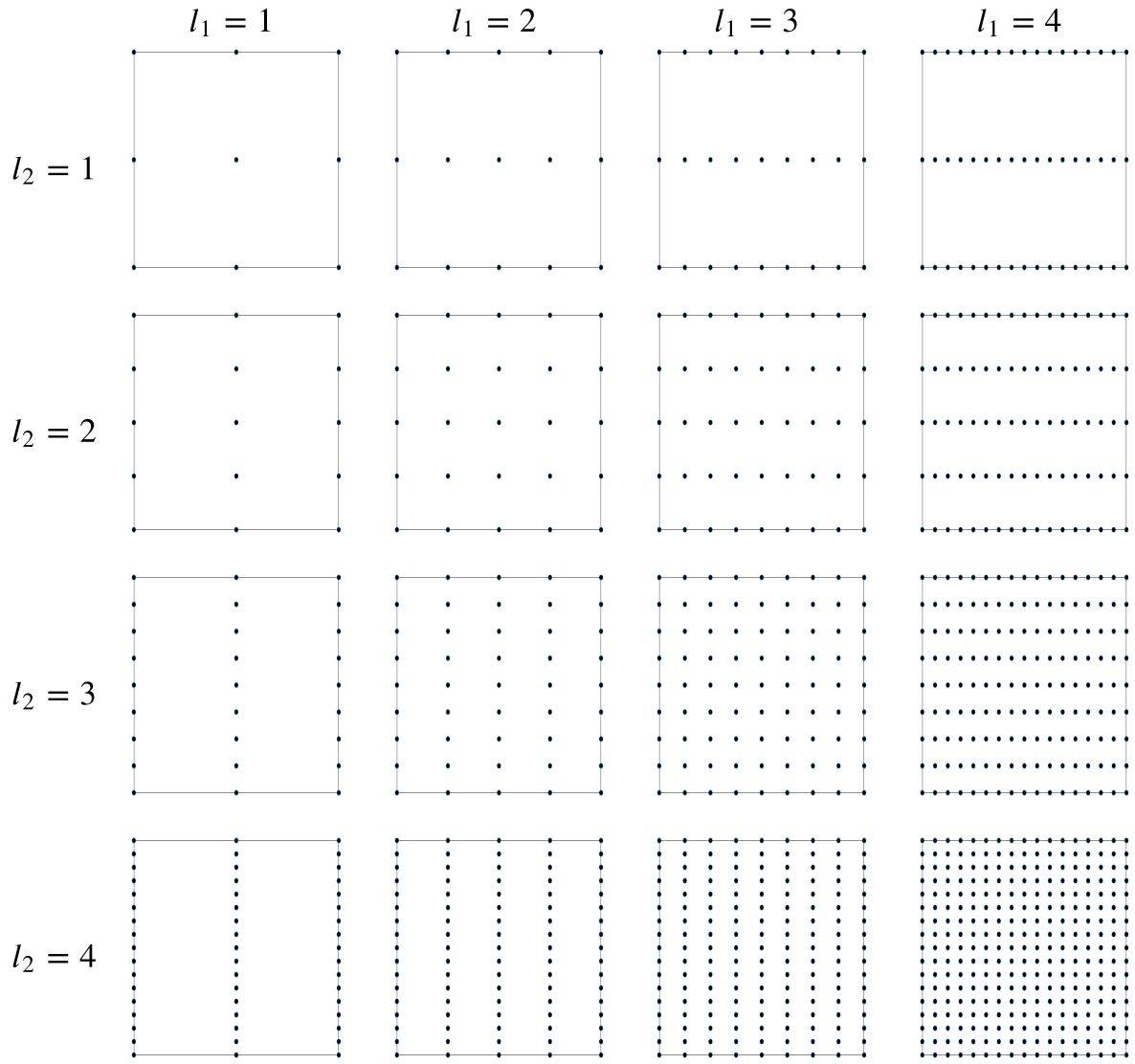

direct sparse grid methods, the number of evaluation points will be slightly larger but the efficiency due to the well-behaved full grids and the possibility to parallelize outweigh this disadvantage. Spatial adaptivity is not possible with the combination method.

Let us again start with a 2-dimensional problem. Remember that N_d denotes the number of points in dimension d. $\overline{X_d}$ and $\underline{X_d}$ are respectively the maximum and minimum values in both dimensions and $\delta_d = \frac{\overline{X_d} - \underline{X_d}}{N_d - 1}$ is the step size. Define the so called level per dimension by l_d. At the first level in dimension d ($l_d = 1$), we assume that the number of points in that dimension equals 3. When we increase the level by 1, we assume that the step size in that dimension is divided by two. This leads to the following relation between the number of points and the level: $N_d = 2^{l_d} + 1$. In two dimensions, we can therefore define a grid by the level $l = [l_1 \;\; l_2]'$. This is graphically illustrated in figure 3.1.

The combination method combines the finite difference solutions on several of the sub-grids. Define by $g_0^{\delta,l}$ the finite difference solution at $t = 0$ on a full grid with level l. Combining grids is not straightforward since all grids have different grid points. Assume we are interested in the value of g at a point $x = [x^1 \;\; x^2]$. The full grid with level l gives as output the value of g at the grid points $x_i^1 = \underline{X_1} + \delta_1(i-1), \quad i \in \{1, ..., 2^{l_1} + 1\}$ and $x_i^2 = \underline{X_2} + \delta_2(i-1), \quad i \in \{1, ..., 2^{l_2} + 1\}$. To obtain the value of g at the point x, we use linear interpolation. Define the approximation of g at the point x using a level l full grid by $g^{\delta,l}(x, 0)$. Lastly, denote by L the level of the sparse grid. Then the sparse grid combination solution at point x becomes:

$$g_{SG}^{\delta}(x,0) = \sum_{l_1+l_2=L+1} g^{\delta,l}(x,0) - \sum_{l_1+l_2=L} g^{\delta,l}(x,0). \tag{3.24}$$

Figure 3.2 shows graphically how the full sub-grids are combined. For a d-dimensional problem, the intuition of the combination method is similar to the 2-dimensional problem, but the formulas are slightly different. Let d_X be the number of state variables. Then the sparse grid solution becomes:

$$g_{SG}^{\delta,L}(x,0) = \sum_{k=0}^{d_X-1} (-1)^k \binom{d_X - 1}{k} \sum_{l_1+...+l_{d_X}=L+(d_X-1)-k} g^{\delta,l}(x,0). \tag{3.25}$$

3.4 Solution method 2: Stochastic grid method

Regression-based methods are originally proposed to calculate the value of American options. The methods use dynamic programming which makes them suitable for the type of problem that we consider. Traditional value function iteration can become extremely slow for high-dimensional problems. We start with discussing the least squares Monte Carlo algorithms that are used by Tsitsiklis and Van Roy (2001) and Longstaff and Schwartz (2001). We then explain why some adjustments to this method are useful in our setting.

3.4.1 Least squares Monte Carlo algorithm for option pricing

The algorithm that we discuss here is the algorithm described in Tsitsiklis and Van Roy (2001). The algorithm used by Longstaff and Schwartz (2001) is quite similar but is more

Figure 3.2: *The combination method to obtain a sparse grid with level $L = 4$ in two dimensions.*

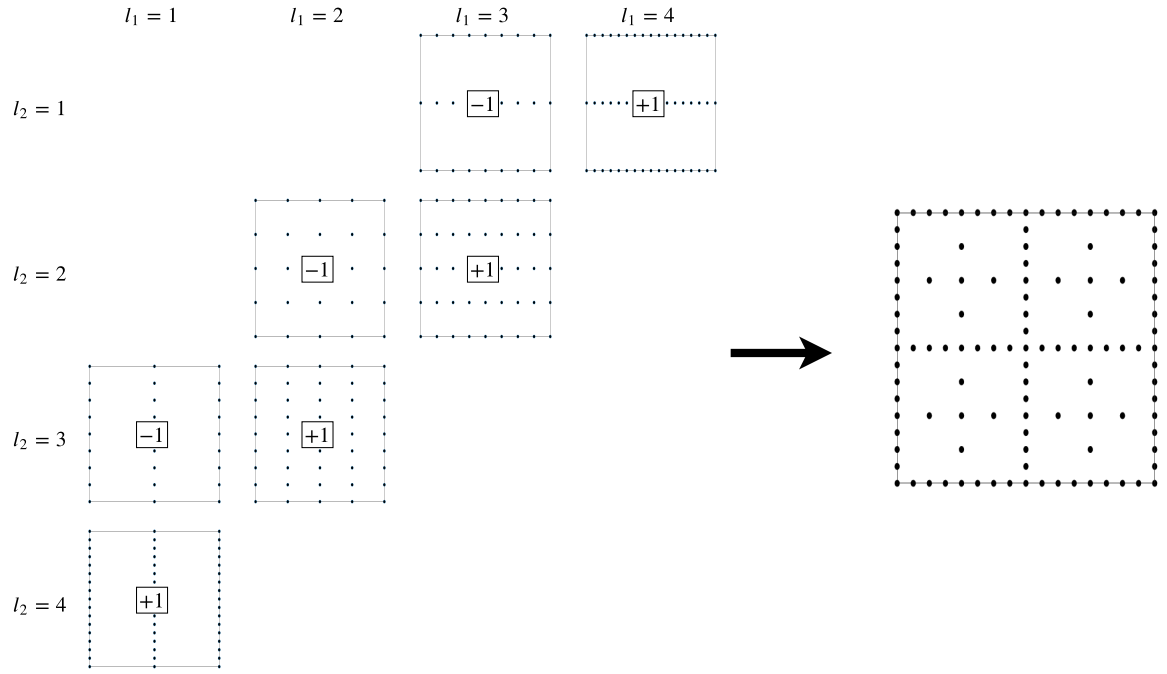

focused on optimal stopping times for American options and is therefore less useful to compare with our method.

Assume that the american option can be excercised at time points $t_0 = 0, t_1 = \delta_t, ..., t_N = T$. Note that this is an approximation since in reality the american option can be evaluated at any time. Define the value of the option as a function of the stock price by $V(X_t, t)$. The idea of the algorithm is as follows. Starting with the initial stock price X_0, simulate K trajectories forward up to time T. Define by $\hat{V}$ the approximate value of the option. At time T, the value of an american call option in trajectory k equals $\hat{V}(X_T(k), T) = h(X_T(k))$ where $h(x) = \max(0, x - A)$ and A is the strike price. The value of the option one period earlier is described by the following recursive relation:

$$V\Big(X_{t_i}(k), t_i\Big) = \max\Big(h(X_{t_i}(k)), e^{-r\delta_t} E_{t_i}[V_{t_{i+1}} | X_{t_i}(k)]\Big). \tag{3.26}$$

The conditional expectation is then approximated using a set of basis functions $B\big(X_t\big) = [B_1\big(X_t\big) \quad ... \quad B_{N_b}\big(X_t\big)]$. The idea is to regress $V_{t_{i+1}}(k)$ on the vector of basis functions $B(X_{t_i}(k))$, which yields an $1 \times N_b$ vector of coefficients ν_{t_i}. The conditional expectation is then approximately equal to: $E_{t_i}[V_{t_{i+1}} | X_{t_i}(k)] \approx \nu'_{t_i} B(X_{t_i}(k))$. Given this approximation of the conditional expectation, we can use equation (3.26) to calculate $V\Big(X_{t_i}(k), t_i\Big)$.

Repeating these steps for all time periods, we are able to find the price of the option at the initial date.

The first issue with using this algorithm to solve for the value function in our setting is that the value function at the terminal date T is unknown, in contrast to the option case where the value of the option at the terminal date is known. This issue can be resolved by using a guess for the value function at the terminal date. It is then important to choose the date T far enough in the future, such that the guess does not influence the initial outcomes.

The second issue is that it is not possible to simulate state variables forward, since the evolution of the state variables depends on the unknown control variable. One way to deal with this is to use random control variables in the simulation stage. When solving the problem backwards, the optimal policy can be calculated. Another possibility, and the approach that we use, is to apply the stochastic grid method (Jain & Oosterlee, 2012). This method relies on random grid points instead of simulating the state variables forward. The advantage of this method is that the only randomness in the solution method comes from the random grid points and therefore much fewer simulations are necessary for the same accuracy. Furthermore, it is very easy to calculate derivatives of the value function using this method which is necessary to efficiently solve for optimal policy every time period.

Additional to the fact that we use random grid points instead of actually simulating the state variables forward, the main difference lies in the regression stage. In the least squares Monte Carlo algorithm, the value function at time t_{i+1} is regressed on basis functions at time t_i to approximate the conditional expectation. We are not able to perform that regression since we do not simulate the state variables forward. In the stochastic grid algorithm, the value function at time t_i is regressed on basis functions of state variables at time t_i. We then use (closed-form) conditional expectations of the basis functions to approximate the conditional expectation of the value function.

Jain and Oosterlee (2012) use the stochastic grid method to calculate the value of american options. Our main contribution to this method is that we use this method to solve for the value function in a DSGE model with recursive preferences. Additionally, we show that the Hamilton-Jacobi-Bellman equation can be used to efficiently calculate optimal control variables. Calculating the value of the option does not involve the calculation of optimal control variables.

3.4.2 Stochastic grid method

We now outline the algorithm for the stochastic grid method. Similar to the option pricing case, we start with a dynamic programming equation. Since we look at recursive preferences, we can not use the standard dynamic programming equation for value functions. Instead, we use the discrete time Epstein-Zin recursive equation. Assume that the time step equals δ_t. The standard discrete time Epstein-Zin equation equals:

$$U_t = \max_{u_t} \left((1 - e^{-\beta\delta_t}) C_t^{1-1/\epsilon} + e^{-\beta\delta_t} E_t[U_{t+\delta_t}^{1-\gamma}]^{1/\zeta} \right)^{\frac{1}{1-1/\epsilon}}. \tag{3.27}$$

Instead of using the standard discrete time equation of the Epstein-Zin preferences, we again use an ordinally equivalent version to be in line with the stochastic differential utility setting. Define $V_t = \frac{U_t^{1-\gamma}}{1-\gamma}$. We have derived that $V_t = \frac{g(X_t,t)Y_t^{1-\gamma}}{1-\gamma}$. We again assume that $\gamma > 1$. After substitution of V_t and rearranging we obtain the following equation:

$$g(X_t,t)Y_t^{1-\gamma} = \min_{u_t}\left((1-e^{-\beta\delta_t})C_t^{1-1/\epsilon} + e^{-\beta\delta_t}\Big(E_t\big[g(X_{t+\delta_t},t+\delta_t)Y_{t+\delta_t}^{1-\gamma}\big]\Big)^{1/\zeta}\right)^{\zeta}. \quad (3.28)$$

Note that the maximization has become a minimization problem, since $\gamma > 1$. Dividing both sides by $Y_t^{1-\gamma}$ and rearranging gives:

$$g(X_t,t) = \min_{u_t}\left((1-e^{-\beta\delta_t})\xi_t^{1-1/\epsilon} + e^{-\beta\delta_t}\Big(E_t\Big[g(X_{t+\delta_t},t+\delta_t)\frac{Y_{t+\delta_t}^{1-\gamma}}{Y_t^{1-\gamma}}\Big]\Big)^{1/\zeta}\right)^{\zeta}. \quad (3.29)$$

For small time steps δ_t, it is reasonable to assume that $E_t\Big[g(X_{t+\delta_t},t+\delta_t)\frac{Y_{t+\delta_t}^{1-\gamma}}{Y_t^{1-\gamma}}\Big] \approx E_t[g(X_{t+\delta_t},t+\delta_t)]E_t\Big[\frac{Y_{t+\delta_t}^{1-\gamma}}{Y_t^{1-\gamma}}\Big]$. The quadratic covariation between $g(X_t)$ and Y_t is equal to 0, which implies that for small enough time steps we can separate the expectations. The idea behind this is that there is no correlation between the shocks that drive Y_t and X_t. The correlation occurs through the drift μ, standard deviation σ and arrival rate λ. However, it takes some time for a shock in X_t to have an effect on Y_t through μ, σ and λ.

Applying Itô calculus, we can derive a closed form expression for $\frac{Y_{t+\delta_t}^{1-\gamma}}{Y_t^{1-\gamma}}$:

$$\begin{aligned}\frac{Y_{t+\delta_t}^{1-\gamma}}{Y_t^{1-\gamma}} = \exp\Big((1-\gamma)\int_t^{t+\delta_t}\Big(\mu(X_s,u_s^*,s) - \sigma(X_s,u_s^*,s)^2/2\Big)ds \\ + (1-\gamma)\int_t^{t+\delta_t}\sigma(X_s,u_s^*,s)dZ_s^c + (1-\gamma)\sum_{m=1}^{M}\sum_{i=1}^{N_{m,t+\delta_t}-N_{m,t}}\log(1+J_{m,i})\Big).\end{aligned} \quad (3.30)$$

If $N_{m,t+\delta_t} - N_{m,t} \geq 2$, i.e. when there are more than two jump processes of type m over the period $[t, t+\delta_t]$, then $J_{m,i}, \quad i = 1, ..., N_{m,t+\delta_t} - N_{m,t}$ are independent realizations of J_m. Then depending on the processes $\mu(X_t,u_t^*,t), \sigma(X_t,u_t^*,t)$ and $\lambda(X_t,u_t^*,t)$ we are either able to calculate the conditional expectation for the ratio in closed form or we can approximate it.

The unknowns in the recursive equation are therefore the conditional expectation and the vector of optimal control variables u_t^*.

We now describe the main characteristics of the algorithm in the one-dimensional case with single state variable X_t. The detailed algorithm for the multi-dimensional case is given in appendix 3.E. Similar to value function iteration, the algorithm starts at time T far in the future and we solve the problem backwards. Instead of using an equally spaced grid, we randomly draw grid points every time period from a uniform distribution. The advantage is that the grid points are better spread over the parameter space. We redraw the grid points every time period and even allow the boundaries of the grid to depend on the time period. It can be useful to have a time-varying boundary if the range of a state

Figure 3.3: *An example of a stochastic grid in the one-dimensional case with* $T = 10$ *and* $\delta_t = 1$.

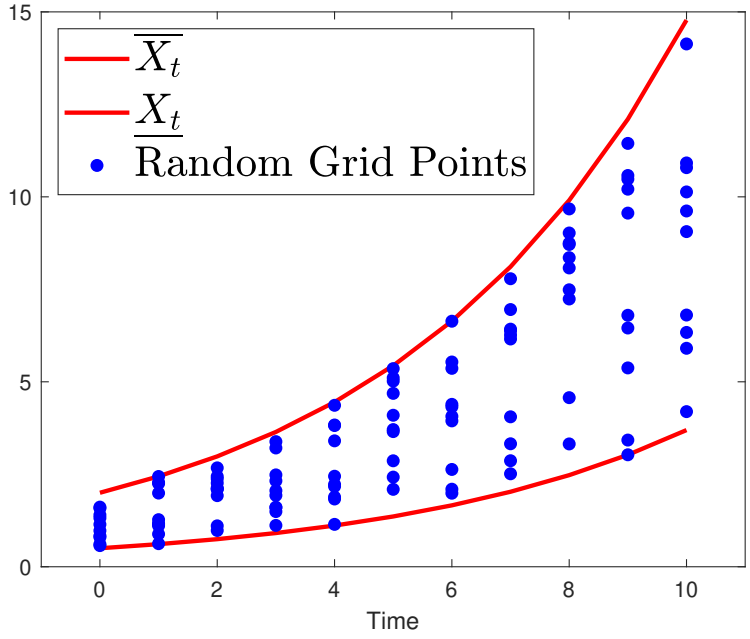

variable that you are interested in varies over time, for example if the state variable is exponentially growing. An example of a stochastic grid is given in figure 3.3.

Now assume that at time $t+\delta_t$ we know the function $g_{t+\delta_t} = g(X_{t+\delta_t}, t+\delta_t)$ at random grid points $X_{t+\delta_t}(1)$ up to $X_{t+\delta_t}(K)$. We perform the following steps to obtain the value function at time t. First, the value function is regressed on the polynomial basis functions 1, $X_{t+\delta_t}$, $X^2_{t+\delta_t}$, ..., $X^L_{t+\delta_t}$ where L controls the highest order of the polynomial basis functions. This regression gives coefficients $\nu_{0,t+\delta_t}$ up to $\nu_{L,t+\delta_t}$ and we then approximately have:

$$g(X_{t+\delta_t}, t+\delta_t) \approx \sum_{i=0}^{L} \nu_{i,t+\delta_t} X^i_{t+\delta_t}. \tag{3.31}$$

We now know the (approximate) value of $g_{t+\delta_t}$ at the entire parameter space. Some examples of function approximation for different levels of L are given in figure 3.4. To calculate optimal policy, we use a non-linear solver to solve the first order condition. Optimal policy u^* is an implicit function of the derivative of $g_{t+\delta_t}$ with respect to $X_{t+\delta_t}$, which can easily be calculated as: $\frac{\partial g(X_{t+\delta_t}, t+\delta_t)}{\partial X_{t+\delta_t}} \approx \sum_{i=1}^{L} i\nu_{i,t+\delta_t} X^{i-1}_{t+\delta_t}$.

The next step is to draw random grid points $X_t(1)$ up to $X_t(K)$ and to calculate the conditional expectation of the value function $E_t\big[g_{t+\delta_t}|X_t(k)\big]$ for each of the random grid points $X_t(k)$, $k = 1, ..., K$. Using our functional form for $g_{t+\delta_t}$, we have:

$$E_t\Big[g_{t+\delta_t}|X_t(k)\Big] \approx \sum_{i=0}^{L} \nu_{i,t+\delta_t} E_t\Big[X^i_{t+\delta_t}|X_t(k)\Big]. \tag{3.32}$$

We use Itô calculus to calculate the conditional expectations of the state variables. For

Figure 3.4: *Some examples of function approximation using basis function regression for different levels of L. L controls the highest order of the basis functions.*

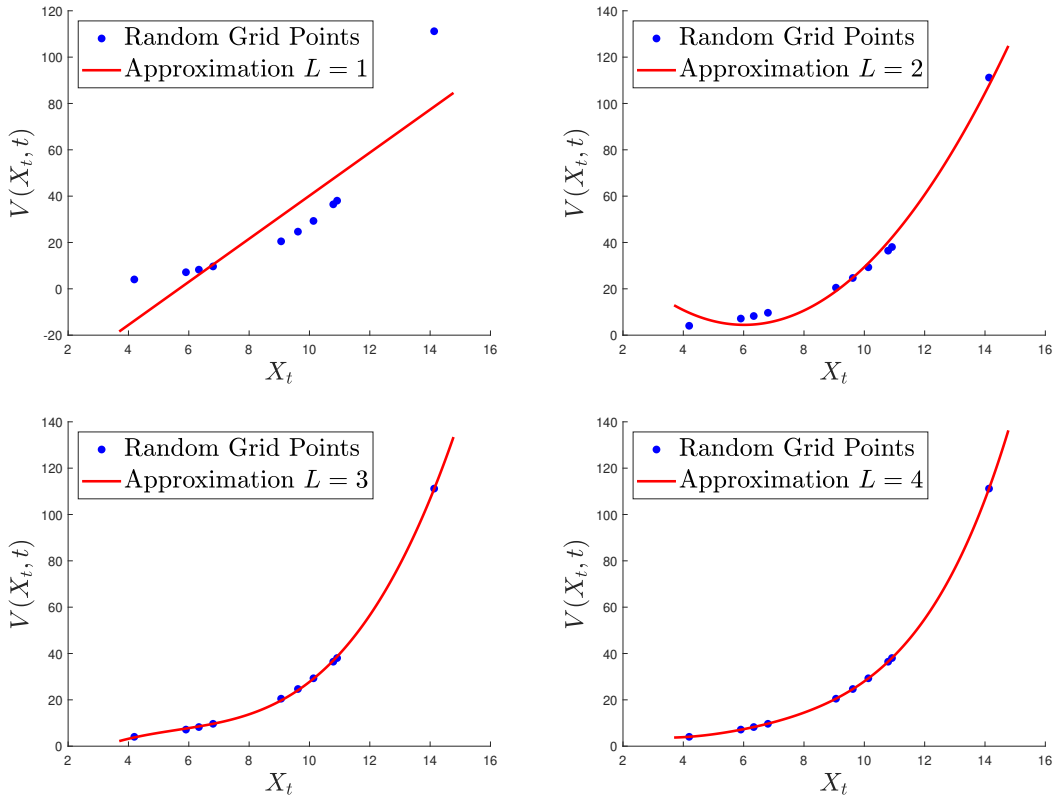

example, if $dX_t = \mu dt + \sigma dZ_t$, we can apply Itô's lemma to obtain:

$$dX_t^i = \Big(i\mu X_t^{i-1} + \frac{1}{2}i(i-1)\sigma^2 X_t^{i-2}\Big)dt + iX_t^{i-1}\sigma dZ_t. \tag{3.33}$$

For small time steps the following approximation is reasonable:

$$E_t\Big[X_{t+\delta_t}^i | X_t(k)\Big] \approx X_t(k)^i + \Big(i\mu X_t(k)^{i-1} + \frac{1}{2}i(i-1)\sigma^2 X_t(k)^{i-2}\Big)\delta_t. \tag{3.34}$$

Applying (3.29) then yields the value function $g(X_t, t)$ at the random grid points $X_t(1)$ up to $X_t(K)$. Starting with a guess at terminal date T and repeating the previous steps every time period, we obtain an approximation of the true value function at time 0 for the entire parameter space.

The main advantage of this algorithm is that the random grid points are spread well over the parameter space. The number of grid points can be much smaller compared to conventional equally spaced grids, without losing much accuracy. Furthermore, compared to other least squares solution methods, the only randomness in this method are the grid points. We do not have to simulate shocks, since we use the closed form conditional expectations of the basis functions. This combination makes the algorithm efficient to solve high-dimensional optimal control problems.

3.5 Results

In this section we present several numerical results. All computations are performed on a laptop with 7-th generation intel i7 processor, 4 cores and 16GB RAM. The first example that we consider is the asset pricing model of Wachter (2013).

3.5.1 Time-varying jump risk

Wachter (2013) considers a jump risk model where the arrival rate is time-varying. The model can be solved analytically when it is assumed that $\epsilon = 1$, but in this example we deviate from this assumption. Furthermore, we use a different jump size distribution for tractability. Except from that, the model is identical to the model developed in Wachter (2013). The growth rate μ and volatility σ of the endowment process are constant. There is a single Poisson process with arrival rate λ_t, which is time-varying. The jump size $1+J$ follows a power distribution with parameter α_J and pdf $f(x) = \alpha_J x^{\alpha_J - 1}, \quad 0 < x < 1$. This gives: $E[J] = \frac{-1}{\alpha_J + 1}$ and $E\Big[(1+J)^n\Big] = \frac{\alpha_J}{\alpha_J + n}$.

The model has a single state variable, namely the arrival rate λ_t. λ_t follows a Cox-Ingersoll-Ross (CIR) process:

$$\lambda_t = \kappa_\lambda(\overline{\lambda} - \lambda_t)dt + \sigma_\lambda\sqrt{\lambda_t}dZ_t^\lambda. \tag{3.35}$$

The calibration is given in table 3.1. This problem does not have any control variables and $\xi_t = 1$ which implies that endowment and consumption are equal in equilibrium: $Y_t = C_t$.

Table 3.1: *Calibration.*

Parameter	Value
γ	4
ϵ	1.5
β	0.02
μ	0.025
σ	0.03
$\overline{\lambda}$	0.035
κ	0.08
σ_λ	0.07
α_J	6.5

Table 3.2: *Consumption-wealth ratio, the function g, interest rate, risk premium and computation time for different number of points N* ($\lambda_t = \overline{\lambda}$).

# points	$k = \frac{C}{S}$	g	$\frac{\partial g}{\partial \lambda_t}$	Interest rate	Risk premium	time (s)
201	1.724%	0.263	3.410	0.922%	2.849%	0.03
2001	1.708%	0.242	3.053	0.931%	2.831%	0.04
20001	1.707%	0.240	3.021	0.932%	2.830%	0.13
200001	1.706%	0.240	3.018	0.932%	2.829%	1.49

Finite Difference Method This problem is an infinite horizon problem without explicit time dependency, which implies that the time derivative is equal to zero. Furthermore, the problem is one-dimensional which implies we do not have to use the sparse grid method. We use an equally spaced one-dimensional grid to discretize the problem. The only state variable is the arrival rate: $X_t = \lambda_t$. The following parameters are used: $[\underline{X}, \overline{X}] = [0, 1]$, $\Delta = 50$, $crit = 10^{-6}$ and we vary the number of points. The right boundary is chosen such that increasing the boundary does not change the results anymore. As initial guess, we choose g_T^δ such that g_T^δ solves $R(X_t, g_t, t) = 0$ at the grid points. This initial guess is chosen since it makes sure that the finite difference scheme satisfies the stability conditions.

Table 3.2 illustrates the results for $\lambda_t = \overline{\lambda}$. Since the problem is only one-dimensional, the finite-difference scheme is very fast. When λ_t is at its average value, the model generates a risk-free rate of 0.9% and a risk premium of 2.8%. The consumption-wealth ratio is around 1.7%. The risk-free rate is close to the historical observed real risk-free rate. The risk-premium is bit lower than the historical equity premium, which implies that this model does not fully solve the equity premium puzzle (Mehra & Prescott, 1985). Dimson, Marsh, and Staunton (2011) estimate the world-wide historical equity premium to be around 4.5%, which shows that the model implied equity premium is on the low side. One way to obtain a more realistic equity premium is to introduce leverage, as Wachter (2013) does. However, since it is not our main purpose to solve this puzzle, we will not consider this extension.

Stochastic Grid Method We compare the stochastic grid method with the finite difference method. λ_t follows a CIR-process. Shao (2012) shows that this implies that the increments of the arrival rate follow a non-central χ^2 distribution:

$$\begin{aligned}
&\lambda_{t_{i+1}}|\lambda_{t_i}(k) \sim a_2\chi^2_{a_1}(a_3\lambda_{t_i}(k)) \text{ where} \\
&a_1 = \frac{4\kappa_\lambda\overline{\lambda}}{\sigma_\lambda^2}, \quad a_2 = \frac{\sigma_\lambda^2(1-e^{-\kappa_\lambda\delta_t})}{4\kappa} \text{ and } a_3 = \frac{4\kappa_\lambda e^{-\kappa_\lambda dt}}{\sigma_\lambda^2(1-e^{-\kappa_\lambda\delta_t})}.
\end{aligned} \tag{3.36}$$

As basis functions we use standard polynomials: $B_j\big(\lambda_t\big) = \lambda_t^j$. Therefore, $E_{t_i}[B(\lambda_{t_{i+1}})|\lambda_{t_i}(k)]$ is just a vector of moments of the non-central χ^2-distribution, which are known in closed form. Also $E_{t_i}\Big[\frac{Y_{t_{i+1}}^{1-\gamma}}{Y_{t_i}^{1-\gamma}}|\lambda_{t_i}(k)\Big]$ can be calculated in closed form:

$$\begin{aligned}
&E_{t_i}\Big[\frac{Y_{t_{i+1}}^{1-\gamma}}{Y_{t_i}^{1-\gamma}}|\lambda_{t_i}(k)\Big] = E_{t_i}\Big[\exp\Big((1-\gamma)(\mu-\sigma^2/2)\delta_t + (1-\gamma)\sigma(Z^c_{t_{i+1}} - Z^c_{t_i}) \\
&+ (1-\gamma)\sum_{j=1}^{N_{t_{i+1}}-N_{t_i}}\log(1+J_j)\Big)\Big] = \exp\Big((1-\gamma)(\mu-\sigma^2/2)\delta_t \\
&+ \frac{1}{2}(1-\gamma)^2\sigma^2\delta_t + E_{t_i}\Big[\int_{t_i}^{t_{i+1}}\lambda_s ds|\lambda_{t_i}(k)\Big]E[(1+J)^{1-\gamma}-1]\Big).
\end{aligned} \tag{3.37}$$

We approximate $E_{t_i}\Big[\int_{t_i}^{t_{i+1}}\lambda_s ds|\lambda_{t_i}(k)\Big]$ by $\lambda_{t_i}(k)\delta_t$, which is a decent approximation for small time steps.

We have to choose several algorithmic parameters. First, we fix T at 500 years. For larger values of T the outcomes do not change anymore. When there is no jump risk, the problem can be solved in closed form. We use the g that belongs to the problem without jump risk as guess for g at terminal time for all grid points. The number of grid points equals: $K = 1000$. Increasing K doesn't change the results. Since there is no explicit time dependence, we choose $\overline{X_{t_i}} = 0.1$ and $\underline{X_{t_i}} = 0$ for any t_i.

Table 3.3 shows the results for the stochastic grid method. In the first step, we start with a fast run. After that run we change several algorithmic parameters to see how that influences the estimate. The first run uses 3 basis functions (up to quadratic) and has a time step δ_t of 1 year. The algorithm is fast but is also not very accurate. Increasing the number of basis function to 9 improves the estimate a lot. To verify how important the discretization error is, we then decrease the time step to δ_t to 0.1. This is a slight improvement. This run takes about 9 seconds. In the last step we again decrease the time step ($\delta_t = 0.01$). The run now takes around 90 seconds. There is only modest improvement now. If we compare the results of the last run to the results of the finite difference method, the two are very close.

The computation time depends a lot on the discount rate β. In this example we use a discount rate $\beta = 2\%$. However, if we would choose e.g. $\beta = 5\%$, the problem will converge in much shorter time period and we could choose T smaller.

Graphical results We have now presented the results at one specific point, namely $\lambda_t = \overline{\lambda}$. In this section we present graphically the results for an entire grid of values

Table 3.3: *Consumption-wealth ratio, the function g, interest rate, risk premium and computation time for different algorithmic parameters.*

N_b	δ_t	$k = \frac{C}{S}$	g	$\frac{\partial g}{\partial \lambda_t}$	r	rp	time (s)
3	1	1.657%	0.184	2.066	0.966%	2.762%	0.2
6	1	1.698%	0.229	2.872	0.934%	2.826%	0.6
9	1	1.704%	0.236	3.004	0.929%	2.836%	1.0
9	0.1	1.705%	0.238	3.001	0.932%	2.829%	8.6
9	0.01	1.706%	0.239	3.001	0.933%	2.828%	88.9

for λ_t. The results are shown in figure 3.5. The consumption-wealth ratio is not very responsive to changes in the arrival rate. However, the risk-free rate and the equity premium do react a lot. The risk-free rate even becomes negative if the arrival rate is large enough. The risk premium also increases a lot for large values of λ_t.

Concluding, the stochastic grid method provides accurate solutions in a reasonable time for this example, but in a one-dimensional setting the finite difference method is much faster. It is clear that this model is quite non-linear, since relatively many points are needed for the finite difference method to converge. Also for the stochastic grid method, three basis functions are not enough to capture the curvature of the function g. This example illustrates the capability of these methods to solve non-linear problems.

3.5.2 Multidimensional climate problem

The second problem we consider is a multidimensional climate problem similar to the model in chapter 2. However, instead of having a deterministic climate model we assume that the climate model is stochastic. We take our climate model from Aengenheyster, Feng, Van der Ploeg, and Dijkstra (2018), who develop a stochastic climate model. In their paper, the stochastic climate model is used to answer the following question: by how much should carbon emissions be reduced to meet the 2 degrees target with 67% probability in 2100? We integrate the stochastic model in a consumption based asset pricing model with an exogenous emissions path to calculate the social cost of carbon.

The model setup is as follows. $\mu_t = \mu$ and $\sigma_t = \sigma$ are constant. There are two Poisson processes: $N_{1,t}$ and $N_{2,t}$. $N_{1,t}$ reflects economic disasters as in the example of the previous subsection. In contrast to the previous model, we now assume that the arrival rate $\lambda_{1,t} = \lambda_1$ is constant. J_1 has again a power distribution with parameter α_{J_1}. The second type of disasters are climate disasters. The arrival rate of climate disasters is assumed to increase with the temperature: $\lambda_{2,t} = \lambda_2 T_t$. J_2 also follows a power distribution with parameter α_{J_2}.

Carbon emissions E_t (in GtC) are an exogenous function of time and calibrated to match the business-as-usual scenario of the DICE model (Nordhaus, 2017): $E_t = 1450.84 \exp(-4.933e^{-0.0075t} - 0.02t)$.

The vector of state variables equals $X_t = [M_{P,t} \;\; M_{1,t} \;\; M_{2,t} \;\; M_{3,t} \;\; T_{0,t} \;\; T_{1,t} \;\; T_{2,t}]'$. $M_t = M_{P,t} + M_{1,t} + M_{2,t} + M_{3,t}$ is the atmospheric carbon concentration and $T_t = T_{0,t} + T_{1,t} + T_{2,t}$ is

Figure 3.5: *The consumption-wealth ratio, risk-free rate and the risk premium as a function of the state variable* λ_t.

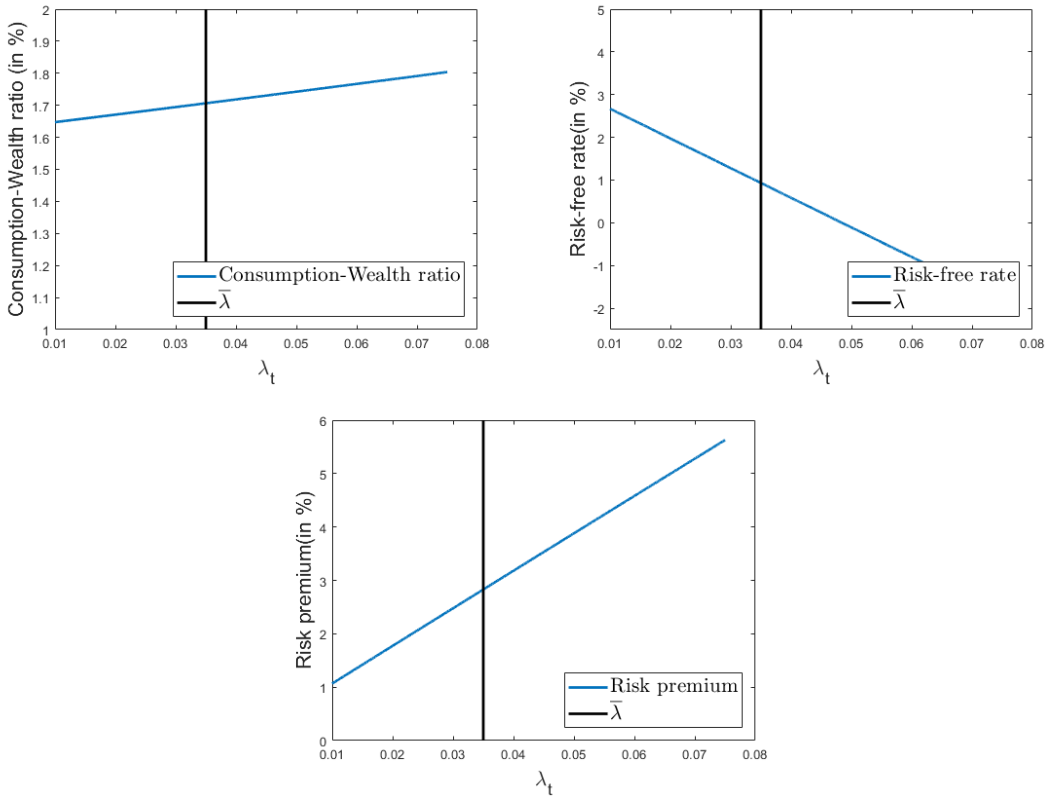

the temperature anomaly. The idea is to model artificial carbon and temperature boxes in order to mimic the dynamics of the complex climate system. Atmospheric carbon concentration is measured in GtC and temperature in ^oC. Define radiative forcing at time t as $F_t = A \log\left(\frac{M_t}{M_{pre}}\right)$. The drift and volatility vectors are defined as:

$$\mu_X = \begin{bmatrix} a_0 E_t \\ a_1 E_t - \frac{1}{\tau_1} M_{1,t} \\ a_2 E_t - \frac{1}{\tau_2} M_{2,t} \\ a_3 E_t - \frac{1}{\tau_3} M_{3,t} \\ b_0 F_t - \frac{1}{\tau_{b_0}} T_{0,t} \\ b_1 F_t - \frac{1}{\tau_{b_1}} T_{1,t} \\ b_2 F_t - \frac{1}{\tau_{b_2}} T_{2,t} \end{bmatrix}, \quad \sigma_X = \begin{bmatrix} 0 & 0 & 0 & 0 & 0 & 0 & 0 \\ 0 & 0 & 0 & 0 & 0 & 0 & 0 \\ 0 & 0 & \sigma_{M_2} & 0 & 0 & 0 & 0 \\ 0 & 0 & 0 & 0 & 0 & 0 & 0 \\ 0 & 0 & 0 & 0 & \sigma_{T_0} & 0 & 0 \\ 0 & 0 & 0 & 0 & 0 & 0 & 0 \\ 0 & 0 & 0 & 0 & 0 & 0 & \sigma_{T_2} T_t \end{bmatrix}. \tag{3.38}$$

Note that this implies that there is one permanent carbon box $M_{P,t}$ that does never decay. The coefficients a_0, a_1, a_2 and a_3 sum up to 1, such that a percentage a_i of one unit of emissions ends up in the artificial carbon box $M_{i,t}$. The calibration of the model is given in table 3.4.

One of the variables of interest for a climate model is the social cost of carbon, which is the welfare loss of emitting one unit of carbon emissions in terms of consumption units

Table 3.4: *Calibration.*

Par.	Value		Par.	Value		Par.	Value		Par.	Value
γ	4		α_{J_2}	35		τ_3	4.304		τ_{b_1}	1.427062
ϵ	1.5		C_0	80×10^{12}		σ_{M^2}	0.65		τ_{b_2}	8.021185
β	0.02		a_0	0.2173		M_{pre}	592.25		σ_{T^0}	0.015
μ	0.025		a_1	0.2240		A	7.92		σ_{T^2}	0.13
σ	0.03		a_2	0.2824		b_0	0.001152			
λ_1	0.035		a_3	0.2763		b_1	0.109680			
α_{J_1}	6.5		τ_1	394.4		b_2	0.033611			
λ_2	0.015		τ_2	36.54		τ_{b_0}	400			

at time t. In this model it is not straightforward to define the social cost of carbon, since we have four artificial carbon boxes. One unit of emissions will lead to an increase of a_0 units of $M_{P,t}$, a_1 units of $M_{1,t}$, a_2 units of $M_{2,t}$ and a_3 units of $M_{3,t}$. The social cost of carbon then becomes:

$$SCC_t = -\frac{a_0\frac{\partial V_t}{\partial M_{P,t}} + a_1\frac{\partial V_t}{\partial M_{1,t}} + a_2\frac{\partial V_t}{\partial M_{2,t}} + a_3\frac{\partial V_t}{\partial M_{3,t}}}{f_C(C_t, V_t)}. \tag{3.39}$$

Note that the social cost of carbon scales with the endowment or consumption level, since damages are a fraction of endowment. Therefore the social cost of carbon will grow over time. The social cost of carbon in this paper is measured in \$ per ton carbon. To get the social cost of carbon per ton CO_2, the social cost of carbon must be divided by 3.67. As initial consumption level, we use $Y_0 = C_0 = 80$ trillion US \$ where the base year is chosen to be 2015. This is a proxy for world consumption using purchasing power parity (instead of exchange rates) in 2015. The vector of initial points at the base year 2015 is given by: $X_0 = [680.2 \;\; 83.2 \;\; 56.9 \;\; 11.1 \;\; 0.11 \;\; 0.41 \;\; 0.62]'$.

Finite Difference Method The problem that we have to solve is a 7-dimensional problem with explicit time dependence. We choose $\overline{X} = [3000 \;\; 2000 \;\; 250 \;\; 50 \;\; 8 \;\; 3 \;\; 10]'$ and $\underline{X} = [600 \;\; 0 \;\; 0 \;\; 0 \;\; 0 \;\; 0 \;\; 0]'$. With these bounds, except for $M_{P,t}$, all state variables on the left of the grid have a positive drift and on the right of the drift have a negative drift. Therefore, we use as boundary condition that the second derivative vanishes, except for $M_{P,t}$. The drift of $M_{P,t}$ is always positive. Therefore we can again set the second derivative to zero at the left boundary. At the right boundary of $M_{P,t}$, we assume that the first derivative is equal to zero.

To get a good starting guess, we first solve the problem with the finite difference method at $T = 250$ with $\Delta = 50$ and $crit = 10^{-6}$ assuming that there are no emissions: $E_{250} = 0$. The time derivative of g_t comes from carbon emissions and therefore $\frac{\partial g_t}{\partial t} = 0$ in this setup. We use the outcome as our initial guess. Given our initial guess, we solve the actual problem with explicit time dependence starting from $T = 250$ and working backwards in time. A more 'stupid' initial guess would also work, as long as the stability conditions are met using that guess. The algorithm might take longer to converge, so T might have to be chosen larger in that case.

Table 3.5: *Consumption-wealth ratio, g, social cost of carbon, interest rate, risk premium and computation time for different algorithmic parameters.*

L	N	δ_t	$k = \frac{C}{S}$	g	SCC (\$)	r	rp	time (s)
1	1	1	1.600%	0.134	242.2	1.058%	2.506%	2.8
2	8	1	1.601%	0.135	250.0	1.058%	2.506%	8.6
3	36	1	1.603%	0.136	253.0	1.058%	2.506%	57.4
4	120	1	1.603%	0.137	253.4	1.058%	2.506%	287.7
5	330	1	1.603%	0.137	253.0	1.058%	2.506%	1440.1
1	1	0.1	1.600%	0.134	242.3	1.058%	2.506%	17.9
2	8	0.1	1.602%	0.135	250.2	1.058%	2.506%	71.4
3	36	0.1	1.603%	0.136	253.2	1.058%	2.506%	501.6

We use the sparse grid combination method and try different combinations of L and δ_t. Define by N the number of sub-problems that are solved, so N depends on the level of the sparse grid L. We use the semi-implicit method in all runs. The explicit method is not much faster and the semi-implicit method is more stable. One of the outputs of the finite difference method is the first derivative of g_t with respect to the vector of state variables X_t. This derivative is used to calculate the social cost of carbon. The results are given in table 3.5.

If we look at the table, it is clear that the run on a single grid ($L = 1$) and $\delta_t = 1$ already gives a reasonable approximation of the outcomes. This implies that the model is not very non-linear. If we increase the level L to 2 or 3, we see that the social cost of carbon becomes approximately 250\$. Increasing L even further does not change the outcomes much, and also choosing a smaller time step has little effect.

Stochastic Grid Method We use again standard power functions as basis functions. However, in the multidimensional setting we also consider cross terms. Define in this case the highest order of the basis functions by L. Then if $L = 1$, we only consider the vector of linear first order basis functions:

$$B(X_t) = [1 \;\; M_{P,t} \;\; M_{1,t} \;\; M_{2,t} \;\; M_{3,t} \;\; T_{0,t} \;\; T_{1,t} \;\; T_{2,t}]'. \tag{3.40}$$

When $L = 2$, we use basis functions up to order two, for example $(M_{P,t})^2$ and the cross-term $M_{P,t}M_{1,t}$. And for order $L = 3$ we consider e.g. $M^3_{P,t}$, $M^2_{P,t}M_{1,t}$ and $M_{P,t}M_{1,t}M_{2,t}$, so all possible basis functions up to third order. This can be extended to any higher order. We define the number of basis functions again by N_b.

For this setup, there are no closed form expectations of the basis functions available. Using the Euler method, we can still find closed form approximate conditional expectations. The conditional expectation for the linear basis functions are straightforward: $E[X_{t_{i+1}}|X_{t_i}] = X_{t_i} + \mu_X(X_{t_i})\delta_t$. For the higher order and cross terms, we can use Itô-

Table 3.6: *Consumption-wealth ratio, g, social cost of carbon, interest rate, risk premium and computation time for different algorithmic parameters.*

L	N_b	δ_t	$k = \frac{C}{S}$	g	SCC (\$)	r	rp	time (s)
1	8	1	1.606%	0.139	259.2	1.058%	2.506%	0.3
2	36	1	1.606%	0.139	249.5	1.058%	2.506%	1.1
3	120	1	1.373%	0.034	16602.7	1.055%	2.511%	4.7
4	330	1	1.803%	0.394	1127.8	1.058%	2.506%	19.0
1	8	0.1	1.603%	0.137	261.0	1,058%	2.506%	2.7
2	36	0.1	1.604%	0.137	251.4	1.058%	2.506%	10.3
3	120	0.1	1.604%	0.137	250.4	1.058%	2.506%	49.7
4	330	0.1	1.604%	0.137	250.4	1.058%	2.506%	224.2
1	8	0.01	1.603%	0.136	261.1	1.058%	2.506%	27.3
2	36	0.01	1.603%	0.137	251.6	1.058%	2.506%	101.7
3	120	0.01	1.603%	0.137	250.6	1.058%	2.506%	496.1
4	330	0.01	1.603%	0.137	250.6	1.058%	2.506%	2333.7

calculus and then use the Euler method approximation. For example:

$$\begin{aligned} dM_{2,t}^2 &= 2M_{2,t}dM_{2,t} + d[M_2, M_2]_t \\ &= \Big(2M_{2,t}(a_2E_t - \frac{1}{\tau_2}M_{2,t}) + \sigma_{M_2}^2\Big)dt + 2M_{2,t}\sigma_{M_2}dZ_t^{M^2}, \\ E[M_{2,t_{i+1}}^2|M_{2,t_i}] &\approx M_{2,t_i}^2 + \Big(2M_{2,t_i}(a_2E_{t_i} - \frac{1}{\tau_2}M_{2,t_i}) + \sigma_{M_2}^2\Big)\delta_t. \end{aligned} \tag{3.41}$$

The conditional expectation for Y_t becomes:

$$\begin{aligned} E\Big[\frac{Y_{t_{i+1}}^{1-\gamma}}{Y_{t_i}^{1-\gamma}}|X_{t_i}(k)\Big] &= \exp\Big((1-\gamma)(\mu - \sigma^2/2)\delta_t \\ &+ \frac{1}{2}(1-\gamma)^2\sigma^2\delta_t + \lambda_1\delta_t(E[(1+J_1)^{1-\gamma}] - 1) \\ &+ \lambda_2(T_{0,t_i}(k) + T_{1,t_i}(k) + T_{2,t_i}(k))\delta_t(E[(1+J_2)^{1-\gamma}] - 1)\Big). \end{aligned} \tag{3.42}$$

The algorithmic parameters that we use are $T = 500$ and $K = 1000$. To obtain the time-dependent grid boundaries, we first calculate the expected path of the state variables. This can be easily found by setting $\sigma_X = 0$ and solving the system forward using a standard differential equation solver. Around the expected path, we then create an interval for the simulation. Define by X_t^{av} the expected value of the vector of state variables at time t. Then at time t_i, we define the boundaries as: $\overline{X_{t_i}} = X_{t_i}^{av} + [150 \;\; 75 \;\; 37.5 \;\; 7.5 \;\; 1.5 \;\; 0.75 \;\; 1.5]'$ and $\underline{X_{t_i}} = X_{t_i}^{av} - [100 \;\; 50 \;\; 25 \;\; 5 \;\; 1 \;\; 0.5 \;\; 1]'$. If the lower bound becomes negative, we set it equal to zero.

Table 3.6 shows the results for different combinations of L and δ_t. We start with $\delta_t = 1$. The first run with only linear basis functions already gives reasonable results. This again shows that the function g is not very non-linear in the state variables. Increasing L to 2 improves the results, but when L is increased to 3 or 4 the results become unstable.

The SCC explodes. The reason for this is that the conditional expectations of the basis functions are an approximation that depends on the time step, in contrast to the time-varying jump risk example where the conditional expectations could be calculated in closed form. Especially for the higher order basis functions, this approximation seems to be not very accurate. If we decrease the time step δ_t to 0.1 or 0.01, the results also become stable for $L = 3$ and $L = 4$.

Graphical results In this section, we present some graphical results of the evolution of the problem over time. Since the problem is stochastic, we do not know the exact future path of the state variables. The output of the solution methods gives the value function and therefore the social cost of carbon at any time t for any combination of the state variables. The results are graphically presented for the expected path of the state variables. Figure 3.6 shows the climate variables, social cost of carbon, consumption-wealth ratio, risk-free rate and risk premium. Emissions are exogenous and are modeled to peak at the end of the century. Both the carbon concentration and the temperature keep increasing over time. The social cost of carbon at 2015 is approximately 250$ and grows over time, since endowment also grows over time. The risk-free rate slightly declines over time and the risk premium increases due to higher climate risk, but both effects are quantitatively small.

In terms of computation time, the stochastic grid method is more efficient. However, both methods are able to solve this multidimensional problem in reasonable computation time.

3.5.3 Multidimensional climate problem with control variable

In the last example we consider a very similar model as in the previous example, but we add a control variable. In the previous example emissions were entirely exogenous. In this example, the agent can reduce emissions using abatement policy. Assume that $\tilde{E}_t = E_t(1 - u_t)$ are actual carbon emissions where E_t are business-as-usual carbon emissions. u_t is called the emissions control rate. In this example we assume that endowment Y_t can be spent on consumption C_t and abatement A_t. Abatement costs are proportional to output: $A_t = c_{1,t}u_t^{c_2}Y_t$ where $c_2 > 1$ is used to capture that the marginal cost of abatement increases in the emissions control rate and $c_{1,t}$ is declining over time to take into account technological process in abatement technologies. This yields $C_t = Y_t - A_t = (1-c_{1,t}u_t^{c_2})Y_t = \xi_t Y_t$ where $\xi_t = 1-c_{1,t}u_t^{c_2}$. We assume that $u_t \leq 1$, so that it is not possible to take carbon out of atmosphere. At best, it is possible to reduce carbon emissions to zero.

The set of state variables and initial conditions is the same as in the previous example. The only difference is that now in the drift μ_X of the state variables, business-as-usual emissions E_t are replaced by controlled emissions $\tilde{E}_t$. The calibration is also identical, but we have two additional abatement parameters now. These are calibrated to match the abatement function of the DICE model (Nordhaus, 2017): $c_{1,t} = 0.074\exp(-0.019t)$ and $c_2 = 2.8$. As initial endowment level, we take $Y_0 = 80$ trillion US \$. The HJB-equation

Figure 3.6: *The expected paths of emissions, carbon concentration, temperature, social cost of carbon, consumption-wealth ratio, risk-free rate and the risk premium over time.*

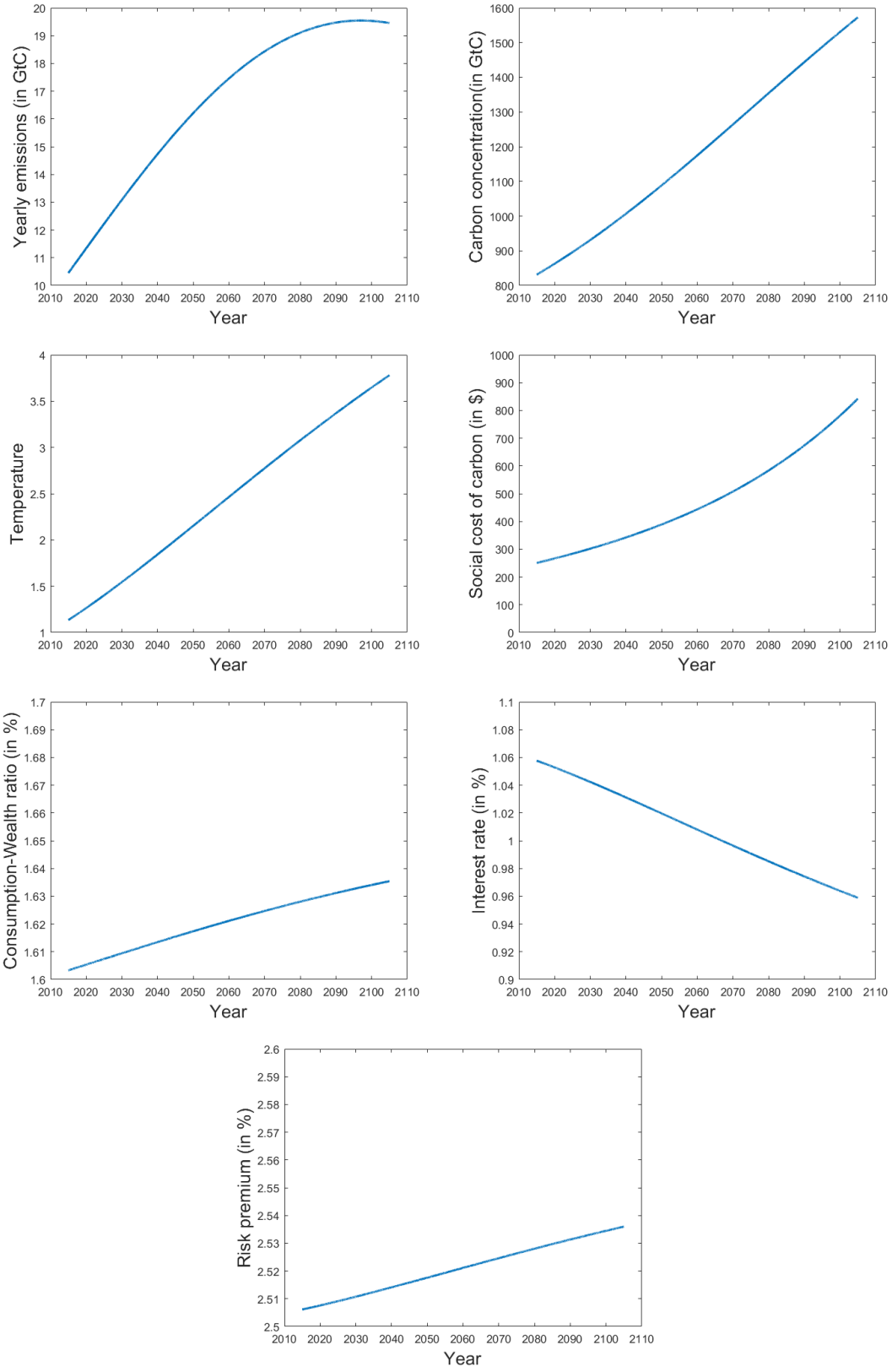

Table 3.7: *Consumption-wealth ratio, g, social cost of carbon, optimal abatement policy, interest rate, risk premium and computation time for different algorithmic parameters.*

L	N	δ_t	$k = \frac{C}{S}$	g	SCC (\$)	u^*	r	rp	time (s)
1	1	1	1.584%	0.125	290.0	38.9%	1.045%	2.506%	11.7
2	8	1	1.586%	0.126	312.2	40.5%	1.043%	2.506%	38.7
3	36	1	1.587%	0.127	325.7	41.5%	1.042%	2.506%	303.4
4	120	1	1.587%	0.127	332.6	42.0%	1.042%	2.506%	2153.4
5	330	1	1.588%	0.128	333.5	42.0%	1.042%	2.506%	12373.5
1	1	0.1	1.584%	0.125	290.0	38.9%	1.045%	2.506%	90.3
2	8	0.1	1.586%	0.126	312.1	40.5%	1.043%	2.506%	344.6
3	36	0.1	1.587%	0.127	325.6	41.5%	1.042%	2.506%	3108.6

corresponding to this problem is:

$$\begin{aligned} 0 = \min_{u_t} \Big\{ \Big(\beta\zeta \Big(g_t^{-\frac{1}{\zeta}} \xi_t^{1-1/\epsilon} - 1 \Big) + (1-\gamma) \Big(\mu - \frac{1}{2}\gamma\sigma^2 + \lambda_1 E\Big[\frac{(1+J_1)^{1-\gamma}-1}{1-\gamma} \Big] \\ + \lambda_2 T_t E\Big[\frac{(1+J_2)^{1-\gamma}-1}{1-\gamma} \Big] \Big) \Big) g_t + \frac{\partial g_t}{\partial t} + g_X \mu_X + \frac{1}{2} tr\Big(g_{XX} \sigma_X \sigma_X' \Big) \Big\}. \end{aligned} \tag{3.43}$$

Taking the first derivative, we obtain the first order condition for u_t:

$$\begin{aligned} 0 = &-\beta(1-\gamma) g_t^{1-\frac{1}{\zeta}} \xi_t^{-1/\epsilon} c_{1,t} c_2 u_t^{c_2-1} \\ &- a_0 \frac{\partial g_t}{\partial M_{P,t}} E_t - a_1 \frac{\partial g_t}{\partial M_{1,t}} E_t - a_2 \frac{\partial g_t}{\partial M_{2,t}} E_t - a_3 \frac{\partial g_t}{\partial M_{3,t}} E_t. \end{aligned} \tag{3.44}$$

This first order condition cannot be solved in closed-form for u_t and therefore the optimal policy u_t is implicitly defined by the first order condition.

Finite difference We use exactly the same algorithmic parameters and boundary conditions as in the previous example. The only difference is that we calculate optimal policy at every time period and grid point. So again we first solve the problem with $E_{250} = 0$ and then solve the problem with explicit time dependence backward in time. The results of the finite difference methods are presented in table 3.7. Compared to the previous problem, this time we need a higher level L for the problem to converge. $L = 3$ already gives relatively accurate results. The time step again does not play an important role, $\delta_t = 1$ seems to be accurate enough. It is also clear that solving for the optimal control variable increases the computation time quite a lot, especially for the higher sparse grid levels.

Stochastic grid method We again assume $T = 500$ but in this case choose $K = 2500$. The reason that we increase K is because the problem is more non-linear compared to the problem without control variable. The non-linearity is due to the cap on the emissions control rate. As lower bound we take the following bounds for any period in time: $\underline{X} = [600 \;\; 0 \;\; 0 \;\; 0 \;\; 0 \;\; 0 \;\; 0]'$. To obtain an upper bound, we first assume a constant

Table 3.8: *Consumption-wealth ratio, g, social cost of carbon, optimal abatement policy, interest rate, risk premium and computation time for different algorithmic parameters.*

L	N_b	δ_t	$k = \frac{C}{S}$	g	SCC (\$)	u^*	r	rp	time (s)
1	8	1	1.590%	0.129	347.4	43.0%	1.041%	2.506%	4.4
2	36	1	1.591%	0.130	326.5	41.5%	1.042%	2.506%	8.6
3	120	1	-	-	-	-	-	-	-
4	330	1	-	-	-	-	-	-	-
1	8	0.1	1.586%	0.127	350.7	43.2%	1.041%	2.506%	39.4
2	36	0.1	1.588%	0.128	329.4	41.7%	1.042%	2.506%	77.5
3	120	0.1	1.588%	0.128	327.8	41.6%	1.042%	2.506%	217.8
4	330	0.1	1.588%	0.128	327.7	41.6%	1.042%	2.506%	832.4
1	8	0.01	1.586%	0.127	351.0	43.2%	1.041%	2.506%	387.4
2	36	0.01	1.587%	0.127	329.7	41.7%	1.042%	2.506%	774.8
3	120	0.01	1.587%	0.127	328.1	41.6%	1.042%	2.506%	2237.2
4	330	0.01	1.587%	0.127	328.0	41.6%	1.042%	2.506%	8156.5

policy rule of $u = 0.5$. We then calculate the expected path of state variables X_t^{av} given $u = 0.5$ by solving the system forward with $\sigma_X = 0$. At time t_i, we define the upper boundary as: $\overline{X_{t_i}} = X_{t_i}^{av} + [150 \quad 75 \quad 37.5 \quad 7.5 \quad 1.5 \quad 0.75 \quad 1.5]'$. We tried different choices for u and this does not seem to matter much, as long as the resulting interval turns out to be roughly around the optimal expected path of state variables. In general, the results seem to be robust against differences in the boundaries.

The outcomes and computation times are given in table 3.8. Taking $L = 2$ and $\delta_t = 1$ provides reasonable results in a short computation time. In this case, the problem does not even converge for $L > 2$ and $\delta_t = 1$, due to the approximation error of the conditional expectations. Decreasing δ_t to 0.1 and choosing $L = 3$ gives accurate results in a few minutes. Increasing L or decreasing δ_t even further does not change the results much.

Graphical results Again, we present results for the expected path of state variables over time. Since we do not know the optimal emissions control rate before solving the problem, we first solve the problem backward and then iterate forward to obtain the expected path of state variables. The graphs are presented in figure 3.7. The optimal emissions control rate equals roughly 40% in 2015 and increases over time. The reason of this increase over time is that the abatement costs are assumed to decrease over time. In the optimal policy scenario the emissions control rate reaches 100% between 2065 and 2070. The temperature level peaks at 1.7 degrees, which is in line with the Paris climate agreement.

The social cost of carbon at 2015 is approximately 330\$, which is larger than in the business-as-usual scenario. If we look at the consumption-endowment ratio, we see that the slope of ξ_t changes at the point where the emissions control rate reaches its upper bound of 100%. Up to that moment, the amount of endowment that is spent on abatement is increasing. Although abatement becomes cheaper, the emissions control rate increases fast enough to make the total amount increasing. However, when the upper bound is

Figure 3.7: *The expected paths of emissions, carbon concentration, temperature, social cost of carbon, consumption-endowment ratio, risk-free rate and the risk premium over time.*

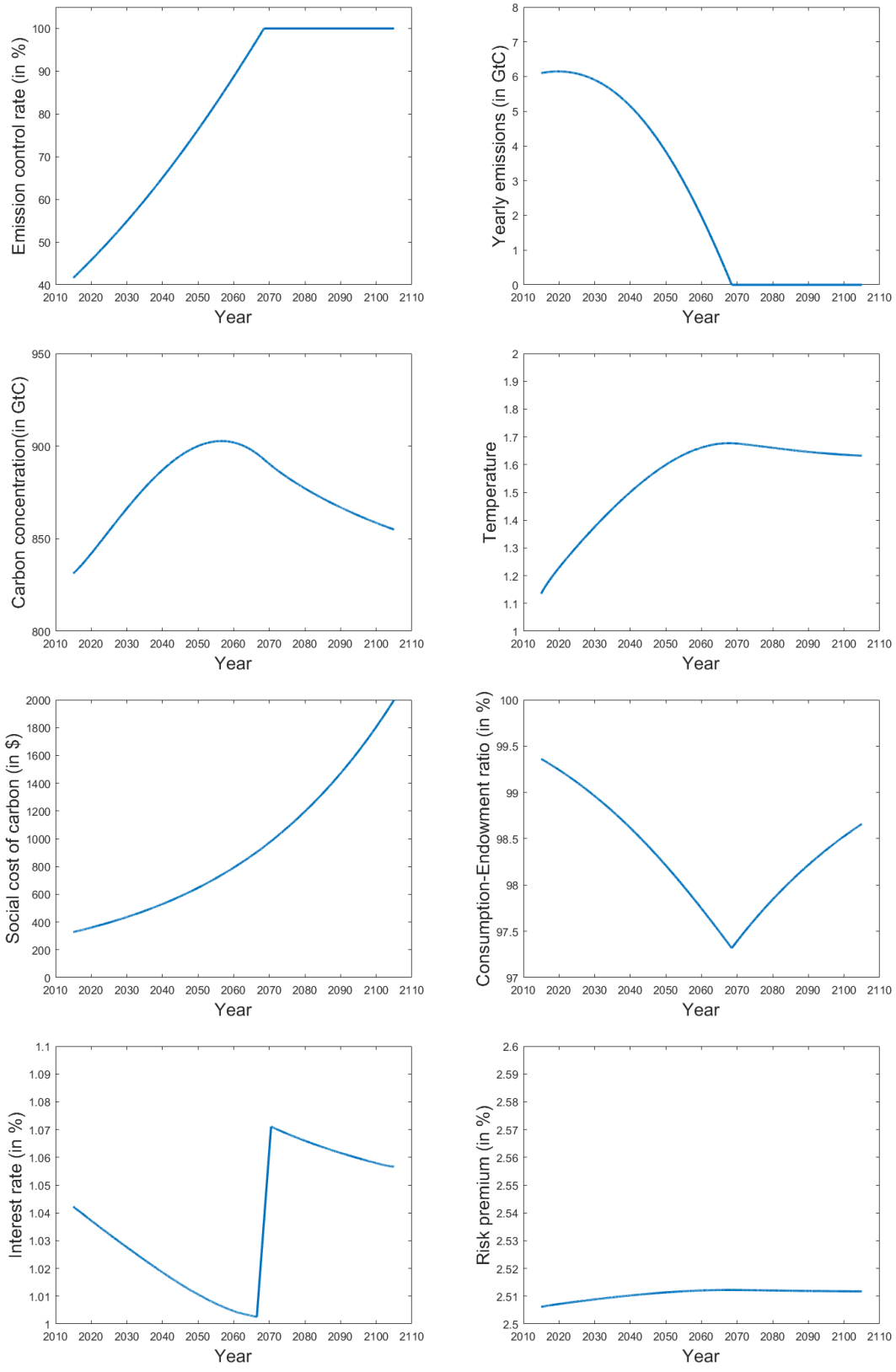

reached, the amount spent on abatement decreases over time. At the moment that u_t^* reaches its upper bound there is a jump in the interest rate, since the growth rate of the endowment-consumption ratio (μ_ξ) jumps. However, quantitatively the effect of climate change on the risk-free rate and risk premium is not very large.

Comparing the two methods in this case, it is clear that the stochastic grid method outperforms the finite difference method. The stochastic grid method converges faster and the computation time increases not as fast when the accuracy of the solution method is increased. The main reason is that the number of grid points increases much faster for the finite difference method than for the stochastic grid method. One of the most time-consuming parts of the algorithm is to find the optimal policy at every grid point. This leads to very large computation times for more accurate runs of the finite difference method. For multi-dimensional problems with optimal policy, it is therefore more efficient to use the stochastic grid method.

3.6 Conclusion

We have developed and compared two solution methods that are suitable to solve multi-dimensional DSGE models. The finite difference method has recently been popular to solve macro-models. We extend this method to the setting with Epstein-Zin preferences and show how to easily apply the finite difference method on sparse grids using the combination method. This method is capable of solving the 7-dimensional optimal control example of an economic model with a climate change externality. However, the computation time increases substantially for denser grids, which might be problematic if one wants to solve high-dimensional problems that are very non-linear.

The second method that we have discussed is the stochastic grid method that up to now is mostly applied to option pricing applications. We show that this method is very suitable to solve optimal control DSGE models with multiple state variables. The method is able to solve the example problem within a few minutes. It does not suffer from the curse of dimensionality. The conditional expectations are straightforward to calculate for any set of basis functions by applying Itô calculus. This makes the method flexible and makes it also able to solve non-linear problems. The order of basis functions can be increased to capture the non-linearities.

In this paper only three numerical examples have been considered. It would be interesting to see how these methods perform on problems with different characteristics. As mentioned before, another topic for further research is to see how the methods perform if there is correlation between the state variables.

3.A Asset prices

3.A.1 Consumption-wealth ratio

S_t equals the total wealth of the representative agent. At the optimum, the following condition is satisfied: $f_C = V_S$ (see for example Tsai and Wachter (2018)). Now define the consumption-wealth ratio by $k_t = \frac{C_t}{S_t}$. Using the chain rule, this implies that $V_S = V_C k_t$. The optimality condition then implies that: $k_t = \frac{f_C}{V_C}$. We can calculate f_C:

$$f_C(C,V) = \frac{\beta C^{-1/\epsilon}}{\big((1-\gamma)V\big)^{\frac{1}{\zeta}-1}}. \tag{3.45}$$

Substituting in $f_c, V_t = g_t \frac{Y_t^{1-\gamma}}{1-\gamma} = g_t \frac{(\frac{C_t}{\xi_t})^{1-\gamma}}{1-\gamma}$ and $V_C = g_t \xi_t^{\gamma-1} C_t^{-\gamma}$ gives:

$$k_t = \beta g_t^{-\frac{1}{\zeta}} \xi_t^{1-1/\epsilon}. \tag{3.46}$$

3.A.2 Stochastic discount factor

Duffie and Epstein (1992a) derive that the stochastic discount factor with stochastic differential utility equals $\pi_t = \exp\Big\{ \int_0^t f_V(C_s,V_s)ds \Big\} f_C(C_t,V_t)$.

We will start with deriving the explicit stochastic differential equation of the stochastic discount factor. First we calculate the derivatives of $f(C,V)$ with respect to V (the derivative with respect to C is given in the previous subsection):

$$f_V(C,V) = \beta\zeta\Big\{ \Big(1-\frac{1}{\zeta}\Big)\Big((1-\gamma)V\Big)^{-\frac{1}{\zeta}} C^{1-1/\epsilon} - 1 \Big\}. \tag{3.47}$$

Substituting $V_t = g_t \frac{Y_t^{1-\gamma}}{1-\gamma}$ and $C_t = \xi_t Y_t$ into $f_C(C,V)$ and $f_V(C,V)$ we obtain:

$$f_C(C_t,V_t) = \beta \xi_t^{-1/\epsilon} g_t^{1-\frac{1}{\zeta}} Y_t^{-\gamma}, \tag{3.48}$$

$$f_V(C_t,V_t) = \beta\zeta\Big\{ g_t^{-\frac{1}{\zeta}} \xi_t^{1-1/\epsilon}\Big(1-\frac{1}{\zeta}\Big) - 1 \Big\}. \tag{3.49}$$

This gives:

$$\pi_t = \exp\left(\int_0^t \beta\zeta\Big\{ g_s^{-\frac{1}{\zeta}} \xi_s^{1-1/\epsilon}\Big(1-\frac{1}{\zeta}\Big) - 1 \Big\} ds \right) \beta \xi_t^{-1/\epsilon} g_t^{1-\frac{1}{\zeta}} Y_t^{-\gamma}. \tag{3.50}$$

Write as a differential equation:

$$\frac{d\pi_t}{\pi_{t-}} = \beta\zeta\Big\{ g_t^{-\frac{1}{\zeta}} \xi_t^{1-1/\epsilon}\Big(1-\frac{1}{\zeta}\Big) - 1 \Big\} dt + \frac{dY_t^{-\gamma}}{Y_{t-}^{-\gamma}} + \frac{dg_t^{1-1/\zeta}}{g_t^{1-1/\zeta}} + \frac{d\xi_t^{-1/\epsilon}}{\xi_t^{-1/\epsilon}} + \frac{d[g_t^{1-1/\zeta}, \xi_t^{-1/\epsilon}]}{g_t^{1-1/\zeta}\xi_t^{-1/\epsilon}}. \tag{3.51}$$

Applying Itô's lemma to $Y_t^{-\gamma}$ gives:

$$dY_t^{-\gamma} = -\gamma\Big(\mu_t - \frac{1}{2}(\gamma+1)\sigma_t^2\Big)Y_t^{-\gamma}dt - \gamma\sigma_t Y_t^{-\gamma}dZ_t^c + \sum_{m=1}^{M}\Big((1+J_m)^{-\gamma}-1\Big)Y_{t-}^{-\gamma}dN_{m,t}. \quad (3.52)$$

We can also apply Itô's lemma to $g_t^{1-1/\zeta}$:

$$\begin{aligned} dg_t &= \Big(\frac{\partial g_t}{\partial t} + g_X\mu_X + \frac{1}{2}tr(g_{XX}\sigma_X\sigma_X')\Big)dt + g_X\sigma_X dZ_t^X, \\ dg_t^{1-1/\zeta} &= (1-1/\zeta)\Bigg(\frac{\frac{\partial g_t}{\partial t}}{g_t} + \frac{g_X}{g_t}\mu_X + \frac{1}{2}tr\Big(\frac{g_{XX}}{g_t}\sigma_X\sigma_X'\Big) \\ &\quad - \frac{1}{2}\frac{1}{\zeta}tr\Big(\frac{g_X'g_X}{g_t^2}\sigma_X\sigma_X'\Big)\Bigg)g_t^{1-1/\zeta}dt + (1-1/\zeta)\frac{g_X}{g_t}g_t^{1-1/\zeta}\sigma_X dZ_t^X. \end{aligned} \quad (3.53)$$

And lastly, applying Itô's lemma to $\xi_t^{-1/\epsilon}$ gives:

$$\begin{aligned} d\xi_t &= \Big(\frac{\partial \xi_t}{\partial t} + \xi_X\mu_X + \frac{1}{2}tr(\xi_{XX}\sigma_X\sigma_X')\Big)dt + \xi_X\sigma_X dZ_t^X, \\ d\xi_t^{-1/\epsilon} &= -1/\epsilon\Bigg(\frac{\frac{\partial \xi_t}{\partial t}}{\xi_t} + \frac{\xi_X}{\xi_t}\mu_X + \frac{1}{2}tr\Big(\frac{\xi_{XX}}{\xi_t}\sigma_X\sigma_X'\Big) \\ &\quad - \frac{1}{2}(1+1/\epsilon)tr\Big(\frac{\xi_X'\xi_X}{\xi_t^2}\sigma_X\sigma_X'\Big)\Bigg)\xi_t^{-1/\epsilon}dt - 1/\epsilon\frac{\xi_X}{\xi_t}\xi_t^{-1/\epsilon}\sigma_X dZ_t^X. \end{aligned} \quad (3.54)$$

The quadratic covariation between $g_t^{1-1/\zeta}$ and $\xi_t^{-1/\epsilon}$ equals:

$$\frac{d[g_t^{1-1/\zeta}, \xi_t^{-1/\epsilon}]}{g_t^{1-1/\zeta}\xi_t^{-1/\epsilon}} = -1/\epsilon(1-1/\zeta)tr\Big(\frac{g_X'\xi_X}{g_t\xi_t}\sigma_X\sigma_X'\Big)dt. \quad (3.55)$$

Define $\mu_g = \frac{\frac{\partial g_t}{\partial t}}{g_t} + \frac{g_X}{g_t}\mu_X + \frac{1}{2}tr\Big(\frac{g_{XX}}{g_t}\sigma_X\sigma_X'\Big)$ and $\mu_\xi = \frac{\frac{\partial \xi_t}{\partial t}}{\xi_t} + \frac{\xi_X}{\xi_t}\mu_X + \frac{1}{2}tr\Big(\frac{\xi_{XX}}{\xi_t}\sigma_X\sigma_X'\Big)$. Combining everything gives:

$$\begin{aligned} \frac{d\pi_t}{\pi_{t-}} =& \Big\{\beta\zeta\Big(g_t^{-\frac{1}{\zeta}}\xi_t^{1-1/\epsilon}\big(1-\frac{1}{\zeta}\big)-1\Big) - \gamma\Big(\mu_t - \frac{1}{2}(\gamma+1)\sigma_t^2\Big) \\ &- 1/\epsilon\Big(\mu_\xi - \frac{1}{2}(1+1/\epsilon)tr\Big(\frac{\xi_X'\xi_X}{\xi_t^2}\sigma_X\sigma_X'\Big)\Big) - 1/\epsilon(1-1/\zeta)tr\Big(\frac{g_X'\xi_X}{g_t\xi_t}\sigma_X\sigma_X'\Big) \\ &+ (1-1/\zeta)\Big(\mu_g - \frac{1}{2}\frac{1}{\zeta}tr\Big(\frac{g_X'g_X}{g_t^2}\sigma_X\sigma_X'\Big)\Big)\Big\}dt \\ &- \gamma\sigma_t dZ_t^c + \Big((1-1/\zeta)\frac{g_X}{g_t}\sigma_X - 1/\epsilon\frac{\xi_X}{\xi_t}\sigma_X\Big)dZ_t^X + \sum_{m=1}^{M}\Big((1+J_m)^{-\gamma}-1\Big)dN_{m,t}. \end{aligned} \quad (3.56)$$

We can now substitute the HJB-equation into the stochastic discount factor. Note that we can rewrite the HJB-equation as:

$$\mu_g = -\beta\zeta\Big(g_t^{\frac{-1}{\zeta}}\xi_t^{1-1/\epsilon}-1\Big) - (1-\gamma)\Big(\mu_t - \frac{1}{2}\gamma\sigma_t^2 + \sum_{m=1}^{M}\lambda_{m,t}E\Big[\frac{(1+J_m)^{1-\gamma}-1}{1-\gamma}\Big]\Big). \quad (3.57)$$

Substituting this gives:

$$\begin{aligned}\frac{d\pi_t}{\pi_{t-}} =& \Big\{ -\beta - \frac{\mu_t}{\epsilon} + \Big(1+\frac{1}{\epsilon}\Big)\frac{\gamma}{2}\sigma_t^2 + \Big(\gamma - \frac{1}{\epsilon}\Big)\sum_{m=1}^{M}\lambda_t^m E\Big[\frac{(1+J^m)^{1-\gamma}-1}{1-\gamma}\Big] \\ & - 1/\epsilon\Big(\mu_\xi - \frac{1}{2}(1+1/\epsilon)tr\Big(\frac{\xi_X'\xi_X}{\xi_t^2}\sigma_X\sigma_X'\Big)\Big) - 1/\epsilon(1-1/\zeta)tr\Big(\frac{g_X'\xi_X}{g_t\xi_t}\sigma_X\sigma_X'\Big) \\ & - \frac{1}{2}\frac{1}{\zeta}(1-1/\zeta)tr\Big(\frac{g_X'g_X}{g_t^2}\sigma_X\sigma_X'\Big)\Big\}dt - \gamma\sigma_t dZ_t^c \\ & + \Big((1-1/\zeta)\frac{g_X}{g_t}\sigma_X - 1/\epsilon\frac{\xi_X}{\xi_t}\sigma_X\Big)dZ_t^X + \sum_{m=1}^{M}\Big((1+J_m)^{-\gamma}-1\Big)dN_{m,t}.\end{aligned} \tag{3.58}$$

Therefore π_t is of the form: $\frac{d\pi_t}{\pi_{t-}} = \mu_\pi dt - \gamma\sigma_t dZ_t^c + \sigma_\pi dZ_t^X + \sum_{m=1}^{M}\Big((1+J_m)^{-\gamma}-1\Big)dN_{m,t}$.

3.A.3 Interest rate

Let B_t be the price of the risk-free asset with continuous return r_t: $dB_t = r_t B_t dt$. Using a no-arbitrage argument, $\pi_t B_t$ must be a martingale:

$$\frac{d\pi_t B_t}{\pi_{t-}B_t} = (r_t + \mu_\pi)dt - \gamma\sigma_t dZ_t^c + \sigma_\pi dZ_t^X + \sum_{m=1}^{M}\Big((1+J_m)^{-\gamma}-1\Big)dN_{m,t}. \tag{3.59}$$

This is a martingale if $r_t = -\mu_\pi - \sum_{m=1}^{M}\lambda_{m,t}E\Big[(1+J_m)^{-\gamma}-1\Big]$. Therefore the interest rate equals:

$$\begin{aligned}r_t =& \beta + \frac{\mu_t}{\epsilon} - \Big(1+\frac{1}{\epsilon}\Big)\frac{\gamma}{2}\sigma_t^2 - \frac{1}{2}\frac{1}{\zeta}(1/\zeta-1)tr\Big(\frac{g_X'g_X}{g_t^2}\sigma_X\sigma_X'\Big) \\ & + 1/\epsilon\Big(\mu_\xi - \frac{1}{2}(1+1/\epsilon)tr\Big(\frac{\xi_X'\xi_X}{\xi_t^2}\sigma_X\sigma_X'\Big)\Big) - 1/\epsilon(1/\zeta-1)tr\Big(\frac{g_X'\xi_X}{g_t\xi_t}\sigma_X\sigma_X'\Big) \\ & - \Big(\gamma - \frac{1}{\epsilon}\Big)\sum_{m=1}^{M}\lambda_{m,t}E\Big[\frac{(1+J_m)^{1-\gamma}-1}{1-\gamma}\Big] - \sum_{m=1}^{M}\lambda_{m,t}E\Big[(1+J_m)^{-\gamma}-1\Big].\end{aligned} \tag{3.60}$$

3.A.4 Risk premium

Let S_t be the ex-dividend price of the stock that pays dividend at a rate C_t and denote by S_t^d the cum-dividend price. Then by no arbitrage, $\pi_t S_t^d$ must be a martingale. Furthermore, we use the relationship $S_t = \frac{\xi_t}{k(X_t,t)}Y_t = \frac{\xi_t^{1/\epsilon}g_t^{1/\zeta}Y_t}{\beta}$. The dynamics of S_t^d are given by:

$$dS_t^d = dS_t + C_t dt = S_t\frac{dY_t}{Y_t} + S_t\frac{dg_t^{1/\zeta}}{g_t^{1/\zeta}} + S_t\frac{d\xi_t^{1/\epsilon}}{\xi_t^{1/\epsilon}} + S_t\frac{d[g_t^{1/\zeta},\xi_t^{1/\epsilon}]}{g_t^{1/\zeta}\xi_t^{1/\epsilon}} + \beta\xi_t^{1-1/\epsilon}g_t^{-1/\zeta}S_t dt. \tag{3.61}$$

Now we calculate $dg_t^{1/\zeta}$ and $d\xi_t^{1/\epsilon}$ and the quadratic covariation:

$$\begin{aligned}
\frac{dg_t^{1/\zeta}}{g_t^{1/\zeta}} &= 1/\zeta\left(\mu_g + \frac{1}{2}(1/\zeta - 1)tr\Big(\frac{g_X' g_X}{g_t^2}\sigma_X\sigma_X'\Big)\right)dt + 1/\zeta\frac{g_X}{g_t}\sigma_X dZ_t^X, \\
\frac{d\xi_t^{1/\epsilon}}{\xi_t^{1/\epsilon}} &= 1/\epsilon\left(\mu_\xi + \frac{1}{2}(1/\epsilon - 1)tr\Big(\frac{\xi_X'\xi_X}{\xi_t^2}\sigma_X\sigma_X'\Big)\right)dt + 1/\epsilon\frac{\xi_X}{\xi_t}\sigma_X dZ_t^X, \\
\frac{d[g_t^{1/\zeta}, \xi_t^{1/\epsilon}]}{g_t^{1/\zeta}\xi_t^{1/\epsilon}} &= \frac{1}{\epsilon}\frac{1}{\zeta}tr\Big(\frac{g_X'\xi_X}{g_t\xi_t}\sigma_X\sigma_X'\Big).
\end{aligned} \tag{3.62}$$

Substituting this into (3.61) yields:

$$\begin{aligned}
\frac{dS_t^d}{S_t} = &\left\{\mu_t + 1/\zeta\left(\mu_g + \frac{1}{2}(1/\zeta - 1)tr\Big(\frac{g_X' g_X}{g_t^2}\sigma_X\sigma_X'\Big)\right)\right. \\
&\left. + 1/\epsilon\left(\mu_\xi + \frac{1}{2}(1/\epsilon - 1)tr\Big(\frac{\xi_X'\xi_X}{\xi_t^2}\sigma_X\sigma_X'\Big)\right) + \frac{1}{\epsilon}\frac{1}{\zeta}tr\Big(\frac{g_X'\xi_X}{g_t\xi_t}\sigma_X\sigma_X'\Big)\right\}dt \\
&+ \Big(1/\zeta\frac{g_X}{g_t}\sigma_X + 1/\epsilon\frac{\xi_X}{\xi_t}\sigma_X\Big)dZ_t^X + \sigma_t dZ_t^c + \sum_{m=1}^{M} J_m dN_{m,t}.
\end{aligned} \tag{3.63}$$

Substituting μ_g (3.57) and taking everything together gives:

$$\begin{aligned}
\mu_S = &\beta + \frac{\mu_t}{\epsilon} - \frac{1}{2}(1/\epsilon - 1)\gamma\sigma_t^2 + (1/\epsilon - 1)\sum_{m=1}^{M}\lambda_{m,t}E\Big[\frac{(1+J_m)^{1-\gamma} - 1}{1-\gamma}\Big] \\
&+ \frac{1}{2}\frac{1}{\zeta}(1/\zeta - 1)tr\Big(\frac{g_X' g_X}{g_t^2}\sigma_X\sigma_X'\Big) + 1/\epsilon\Big(\mu_\xi + \frac{1}{2}(1/\epsilon - 1)tr\Big(\frac{\xi_X'\xi_X}{\xi_t^2}\sigma_X\sigma_X'\Big)\Big) \\
&+ \frac{1}{\epsilon}\frac{1}{\zeta}tr\Big(\frac{g_X'\xi_X}{g_t\xi_t}\sigma_X\sigma_X'\Big).
\end{aligned} \tag{3.64}$$

From this equation we can calculate the risk premium rp_t:

$$\begin{aligned}
rp_t = \mu_S + \sum_{m=1}^{M}\lambda_{m,t}E[J_m] - r_t = &\gamma\sigma_t^2 + \sum_{m=1}^{M}\lambda_{m,t}E\Big[J_m + (1+J_m)^{-\gamma} - (1+J_m)^{1-\gamma}\Big] \\
&+ \frac{1}{\zeta}(1/\zeta - 1)tr\Big(\frac{g_X' g_X}{g_t^2}\sigma_X\sigma_X'\Big) + \frac{1}{\epsilon^2}tr\Big(\frac{\xi_X'\xi_X}{\xi_t^2}\sigma_X\sigma_X'\Big) + \frac{1}{\epsilon}\Big(\frac{2}{\zeta} - 1\Big)tr\Big(\frac{g_X'\xi_X}{g_t\xi_t}\sigma_X\sigma_X'\Big).
\end{aligned} \tag{3.65}$$

3.B Definition of finite difference matrix

We first define the backward, central and forward parameters α for the interior grid points.

$$\begin{aligned}
&\alpha^C_{i,j,t} = -\sum_{d=1}^{2} \frac{|(\mu_{Xi,j,t})_d|}{\delta_d} - \sum_{d=1}^{2} \frac{\left(\sigma_{Xi,j,t}\sigma'_{Xi,j,t}\right)_{d,d}}{\delta_d^2}, \quad i \in \{2,...,N_1-1\},\ j \in \{2,...,N_2-1\} \\
&\alpha^B_{i,j,t,d} = \frac{(\mu^-_{Xi,j,t})_d}{\delta_d} + \frac{1}{2}\frac{\left(\sigma_{Xi,j,t}\sigma'_{Xi,j,t}\right)_{d,d}}{\delta_d^2} \quad \alpha^F_{i,j,t,d} = \frac{(\mu^+_{Xi,j,t})_d}{\delta_d} + \frac{1}{2}\frac{\left(\sigma_{Xi,j,t}\sigma'_{Xi,j,t}\right)_{d,d}}{\delta_d^2} \\
&d=1,\ i \in \{2,...,N_1-1\},\ j \in \{1,...,N_2\}, \quad d=2,\ i \in \{1,...,N_1\},\ j \in \{2,...,N_2-1\}
\end{aligned} \tag{3.66}$$

In this example, assume that $(\mu_{Xi,j,t})_1 > 0$ when $i = 1$, $(\mu_{Xi,j,t})_2 > 0$ when $j = 1$, $(\mu_{Xi,j,t})_1 < 0$ when $i = N_1$ and $(\mu_{Xi,j,t})_2 < 0$ $j = N_2$. This implies that at all left boundaries, the forward difference is used and at all right boundaries, the backward difference is always used in the upwind scheme. At the boundary points we then assume that the second derivative vanishes. The α parameters at the boundaries then become.

$$\begin{aligned}
&\alpha^C_{i,j,t} = -\sum_{d=1}^{2} \frac{|(\mu_{Xi,j,t})_d|}{\delta_d}, \quad (i,j) \in \{(1,1),(1,N_2),(N_1,1),(N_1,N_2)\} \\
&\alpha^C_{i,j,t} = -\sum_{d=1}^{2} \frac{|(\mu_{Xi,j,t})_d|}{\delta_d} - \frac{\left(\sigma_{Xi,j,t}\sigma'_{Xi,j,t}\right)_{2,2}}{\delta_2^2}, \quad i \in \{1,N_1\},\ j \in \{2,...,N_2-1\} \\
&\alpha^C_{i,j,t} = -\sum_{d=1}^{2} \frac{|(\mu_{Xi,j,t})_d|}{\delta_d} - \frac{\left(\sigma_{Xi,j,t}\sigma'_{Xi,j,t}\right)_{1,1}}{\delta_1^2}, \quad i \in \{2,..,N_1-1\},\ j \in \{1,N_2\}
\end{aligned} \tag{3.67}$$

$$\begin{aligned}
&\alpha^B_{1,j,t,1} = 0, \quad j \in \{1,...,N_2\}, \quad \alpha^B_{i,1,t,2} = 0, \quad i \in \{1,...,N_1\} \\
&\alpha^B_{N_1,j,t,1} = \frac{(\mu^-_{XN_1,j,t})_1}{\delta_1}, \quad j \in \{1,...,N_2\}, \quad \alpha^B_{i,N_2,t,2} = \frac{(\mu^-_{Xi,N_2,t})_2}{\delta_2}, \quad i \in \{1,...,N_1\} \\
&\alpha^F_{1,j,t,1} = \frac{(\mu^+_{X1,j,t})_1}{\delta_1}, \quad j \in \{1,...,N_2\}, \quad \alpha^F_{i,1,t,2} = \frac{(\mu^+_{Xi,1,t})_2}{\delta_2}, \quad i \in \{1,...,N_1\} \\
&\alpha^F_{N_1,j,t,1} = 0, \quad j \in \{1,...,N_2\}, \quad \alpha^F_{i,N_2,t,2} = 0, \quad i \in \{1,...,N_1\}
\end{aligned} \tag{3.68}$$

Putting everything together, we can construct the matrix D_t^δ.

$$D_{j,t}^C = \begin{bmatrix} \alpha_{1,j,t}^C & \alpha_{1,j,t,1}^F & 0 & 0 & \dots & 0 & 0 & 0 & 0 \\ \alpha_{2,j,t,1}^B & \alpha_{2,j,t}^C & \alpha_{2,j,t,1}^F & 0 & \dots & 0 & 0 & 0 & 0 \\ 0 & \alpha_{3,j,t,1}^B & \alpha_{3,j,t}^C & \alpha_{3,j,t,1}^F & \dots & 0 & 0 & 0 & 0 \\ \vdots & \vdots & \vdots & \vdots & \ddots & \vdots & \vdots & \vdots & \vdots \\ 0 & 0 & 0 & 0 & \dots & \alpha_{N_1-2,j,t,1}^B & \alpha_{N_1-2,j,t}^C & \alpha_{N_2-2,j,t,1}^F & 0 \\ 0 & 0 & 0 & 0 & \dots & 0 & \alpha_{N_1-1,j,t,1}^B & \alpha_{N_1-1,j,t}^C & \alpha_{N_1-1,j,t,1}^F \\ 0 & 0 & 0 & 0 & \dots & 0 & 0 & \alpha_{N_1,j,t,q}^B & \alpha_{N_1,j,t}^C \end{bmatrix}$$

$$D_{j,t}^B = \begin{bmatrix} \alpha_{1,j,t,2}^B & 0 & \dots & 0 & 0 \\ 0 & \alpha_{2,j,t,2}^B & \dots & 0 & 0 \\ \vdots & \vdots & \ddots & \vdots & \vdots \\ 0 & 0 & \dots & \alpha_{N_1-1,j,t,2}^B & 0 \\ 0 & 0 & \dots & 0 & \alpha_{N_1,j,t,2}^B \end{bmatrix}$$

$$D_{j,t}^F = \begin{bmatrix} \alpha_{1,j,t,2}^F & 0 & \dots & 0 & 0 \\ 0 & \alpha_{2,j,t,2}^F & \dots & 0 & 0 \\ \vdots & \vdots & \ddots & \vdots & \vdots \\ 0 & 0 & \dots & \alpha_{N_1-1,j,t,2}^F & 0 \\ 0 & 0 & \dots & 0 & \alpha_{N_1,j,t,2}^F \end{bmatrix}$$

$$D_t^\delta = \begin{bmatrix} D_{1,t}^C & D_{1,t}^F & 0 & 0 & \dots & 0 & 0 & 0 & 0 \\ D_{2,t}^B & D_{2,t}^C & D_{2,t}^F & 0 & \dots & 0 & 0 & 0 & 0 \\ 0 & D_{3,t}^B & D_{3,t}^C & D_{3,t}^F & \dots & 0 & 0 & 0 & 0 \\ \vdots & \vdots & \vdots & \vdots & \ddots & \vdots & \vdots & \vdots & \vdots \\ 0 & 0 & 0 & 0 & \dots & D_{N_2-2,t}^B & D_{N_2-2,t}^C & D_{N_2-2,t}^F & 0 \\ 0 & 0 & 0 & 0 & \dots & 0 & D_{N_2-1,t}^B & D_{N_2-1,t}^C & D_{N_2-1,t}^F \\ 0 & 0 & 0 & 0 & \dots & 0 & 0 & D_{N_2,t}^C & D_{N_2,t}^F \end{bmatrix} \tag{3.69}$$

3.C Consistency, convergence and stability

A proper finite difference scheme should satisfy the following three properties: consistency, convergence and stability. We will briefly cover these three properties, see Thomas (2013) for more details. Let us start with consistency. Denote the true solution at the grid points at time t_i by g_{t_i} and the approximate solution by $g_{t_i}^\delta$. A scheme $g_{t_i}^\delta = A g_{t_{i+1}}^\delta$ is consistent with respect to the norm $||.||$ if g_{t_i} satisfies:

$$g_{t_i} = A g_{t_{i+1}} + \delta_t \tau_{t_{i+1}}, \quad \text{and } ||\tau_{t_i}|| \to 0 \ \text{ as } \delta_t, \delta_1, \delta_2 \to 0. \tag{3.70}$$

τ_{t_i} is the error vector of the finite difference approximation. We did not yet explicitly specify the norm, but one can use for example the absolute sum ($||.||_1$), the Euclidean norm ($||.||_2$) or the max absolute value ($||.||_\infty$). If the function g is sufficiently smooth (bounded and existing derivatives), then consistency is satisfied. One can for example verify consistency by writing out the error terms of the Taylor approximations of the finite difference schemes.

Convergence and stability are less straightforward to show. We now first consider stability. We use the following definition for stability. A finite difference scheme is said to be stable with respect to the norm $||.||$ if there exist positive constants $\Delta_1, \Delta_2, \Delta_t$ and a non-negative constant K such that:

$$||g_0^\delta|| \leq K||g_T^\delta||, \quad \text{for } \ 0 < \delta_1 \leq \Delta_1, \ 0 < \delta_2 \leq \Delta_2, \ 0 < \delta_t \leq \Delta_t. \tag{3.71}$$

The stability condition implies that when you let the time steps go from $\Delta_1, \Delta_2, \Delta_t$ towards zero, the norm of the solution remains bounded. It turns out that when considering a consistent linear scheme of the form $g_{t_i}^\delta = Ag_{t_{i+1}}^\delta$, the scheme is convergent if and only if it is stable. This is the so called Lax Equivalence theorem. So the only thing that we have to verify is the stability of the scheme.

Let us first consider a simplified example of the PDE that we are trying to solve. Assume that $R = -r$ where $r > 0$ is the interest rate. Furthermore, assume that $\mu_X = [rX_{1,t} \ \ rX_{2,t}]$ and $\sigma_X = \begin{bmatrix} \sigma_1 X_{1,t} & 0 \\ 0 & \sigma_2 X_{2,t} \end{bmatrix}$, so there is no optimal control. Then the PDE becomes:

$$0 = \frac{\partial g_t}{\partial t} + rX_{1,t}\frac{\partial g_t}{\partial X_{1,t}} + rX_{2,t}\frac{\partial g_t}{\partial X_{2,t}} + \frac{1}{2}(\sigma_1 X_{1,t})^2\frac{\partial^2 g_t}{(\partial X_{1,t})^2} + \frac{1}{2}(\sigma_1 X_{2,t})^2\frac{\partial^2 g_t}{(\partial X_{2,t})^2} - rg_t. \tag{3.72}$$

This is the two-dimensional Black-Scholes PDE when the assets are uncorrelated. Note that the drifts are always positive, so the upwind scheme implies that only forward differences are used. Since the drift is always positive in this case, we assume that the first derivative vanishes at the boundary. Every European style two-asset option satisfies this equation. We can again write the scheme as $g_{t_i}^\delta = Ag_{t_{i+1}}^\delta$ where A is independent of time since μ_X, σ_X and R are independent of time.

Due to the upwind scheme, the matrix D^δ satisfies the following properties:

$$\begin{aligned} (D^\delta)_{i,i} < 0, \quad (D^\delta)_{i,j} \geq 0 \ j \neq i, \\ \sum_j (D^\delta)_{i,j} = 0 \quad \forall i. \end{aligned} \tag{3.73}$$

Then it can be shown that $||A^I||_\infty \leq \frac{1}{1+r\delta_t}$ (see Lapeyre et al. (2005), Theorem 7.2.3). Since we can write $||g_0^\delta||_\infty = ||(A^I)^{N_t} g_T^\delta||_\infty \leq \left(||A^I||_\infty\right)^{N_t} ||g_T^\delta||_\infty \leq ||g_T^\delta||_\infty$, the implicit scheme is stable for any time step δ_t. The $||.||_\infty$ for a matrix corresponds to the maximum absolute row sum of a matrix. Note that the implicit scheme in this case is fully implicit, since R does not depend on g_t.

Similarly, $||A^E||_\infty \leq \frac{1}{1+r\delta_t}$ when the additional condition $\delta_t \leq \frac{1}{|(D^\delta)_{i,i}|} \ \ \forall i$ is satisfied. So given a small enough time step, the explicit scheme is stable as well. However, this condition can be quite restrictive in some cases. It might lead to an unnecessary small time step which will make the algorithm slower compared to the implicit method which is stable for any time step.

But in the general case there is no guarantee that $R(X_t, g_t, u_t, t)$ is negative for any X_t. Now consider again a simplified problem where $R(X_t, u_t)$ does not depend on time or on g_t, but possibly on the states X_t and the control u_t and $R(X_t, u_t)$ can be both negative

and positive. Furthermore, assume that μ_X and σ_X are independent of t such that the matrix A does not depend on time. Define the spectral radius as: $\rho(A) \equiv \max\{|\lambda| : \lambda \text{ is an eigenvalue of A}\}$, i.e. the maximum absolute eigenvalue. A necessary condition for stability is then that the spectral radius must be smaller or equal to one: $\rho(A) \leq 1$. The idea behind this condition is the following. We can write: $||g_0^\delta|| = ||A^{N_t} g_T^\delta||$. Since $||A^n|| \geq \rho(A)^n \quad \forall n$, $\rho(A) \leq 1$ is a necessary condition for stability. So if we want the norm of the matrix A to the power n to be bounded for large n, the spectral radius must be less or equal to one. This condition is also a sufficient condition when the matrix A is symmetric. When A is not symmetric (which is often the case), in practice this condition turns out to still be useful.

Consider now the general problem where A_t depends on time since μ_X, σ_X and $R(X_t, g_t, u_t, t)$ might depend on time. In this case we can write $||g_0^\delta|| = ||A_{t_1} ... A_{t_N} g_T^\delta|| \leq ||A_{t_1} ... A_{t_N}||\ ||g_T^\delta||$. We therefore must find a bound on the product of a sequence of matrices, which is not straightforward. We can use the following inequality: $||A_{t_1} ... A_{t_N}|| \leq ||A_{t_1}|| ... ||A_{t_N}||$. This implies that if we can establish that the norm of the matrix A_t is less than or equal to one for every t, the scheme is stable. Since $||A_t|| \geq \rho(A_t) \quad \forall t$, it is again useful to verify whether the spectral radius of A_t is bounded by one for each t. It might take some time to calculate the spectral radius of the matrix A_t, especially when A_t is very large. Therefore, one should only calculate the spectral radius when there are serious concerns about stability. It could be useful to calculate the spectral radius at least for the first time step (A_{t_N}) or every n-th iteration.

Lastly, we discuss oscillatory behavior. Even when the scheme is stable, there might be oscillations if the time step is too large. In our specific setting, the function $R(X_t, g_t, u_t, t)$ contains a term $g_t^{\frac{-1}{\zeta}}$. When g_t becomes negative, this term might lead to complex numbers which is unsatisfactory. The scheme is free of oscillatory behavior when all eigenvalues of the matrix A are non-negative (Harwood, 2017). Note that this is a sufficient condition and that the condition is not necessary.

Summarizing, it is not straightforward to derive precise stability conditions for the general problem. In the simpler setting, it is shown that the implicit upwind scheme is unconditionally stable. Although we cannot guarantee that this will also lead to a stable scheme in the more general setting, in practice the implicit upwind scheme is often stable. It can still be useful to verify, e.g. in the first step, whether the eigenvalues of the matrix A are between 0 and 1 (up to numerical precision). If this is not the case, this indicates an unstable algorithm. It is expensive in terms of computation time to do this often but if there are concerns this gives at least some guidance in whether the scheme is stable or not.

3.D Finite difference without time derivative

The problem that we are solving becomes:

$$\begin{aligned} 0 &= \min_{u_t} \Big\{ R(X_t, g_t, u_t) g_t + D g_t \Big\} \\ \text{where} \quad D g_t &= \sum_{d=1}^{d_X} (\mu_X)_d \frac{\partial g_t}{\partial X_{d,t}} + \frac{1}{2} \sum_{d=1}^{d_X} (\sigma_X \sigma_X')_{d,d} \frac{\partial^2 g_t}{(\partial X_{d,t})^2}. \end{aligned} \tag{3.74}$$

Then our finite difference solution would solve the following equation:

$$0 = \left(D^{\delta}\big(u^*(g^{\delta})\big) + diag\Big(R^{\delta}\big(g^{\delta}, u^*(g^{\delta})\big)\Big)\right) g^{\delta}. \tag{3.75}$$

Note that the matrix D^{δ} and the vector R^{δ} are independent of time. One possibility is to solve this equation directly using a non-linear solver. Another way to solve this equation is to use an iterative approach and add a 'false transient' with step size Δ to (3.75). Define $D_n^{\delta} = D^{\delta}\big(u^*(g_n^{\delta})\big)$ and $R_n^{\delta} = R^{\delta}(g_n^{\delta}, u^*(g_n^{\delta})\Big)$. This gives the following equation:

$$\frac{g_{n+1}^{\delta} - g_n^{\delta}}{\Delta} = \Big(D_n^{\delta} + diag(R_n^{\delta})\Big) g_{n+1}^{\delta}. \tag{3.76}$$

We can use a similar algorithm as for the problem with time derivative to solve for g^{δ}.

The algorithm

Step 1: Start with an initial guess for the g_0^{δ} .
Starting with $n = 0$, repeat the following steps until $|g_{n+1}^{\delta} - g_n^{\delta}| < crit$ where $crit$ is some small number.
Step 2: g_n^{δ} is obtained from the previous iteration. Calculate the optimal policy $u^*(g_n^{\delta})$ using either a closed form or implicit expression that follows from the first order conditions. This requires as input g_n^{δ} and its derivatives. The derivatives can easily be calculated using central finite differences.
Step 3: Use u_n^* to calculate μ_X and σ_X.
Step 4: Construct D_n^{δ} (see appendix 3.B).
Step 5: Use g_n^{δ} and u_n^* to calculate R_n^{δ}.
Step 6: Given g_n^{δ}, D_n^{δ} and R_n^{δ}, we can use a semi-implicit scheme to obtain g_{n+1}^{δ}: $g_{n+1}^{\delta} = A_n^I g_n^{\delta} = \left(I_{N_1 N_2} - \Delta\Big(D_n^{\delta} + diag(R_n^{\delta})\Big)\right)^{-1} g_n^{\delta}$.
Optional: Step 7. To obtain the risk-free rate and the risk premium, ξ and its derivatives can be calculated using (central) finite differences. Result: After convergence, we obtain the function g^{δ} and the optimal policy $u^*(g^{\delta})$.

The idea of the 'false transient' is to use an iterative method to solve (3.75). Δ in this case can be seen as a stability parameter in contrast to an actual time step. However, the algorithm is basically identical to the algorithm for the problem with time derivative. A small Δ restricts the updated g_{n+1}^{δ} to be close to the previous step g_n^{δ}. This leads to a stable scheme, but it might take a long time before the algorithm converges. A larger Δ will lead to faster convergence, but for a too large Δ the matrix A_n^I might not satisfy the stability conditions discussed in the previous section. In contrast to the problem with time derivative, the accuracy of the scheme does not depend on Δ. It is therefore efficient to choose Δ quite large but to make sure that the stability conditions are met. The semi-implicit scheme is stable for much larger Δ compared to the explicit scheme and therefore we do not consider the explicit scheme in this case.

3.E Stochastic Grid Method: Algorithm

The algorithm

Initialization: First we determine some algorithm parameters. We must cut-off the infinite horizon problem at some time T in the future. T must be far enough away, such that choosing a larger T does not change the solution anymore. We then discretize the problem in the time dimension. The second choice is therefore the time step δ_t. Define the grid of time points as: $[t_0 = 0,\ t_1 = \delta_t,\ \ldots, t_N = T]$. Next we define the boundaries of the random grid for the state variables X_t at every time point t. Since we do not know the optimal policy u_t^* yet, we do not know exactly what the distribution of the state variables is. However, it is still possible to choose a wide enough grid for the state variables. Denote the vector with upper bounds of X_{t_i} at period t_i by $\overline{X_{t_i}}$ and the vector of lower bounds by $\underline{X_{t_i}}$. Note that the boundaries of the grid are allowed to be time-dependent.

Step 1: Simulate K random grid points of the state variables at time T. The easiest way to do this is to simulate draws from a uniform distribution with boundaries $\underline{X_T}$ and $\overline{X_T}$. This gives the random grid points $X_T(k),\ k = 1, ..., K$. If it is very clear that it is more important to have a good fit of the value function in the middle of the grid, one could for example also use a beta distribution or some other distribution to obtain random grid points.

Step 2: Guess the function $\hat{g}(X_T(k), T)$ at terminal time T. A good approximation at terminal time implies that the solution will converge using a shorter time horizon.

Then start at one step before terminal time t_{N-1}. Backwards in time, for every time step t_i, $i = N-1, ..., 1$ we perform the following steps.

Step 3: Approximating g as a function of the state variables. To approximate $g\big(X_{t_{i+1}}, t_{i+1}\big)$, choose a vector of N_b basis functions:

$$B\big(X_t\big) = [B_1\big(X_t\big)\ \ \ldots\ \ B_{N_b}\big(X_t\big)]'. \tag{3.77}$$

Then using the sample of K grid points, regress $\hat{g}\big(X_{t_{i+1}}(k), t_{i+1}\big)$ on $B\big(X_{t_{i+1}}(k)\big)$ to obtain an N_b dimensional column vector of coefficients $\nu_{t_{i+1}}$.

Step 4: Simulation. Simulate K random grid points at time t_i, using a uniform distribution with boundaries $\underline{X_{t_i}}$ and $\overline{X_{t_i}}$.

Step 5: Calculating the optimal policy. To calculate $u_{t_i}^*$, we use the first order condition from the HJB-equation, which needs as input the derivatives of g. To calculate these derivatives, we use the following approximation of $g(X_{t_i}, t_i)$:

$$\hat{g}(X_{t_i}(k), t_i) = \nu'_{t_{i+1}} B(X_{t_i}(k)) = \sum_{j=1}^{N_b} (\nu_{t_{i+1}})_j B_j(X_{t_i}(k)). \tag{3.78}$$

Note that we have to use the coefficients α of the previous time period, since ν_{t_i} is still unknown. This does not matter much if the time step δ_t is small. The vector of first

derivatives with respect to the state variables can then be calculated as:[14]

$$\hat{g}_X(X_{t_i}(k), t_i) = \frac{\partial \hat{g}(X_t, t_i)}{\partial X_t}\Big|_{X_{t_i}(k)} = \sum_{j=1}^{n_b} (\nu_{t_{i+1}})_j \frac{\partial B_j(X_t)}{\partial X_t}\Big|_{X_{t_i}(k)}. \tag{3.79}$$

Similarly, we can find the second derivative $\hat{g}_{XX}$. Using these derivatives and the first order condition, we can calculate $u^*_{t_i}$. If $u^*_{t_i}$ does not have a closed form expression, a non-linear equation has to be solved. It pays off to supply the analytical Jacobian of the first order conditions to the solver. We use a trust-region algorithm with analytical Jacobian to calculate the optimal policy function.

Step 6: Approximating the conditional expectation. We want to approximate for each (d_X-dimensional) grid point $X_{t_i}(k)$ the conditional expectation $E_{t_i}\Big[g(X_{t_{i+1}}, t_{i+1})|X_{t_i}(k)\Big]$, $k = 1, ..., K$. We use the following relation:

$$E_{t_i}\Big[\hat{g}\big(X_{t_{i+1}}, t_{i+1}\big)|X_{t_i}(k)\Big] = \nu'_{t_{i+1}} E_{t_i}\Big[B\big(X_{t_{i+1}}\big)|X_{t_i}(k)\Big]. \tag{3.80}$$

Here $E_{t_i}\Big[B\big(X_{t_{i+1}}\big)|X_{t_i}(k)\Big]$ is known in closed form or has an analytic approximation. Note that this conditional expectation also depends on $u^*_{t_i}$.

Step 7: In this step we use the recursive equation to calculate the function g at time t_i:

$$\begin{aligned}\hat{g}(X_{t_i}(k), t_i) = \Bigg(&(1 - e^{-\beta\delta_t})\xi_t^{1-1/\epsilon} + e^{-\beta\delta_t} \\ &\left(E_{t_i}\Big[\hat{g}(X_{t_{i+1}}, t_{i+1})|X_{t_i}(k)\Big] E_{t_i}\Big[\frac{Y_{t_{i+1}}^{1-\gamma}}{Y_{t_i}^{1-\gamma}}|X_{t_i}(k)\Big] \right)^{1/\zeta} \Bigg)^{\zeta}.\end{aligned} \tag{3.81}$$

Optional: Step 8. To calculate the risk-free rate and the risk premium, we have to calculate the derivatives of ξ_{t_i}. If $u^*_{t_i}$ has a closed form expression in terms of g_{t_i} and its derivatives, it might be possible to express the derivatives of ξ_{t_i} as a function of the derivatives of g_{t_i}. If this is not possible, we can calculate the derivatives numerically. Note that we can calculate g_{t_i} and its derivatives at any state-space point X_{t_i} and time point t_i using $\hat{g}(x, t_i) = \nu'_{t_i} B(x)$. Therefore we can also calculate $\xi_{t_i} = \xi(X_{t_i}, u^*_{t_i}, t_i)$ at any state-space and time point t_i. An easy way to calculate the derivatives of ξ_{t_i} numerically is to use a finite difference approximation.

After iterating until $i = 1$, we obtain an estimate of g at time t_0. Calculate u^*_0 once more to obtain the optimal policy at time 0.

[14]Similar to Jain and Oosterlee (2015) we assume that $\frac{\partial \nu_{t_i}}{\partial X_{t_i}} = 0$. This makes it much simpler to calculate the derivatives and this derivative is generally very close to zero. In a follow up paper, Jain, Leitao, and Oosterlee (2019) relax this assumption and they show how to calculate the derivatives recursively. We do not consider this extension.

4 The social cost of carbon: Optimal policy versus business-as-usual

4.1 Introduction

The earth is warming due to man-made greenhouse gas emissions, which makes the problem of climate change a global externality: polluting has a negative effect on economic activity but the cost of pollution is not priced. Since private interest and social interest are not aligned, one solution is to levy a tax that is equal to the social cost of pollution as proposed by Pigou (1920). Due to its slow decay, carbon dioxide is the most important greenhouse gas. To be able to set a carbon tax, one must know the welfare loss of carbon emissions expressed in dollar terms. This metric is called the social cost of carbon (SCC): the marginal social cost of carbon emissions. This social cost consists of the discounted sum of all future damages caused by emitting one unit of carbon today.

The most straightforward way to internalize the externality is to implement a global carbon tax and set the carbon tax equal to the social cost of carbon. However, there are several issues that prevent countries to implement a joint climate policy. Carbon abatement is a clear example of a free-rider problem where a country benefits from good behaviour of other countries. Furthermore, there is a lot of heterogeneity in the impact of climate change and this makes some countries care less about climate change than others. Additionally, there is discussion about the distribution of the financial burden between the developed and developing countries since it were the developed countries that have caused the largest part of the problem.

The first-best solution would be to consider the optimal policy scenario, calculate the social cost of carbon and implement a global carbon tax that equals the social cost of carbon. However, climate policy is currently far away from optimal. The benefit of abating a unit of carbon today is equal to the social cost of carbon given the current policy scenario. If coordination on a carbon tax is not possible, the SCC given the current policy scenario should be used in current cost-benefit analysis. Directly implementing a carbon tax for the entire world is currently infeasible and the more realistic scenario is that carbon taxes will be implemented region by region. For regions currently implementing a carbon tax, the tax should be equal to the benefit of emissions abatement given the current policy scenario. If more and more regions implement a carbon tax, the actual policy scenario will change and this should be taken into account when calculating the social cost of carbon. In the literature, both the optimal policy scenario and business-as-usual scenario are used to calculate the social cost of carbon.[15] This paper studies how sensitive the SCC is to the policy scenario and which assumptions matter for the difference between the two scenarios.

We set up a global climate-economy model (also called integrated assessment model) to analyze the social cost of carbon. The model is based on a pure exchange economy (or

[15] Nordhaus (2014a, pp. 274-275) for example states: "There is some inconsistency in the literature on the definition of the path along which the SCC should be calculated. This paper will generally define the SCC as the marginal damages along the baseline path of emissions and output and not along the optimized emissions path."

Lucas-tree economy) with a representative agent with Epstein-Zin preferences.[16] We add both climate disaster risk and economic disaster risk to the standard pure exchange model. By adding a climate model and climate disasters, we are able to analyze the externality of global warming. Economic growth leads to carbon emissions, which accumulate in the atmosphere. This in turn leads to a rise in the temperature level. The frequency of the climate disasters is assumed to be increasing in the temperature level. Both the timing of climate disasters and the size is stochastic: we are not able to predict the exact damages of climate change in the future. Abatement policy can reduce the amount of carbon emissions, so there is a trade-off between consuming more today and having less disasters in the future.

We start with some simplifying assumptions. First, we assume that carbon emissions are exogenous. Second, the carbon concentration decays at a constant rate and is a deterministic function of emissions. Lastly, there is a single deterministic equation that describes the link between carbon concentration and temperature. These assumptions allow us to derive an intuitive expression for the social cost of carbon and to highlight the two offsetting effects of abatement policy on the SCC. A less stringent climate policy (BAU) compared to a more stringent policy (optimal) has two offsetting effects on the social cost of carbon. On the one hand, increasing the carbon concentration by one unit has a smaller effect on temperature when the carbon concentration is already high. On the other hand, marginal damages are increasing in temperature. Since both effects work in opposite directions, a quantitative estimation of the social cost of carbon is needed.

To quantitatively estimate the social cost of carbon, we relax the simplifying assumptions, extend the climate model and solve the model numerically. Emissions are no longer exogenous but depend on the level of economic activity. Furthermore, we use multiple state variables for both the carbon concentration and temperature dynamics to make sure these dynamics are in line with complex climate models. Lastly, we add random shocks to both the carbon concentration and temperature dynamics to reflect uncertainty within the climate system. Additional to the climate model and disaster specifications, the preference parameters and the economic risk structure are important for the discount rate that is used to discount future climate damages.[17] All these ingredients together are then incorporated in the social cost of carbon.

Using the DICE model, Nordhaus (2014a) calculates the SCC both for the business-as-usual case and the optimal case. The difference turns out to be rather small. Hope and Newbery (2007) also find that the SCC is insensitive to the policy scenario using the PAGE model and argue that this result is not trivial. The reason that the policy scenario does not play a large role in determining the social cost of carbon is that the

[16] This type of model is often used in an asset pricing setting. Although at first sight the two might not have much to do with each other, determining the social cost of carbon is basically calculating the value today of a risky cash-flow (the climate disasters) that materializes in the future. Therefore this type of model is suitable for the analysis.

[17] It is well known that the standard Lucas-tree model with power utility is not able to solve the equity premium puzzle (Mehra & Prescott, 1985), but the combination of Epstein-Zin preferences and economic disasters is able to generate a more realistic interest rate and risk premium. Although we are not trying to solve the equity premium puzzle, the interest rate and risk premium are part of the discount rate that is used to discount future damages within the social cost of carbon. We therefore make sure that the interest rate and risk premium are in line with historical averages.

two previously mentioned offsetting effects cancel out in their model. This result however depends crucially on the calibration of the damage function.

In the literature there is no clear consensus about the convexity and calibration of the damage function. Especially the effects of larger temperature increases above 3 degrees Celsius are hard to obtain estimates for since we have not experienced such global warming in the recent past. Bretschger and Pattakou (2019) stress that there is no agreement on the form of the damage function and consider different polynomial specifications for the damage function, ranging from linear to quartic. Nordhaus (2017) calibrates the damage function in the DICE model to be a quadratic function of temperature. Weitzman (2012) argues that the damage function in DICE is not convex enough and that damages are underestimated for large temperature increases. He proposes to add an additional term to the quadratic damage function that kicks in after roughly three degrees warming. Dietz and Stern (2015) integrate the more convex specification of Weitzman (2012) within Nordhaus's DICE framework and additionally consider a scenario in which damages are even larger. On the other hand, Karydas and Xepapadeas (2019) develop an integrated assessment model where climate change affects the economy via disasters, similar to our framework. Based on data of climate disasters between 1955 and 2015, they find that there has been historically a linear relationship between the temperature anomaly and the arrival rate of disasters. Summarizing, the jury is still out on the form and convexity of the damage function. In the quantitative part of the paper, we therefore vary the convexity of damages in temperature and analyze the effect on the sensitivity of the SCC to the policy scenario. We show that for the convex specification the social cost of carbon in the business-as-usual scenario is 41% higher than in the optimal policy scenario.

This paper is related to the literature on climate-economy or integrated assessment models. The well-known DICE model forms the basis of this literature. It combines a neoclassical economic growth model with a deterministic climate model. The earliest version is Nordhaus (1992). After that the model was regularly updated, the most recent version is the DICE 2016 model (Nordhaus, 2017). Another well known integrated assessment model is PAGE (Hope, 2006). DICE and PAGE are deterministic models and uncertainty is captured by drawing random parameters instead of actually capturing uncertainty within the model. More recently, several papers have studied the effects of risk, uncertainty and more complex preferences on the social cost of carbon. This paper fits within this literature, since we integrate Epstein-Zin preferences and different types of risk into our climate-economy model.

Our model builds on the model from chapter 2, which also extends a pure exchange economy with climate disasters to analyze the social cost of carbon. We additionally include economic disasters and study optimal policy decisions, where chapter 2 includes ambiguity aversion and only considers the social cost of carbon in the BAU scenario. Jensen and Traeger (2014) add long term economic growth uncertainty to their integrated assessment model and stress the impact on discounting. Crost and Traeger (2014) focus rather on damage uncertainty given the temperature level. Cai and Lontzek (2019) include economic uncertainty and climate tipping into the DICE model. Van den Bremer and Van der Ploeg (2021) develop a model with both economic and climate risk and obtain closed-form approximate solutions for the social cost of carbon. Hambel et al. (2021) study temperature feedback in a stochastic equilibrium model with climate change. Lastly,

Karydas and Xepapadeas (2019) develop an asset pricing model with both economic and climate disasters. Their model is used to study the social cost of carbon and the effect of both physical climate risk and transition risk on the portfolio allocation of carbon intensive assets.

Where the earlier integrated assessment models (DICE and PAGE) use the BAU scenario as the benchmark to calculate the social cost of carbon, the standard in the more recent literature focusing on risk and uncertainty is to calculate the social cost of carbon solely in the optimal scenario. We develop a climate-economy model in line with recent advances in both the economic and climate literature to properly calculate the social cost of carbon. We then use this model to look at the scenario dependence of the social cost of carbon, since that has received little attention within the literature.

We additionally study the implications of a hybrid policy scenario, in which no climate policy is implemented in the first 20 years, and after that optimal policy is implemented. Our simulations show that with convex damages, delay is costly. Furthermore, after the delay of optimal policy carbon taxes must be set even higher compared to the optimal policy scenario.

4.2 Model

We extend the stochastic pure exchange economy (Lucas Jr, 1978) in continuous time with a climate model and both climate and economic disasters. We assume for simplicity that there is a single representative agent. Instead of specifying a production function with input factors, the representative agent owns an asset that pays as dividends a stream of endowment. The asset can be seen as a tree that yields an amount of fruit every period. The endowment or the yield of the tree is stochastic. We differentiate between two types of risk: diffusion risk and disaster risk. Diffusion risk represents 'standard' risk in the economy: there are continuous fluctuations in the endowment. On the other hand, the economy is also subject to disaster risk. We consider both economic disasters and climate disasters where economic disasters represent any non-climate type of disaster. Examples are economic crises, financial crises and wars. Non-climate disasters also have an effect on the valuation of climate disasters since the exchange model is a general equilibrium model: the risk structure of the endowment process has an effect on all asset prices in the economy.

The main focus of this paper is on the climate disasters. Due to global warming, the frequency of climate-related disasters is expected to increase and historically there has already been a positive relationship between the temperature level (with respect to the pre-industrial temperature) and the number of climate-related disasters (Karydas & Xepapadeas, 2019). We model this by assuming that the arrival rate of climate disasters is an increasing function of temperature. We consider both linear and more convex specifications.

In the pure exchange economy the endowment cannot be stored: it must be consumed directly. In the standard exchange economy this implies that in equilibrium, consumption is equal to endowment in every period. We allow the agent to spend the endowment on two goods: abatement and consumption. Abatement reduces carbon emissions and therefore reduces the risk of climate disasters in the future. Consumption directly enters

the utility function.

The exchange economy might look very simplistic. It does not consider investment and production and the output in the economy is basically an exogenous process. However, this type of model does allow for a rich risk structure: we feed different types of risk into the model. In a general equilibrium model the risk sources are important since they affect discount rates and asset prices.

In this section, the climate model consists of just two state variables: the atmospheric carbon concentration and the temperature level. We start with a simple climate model to obtain an intuitive expression of the social cost of carbon. We will specifically look at the difference of the social cost of carbon in the business-as-usual (BAU) scenario and the optimal policy scenario. Later in this paper, a more realistic (climate) model is numerically solved to obtain quantitative estimations of the social cost of carbon.

The mathematical formulation of the model is as follows. Consider a single representative agent with stochastic differential utility (Duffie & Epstein, 1992b). This is the continuous time equivalent of Epstein-Zin utility (Epstein & Zin, 1989) and allows us to separate the risk aversion coefficient γ from the elasticity of intertemporal substitution ϵ. Especially since the climate change problem has such a long horizon and risk plays an important role, it is necessary to disentangle these. Let β be the rate of time preference. The value function V_t is then recursively defined:

$$V_t = E_t\Big[\int_t^\infty f(C_s, V_s)ds\Big]$$

where

$$f(C,V) = \frac{\beta}{1-1/\epsilon}\frac{C^{1-1/\epsilon} - \big((1-\gamma)V\big)^{\frac{1}{\zeta}}}{\big((1-\gamma)V\big)^{\frac{1}{\zeta}-1}} \quad \text{for } \epsilon \neq 1 \tag{4.1}$$

$$\text{with } \zeta = \frac{1-\gamma}{1-1/\epsilon}.$$

The exogenous endowment Y_t follows a geometric Brownian motion with two additional jump (Poisson) processes. The growth rate μ and volatility σ are constant. The first jump process captures economic disasters as in Barro (2009). It is important to add economic disasters in a climate-economy model since disaster risk plays an important role in the valuation of uncertain future payoffs. Economic disaster risk affects the discount rate that is used to discount future climate disasters and therefore has an impact on the social cost of carbon. These economic disasters in combination with Epstein-Zin utility yield a more realistic risk-free rate and equity premium. Next to economic disasters, we also consider climate disasters of which the arrival rate is temperature-dependent.

The dynamics of Y_t are given by:

$$dY_t = \mu Y_t dt + \sigma Y_t dZ_t - J_1 Y_{t-} dN_{1,t} - J_2 Y_{t-} dN_{2,t}. \tag{4.2}$$

Z_t is a standard Brownian motion, Y_{t-} denotes aggregate endowment just before a jump ($Y_{t-} = \lim_{h \downarrow 0} Y_{t-h}$). $N_{1,t}$ is the Poisson process for economic disasters with constant arrival rate λ_1 and jump size J_1, where J_1 can be interpreted as the percentage loss of endowment when a disasters strikes. We assume that $x = (1 - J_1)$ follows a power distribution with

parameter α_1 and probability density function $f(x) = \alpha_1 x^{\alpha_1 - 1}$, $0 < x < 1$. This implies that $E[J_1] = \frac{1}{\alpha_1+1}$ and $E\Big[(1-J_1)^n] = \frac{\alpha_1}{\alpha_1+n}$. The Poisson process $N_{2,t}$ for climate disasters has arrival rate

$$\lambda_{2,t} = \lambda_2 T_t^{\theta}, \tag{4.3}$$

where T_t is the temperature compared to the pre-industrial level and θ controls the convexity of the arrival rate in temperature. Since there is no agreement within the literature about the convexity parameter θ, we will vary this parameter in the numerical part of the paper. The jump size of climate disasters J_2 follows the same distribution as J_1, but with parameter α_2.

Business-as-usual carbon emissions E_t are assumed to be exogenous. This assumption will later be relaxed in the extended version of the model. The agent can reduce BAU emissions using abatement policy: $\tilde{E}_t = E_t(1 - u_t)$ are actual carbon emissions where E_t are business-as-usual carbon emissions and u_t is the emissions control rate. Endowment Y_t can thus be spent on consumption C_t and abatement A_t where $A_t = c_{1,t} u_t^{c_2} Y_t$ represents the cost of abatement policy u_t. This yields $C_t = Y_t - A_t = \xi_t Y_t$ where $\xi_t = \frac{C_t}{Y_t} = 1 - c_{1,t} u_t^{c_2}$ is the consumption-endowment ratio.

Define by M_t the atmospheric carbon concentration compared to the pre-industrial level M_{pre}. Emissions accumulate in the atmosphere and carbon is assumed to decay at a constant rate δ_M:

$$dM_t = (\tilde{E}_t - \delta_M M_t)dt. \tag{4.4}$$

An increase in the atmospheric carbon concentration will lead to positive radiative forcing due to the greenhouse effect, which in turn leads to a higher temperature.[18] Radiative forcing is a concave function of the carbon concentration compared to the pre-industrial level: $F_t = \alpha_F \ln\left(\frac{M_t + M_{pre}}{M_{pre}}\right)$. Temperature increases with radiative forcing and has the following dynamics:

$$dT_t = (bF_t - \tau_T T_t)dt. \tag{4.5}$$

4.2.1 Asset prices

Appendix 4.A shows the derivations of the endogenous risk-free rate and risk premium. The interest rate and risk premium are important drivers of the social cost of carbon, which we will discuss in the next section.

Let π_t be the stochastic discount factor of this economy. First, define by B_t a risk free asset that pays 1 at a future date T. The price of this asset equals: $B_t = E_t\Big[\frac{\pi_T}{\pi_t}\Big]$. The return of the risk free asset at time t is the risk free interest rate r_t. Furthermore, let S_t be the price of the asset that gives a claim on the consumption stream. Therefore S_t pays continuous dividends equal to C_t. More formally: $S_t = E_t\Big[\int_t^{\infty} \frac{\pi_s}{\pi_t} C_s ds\Big]$. The risk premium is defined by the difference between the return on S_t (including dividend payments) and the return on the risk-free asset:

[18] Radiative forcing is the difference between energy coming into the Earth and energy leaving the Earth.

$$
\begin{aligned}
r_t &= \underbrace{\beta + \frac{\mu_{c,t}}{\epsilon} - \Big(1+\frac{1}{\epsilon}\Big)\frac{\gamma}{2}\sigma^2}_{\text{Standard interest rate}} + \underbrace{\lambda_1\Big(\frac{\gamma-\frac{1}{\epsilon}}{\alpha_1+1-\gamma} - \frac{\gamma}{\alpha_1-\gamma}\Big)}_{\text{Economic disaster risk}} \\
&\quad + \underbrace{\lambda_{2,t}\Big(\frac{\gamma-\frac{1}{\epsilon}}{\alpha_2+1-\gamma} - \frac{\gamma}{\alpha_2-\gamma}\Big)}_{\text{Climate disaster risk}}, \\
rp_t &= \underbrace{\gamma\sigma^2}_{\text{Standard risk premium}} + \underbrace{\lambda_1\Big(\frac{-1}{\alpha_1+1} + \frac{\alpha_1}{\alpha_1-\gamma} - \frac{\alpha_1}{\alpha_1+1-\gamma}\Big)}_{\text{Economic disaster risk}} \\
&\quad + \underbrace{\lambda_{2,t}\Big(\frac{-1}{\alpha_2+1} + \frac{\alpha_2}{\alpha_2-\gamma} - \frac{\alpha_2}{\alpha_2+1-\gamma}\Big)}_{\text{Climate disaster risk}}.
\end{aligned}
\tag{4.6}
$$

The key determinants of the interest rate and the risk premium are the preference parameters (rate of time preference, elasticity of intertemporal substitution and risk aversion coefficient) and the structure of endowment (growth rate, volatility and disaster parameters). The standard interest rate without jump risk depends on three terms. The first reason for a positive interest rate is the pure rate of time preference β; the agent would rather like to consume earlier than later. Second, since consumption is growing over time, the marginal utility of consumption is declining over time and this gives rise to a higher interest rate. The magnitude of this effect is controlled by the elasticity of intertemporal substitution ϵ. The third term is negative and captures diffusion risk and risk aversion. Due to a flight to safety argument, risk lowers the interest rate. This term scales with risk aversion γ and volatility σ^2. Economic and climate disaster risk have qualitatively a similar effect to the interest rate: disasters depress the interest rate. The magnitude of the disaster terms depends again on risk aversion and on the jump parameters.

The standard risk premium without jump risk equals $\gamma\sigma^2$. Economic and climate disasters lead to a higher risk premium and again risk aversion γ is a key parameter for the risk premium. With the right calibration, we can match the historical risk-free rate and risk premium.

4.2.2 Social cost of carbon

The social cost of carbon is the marginal welfare loss of carbon emissions expressed in current consumption units. Formally, it is defined as: $SCC_t = -\frac{\partial V_t/\partial M_t}{f_C(C_t,V_t)}$. Intuitively, the social cost of carbon equals the discounted value of future damages caused by emitting one unit of carbon today.

As an intermediate step, it is useful to define a consumption strip. A consumption strip is an asset that pays a unit of consumption at a future date. Assume that currently we are at time 0 and that this asset pays out at time t. The expected payoff equals: $E_0[C_t] = C_0 \exp\Big\{\int_0^t \Big(\mu_{c,u} - \frac{\lambda_1}{\alpha_1+1} - \frac{\lambda_{2,u}}{\alpha_2+1}\Big)du\Big\}$ where $\mu_{c,t}$ is the growth rate of consumption at time t when there are no disasters. Since jumps have a negative effect on endowment and therefore on consumption, $\frac{\lambda_1}{\alpha+1}$ and $\frac{\lambda_{2,t}}{\alpha_2+1}$ must be subtracted from $\mu_{c,t}$ to obtain the expected growth rate. The price of this asset is smaller than the expected payoff due to

discounting. The appropriate discount rate for a risk-free payoff is the risk-free interest rate, but since C_t is risky we should include the risk premium. Therefore, the price of the asset equals:

$$E_0\Big[\frac{\pi_t}{\pi_0}C_t\Big] = \exp\Big\{-\int_0^t (r_u + rp_u)du\Big\}E_0[C_t]. \tag{4.7}$$

The social cost of carbon can be calculated as follows (detailed derivations are given in appendix 4.B):

$$SCC_0 = -\frac{\partial V_0/\partial M_0}{f_C(C_0, V_0)} = -\frac{\partial S_0/\partial M_0}{1-1/\epsilon} - \frac{\partial \xi_0/\partial M_0}{\xi_0}S_0. \tag{4.8}$$

Using the product rule, the social cost of carbon in the optimal policy scenario equals the discounted sum of future marginal damages given the initial policy (the first term) plus the welfare effect of a change in policy due to a change in M_0 (the second term). Note that the second term of the SCC is not present for any exogenous policy path u_t, since in that case the consumption-endowment ratio $\xi_t = c_{1,t}u_t^{c_2}$ does not change when the carbon concentration M_t changes. A special case of an exogenous policy path is the business-as-usual scenario where the emissions control rate $u_t = 0$ for all t. The second term in the SCC formula is quantitatively negligible and for illustrative purposes not very interesting. If we impose that $\partial u_0^*/\partial M_0 \approx 0$, we obtain the following formula for the SCC:

$$SCC_0 \approx \int_0^\infty \underbrace{\int_0^t \frac{\partial \lambda_{2,s}}{\partial M_0}ds}_{\substack{\text{Change in probability of} \\ \text{disaster between 0 and } t}} \underbrace{\frac{1}{\alpha_2 + 1 - \gamma}}_{\substack{\text{Certainty equivalent} \\ \text{of climate disaster}}} \underbrace{\exp\Big\{-\int_0^t (r_u + rp_u)du\Big\}E_0[C_t]}_{\substack{\text{Price of} \\ \text{consumption strip}}} dt. \tag{4.9}$$

Consider the effect of pulse of carbon emissions at time 0. This will change the expected payoff of consumption strips at any time t in the future. The atmospheric carbon concentration and temperature affect the consumption dynamics via the climate disasters. The first term in the social cost of carbon denotes the change in the arrival rate of disasters due to the carbon pulse. Note that any disaster between time 0 and time t affects the level of consumption at time t. Therefore, the derivative of the arrival rate with respect to the carbon concentration is integrated from 0 to t to obtain the change in the probability of a disaster taking place between time 0 and t. The second term is the certainty equivalent of the disaster size. When the agent is risk neutral ($\gamma = 0$), the certainty equivalent equals the expected disaster size. Since the agent is risk averse, the certainty equivalent is larger than the expected disaster size. The last term in the social cost of carbon is the price of a consumption strip. Since the disaster size is defined as a percentage of endowment and therefore of consumption, the first two terms are multiplied with the price of a consumption strip. The social cost of carbon integrates the product of these three terms over all future periods.

The future expected damages within the SCC are discounted at a rate equal to the interest rate plus the risk premium. The effects of the elasticity of intertemporal substitution ϵ and the pure rate of time preference β work through the discount rates. A higher elasticity or a lower rate of time preference lowers the interest rate and therefore affects the SCC. Risk aversion has multiple effects. A higher risk aversion lowers the interest rate

(flight to safety) and increases the risk premium. The effect on discounting is ambiguous and depends on ϵ.[19] Non-climate disasters also influence the SCC through the discount rate. Risk aversion also plays a direct role in the SCC since the certainty equivalent of the climate disasters depends on risk aversion.

The role of the policy scenario u_t in the SCC is not directly clear from the formula. To get a better idea, we can look in more detail at the derivative: $\frac{\partial \lambda_{2,s}}{\partial M_0} = \lambda_2 \theta T_s^{\theta-1} \frac{\partial T_s}{\partial M_0}$. Due to the specific setting of our climate model, we can also calculate the derivative of temperature with respect to the carbon concentration in closed form:

$$\begin{aligned} \frac{\partial T_s}{\partial M_0} &= \int_0^s e^{-\tau_T(s-i)} b \frac{\partial F_i}{\partial M_0} di = \int_0^s e^{-\tau_T(s-i)} \alpha_F b \frac{1}{M_i} \frac{\partial M_i}{\partial M_0} di \\ &= e^{-\delta_M s} \int_0^s e^{-(\tau_T - \delta_M)(s-i)} \alpha_F b \frac{1}{M_i} di. \end{aligned} \tag{4.10}$$

Let us start with the special case in which the arrival rate is a linear function of temperature ($\theta = 1$). In that case, $\frac{\partial \lambda_{2,s}}{\partial M_0} = \lambda_2 \frac{\partial T_s}{\partial M_0}$. The derivative of T_s with respect to M_0 depends on the policy scenario. Radiative forcing $F_t = \alpha_F \ln\left(\frac{M_t + M_{pre}}{M_{pre}}\right)$ is a concave function of the atmospheric carbon concentration and thus $\frac{\partial F_t}{\partial M_t}$ is decreasing in M_t. When the carbon concentration is already very high, an additional unit has a small effect on radiative forcing and therefore on temperature.

Consider two abatement policies $\overline{u_t}$ and $\underline{u_t}$, where $\overline{u_t} > \underline{u_t}$ for all t. This in turn implies that $\overline{M_t} < \underline{M_t}$ since more abatement leads to a lower carbon concentration. From (4.10) it then becomes clear that $\overline{\partial T_s / \partial M_0} > \underline{\partial T_s / \partial M_0}$ due to the concavity of radiative forcing. Therefore we have $\overline{SCC_0} > \underline{SCC_0}$. This directly implies that the SCC in the optimal policy scenario is larger than the SCC in the business-as-usual scenario.

However, damages are often assumed to be a convex function of temperature, i.e. $\theta > 1$. In that case, $\frac{\partial \lambda_{2,s}}{\partial M_0} = \lambda_2 \theta T_s^{\theta-1} \frac{\partial T_s}{\partial M_0}$. Again consider the two abatement strategies $\overline{u_t}$ and $\underline{u_t}$. We still have that $\overline{\partial T_s / \partial M_0} > \underline{\partial T_s / \partial M_0}$, but additionally $\overline{T_s} < \underline{T_s}$ and these two effects work in opposite directions.

If we compare the optimal scenario to the BAU scenario, then both the future temperature and the future carbon concentration are lower in the optimal scenario. The lower carbon concentration in the optimal scenario implies that a unit of carbon emissions has a larger effect on radiative forcing and therefore on temperature (concavity of F_t in M_t). But on the other hand, marginal damages are now increasing in temperature since $\theta > 1$ (convexity of $\lambda_{2,t}$ in T_t). Therefore, future marginal damages are smaller in the optimal scenario since future temperature is smaller. θ controls the strength of the latter effect and is therefore an important driver of the difference between the SCC in the optimal and the BAU scenario. To figure out in which scenario the SCC is largest when $\theta > 1$, we will numerically determine which effect dominates.

[19] See chapter 2 for a detailed discussion of the effect of preference parameters on discounting within the SCC.

4.3 Extended climate model

In the previous section, we developed an integrated assessment model with some simplifying assumptions and analyzed the analytic formula for the social cost of carbon. In this section a more realistic model is presented, which will be solved numerically.

First, emissions are not exogenous but do clearly depend on economic activity itself. We therefore model emissions now as the product of the carbon intensity and endowment, where the carbon intensity declines over time to represent technological progress. This formulation captures that emissions are higher in booms, while in crisis times emissions decline together with the economy. Second, the climate model in the previous section was useful for illustrative purposes but is too simple to properly capture climate dynamics. This will certainly affect quantitative outcomes and simplifying the climate model can have non-negligible effects. Lemoine and Rudik (2017) use a single state variable for both the carbon cycle and temperature dynamics to look at optimal abatement policy. In a comment, Mattauch et al. (2019) show that allowing for multiple state variables in both the carbon cycle and the temperature module does lead to significantly different outcomes. Lastly, not only damages are stochastic, but also the climate variables: we cannot predict exactly what the carbon concentration and temperature will be given the abatement policy. We therefore also allow for randomness in the climate state variables.

Endowment has the same structure as in (4.2):

$$dY_t = \mu Y_t dt + \sigma Y_t dZ_t - J_1 Y_{t-} dN_{1,t} - J_2 Y_{t-} dN_{2,t}, \tag{4.11}$$

where again the arrival rate of climate disasters depends on temperature: $\lambda_{2,t} = \lambda_2 T_t^\theta$. The business-as-usual emissions in the extended model are proportional to endowment: $E_t = \psi_t Y_t$, where ψ_t is the carbon intensity. The carbon intensity is declining over time to represent technological progress. We use the following functional form for the carbon intensity: ψ_t declines at a rate $\delta_t^\psi = \delta_0^\psi e^{-\alpha_\psi t} + \delta_\infty^\psi (1 - e^{-\alpha_\psi t})$. Initially, the decline rate of the carbon intensity δ_0^ψ is smaller than the growth of the economy and emissions are increasing. In the long run, δ_∞^ψ is larger than the growth of the economy so emissions will eventually go towards zero even in the BAU scenario. Eventually emissions must decline, simply because fossil fuels are of finite supply. Actual emissions are then $\tilde{E}_t = E_t(1 - u_t)$. Abatement costs are proportional to endowment and have the same form as in Nordhaus (2017): $A_t = c_{1,t} u_t^{c_2} Y_t$. $c_2 > 1$ captures that the marginal cost of abatement increases in the emissions control rate and $c_{1,t}$ is declining over time at a constant rate δ^c to take into account technological process in abatement technologies. We assume that it is not possible to have net negative emissions, which implies that u_t has an upper bound equal to 1. Although it might technically be possible to take carbon out of the atmosphere, these techniques are expensive and net negative emissions on a large scale seem currently unrealistic. The representative agent consumes what is not spent on endowment, which implies $C_t = Y_t - A_t = \xi_t Y_t$ where $\xi_t = \frac{C_t}{Y_t} = 1 - c_{1,t} u_t^{c_2}$ is the consumption-endowment ratio.

We integrate the climate model developed in Aengenheyster et al. (2018) into our economic model. Aengenheyster et al. (2018) use this stochastic climate model to analyze how early policymakers must at least start with stricter abatement policies in order to keep temperature below two degrees with a 66% probability. We rather use the model to look at optimal policy and the social cost of carbon.

The simple model assumed that there is a single constant decay rate of carbon concentration. In reality the dynamics of the carbon concentration are more complex and a constant decay rate does not hold. Joos et al. (2013) perform a multi-model comparison of different climate models and propose a four-box specification for the carbon model to fit the mean response of the carbon concentration to different emission runs. A fraction a_0 of emissions $\tilde{E}_t$ ends up in the permanent carbon box $M_{0,t}$, which does not decay. Similarly, a fraction a_i ends up in carbon box $M_{i,t}$, $i \in \{1,2,3\}$ where a higher index belongs to a box with a faster decay. The fractions add up to 1: $a_0 + a_1 + a_2 + a_3 = 1$. The carbon concentration compared to the pre-industrial level is then the sum of the four boxes: $M_t = M_{0,t} + M_{1,t} + M_{2,t} + M_{3,t}$. These four boxes should not be interpreted to physically exist but this is rather a reduced form method to match the carbon dynamics of more sophisticated models. The dynamics of the boxes are given by:

$$\begin{aligned}
dM_{0,t} &= a_0 \tilde{E}_t dt, \\
dM_{1,t} &= \Big(a_1 \tilde{E}_t - \frac{M_{1,t}}{\tau_{M_1}}\Big) dt, \\
dM_{2,t} &= \Big(a_2 \tilde{E}_t - \frac{M_{2,t}}{\tau_{M_2}}\Big) dt + \sigma_{M_2} dZ_t^{M_2}, \\
dM_{3,t} &= \Big(a_3 \tilde{E}_t - \frac{M_{3,t}}{\tau_{M_3}}\Big) dt, \\
&\tau_{M_1} > \tau_{M_2} > \tau_{M_3}.
\end{aligned} \tag{4.12}$$

This model can capture the dynamics of a carbon pulse: part of the pulse will decay relatively fast within one or two decades but after that decay is slow and a fraction of the pulse will stay in the atmosphere for multiple centuries. The latter effect is captured by having a permanent carbon box that does not decay. The Brownian motion $dZ_t^{M_2}$ captures uncertainty about the carbon concentration given a certain emissions scenario.

Radiative forcing $F_t = \alpha_F \log\left(\frac{M_{pre}+M_t}{M_{pre}}\right)$ is increasing in the carbon concentration, where M_{pre} is the pre-industrial level of carbon concentration. Temperature increases due to radiative forcing. To calibrate the temperature dynamics, Aengenheyster et al. (2018) look at the temperature response of climate models to different representative concentration pathways (RCPs). These RCPs are different standardized carbon concentration scenarios. Aengenheyster et al. (2018) find that three temperature boxes are sufficient to fit the mean temperature response of multiple climate models to different RCPs. We therefore use three artificial temperature boxes $T_{i,t}$, $i \in \{0,1,2\}$. The temperature anomaly is then the sum of the three boxes: $T_t = T_{0,t} + T_{1,t} + T_{2,t}$, with dynamics:

$$\begin{aligned}
dT_{0,t} &= \Big(b_0 F_t - \frac{T_{0,t}}{\tau_{T_0}}\Big) dt + \sigma_{T_0} dZ_t^{T_0}, \\
dT_{1,t} &= \Big(b_1 F_t - \frac{T_{1,t}}{\tau_{T_1}}\Big) dt, \\
dT_{2,t} &= \Big(b_2 F_t - \frac{T_{2,t}}{\tau_{T_2}}\Big) dt + \sigma_{T_2} T_{2,t} dZ_t^{T_2}.
\end{aligned} \tag{4.13}$$

Note that the standard deviation of $T_{2,t}$ is multiplicative, so volatility increases with the temperature level. This is in line with the finding that the uncertainty about future tem-

perature levels given a carbon concentration scenario is increasing with the temperature level itself.

In this model we can not directly use the same definition for the social cost of carbon, since we have four artificial carbon boxes. One unit of emissions will lead to an increase of a_0 units of $M_{0,t}$, a_1 units of $M_{1,t}$, a_2 units of $M_{2,t}$ and a_3 units of $M_{3,t}$. The social cost of carbon then becomes:

$$SCC_t = -\frac{a_0 \frac{\partial V_t}{\partial M_{0,t}} + a_1 \frac{\partial V_t}{\partial M_{1,t}} + a_2 \frac{\partial V_t}{\partial M_{2,t}} + a_3 \frac{\partial V_t}{\partial M_{3,t}}}{f_C(C_t, V_t)}. \tag{4.14}$$

4.3.1 Hamilton-Jacobi-Bellman equation and optimal policy

The representative agent maximizes welfare by choosing optimal abatement given the dynamics of equations (4.11), (4.12) and (4.13):

$$V_t = \max_{\{u_s\}_{s \geq t}} E_t \Big[\int_t^\infty f(C_s, V_s) ds \Big]. \tag{4.15}$$

The value function V_t must then satisfy the Hamilton-Jacobi-Bellman equation. We denote derivatives with subscripts:

$$\begin{aligned}
0 = \max_{u_t} & \Big\{ f(C_t, V_t) + V_{M_0} a_0 \tilde{E}_t + \sum_{i=1}^{3} V_{M_i} \Big(a_i \tilde{E}_t - \frac{M_{i,t}}{\tau_{M_i}} \Big) \Big\} \\
& + \frac{\partial V}{\partial t} + V_Y \mu Y_t + \sum_{i=0}^{2} V_{T_i} \Big(b_i F_t - \frac{T_{i,t}}{\tau_{T_i}} \Big) \\
& + \frac{1}{2} V_{YY} \sigma^2 Y_t^2 + \frac{1}{2} V_{M_2 M_2} \sigma_{M_2}^2 + \frac{1}{2} V_{T_0 T_0} \sigma_{T_0}^2 + \frac{1}{2} V_{T_2 T_2} \sigma_{T_2}^2 T_{2,t}^2 \\
& + \lambda_1 E \Big[V \Big(Y_{t-}(1 - J_1), M_{0,t}, M_{1,t}, M_{2,t}, M_{3,t}, T_{0,t}, T_{1,t}, T_{2,t}, t \Big) - V_{t-} \Big] \\
& + \lambda_{2,t} E \Big[V \Big(Y_{t-}(1 - J_2), M_{0,t}, M_{1,t}, M_{2,t}, M_{3,t}, T_{0,t}, T_{1,t}, T_{2,t}, t \Big) - V_{t-} \Big].
\end{aligned} \tag{4.16}$$

Optimal policy balances the trade-off between a higher consumption level today and less climate damages in the future. Consumption today equals endowment minus abatement costs: $C_t = Y_t - A_t = \xi_t Y_t$ where the consumption-endowment ratio equals: $\xi_t = 1 - c_{1,t} u_t^{c_2}$. So when the emissions control rate goes up, consumption goes down and therefore also the instantaneous utility $f(C_t, V_t)$ is affected. On the other hand, actual emissions depend on the control rate: $\tilde{E}_t = (1 - u_t) E_t$. Furthermore, a higher carbon concentration leads to more warming and more damages. Therefore, future consumption will benefit (at least in expectation) from abatement. The optimal abatement can therefore be seen as a trade-off between consumption today and in the future. The first order condition for optimal policy equals:

$$0 = -f_C(C_t, V_t) c_{1,t} c_2 u_t^{c_2 - 1} Y_t - \sum_{i=0}^{3} V_{M_i} a_i E_t. \tag{4.17}$$

This condition is equivalent to: $SCC_t = MAC_t$ where $MAC_t = \frac{\partial A_t/\partial u_t}{E_t} = \frac{c_{1,t}c_2 u_t^{c_2-1} Y_t}{E_t}$. In words, in the optimal policy scenario the social cost of carbon is equal to the marginal abatement cost. We have to divide $\frac{\partial A_t}{\partial u_t}$ by the emissions level since u_t is the fraction of total emissions that is abated, while the marginal abatement costs are the costs of reducing emissions by one unit. This equation cannot be solved in closed form for u_t but u_t^* is implicitly defined as a function of V_t, its derivatives and Y_t.

4.3.2 Calibration

The next step is to calibrate the model. First, consider the endowment process except for the climate disasters. We assume that the growth rate of endowment in normal non-disaster times equals $\mu = 3\%$, which is the projected long-run global growth rate in Johansson et al. (2012). Volatility is set to 2.5%. Barro and Jin (2011) estimate the probability and size of economic disasters based on historical data of several countries. These estimations yield $\lambda_1 = 0.038$ (on average once every 26 years a disaster) and an expected disaster size of approximately 20%. However, Barro and Jin (2011) use a minimum disaster size of 9.5%. We do not consider such a cut-off and therefore the arrival rate of $\lambda_1 = 0.038$ is too low and the expected disaster size is too high. Following Hambel, Kraft, and Van der Ploeg (2020), we can derive the arrival rate and expected size without the cut-off. This yields $\lambda_1 = 0.088$ (on average every 11.4 years a disaster) and $\alpha_1 = 8$ (mean disaster size of 11%). Abatement is only a small fraction of endowment and therefore we set the initial endowment level equal to the world consumption level. We can not just use GDP because our asset pricing model does not take into account investments. The base year is 2015. World consumption (using purchasing power parities) is set equal to 83 trillion US dollars in 2015.

To calibrate the preference parameters, we use the following procedure. The interest rate and risk-premium in the model depend on the endowment process and the preference parameters. We choose our preference parameters such that the interest rate and equity premium in the model match historical data. Note that in the past, climate change did not play a big role in both the interest rate and equity premium. For the calibration we therefore consider the interest rate and risk premium assuming there is no climate risk ($\lambda_{2,t} = 0$). Since climate disasters are relatively small compared to economic disasters, the effect of climate risk on the interest rate and risk premium will be modest anyhow. The observed world-wide averages over the period 1900-2010 of the worldwide risk-free interest rate and risk premium were respectively 1% and 4.5% (Dimson et al., 2011). However, Dimson et al. (2011) argue that the historical equity premium might be overoptimistic, since the second half of the 20th century was a period with high returns which turned out better than expected. Based on dividend projections, the authors expect the future equity premium to be in the range of $3\% - 3.5\%$. The combination $\gamma = 4.25$, $\epsilon = 1.5$ and $\beta = 2.5\%$ yields a risk-free rate and an equity premium (without climate risk) of 0.94% and 3.24% respectively. Note that the disentangling of risk aversion and the elasticity of intertemporal substitution is necessary to be able to obtain a reasonable risk-free rate and equity premium. We are fully aware of the fact that the outcomes are very sensitive to the preference calibration. However, the focus of this paper is not to discuss the effect of different preference calibrations on the social cost of carbon and optimal policy.

The emissions parameters are set such that the expected business-as-usual emissions scenario is comparable to the BAU scenario in Nordhaus (2017). The emissions are assumed to peak at the beginning of the next century and start decreasing after that. The abatement costs are also calibrated to resemble the abatement cost function in Nordhaus (2017).

For the climate model, we take over the calibration of Aengenheyster et al. (2018). The authors base the calibrations on a multi-model comparison of the Coupled Model Intercomparison Project (CMIP). CMIP develops standardized experiments that make it possible to compare different climate models. The parameters a_i and τ_{M_i} (carbon cycle) and b_i and τ_{T_i} (temperature model) are calibrated to the match the mean of the multiple climate models. The volatility parameters (σ_{M_2},σ_{T_0},σ_{T_2}) are chosen to match the standard deviation of the multi-model comparison.

The last part is the calibration of the climate disasters. Climate damages are often assumed to have a level effect. The well-known DICE model uses an inverse quadratic damage function: $D_t = \frac{1}{1+0.00266T_t^2}$ (Nordhaus, 2014a). Weitzman (2012) argues that this specification underestimates damages for high temperature levels and proposes to use: $D_t = \frac{1}{1+(\frac{T_t}{20.46})^2+(\frac{T_t}{6.081})^{6.754}}$. On the contrary, our setup with climate disasters yields on average a growth effect instead of a level effect. Hambel et al. (2021) study both growth and level effects in a stochastic climate economy model. They show that the level effects are very similar to the following growth effects: $0.00026T_t$ (Nordhaus) and $0.000075T_t^{3.25}$ (Weitzman). The similarity is reflected in both the output loss over the first century and the social cost of carbon. We use these growth damages to calibrate our climate disasters. We fix the size of a disaster at 3%. We then consider two specifications of the arrival rate: $\lambda_{2,t} = 0.0087T_t$ (linear) or $\lambda_{2,t} = 0.0025T_t^{3.25}$ (convex), such that on average the growth impact is equal to the impact of Hambel et al. (2021).

4.4 Results

In this section we present several numerical results. All computations are performed on a laptop with 7-th generation intel i7 processor and 16GB RAM.

4.4.1 Computation times and algorithm convergence

We solve the model using the stochastic grid method discussed in chapter 3. The details of the solution method are described in appendix 4.D. Before analyzing the outcomes, we first look at the trade-off between computation time and accuracy. We set the number of trajectories K equal to 2500 and the terminal date T to 500. It turns out that increasing either one does not really change the results.

The outcomes and computation times are given in tables 4.1 (linear case) and 4.2 (convex case). We show the value function at the initial date V_0, the initial social cost of carbon SCC_0 and the optimal policy u_0^*. The number of basis functions in the algorithm is varied by changing the number of basis functions (by changing the parameter L) and the results are also given for different time steps δ_t. Both the linear case (table 4.1) and the convex case (table 4.2) are evaluated to see what the effect is of non-linearity in the model.

Table 4.1: *Calibration:* $\theta = 1, \lambda_2 = 0.87\%$. *The value function, social cost of carbon (in US dollars), optimal abatement policy and computation time (in seconds) for different algorithmic parameters.*

			Optimal				BAU			
L	N_b	δ_t	V_0	SCC_0	u_0^*	time	V_0	SCC_0	u_0	time
1	9	2^{-1}	-263.1	116.0	0.191	23	-263.5	88.5	0	8
2	45	2^{-1}	-262.3	109.4	0.184	45	-263.0	106.5	0	24
3	165	2^{-1}	-262.1	110.8	0.186	123	-263.0	108.0	0	83
4	495	2^{-1}	-262.0	111.7	0.187	422	-263.0	107.9	0	313
1	9	2^{-2}	-263.6	115.2	0.190	44	-264.0	87.9	0	16
2	45	2^{-2}	-262.8	108.9	0.184	87	-263.5	105.4	0	48
3	165	2^{-2}	-262.6	110.1	0.185	242	-263.5	107.3	0	163
4	495	2^{-2}	-262.5	110.9	0.186	888	-263.5	107.2	0	639
1	9	2^{-3}	-263.9	114.8	0.190	89	-264.2	87.5	0	31
2	45	2^{-3}	-263.1	108.6	0.183	181	-263.7	105.1	0	97
3	165	2^{-3}	-262.8	109.7	0.184	496	-263.7	106.9	0	319
4	495	2^{-3}	-262.7	110.6	0.185	1801	-263.8	106.9	0	1293

Starting with the linear damages case, it turns out that the linear approximation of the value function ($L = 1$) is not yet very accurate, especially in the BAU scenario. Including the cross-terms and quadratic terms to the set of basis functions by increasing L to 2 already gives accurate results. Choosing L even larger does not change the outcomes much. Decreasing the time step from 2^{-1} to 2^{-2} and from 2^{-2} to 2^{-3} slightly changes the results but the effects are not large.

When we set $\theta = 3.25$, the problem becomes more non-linear. This is clearly visible in the outcomes: the linear approximation with $L = 1$ is not accurate at all in table 4.2. It understates the social cost of carbon in the optimal scenario and overstates it in the BAU scenario. Increasing L improves the results. In the optimal scenario, $L = 2$ already gives a reasonable outcome. In the BAU scenario the value function is more non-linear and a higher order L is needed to obtain an accurate solution.

The outcomes also clearly show the trade-off between computation time and accuracy. The fastest run takes about 10 seconds, while the slowest run takes around two hours. Increasing the level L by one unit approximately triples the computation time, while halving the time step doubles the computation time. For all following results, we choose to set $L = 3$ in the linear case and $L = 5$ in the convex case.

4.4.2 Social cost of carbon: Optimal policy versus business-as-usual

We now quantitatively investigate the difference between the optimal policy scenario and the business-as-usual scenario. The analytic section highlighted two offsetting effects. In the optimal scenario the future carbon concentration is smaller than in the business-as-usual scenario. Adding one unit of carbon into the atmosphere has a larger effect on temperature when the concentration is small, due to the concavity of radiative forcing in the carbon concentration. When climate damages are a linear function of temperature,

Table 4.2: *Calibration:* $\theta = 3.25, \lambda_2 = 0.25\%$. *The value function, social cost of carbon (in US dollars), optimal abatement policy and computation time (in seconds) for different algorithmic parameters.*

			Optimal				BAU			
L	N_b	δ_t	V_0	SCC_0	u_0^*	time	V_0	SCC_0	u_0	time
1	9	2^{-1}	-264.9	247.5	0.307	19	-284.1	479.8	0	9
2	45	2^{-1}	-261.9	305.4	0.350	48	-272.1	574.1	0	30
3	165	2^{-1}	-261.6	293.2	0.341	139	-281.3	381.2	0	103
4	495	2^{-1}	-261.3	301.2	0.347	489	-278.5	448.1	0	370
5	1287	2^{-1}	-261.2	298.5	0.345	1771	-279.7	420.2	0	1393
1	9	2^{-2}	-265.1	248.3	0.307	38	-283.1	480.7	0	18
2	45	2^{-2}	-262.4	306.9	0.351	95	-270.8	598.1	0	57
3	165	2^{-2}	-262.2	292.9	0.341	283	-281.9	372.6	0	200
4	495	2^{-2}	-261.9	300.2	0.346	957	-279.1	450.7	0	714
5	1287	2^{-2}	-261.8	297.7	0.344	3534	-280.2	420.7	0	2778
1	9	2^{-3}	-265.4	245.8	0.305	82	-283.8	475.7	0	36
2	45	2^{-3}	-262.7	307.6	0.351	192	-271.2	586.8	0	116
3	165	2^{-3}	-262.5	292.2	0.340	570	-282.0	370.7	0	411
4	495	2^{-3}	-262.1	299.6	0.346	2132	-279.3	450.9	0	1558
5	1287	2^{-3}	-262.0	297.4	0.344	7028	-280.5	420.0	0	5557

Table 4.3: *Social cost of carbon (in \$/tC).*

	Linear Damages ($\theta = 1$)	Convex Damages ($\theta = 3.25$)
Opt	111	299
BAU	108	420
$\frac{BAU}{Opt}$	97%	141%

the social cost of carbon is therefore larger in the optimal scenario.

However, when the arrival rate is modeled as a convex function of temperature the situation changes. In the optimal scenario, the future carbon concentration is lower but also the future temperature level. With a convex damage specification, marginal damages are increasing in the temperature level. The arrival rate of climate disasters has the following functional form: $\lambda_{2,t} = \lambda_2 T_t^\theta$.

The quantitative results are given in table 4.3. For the linear specification, the SCC in the business-as-usual scenario is equal to 108\$ per ton carbon, which is 97% of the SCC in the optimal scenario. We will express the SCC in the entire paper in US\$/tC. 108\$ per ton carbon is equivalent to 29\$ per ton CO_2, the conversion factor is 3.67. This result shows that the difference between the SCC in the optimal and BAU scenario is very small in the linear specification. So the concavity of radiative forcing does not play a big role. One reason for this small effect is that optimal climate policy is not very stringent with the linear damages calibration. The optimal abatement rate starts at 19%, which implies that in the beginning the climate state variables of the BAU and optimal scenario will not be very different. When it would be optimal to initially abate much more, for example

because of a higher damages (higher λ_T) or because of cheaper abatement technologies, the difference between the SCC in the optimal and the BAU scenario would be larger.

The takeaway from this table is that if damages are assumed to be convex, which is for example argued by Weitzman (2012) and Dietz and Stern (2015), the difference between the SCC in both scenarios becomes large. Using our convex calibration, the SCC in the optimal scenario equals 299$/tC compared to 420$/tC in the BAU scenario. The SCC is thus 41% larger in the BAU scenario compared to the optimal scenario. The conclusion that it does not matter which scenario to use to evaluate the social cost of carbon is only valid for specific calibrations that are close to linear. Since there is no consensus about the specification of the damage function, it is therefore important to take into account this wedge between the two scenarios and to consider the fact the global climate policy at this moment is far from optimal.

4.4.3 Graphical results

This section presents graphical results over time. In the model, both endowment and the climate variables are stochastic. Therefore, also the optimal policy and the social cost of carbon are stochastic variables.

Figure 4.1 shows that there is considerable uncertainty about the future values of most variables. In the worst case scenario (5th percentile), endowment barely doubles within a period of 100 years which implies an average growth rate (including disasters) of approximately 0.7%. The best case scenario (95th percentile) yields an average growth rate of approximately 2.6%, while the median scenario has a growth rate of 1.8%.

The optimal social cost of carbon initially starts at 111 US$ per ton carbon. Most of the expected growth and the uncertainty of the social cost of carbon is driven by the endowment scenarios. Since damages are proportional to endowment, the SCC is also proportional to endowment. A low economic growth scenario thus leads to a low social cost of carbon. The social cost of carbon in the BAU scenario is below the optimal scenario since $\theta = 1$. Furthermore, it becomes clear that the differences between the BAU scenario and optimal scenario are increasing over time. This is intuitive since in the optimal policy scenario the climate variables reach an equilibrium, whereas in the BAU scenario they keep growing. This amplifies the effects that are already present at time $t = 0$. In the BAU scenario the SCC with $\theta = 1$ grows significantly slower than the growth of the economy. The reason for this is that the carbon concentration is growing. Given the concavity of radiative forcing in the carbon concentration, an additional unit of carbon in the atmosphere has a smaller effect if the concentration is already large.

In the optimal policy case, the emissions control rate is chosen such that the marginal abatement cost is exactly equal to the social cost of carbon. The emissions control rate in the initial period is 19%. This implies that actual emissions are 19% lower in the optimal policy case compared to the business-as-usual case. The emissions control rate is increasing over time since abatement costs go down due to technological progress. The uncertainty about the future emissions control rate also comes mostly from economic uncertainty. When endowment growth turns out to be low, the emissions control rate is also low. Interestingly, there seems to be less variation in the optimal emissions path compared to the control rate. The reason for this is that business-as-usual emissions are

Figure 4.1: *Calibration:* $\theta = 1, \lambda_2 = 0.87\%$. *This graph shows the evolution of endowment, the social cost of carbon, marginal abatement costs, the emissions control rate, yearly emissions, the consumption-endowment ratio, the carbon concentration (in excess of the pre-industrial level) and the temperature anomaly over time. Red solid (dashed) lines denote the median (mean) of the optimal scenario and grey areas denote the 5th and 95th percentiles. Lastly, the blue dotted lines denote the mean of the BAU scenario.*

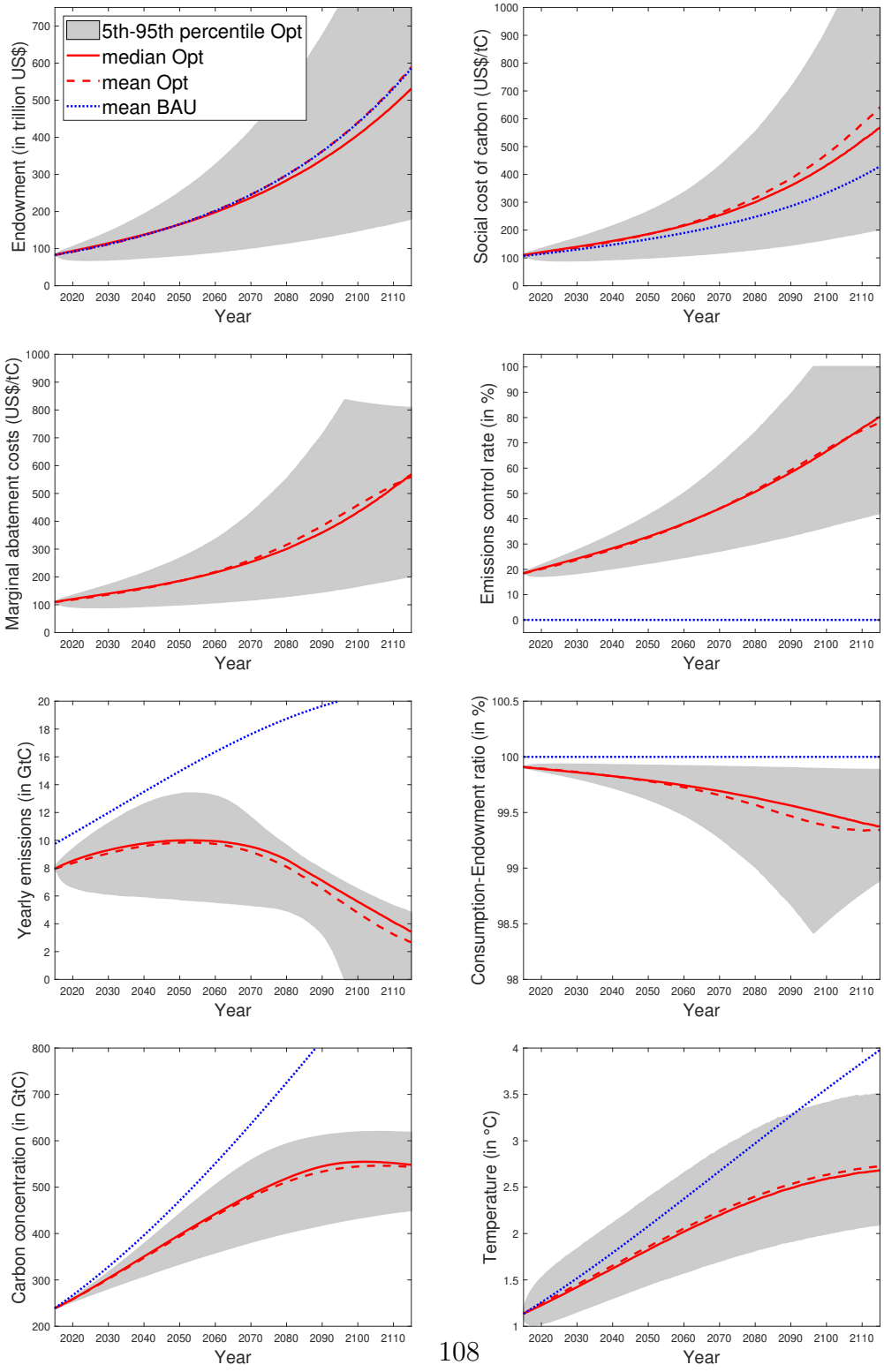

Figure 4.2: *Calibration:* $\theta = 3.25, \lambda_2 = 0.25\%$. *This graph shows the evolution of endowment, the social cost of carbon, marginal abatement costs, the emissions control rate, yearly emissions, the consumption-endowment ratio, the carbon concentration (in excess of the pre-industrial level) and the temperature anomaly over time. Red solid (dashed) lines denote the median (mean) of the optimal scenario and grey areas denote the 5th and 95th percentiles. Lastly, the blue dotted lines denote the mean of the BAU scenario.*

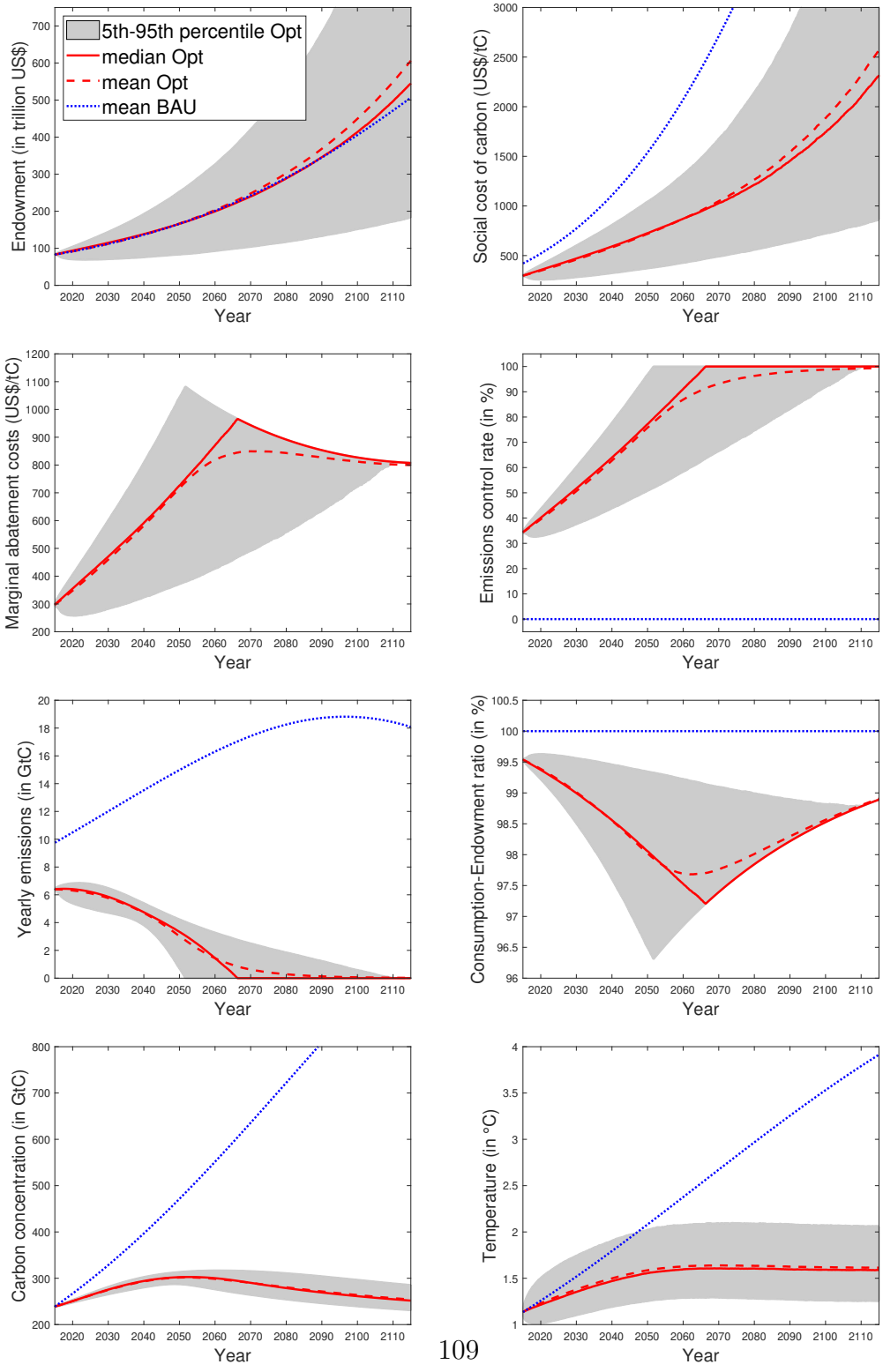

proportional to endowment. When endowment is low, both the emissions control rate is low and the business-as-usual emissions are low. On the other hand, when endowment is high, business-as-usual emissions are high but so is the social cost of carbon and therefore optimal abatement efforts are higher. Both effects somewhat cancel out and this yields less variation in yearly emissions. In the BAU scenario the emissions control rate is simply set to zero. The BAU emissions increase until the end of the century.

Initially, it turns out to be optimal to allocate a very small percentage of endowment to abatement policies. In the median scenario, at the peak it is optimal to spend 0.7% of endowment on emission reduction policies. When u^* is stuck at its maximum level, the abatement fraction starts going down again. This leads to a kink in the consumption-endowment ratio. When the social cost of carbon grows very fast, it is optimal to have a stringent abatement policy and to allocate more resources to abatement. In the 5th percentile scenario, at its peak 1.5% of the resources is spent on abatement, while in the 95th percentile scenario the abatement costs are never above 0.2%.

The carbon concentration in the optimal case reaches its peak around the end of the century, while in the BAU case it would just keep growing. There is some decay of carbon in the atmosphere and therefore the optimal carbon concentration is slightly decreasing after the peak. In our model, we even include a permanent carbon box which implies that the optimal carbon concentration will never reach the original level.

With optimal policy temperature peaks at approximately 2.75 degrees Celsius in the median scenario. This is way above the 2 degrees that is advocated in the Paris agreement. The figure also shows that there is a lot of variation in possible future temperature levels. In the 95th percentile scenario, the temperature peaks at 3.5 degrees. In the BAU scenario the temperature simply keeps growing.

Overall, figure 4.1 shows that uncertainty plays an important role in climate policy. The initial abatement decisions and the initial social cost of carbon are affected by the uncertainty, but the future realizations of these variables are also uncertain. Furthermore, even though policymakers can steer climate policy and react on a specific realization of the state variables when choosing u^*, there is still considerable uncertainty left in the future temperature level. Furthermore we can conclude that the linear damage specification does not induce a stringent optimal policy response. Optimal abatement policy starts only at a 19% reduction and on average the economy is not even carbon neutral at the end of the century.

Figure 4.2 replicates the same graphs in the case of convex damages. Several things are different. First, from the endowment graph it is now clear that no climate policy will really hurt endowment; endowment in the BAU scenario is way below optimal endwoment at the end of the century. Furthermore, when $\theta = 3.25$, the SCC in the BAU scenario is above the optimal scenario. Similar to the previous case, the difference becomes larger over time. The SCC in the BAU scenario is now rising faster than economic growth. The large increase in temperature in the BAU scenario combined with the high convexity pushes up the SCC much faster than in the optimal scenario, where temperature stabilizes at lower levels.

In the convex scenario the median emissions control rate reaches the upper bound of 100% around 2065. At that moment, the entire economy is emissions-neutral. We assume that it is not possible to take carbon out of the atmosphere, which implies that actual

emissions stay at 0 from that moment onward. Abatement policy has reached its upper bound, which implies that after this moment the social cost of carbon is not equal to the marginal abatement costs anymore. As long as u^* has an interior solution, the optimal carbon tax is equal to social cost of carbon, but when u^* reaches 1, a carbon tax equal to the marginal abatement costs will make sure that there will be no more carbon emissions. There is considerable variation in the moment that the economy will be emissions neutral.

With convex damages, abatement spending as a fraction of endowment is also much larger. It is optimal to increase spending on abatement over time up to 2.75% in the median scenario. Temperature stays below two degrees Celsius with a high probability and on average the temperature stabilizes just above 1.5 degrees Celsius. In contrast to the linear specification, the convex damage calibration does induce an optimal policy response that is in line with the Paris agreement.

4.4.4 Risk scenarios and the social cost of carbon

In this section we analyze the effect of the different types of risk on the social cost of carbon. In order to do so, we first solve the deterministic model without any risk. This implies that we set σ, σ_{M_2}, σ_{T_0} and σ_{T_2} equal to zero. To obtain a deterministic equivalent to jump risk, we adjust the growth rate such that the expected growth rate is the same as in the stochastic scenario. In the deterministic scenario, the growth rate of endowment becomes: $\mu - \frac{\lambda_1}{\alpha_1+1} - \frac{\lambda_{2,t}}{\alpha_2+1}$. Then, we first add economic risk by reintroducing economic disaster risk and setting $\sigma > 0$. After that, we add climate risk by setting $\sigma_{M_2} > 0$, $\sigma_{T_0} > 0$ and $\sigma_{T_2} > 0$. In the last step, we also include climate disaster risk. We calculate the social cost of carbon for both scenarios. The results are given in table 4.4.

Compared to the situation with economic risk, the no risk scenario has a substantially higher social cost of carbon. Economic risk affects the social cost of carbon via the discount rate. The effect of risk on the discount rate interacts with the preference calibration. First, the sign of the effect is determined by the elasticity of intertemporal substitution ϵ. In our calibration, we assume $\epsilon > 1$. The discount rate for the social cost of carbon equals the interest rate plus the risk premium. In the no risk scenario, the risk premium equals zero but the interest rate is substantially higher. However, since $\epsilon > 1$ the sum of the two is smaller in the no risk case and therefore the effective discount rate is smaller. This leads to a higher social cost of carbon. When we would choose $\epsilon < 1$, the SCC in the no risk scenario would be smaller compared to the scenario with economic risk.

The change in the discount rate also has an effect on the difference of the SCC between the optimal and BAU scenario. The difference is amplified in the no risk scenario. The reason for this result is that the discount rate is smaller when there is no risk, so more weight is given to the far future. The climate state variables in the BAU scenario are increasing much faster compared to the optimal scenario and the further we get to the future, the larger this difference is. This strengthens the effect that causes the discrepancy of the SCC between the two policy scenarios.

Adding climate risk has a negligible effect when the arrival rate is a linear function of temperature. With more convex specifications, the effects are somewhat larger. When adding disaster risk, the social cost of carbon increases in all scenarios with a similar percentage. The expected loss when a climate disaster strikes is calibrated at 3%. The

Table 4.4: *The social cost of carbon for different risk, policy and parameter scenarios.*

Risk type	$\theta = 1, \lambda_2 = 0.87\%$ Opt	BAU	$\frac{\text{BAU}}{\text{Opt}}$	$\theta = 3.25, \lambda_2 = 0.25\%$ Opt	BAU	$\frac{\text{BAU}}{\text{Opt}}$
No Risk	133.5	118.5	89%	338.9	576.8	170%
Economic	96.7	94.5	98%	251.5	345.3	137%
Economic + Climate	96.8	94.5	98%	268.7	375.1	140%
Economic + Climate + Disaster	110.8	108.0	97%	298.5	420.2	141%

certainty equivalent with risk aversion $\gamma = 4.25$ equals $\frac{1}{\alpha_2+1-\gamma} = 3.4\%$, which is about 14% higher compared to the expected value. If we would set the average disaster size at 6%, the certainty equivalent would be 34% higher. This shows that risk plays a bigger role with infrequent large disasters than with frequent small disasters, even if the expected value of both disasters is the same. The relative differences between the SCC in the optimal and BAU scenario do not change much when climate and disaster risk are included.

Summarizing, table 4.4 shows that it is important to take into account economic risk when calculating the social cost of carbon. Having a realistic economic risk structure generates a plausible interest rate and risk premium and these have a considerable effect on the social cost of carbon. The effects of climate and disaster risk are somewhat smaller with this calibration, but the quantitative effects depend crucially on the calibration. The effect of disaster risk would for example be larger with infrequent large disasters.

4.4.5 Delay of climate policy

In this subsection we analyze the implications of a delay of climate policy. We consider a run in which the abatement control rate is restricted to 0 in the first 20 years, after which optimal policy is implemented. This run therefore is a hybrid between the optimal policy scenario and the BAU scenario. We thus analyze how costly it is to wait with implementing climate policy.

The results for the linear damage specification are given in figure 4.3. The figure shows that after a delay of climate policy, it is not optimal to catch up and start with a higher control rate. With linear damages, the marginal cost of carbon emissions (the SCC) does not increase after 20 years of delayed climate policy. The welfare loss of the delay in policy is also very small. The representative agent is willing to give up less than 0.1% of permanent consumption in order to be able to directly start with optimal abatement policy. One reason for this low welfare loss of delay is that even in the optimal policy scenario, the optimal abatement rate is not very high in the first twenty years. Summarizing, with linear damages delay of climate policy does not seem to be very costly and optimal policy does not change much after the delay.

The picture however changes when we look at the case of convex damages. Figure 4.4 shows that after twenty years of delay optimal abatement policy is significantly above the optimal policy path. This can also be seen from the social cost of carbon, which is higher than the SCC in the optimal policy scenario. The intuition behind this is that a delay in optimal policy leads to higher temperature levels. With convex damages, this

Figure 4.3: *Calibration:* $\theta = 1, \lambda_2 = 0.87\%$. *This graph shows the emissions control rate and the social cost of carbon. Red solid (dashed) lines denote the median (mean) of the scenario in which optimal policy is implemented except for the first 20 years, in which the emissions control rate is restricted to 0. Grey areas denote the 5th and 95th percentiles. Lastly, the blue dotted lines denote the mean of the optimal policy scenario.*

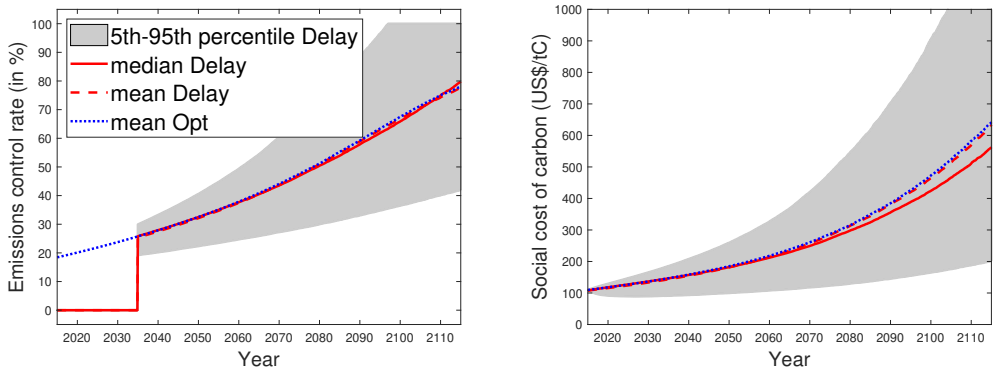

Figure 4.4: *Calibration:* $\theta = 3.25, \lambda_2 = 0.25\%$. *This graph shows the emissions control rate and the social cost of carbon. Red solid (dashed) lines denote the median (mean) of the scenario in which optimal policy is implemented except for the first 20 years, in which the emissions control rate is restricted to 0. Grey areas denote the 5th and 95th percentiles. Lastly, the blue dotted lines denote the mean of the optimal policy scenario.*

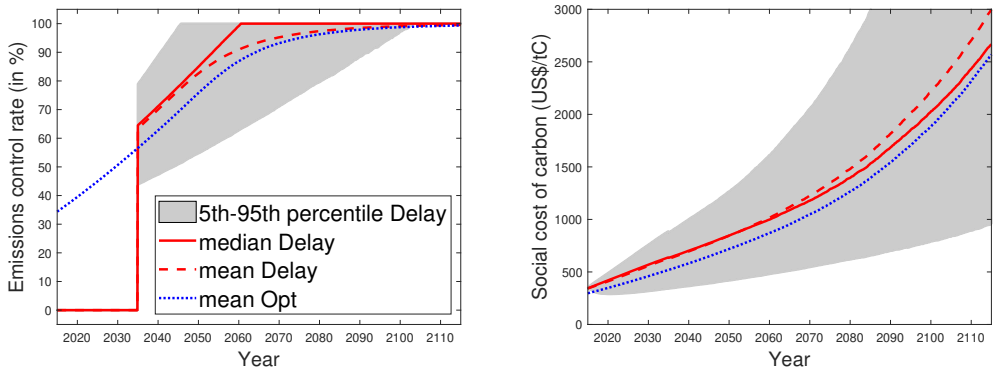

leads to a higher welfare loss of carbon emissions. The representative agent is willing to give up 0.4% of consumption permanently to be able to implement optimal policy in the first twenty years. A 0.4% consumption loss might not sound as much, but note that this is a permanent loss. So the cost of delay equals 0.4% of the value of the claim on consumption. This cost is then equivalent to 17.5% - 20% of yearly consumption. The main point is thus that with convex damages, delay is costly. Besides that, the optimal abatement rate is even higher after the delay compared to the situation where optimal policy is directly implemented.

4.5 Conclusion

We have developed a stochastic climate-economy model to analyze the social cost of carbon. Multi-box carbon and temperature models are integrated into a stochastic pure exchange economy. Our model captures three types of risk: economic risk, climate diffusion risk and climate disaster risk. All three types of risk are inputs of the social cost of carbon, either directly or through discount rates. With this model in hand, we analyze the effect of the policy scenario on the social cost of carbon.

First, using the closed form solution with a simplified climate model we show why and how the policy scenario has an effect on the SCC. On the one hand, radiative forcing is a concave function of the carbon concentration. This implies that emitting a unit of carbon leads to less warming when the carbon concentration is already high, as in the business-as-usual scenario. On the other hand, when damages are convex in temperature, the marginal damages are increasing in the temperature level. This implies that a high temperature level, also as in the business-as-usual scenario, leads to higher marginal damages.

Both effects work in opposite directions and therefore we numerically evaluate the SCC to see which effects dominates. Since we have to solve the model numerically anyhow, we extend our simplified model with endogenous emissions and a stochastic climate model with multiple carbon and temperature boxes to get more realistic climate dynamics. The simulations show that there is considerable uncertainty about future values of the social cost of carbon, optimal policy and the climate variables.

We show that dependence of the SCC on the policy scenario varies with the convexity of the damage function. In the convex calibration with a convexity parameter of 3.25, the SCC in the business-as-usual scenario is 41% higher compared to the optimal scenario. In the ideal world, a global carbon tax equal to the optimal social cost of carbon should be implemented. However, currently global policy is far away from optimal. The SCC in the business-as-usual scenario thus represents the benefit of carbon reduction in the current situation and this metric should currently be leading when implementing climate policy. This chapter additionally shows that delay of climate policy is costly when damages are convex. It is therefore important that policymakers start as soon as possible with implementation of carbon abatement policies.

Our results depend crucially on the convexity parameter of the damage function. As discussed before, there is no clear consensus about what that value should be. A way to explicitly model this uncertainty is to include parameter uncertainty and ambiguity aversion within this framework. An interesting extension for future research is to evaluate the dependency of the social cost of carbon on the emissions path within such a model.

4.A Asset prices

4.A.1 Hamilton-Jacobi-Bellman equation and optimal policy

Derivatives are denoted by subscripts. The value function $V_t = V(Y_t, M_t, T_t, t)$ must satisfy the following Hamilton-Jacobi-Bellman (HJB) equation:

$$\begin{aligned} 0 = \max_{u_t} \Big\{ & f(C_t, V_t) + V_Y \mu Y_t + \frac{1}{2} V_{YY} \sigma^2 Y_t^2 + \frac{\partial V_t}{\partial t} + V_M(\tilde{E}_t - \delta_M M_t) + V_T(bF_t - \tau_T T_t) \\ & + \lambda_1 E\Big[V\Big(Y_t(1-J_1), M_t, T_t, t\Big) - V(Y_t, M_t, T_t, t)\Big] \\ & + \lambda_{2,t} E\Big[V\Big(Y_t(1-J_2), M_t, T_t, t\Big) - V(Y_t, M_t, T_t, t)\Big]\Big\}. \end{aligned} \tag{4.18}$$

Now conjecture: $V(Y_t, M_t, T_t, t) = \frac{g(M_t, T_t, t) Y_t^{1-\gamma}}{1-\gamma}$. We can calculate the derivatives and we can substitute the conjecture of V_t into $f(C, V)$. Substituting our conjecture into $f(C, V)$ gives:

$$\begin{aligned} f(C_t, V_t) &= \frac{\beta}{1 - 1/\epsilon} \frac{\Big(Y_t \xi_t\Big)^{1-1/\epsilon} - \Big(g_t Y_t^{1-\gamma}\Big)^{\frac{1}{\zeta}}}{\Big(g_t Y_t^{1-\gamma}\Big)^{\frac{1}{\zeta}-1}} \\ &= \frac{\beta}{1 - 1/\epsilon} \Big(g_t^{1-\frac{1}{\zeta}} \xi_t^{1-1/\epsilon} Y_t^{1-\gamma} - g_t Y_t^{1-\gamma} \Big) \\ &= \beta\zeta \Big(g_t^{-\frac{1}{\zeta}} \xi_t^{1-1/\epsilon} - 1 \Big) V_t. \end{aligned} \tag{4.19}$$

The partial derivatives of V_t are given by:

$$\begin{aligned} & V_Y = g_t Y_t^{-\gamma}, \quad V_{YY} = -\gamma g_t Y_t^{-\gamma-1} \\ & V_M = \frac{g_M Y_t^{1-\gamma}}{1-\gamma}, \quad V_T = \frac{g_T Y_t^{1-\gamma}}{1-\gamma} \\ & V_t = \frac{\frac{\partial g_t}{\partial t} Y_t^{1-\gamma}}{1-\gamma}. \end{aligned} \tag{4.20}$$

Substituting the derivatives and dividing by $\frac{Y_t^{1-\gamma}}{1-\gamma}$ gives the reduced HJB-equation:

$$\begin{aligned} 0 = \min_{u_t} \Bigg\{ & \Bigg(\beta\zeta \Big(g_t^{-1/\zeta} \xi_t^{1-1/\epsilon} - 1 \Big) + (1-\gamma) \Big(\mu - \frac{1}{2}\gamma\sigma^2 - \lambda_1 \frac{1}{\alpha_1 + 1 - \gamma} \\ & - \lambda_{2,t} \frac{1}{\alpha_2 + 1 - \gamma} \Big) \Bigg) g_t + \frac{\partial g_t}{\partial t} + g_M(\tilde{E}_t - \delta_M M_t) + g_T(bF_t - \tau_T T_t) \Bigg\}. \end{aligned} \tag{4.21}$$

We assume that $\gamma > 1$. Then dividing by $\frac{Y_t^{1-\gamma}}{1-\gamma}$ implies that the maximization problem becomes a minimization problem. We were now able to get rid of one state variable, namely Y_t. Given g_t, the optimal policy can be obtained using the first order condition. Denote the optimal policy by u_t^*, which solves the first order condition:

$$0 = -\beta(1-\gamma) g_t^{1-\frac{1}{\zeta}} \xi_t^{-1/\epsilon} \frac{\partial \xi_t}{\partial u_t} - g_M E_t. \tag{4.22}$$

Optimal policy is implicitly defined by this equation.

4.A.2 Consumption-wealth ratio

S_t equals the total wealth of the representative agent. At the optimum, the following condition is satisfied: $f_C = V_S$ (see for example Tsai and Wachter (2018)). Now define the consumption-wealth ratio by $k_t = \frac{C_t}{S_t}$. Using the chain rule, this implies that $V_S = V_C k_t$. The optimality condition then implies that $k_t = \frac{f_C}{V_C}$. We can calculate f_C:

$$f_C(C,V) = \frac{\beta C^{-1/\epsilon}}{\big((1-\gamma)V\big)^{\frac{1}{\zeta}-1}}. \tag{4.23}$$

Substituting in $f_c, V_t = g_t \frac{Y_t^{1-\gamma}}{1-\gamma} = g_t \frac{(\frac{C_t}{\xi_t})^{1-\gamma}}{1-\gamma}$ and $V_C = g_t \xi_t^{\gamma-1} C_t^{-\gamma}$ gives:

$$k_t = \beta g_t^{-\frac{1}{\zeta}} \xi_t^{1-1/\epsilon}. \tag{4.24}$$

4.A.3 Stochastic discount factor

Duffie and Epstein (1992a) derive that the stochastic discount factor with stochastic differential utility equals $\pi_t = \exp\Big\{\int_0^t f_V(C_s,V_s)ds\Big\} f_C(C_t,V_t)$.

We will start with deriving the explicit stochastic differential equation of the stochastic discount factor. First we calculate the derivatives of $f(C,V)$ with respect to V (the derivative with respect to C is given in the previous subsection):

$$f_V(C,V) = \beta\zeta\Big\{\Big(1-\frac{1}{\zeta}\Big)\Big((1-\gamma)V\Big)^{-\frac{1}{\zeta}} C^{1-1/\epsilon} - 1\Big\}. \tag{4.25}$$

Substituting $V_t = g_t \frac{Y_t^{1-\gamma}}{1-\gamma}$ and $C_t = \xi_t Y_t$ into $f_C(C,V)$ and $f_V(C,V)$ we obtain:

$$\begin{aligned} f_C(C_t,V_t) &= \beta \xi_t^{-1/\epsilon} g_t^{1-\frac{1}{\zeta}} Y_t^{-\gamma}, \\ f_V(C_t,V_t) &= \beta\zeta\Big\{g_t^{-\frac{1}{\zeta}} \xi_t^{1-1/\epsilon}\Big(1-\frac{1}{\zeta}\Big) - 1\Big\}. \end{aligned} \tag{4.26}$$

This gives:

$$\pi_t = \exp\left(\int_0^t \beta\zeta\Big\{g_s^{-\frac{1}{\zeta}} \xi_s^{1-1/\epsilon}\Big(1-\frac{1}{\zeta}\Big) - 1\Big\}ds\right) \beta \xi_t^{-1/\epsilon} g_t^{1-\frac{1}{\zeta}} Y_t^{-\gamma}. \tag{4.27}$$

Write as a differential equation:

$$\frac{d\pi_t}{\pi_{t-}} = \beta\zeta\Big\{g_t^{-\frac{1}{\zeta}} \xi_t^{1-1/\epsilon}\Big(1-\frac{1}{\zeta}\Big) - 1\Big\}dt + \frac{dY_t^{-\gamma}}{Y_{t-}^{-\gamma}} + \frac{dg_t^{1-1/\zeta}}{g_t^{1-1/\zeta}} + \frac{d\xi_t^{-1/\epsilon}}{\xi_t^{-1/\epsilon}}. \tag{4.28}$$

Applying Itô's lemma to $Y_t^{-\gamma}$ gives:

$$\begin{aligned}\frac{dY_t^{-\gamma}}{Y_{t-}^{-\gamma}} = &-\gamma\Big(\mu - \frac{1}{2}(\gamma+1)\sigma^2\Big)dt - \gamma\sigma dZ_t + \Big((1-J_1)^{-\gamma}-1\Big)dN_{1,t} \\ &+ \Big((1-J_2)^{-\gamma}-1\Big)dN_{2,t}.\end{aligned} \tag{4.29}$$

We can also apply Itô's lemma to g_t and ξ_t:

$$\begin{aligned}dg_t &= \frac{\partial g_t}{\partial t} + g_M(\tilde{E}_t - \delta_M M_t) + g_T(bF_t - \tau_T T_t)dt, \\ d\xi_t &= \frac{\partial \xi_t}{\partial t} + \xi_M(\tilde{E}_t - \delta_M M_t) + \xi_T(bF_t - \tau_T T_t)dt.\end{aligned} \tag{4.30}$$

Define $\mu_{g,t} = \frac{\frac{\partial g_t}{\partial t}}{g_t} + \frac{g_M}{g_t}(\tilde{E}_t - \delta_M M_t) + \frac{g_T}{g_t}(bF_t - \tau_T T_t)$ and $\mu_{\xi,t} = \frac{\frac{\partial \xi_t}{\partial t}}{\xi_t} + \frac{\xi_M}{\xi_t}(\tilde{E}_t - \delta_M M_t) + \frac{\xi_T}{\xi_t}(bF_t - \tau_T T_t)$. Applying Itô's lemma once more gives:

$$\frac{dg_t^{1-1/\zeta}}{g_t^{1-1/\zeta}} = (1-1/\zeta)\mu_{g,t}dt, \qquad \frac{d\xi_t^{-1/\epsilon}}{\xi_t^{-1/\epsilon}} = -1/\epsilon\mu_{\xi,t}dt. \tag{4.31}$$

Combining everything gives:

$$\begin{aligned}\frac{d\pi_t}{\pi_{t-}} = &\Big\{\beta\zeta\Big(g_t^{-\frac{1}{\zeta}}\xi_t^{1-1/\epsilon}\big(1-\frac{1}{\zeta}\big)-1\Big) - \gamma\Big(\mu - \frac{1}{2}(\gamma+1)\sigma^2\Big) \\ &- 1/\epsilon\mu_{\xi,t} + (1-1/\zeta)\mu_{g,t}\Big\}dt - \gamma\sigma dZ_t + \Big((1-J_1)^{-\gamma}-1\Big)dN_{1,t} \\ &+ \Big((1-J_2)^{-\gamma}-1\Big)dN_{2,t}.\end{aligned} \tag{4.32}$$

We can now substitute the HJB-equation into the stochastic discount factor. Note that we can rewrite the HJB-equation as:

$$\mu_{g,t} = -\beta\zeta\Big(g_t^{\frac{-1}{\zeta}}\xi_t^{1-1/\epsilon} - 1\Big) - (1-\gamma)\Big(\mu - \frac{1}{2}\gamma\sigma^2 - \lambda_1\frac{1}{\alpha_1+1-\gamma} - \lambda_{2,t}\frac{1}{\alpha_2+1-\gamma}\Big). \tag{4.33}$$

Substituting this gives:

$$\begin{aligned}\frac{d\pi_t}{\pi_{t-}} = &\Big\{ -\beta - \frac{\mu+\mu_{\xi,t}}{\epsilon} + \Big(1+\frac{1}{\epsilon}\Big)\frac{\gamma}{2}\sigma^2 - \Big(\gamma - \frac{1}{\epsilon}\Big)\lambda_1\frac{1}{\alpha_1+1-\gamma} \\ &- \Big(\gamma - \frac{1}{\epsilon}\Big)\lambda_{2,t}\frac{1}{\alpha_2+1-\gamma}\Big\}dt \\ &- \gamma\sigma dZ_t + \Big((1-J_1)^{-\gamma}-1\Big)dN_{1,t} + \Big((1-J_2)^{-\gamma}-1\Big)dN_{2,t}.\end{aligned} \tag{4.34}$$

Therefore π_t is of the form:

$$\frac{d\pi_t}{\pi_{t-}} = \mu_{\pi,t}dt - \gamma\sigma dZ_t + \Big((1-J_1)^{-\gamma}-1\Big)dN_{1,t} + \Big((1-J_2)^{-\gamma}-1\Big)dN_{2,t}. \tag{4.35}$$

4.A.4 Interest rate

Let B_t be the price of the risk-free asset with continuous return r_t: $dB_t = r_t B_t dt$. Using a no-arbitrage argument, $\pi_t B_t$ must be a martingale. This is a martingale if $r_t = -\mu_{\pi,t} - \lambda_1 \frac{\gamma}{\alpha_1 - \gamma} - \lambda_{2,t} \frac{\gamma}{\alpha_2 - \gamma}$. Note that consumption C_t has the following dynamics:

$$\frac{dC_t}{C_{t-}} = (\mu + \mu_{\xi,t})dt + \sigma dZ_t - J_1 dN_{1,t} - J_2 dN_{2,t}. \tag{4.36}$$

Define $\mu_{c,t} = \mu + \mu_{\xi,t}$. The interest rate then equals:

$$\begin{aligned} r_t = \beta + \frac{\mu_{c,t}}{\epsilon} - \Big(1 + \frac{1}{\epsilon}\Big)\frac{\gamma}{2}\sigma^2 + \lambda_1 \Big(\frac{\gamma - \frac{1}{\epsilon}}{\alpha_1 + 1 - \gamma} - \frac{\gamma}{\alpha_1 - \gamma}\Big) \\ + \lambda_{2,t}\Big(\frac{\gamma - \frac{1}{\epsilon}}{\alpha_2 + 1 - \gamma} - \frac{\gamma}{\alpha_2 - \gamma}\Big). \end{aligned} \tag{4.37}$$

4.A.5 Risk premium

Let S_t be the ex-dividend price of the stock that pays dividend at a rate C_t and denote by S_t^d the cum-dividend price. We use the relationship $S_t = \frac{\xi_t}{k_t} Y_t = \frac{\xi_t^{1/\epsilon} g_t^{1/\zeta} Y_t}{\beta}$. The dynamics of S_t^d are given by:

$$dS_t^d = dS_t + C_t dt = S_t \frac{dY_t}{Y_t} + S_t \frac{dg_t^{1/\zeta}}{g_t^{1/\zeta}} + S_t \frac{d\xi_t^{1/\epsilon}}{\xi_t^{1/\epsilon}} + \beta \xi_t^{1-1/\epsilon} g_t^{-1/\zeta} S_t dt \tag{4.38}$$

Now we calculate $dg_t^{1/\zeta}$ and $d\xi_t^{1/\epsilon}$:

$$\frac{dg_t^{1/\zeta}}{g_t^{1/\zeta}} = 1/\zeta \mu_{g,t} dt, \qquad \frac{d\xi_t^{1/\epsilon}}{\xi_t^{1/\epsilon}} = 1/\epsilon \mu_{\xi,t} dt. \tag{4.39}$$

Substituting this into (4.38) yields:

$$\frac{dS_t^d}{S_t} = \Big(\mu + 1/\zeta \mu_{g,t} + 1/\epsilon \mu_{\xi,t}\Big)dt + \sigma dZ_t - J_1 dN_{1,t} - J_2 dN_{2,t}. \tag{4.40}$$

Substituting $\mu_{g,t}$ (4.33) and taking everything together gives:

$$\mu_{S,t} = \beta + \frac{\mu_{c,t}}{\epsilon} - \frac{1}{2}(1/\epsilon - 1)\gamma\sigma^2 - \lambda_1 \frac{1/\epsilon - 1}{\alpha_1 + 1 - \gamma} - \lambda_{2,t} \frac{1/\epsilon - 1}{\alpha_2 + 1 - \gamma}. \tag{4.41}$$

From this equation we can calculate the risk premium rp_t:

$$\begin{aligned} rp_t &= \mu_{S,t} - \lambda_1 E[J_1] - \lambda_{2,t} E[J_2] - r_t \\ &= \gamma\sigma^2 + \lambda_1 \Big(\frac{-1}{\alpha_1 + 1} + \frac{\alpha_1}{\alpha_1 - \gamma} - \frac{\alpha_1}{\alpha_1 + 1 - \gamma}\Big) \\ &\quad + \lambda_{2,t}\Big(\frac{-1}{\alpha_2 + 1} + \frac{\alpha_2}{\alpha_2 - \gamma} - \frac{\alpha_2}{\alpha_2 + 1 - \gamma}\Big). \end{aligned} \tag{4.42}$$

4.A.6 Consumption-wealth ratio

We can find an expression for k_t that does not depend on g_t and ξ_t. First, the stochastic discount factor can be written as:

$$\begin{aligned}\frac{d\pi_t}{\pi_{t-}} =& \Big\{ -r_t - \lambda_1 \frac{\gamma}{\alpha_1 - \gamma} - \lambda_{2,t} \frac{\gamma}{\alpha_2 - \gamma} \Big\} dt - \gamma\sigma dZ_t \\ &+ \Big((1-J_1)^{-\gamma} - 1 \Big) dN_{1,t} + \Big((1-J_2)^{-\gamma} - 1 \Big) dN_{2,t}.\end{aligned} \tag{4.43}$$

Now consider the product of the stochastic discount factor π_t and the consumption stream C_t:

$$\begin{aligned}\frac{d\pi_t C_t}{\pi_t C_t} =& \Big\{ \mu_{c,t} - r_t - \lambda_1 \frac{\gamma}{\alpha_1 - \gamma} - \lambda_{2,t} \frac{\gamma}{\alpha_2 - \gamma} - \gamma\sigma^2 \Big\} dt + \Big(\sigma - \gamma\sigma \Big) dZ_t \\ &+ \Big((1-J_1)^{1-\gamma} - 1 \Big) dN_{1,t} + \Big((1-J_2)^{1-\gamma} - 1 \Big) dN_{2,t}.\end{aligned} \tag{4.44}$$

Thus for $t > 0$:

$$\begin{aligned}\pi_t C_t = \pi_0 C_0 \exp\Big\{ \int_0^t \Big(&\mu_{c,u} - r_u - \lambda_1 \frac{\gamma}{\alpha_1 - \gamma} - \lambda_{2,u} \frac{\gamma}{\alpha_2 - \gamma} - \gamma\sigma^2 \\ &- \frac{1}{2}(\sigma - \gamma\sigma)^2 \Big) du + (\sigma - \gamma\sigma) Z_t \Big\} \prod_{i=1}^{N_{1,t}} (1 - J_1^{(i)})^{(1-\gamma)} \prod_{i=1}^{N_{2,t}} (1 - J_2^{(i)})^{(1-\gamma)}.\end{aligned} \tag{4.45}$$

Here $J_1^{(i)}$ denotes the realization of the i-th jump that occurs within the time interval $[0, t]$. Let a consumption strip be an asset that pays a unit of consumption at some time t in the future. The value of such a consumption strip at time 0 equals:

$$\begin{aligned}E_0\Big[\frac{\pi_t}{\pi_0} C_t\Big] = C_0 \exp\Big\{ \int_0^t \Big(&\mu_{c,u} - r_u - \lambda_1 \frac{\gamma}{\alpha_1 - \gamma} - \lambda_{2,u} \frac{\gamma}{\alpha_2 - \gamma} - \gamma\sigma^2 \\ &+ \lambda_1 \Big(\frac{\alpha_1}{\alpha_1 + 1 - \gamma} - 1 \Big) + \lambda_{2,u} \Big(\frac{\alpha_2}{\alpha_2 + 1 - \gamma} - 1 \Big) \Big) du \Big\}.\end{aligned} \tag{4.46}$$

This is equivalent to:

$$E_0\Big[\frac{\pi_t}{\pi_0} C_t\Big] = C_0 \exp\Big\{ -\int_0^t \Big(r_u + rp_u - (\mu_{c,u} - \frac{\lambda_1}{\alpha_1 + 1} - \frac{\lambda_{2,t}}{\alpha_2 + 1}) \Big) du \Big\}. \tag{4.47}$$

Note that $E_0[C_t] = C_0 \exp\Big\{ \int_0^t \Big(\mu_{c,u} - \frac{\lambda_1}{\alpha_1 + 1} - \frac{\lambda_{2,t}}{\alpha_2 + 1} \Big) du \Big\}$. The consumption-wealth ratio is then equal to:

$$k_0^{-1} = \int_0^\infty E_0\Big[\frac{\pi_t}{\pi_0} \frac{C_t}{C_0}\Big] dt = \int_0^\infty \exp\Big\{ -\int_0^t \Big(r_u + rp_u \Big) du \Big\} E_0[C_t] dt. \tag{4.48}$$

4.B Social cost of carbon

The social cost of carbon can be calculated as the derivative of the value function with respect to the atmospheric carbon concentration scaled by the marginal utility of consumption:

$$\begin{aligned} SCC_0 &= -\frac{\partial V_0/\partial M_0}{f_C(C_0, V_0)} = -\frac{\partial g_0/\partial M_0}{(1-\gamma)\beta\xi_0^{-1/\epsilon} g_0^{1-\frac{1}{\zeta}}} Y_0 = -\frac{\partial g_0/\partial M_0}{g_0(1-\gamma)k_0} C_0 \\ &= -\frac{\partial k_0^{-1}/\partial M_0}{1-1/\epsilon} C_0 - \frac{\partial \xi_0/\partial M_0}{\xi_0} k_0^{-1} C_0. \end{aligned} \tag{4.49}$$

Quantitatively, $\partial u_t^*/\partial M_t$ is negligible and therefore we approximately have:

$$\begin{aligned} SCC_0 &\approx -\frac{\partial k_0^{-1}/\partial M_0}{1-1/\epsilon} C_0 \\ &= -\frac{C_0}{1-1/\epsilon} \int_0^\infty \frac{\partial}{\partial M_0} \exp\Big\{ -\int_0^t \Big(r_u + rp_u\Big) du \Big\} E_0[C_t] dt \\ &= \frac{C_0}{1-1/\epsilon} \int_0^\infty \int_0^t \frac{\partial}{\partial M_0} \Big(r_u + rp_u - (\mu_{c,u} - \frac{\lambda_1}{\alpha_1+1} - \frac{\lambda_{2,t}}{\alpha_2+1})\Big) du \\ &\exp\Big\{ -\int_0^t \Big(r_u + rp_u\Big) du \Big\} E_0[C_t] dt \\ &= C_0 \int_0^\infty \int_0^t \frac{\partial \lambda_{2,t}}{\partial M_0} du \frac{1}{\alpha_2 + 1 - \gamma} \exp\Big\{ -\int_0^t \Big(r_u + rp_u\Big) du \Big\} E_0[C_t] dt. \end{aligned} \tag{4.50}$$

4.C Calibration

Table 4.5: *Parameters for the economic model.*

Par.	Description	Value
Y_0	Initial endowment level (in USD, 2015)	83×10^{12}
μ	Growth rate of endowment during non-disaster times	3%
σ	Volatility of endowment	2.5%
λ_1	Arrival rate of economic disasters	8.8%
α_1	Economic disaster size parameter	8
λ_2	Arrival rate coefficient of climate disasters	0.87% or 0.25%
θ	Convexity parameter	1 or 3.25
α_2	Climate disaster size parameter	32.33
β	Rate of time preference	2.5%
γ	Relative risk aversion coefficient	4.25
ϵ	Elasticity of intertemporal substitution	1.5

Table 4.6: *Parameters for the climate model.*

Par.	Description	Value
E_0	Initial level of total emissions (in GtC, 2015)	9.75
δ_0^{ψ}	Initial decline rate of carbon intensity (2015)	0.5%
δ_{∞}^{ψ}	Long run decline rate of carbon intensity	6.5%
α_{ψ}	Speed of convergence	0.0025
$c_{1,0}$	Initial abatement cost level (2015)	7.41%
δ^c	Decline rate of abatement costs	1.9%
c_2	Convexity parameter of abatement costs	2.6
$M_{0,0}$	Initial level of carbon box 0 (2015)	87.8
$M_{1,0}$	Initial level of carbon box 1 (2015)	83.2
$M_{2,0}$	Initial level of carbon box 2 (2015)	56.9
$M_{3,0}$	Initial level of carbon box 3 (2015)	11.1
M_{pre}	Pre-industrial carbon concentration	592.25
a_0	Fraction of emissions that ends up in carbon box 0	21.73%
a_1	Fraction of emissions that ends up in carbon box 1	22.40%
a_2	Fraction of emissions that ends up in carbon box 2	28.24%
a_3	Fraction of emissions that ends up in carbon box 3	27.63%
τ_{M_1}	Decay parameter of carbon box 1	394.4
τ_{M_2}	Decay parameter of carbon box 2	36.54
τ_{M_3}	Decay parameter of carbon box 3	4.30
σ_{M_2}	Volatility of carbon box 2	0.65
α_F	Radiative forcing parameter	7.92
$T_{0,0}$	Initial level of temperature box 0 (2015)	0.11
$T_{1,0}$	Initial level of temperature box 1 (2015)	0.41
$T_{2,0}$	Initial level of temperature box 2 (2015)	0.62
b_0	Radiative forcing parameter of temperature box 0	0.00115
b_1	Radiative forcing parameter of temperature box 1	0.1097
b_2	Radiative forcing parameter of temperature box 2	0.0336
τ_{T_0}	Temperature parameter of box 0	400
τ_{T_1}	Temperature parameter of box 1	1.43
τ_{T_2}	Temperature parameter of box 2	8.02
σ_{T_0}	Volatility of temperature box 0	0.015
σ_{T_2}	Volatility of temperature box 2	0.13

4.D Solution method

We apply the stochastic grid method as described in chapter 3 to solve this model. One difference is that we cannot substitute out Y_t as a state variable, since emissions are assumed to be a function of endowment. We therefore use the following recursive equation:

$$V_t = \left((1 - e^{-\beta\delta_t}) C_t^{1-1/\epsilon} + e^{-\beta\delta_t} E_t[(1-\gamma) V_{t+\delta_t}]^{1/\zeta} \right)^{\zeta} / (1-\gamma). \tag{4.51}$$

This equation is used instead of the recursive equation for g_t in chapter 3. The vector of state variables equals:

$$X_t = [Y_t \;\; M_{0,t} \;\; M_{1,t} \;\; M_{2,t} \;\; M_{3,t} \;\; T_{0,t} \;\; T_{1,t} \;\; T_{2,t}]'. \tag{4.52}$$

We can then write $V_t = V\big(X_t, t\big)$.

We use the following time-dependent boundaries for the random grid points. Y_t is the only exponentially growing variable. Without climate disasters, Y_t grows in expectation at a rate $\mu - \frac{\lambda_1}{\alpha_1+1}$. Therefore we set the upper bound for $\overline{Y_t}$ equal to $3Y_0 \exp\left((\mu - \frac{\lambda_1}{\alpha_1+1})t\right)$ and the lower bound $\underline{Y_t}$ to $0.1Y_0 \exp\left((\mu - \frac{\lambda_1}{\alpha_1+1})t\right)$. Since Y_t is exponentially growing, the bounds are also time-dependent. For the climate variables, there exists a natural lower bound, namely that $\underline{M_{0,t}} = \underline{M_{1,t}} = \underline{M_{2,t}} = \underline{M_{3,t}} = \underline{T_{0,t}} = \underline{T_{1,t}} = \underline{T_{2,t}} = 0$. The lower bound is the pre-industrial state of the climate. As upper bound, we use the following values:

$$[\overline{M_{0,t}} \;\; \overline{M_{1,t}} \;\; \overline{M_{2,t}} \;\; \overline{M_{3,t}} \;\; \overline{T_{0,t}} \;\; \overline{T_{1,t}} \;\; \overline{T_{2,t}}]' = [250 \;\; 200 \;\; 100 \;\; 25 \;\; 0.6 \;\; 0.6 \;\; 1.5]'. \tag{4.53}$$

So for the climate variables, we use time invariant bounds. Let $\overline{X_t}$ and $\underline{X_t}$ denote the column vectors of upper and lower bounds respectively. It is important to never evaluate the value function at a state variable outside the bounds.

Since there is no abatement in the business-as-usual problem, the climate state variables will just grow over time. We therefore consider a somewhat wider range for the climate state variables in the BAU case:

$$[\overline{M_{0,t}} \;\; \overline{M_{1,t}} \;\; \overline{M_{2,t}} \;\; \overline{M_{3,t}} \;\; \overline{T_{0,t}} \;\; \overline{T_{1,t}} \;\; \overline{T_{2,t}}]' = [500 \;\; 400 \;\; 200 \;\; 50 \;\; 0.9 \;\; 1.2 \;\; 2]'. \tag{4.54}$$

5 On current and future carbon prices in a risky world

5.1 Introduction

Rising temperatures and the threat to our planet and the economy constitute the biggest market failure we know of (Stern et al., 2006). One solution is to price carbon as this reduces demand for carbon-intensive goods, encourages green innovation and carbon capture and sequestration, and locks up fossil fuel in the crust of the earth. This Pigouvian solution charges emissions at a price that implements the optimal policy, namely the price that internalizes the global warming externality (Pigou, 1920). There is a burgeoning debate on how high that tax should be, but with implications for future values of that tax often delivered as a by-product only. Yet future tax rates are a crucial determinant of the investment decisions that need to be taken today to implement an efficient and timely transition to a climate-neutral future. In this paper our emphasis is therefore not only on the level but more on the shape of the time path of the optimal carbon price under a wide range of economic, climatic and damage uncertainties.

Time paths matter as much as the initial price level since much of the adjustment and mitigation efforts will have to take place through new investments and these depend on the trade-off between current costs and future prices. In addition, as investments in both carbon-intensive and green technologies are to a large extent irreversible, there are strong option arguments for announcing a growing path of carbon prices and for policy makers to stick to it so as to lower perceived volatility and thereby reducing the incentive to delay investment (Dixit & Pindyck, 1994).

This price can be implemented as a carbon tax with the revenue rebated in lump-sum manner to the private sector. An alternative and increasingly popular method is to set up a competitive market for emission permits. Instead of the Pigouvian approach, one could also adopt a Coasian approach where property rights to emit or the right to a clean planet are allocated (Coase, 1960), with subsequent trade allowed. If there are other market failures, they should be dealt with using separate instruments. For example, learning-by-doing externalities in the production of green energy require early and direct subsidies of green energy. If this subsidy is lumped together with carbon prices, as is sometimes done in the literature (e.g. Daniel, Litterman, and Wagner (2019)), this leads to an unwarranted early spike in carbon prices which may actually discourage investment in clean technology by rising input costs while not raising future prices commensurately.

In climate economics the Pigouvian price is referred to as the social cost of carbon or the SCC. This is defined as the expected present discounted value of all present and future damages caused by emitting one additional ton of carbon today. Strictly speaking, the SCC is a more general concept than a Pigouvian tax as it can be evaluated along other paths than the optimal path. For example, the SCC evaluated along a business-as-usual path where global warming externalities are not internalized, will be higher than along the optimal path if damages are convex enough (see chapter 4). Policy makers must evaluate the SCC under big uncertainties regarding the wealth of future generations and future global warming damages resulting from emissions today. This involves difficult trade-offs between consumption today and (the risks of) damages from global warming

to consumption in the distant future.

We thus focus on the main drivers for the growth, or decline, of the optimal carbon price. Our benchmark is the case where damages to aggregate production are linear in temperature. Given that recent insights in atmospheric science suggest that temperature is linear in cumulative emissions (Allen et al., 2009; Dietz & Venmans, 2019; Matthews, Gillett, Stott, & Zickfeld, 2009; Van der Ploeg, 2018), the function relating the percentage loss in aggregate production to cumulative emissions is then also linear.[20] We then see that the optimal carbon price grows at the same rate of growth of the economy. The reason for this is that damages are proportional to aggregate production. We then consider step by step four generalizations of our benchmark and how they impact the qualitative pattern of the time path of optimal carbon prices.

First, we show that if damages are a convex function of temperature as has been argued by Weitzman (2012) and Dietz and Stern (2015), the optimal carbon price will start at a higher level and will also grow faster than the economy.

Second, we confirm an earlier result by Daniel et al. (2019) that if there is gradual resolution of uncertainty in the damage ratio, there is a component of the optimal carbon price which falls over time.[21] But we also show that when there is sufficient growth of the economy, this component is outweighed by the growing component of the carbon price resulting from growing damages. The key insight is thus that gradual resolution of uncertainty slows down the rate of growth of the optimal carbon price but under plausible assumptions does not reverse it. Gerlagh and Liski (2018) also find that learning and resolution of uncertainty slows the rise in the optimal carbon price.[22]

Third, we show that climatic and economic tipping points whose arrival rates increase in temperature boost the carbon price. Once a climate tipping point occurs, it will suddenly increase the sensitivity of temperature to cumulative emissions which in turn should prompt policy makers to boost carbon prices and abatement significantly right now. Immediately after the tip has occurred, climate policy is ramped up resulting in an instantaneous further upward jump in the carbon price and abatement. A temperature-dependent risk of an economic tipping point that abruptly leads to a percentage destruction of production also leads to a higher path of carbon prices and abatement ex ante, but immediately after the tip the carbon price and abatement jump down. Different types of tipping points thus have radically different implications.

Fourth, although economists usually take a conventional welfare-maximizing approach, the International Governmental Panel on Climate Change (IPCC) and most countries have adopted the more pragmatic approach of agreeing that policy makers will do their utmost best to keep global mean temperature well below 2 degrees Celsius and aim for 1.5 degrees

[20]This is related to Golosov et al. (2014), who take a different perspective. Their damage function is a convex function of temperature and their temperature relationship is a concave function of the stock of atmospheric carbon. They then notice that their exponential damage function is roughly a linear function of the stock of atmospheric carbon.

[21]Daniel et al. (2019) employ the workhorse recursive dynamic asset pricing model consisting of a discrete-time decision tree with a finite horizon extended to allow for Epstein-Zin preferences and generate optimal carbon dioxide price paths based on probabilistic assumptions about climate damages. They argue that it is optimal to have a high price today that is expected to decline over time as the "insurance" value of mitigation declines and technological change makes emission cuts cheaper.

[22]For learning and optimal climate policy, see also Kelly and Kolstad (1999) and Kelly and Tan (2015).

Celsius. A temperature cap which bites implies that the optimal carbon price should grow at a rate equal to the risk-adjusted interest rate (cf. Gollier (2020)).[23] Once allowance is made for the risk premium, this Hotelling path for the carbon price is typically faster than the rate of growth of the economy (even when the safe return is below the economic growth rate). Hence, the initial carbon price and abatement will be lower upfront but higher in the future. We find that taking into account risk and uncertainty, climate policy is stepped up hugely as temperature gets closer to its cap. The reason is that policy makers must prevent temperature overshooting the cap. If policy makers adopt a tighter cap, they need to boost the carbon price and abatement. We also show that if policy makers take account of a temperature cap and internalize damages from global warming to aggregate production, the optimal carbon price will grow faster than if only damages are internalized but slower than if only a temperature cap is imposed.

Overall, our results suggest that in face of a wide range of risks and uncertainties policy makers should commit to a gradually rising path of carbon prices. This has the added advantage that businesses get clear incentives to invest in long-term projects necessary to make the transition from carbon-intensive to carbon-free production. Our framework of analysis is a simple endowment economy where the endowment is subject to normal economic shocks (modelled by a geometric Brownian motion) and by macroeconomic disasters as in Barro (2006, 2009) and Barro and Jin (2011). Temperature is driven by cumulative emissions, and the fraction of damages lost due to global warming is a power function of temperature and is subject to stochastic shocks with a distribution that is skewed and has mean reversion as in Van den Bremer and Van der Ploeg (2021). Our short-cut approach to modelling gradual resolution of damage uncertainty is slow release of information. We distinguish aversion to risk from aversion to intertemporal fluctuations, so we use recursive preferences (Duffie & Epstein, 1992b; Epstein & Zin, 1989, 1991). This allows for a preference for early resolution of uncertainty when the coefficient of relative risk aversion exceeds the inverse of the elasticity of intertemporal substitution in accordance with empirical evidence.

Our paper is closely related to a recent interesting contribution by Lemoine (2021) who also studies the effect of damage ratio uncertainty and uncertainty about the economic growth rate in an endowment economy and offers analytical insights into the deterministic, precautionary, damage scaling and growth insurance determinants of the optimal social cost of carbon (cf. Van den Bremer and Van der Ploeg (2021)) and crucially gives simulations that show these components of the optimal carbon price. Our model differs in that we distinguish relative risk aversion from the inverse of the elasticity of intertemporal substitution and that that we have more general forms of uncertainty, i.e., we allow for skewness and declining volatility of the shocks to the damage ratio (cf. Daniel et al. (2019)), the risk of rare macroeconomic disasters, and both economic and climatic tipping risks. We also allow for learning-by-doing effects in mitigation and thus for the consequent need for renewable energy subsidies. Furthermore, another contribution of our study is that we analyse the effects of temperature caps under uncertainty (both with and

[23]Gollier (2020) shows in his analysis of the optimal carbon price needed to ensure that a temperature cap is not violated that this rate equals the safe rate plus the beta (the regression coefficient if rate of change in marginal abatement costs is regressed on rate of growth in aggregate consumption) times the aggregate risk premium.

without damages to the economy) on the time paths of the optimal carbon price under uncertainty.

Our paper is also related to an extensive literature on optimal discounting under uncertainty (Gollier, 2002a, 2002b, 2008, 2011, 2012; Weitzman, 1998, 2007, 2009, 2011) and optimal climate policy under uncertainty (Crost & Traeger, 2013, 2014; Jensen & Traeger, 2014; Traeger, 2021; Van den Bremer & Van der Ploeg, 2021). It also relates to a growing literature on optimal climate policy in the presence of climatic and economic tipping points (Cai, Lenton, & Lontzek, 2016; Cai & Lontzek, 2019; Lemoine & Traeger, 2014, 2016; Van der Ploeg & de Zeeuw, 2018).

Our contribution is to present a simple asset pricing model to answer many of the questions regarding uncertainty and tipping points in this literature. Our focus is, however, different in that we aim to understand the qualitative nature of the time path of the path of optimal carbon prices and abatement. A novel contribution of our approach is to also allow for temperature caps. Although Gollier (2020) has analysed these in a 2-period model, we study temperature caps in a continuous-time, infinite-horizon integrated assessment model of the economy and the climate. In the absence of damages from global warming to the economy, we show that the expected growth in the marginal abatement cost and the price of carbon equals the risk-free rate plus the insurance premium. Compared to Gollier (2020), we additionally consider the implementation of a temperature cap while at the same time internalizing the damages to aggregate production caused by climate change. This gives an expected growth of the carbon price that is in the between the growth rate of the economy and the risk-adjusted interest rate.

5.2 An integrated model for optimal climate policy evaluation under risk

To make the trade-off between sacrifices in current consumption against less consumption due to global warming in the future, we use recursive preferences which recursively defines a value function giving the expected welfare from time t onwards, i.e. V_t (Duffie & Epstein, 1992b; Epstein & Zin, 1989, 1991). This formulation distinguishes the coefficient of relative risk aversion, denoted by RA, from the inverse of the elasticity of intertemporal substitution, EIS. Policy makers prefer early (late) resolution of uncertainty if RA exceeds (is less than) 1/EIS. Econometric evidence on financial markets strongly suggests this separation and that RA exceeds 1/EIS (Van Binsbergen et al., 2012; Vissing-Jørgensen & Attanasio, 2003). Hence, the risk-adjusted interest rate incorporates a so-called 'timing premium' (Epstein, Farhi, & Strzalecki, 2014). If RA = 1/EIS as with the power utility function, policy makers are indifferent about the timing of the resolution of uncertainty and there is no timing premium in interest rates. Mathematically, this is represented as follows. All agents have identical preferences and endowments, so all the agents can be replaced by one representative agent. If RA = γ and EIS = ϵ, preferences of this agent

follow recursively from:

$$V_t = \max_{\{u_s\}_{s\geq t}} E_t\Big[\int_t^\infty f(C_s, V_s)ds\Big] \text{ with}$$
$$f(C,V) = \frac{\beta}{1-1/\epsilon}\frac{C^{1-1/\epsilon} - \Big((1-\gamma)V\Big)^{1/\zeta}}{\Big((1-\gamma)V\Big)^{1/\zeta-1}}, \tag{5.1}$$

where $\zeta = (1-\gamma)/(1-1/\epsilon)$ and $\beta > 0$ denotes the utility discount rate or rate of time impatience. If RA = 1/EIS, equation (5.1) boils down to the expected utility approach with no preference for early (or late) resolution of uncertainty.

The endowment of the economy Y_t follows a geometric Brownian motion with drift μ and volatility σ_Y and includes additional terms to allow for disaster shocks with constant mean arrival rate λ_1. The size of the shocks is a random variable with time-invariant distribution. The endowment thus follows the stochastic process:

$$dY_t = \mu Y_t dt + \sigma_Y Y_t dW_t^Y - J_1 Y_t dN_{1,t}, \tag{5.2}$$

where W_t^Y is a standard Brownian motion, $N_{1,t}$ is a Poisson process with arrival rate λ_1, and J_1 is a random variable and corresponds to the share of endowment destroyed if a disaster hits the economy. We assume that $x = 1 - J_1$ follows a power distribution with density $f(x) = \alpha_1 x^{\alpha_1 - 1}$, so $E[x^n] = \alpha_1/(\alpha_1 + n)$ and $0 \leq E[J_1] = 1/(\alpha_1 + 1) \leq 1$. For all moments to exist, we assume that $\gamma < \alpha_1$. This process for the evolution of the economy thus incorporates both normal macroeconomic uncertainty (captured by the geometric Brownian motion) and macroeconomic disaster risks as in Barro (2006, 2009).

Consumption equals:

$$C_t = \frac{1 - A_t}{1 + D_t} Y_t, \tag{5.3}$$

where A_t denotes the fraction of output used for abatement and D_t is the damage ratio associated with global warming. The time path of business-as-usual emissions E_t is assumed to be exogenous. Business-as-usual emissions grow at the decreasing rate $g_t^E = g_0^E e^{-\delta_E t}$, where $\delta_E > 0$ is a constant. Actual emissions are $(1 - u_t)E_t$ where u_t denotes the abatement rate. Without carbon capture and sequestration (CCS), the upper bound of the abatement rate equals 1 in which case all emissions are fully abated and the economy effectively only uses renewable energy.

The cost function for abatement is:

$$A_t = c_0 e^{-c_1 X_t} u_t^{c_2}, \tag{5.4}$$

where X_t is the stock of knowledge and c_1 is the parameter that controls how fast the costs decline over time due to technological progress. The future stock of knowledge is uncertain. We assume that $c_2 > 1$, so abatement costs are a convex function of the abatement rate. We consider two different processes for the stock of knowledge. In the standard case, the stock of knowledge grows exogenously over time, so that:

$$dX_t = 1dt + \sigma_X dW_t^X. \tag{5.5}$$

Technological progress in this case is exogenous. In the absence of abatement cost uncertainty (i.e. $\sigma_X = 0$), the cost function is identical to the cost function in the DICE model (Nordhaus, 2017). In the alternative case we allow for learning-by-doing by assuming that the growth of the stock of knowledge is a function of the cumulative amount of emissions that have been abated:

$$dX_t = u_t E_t dt + \sigma_X dW_t^X. \tag{5.6}$$

Temperature is a linear function of cumulative carbon emissions and its dynamics are described by:

$$dT_t = \chi(1 - u_t)E_t dt, \tag{5.7}$$

where χ denotes the transient climate response to cumulative emissions (TCRCE). The damage ratio is a function of temperature and shocks that take some time to have their full impact and follow a skewed distribution to reflect 'tail' risk. The damage ratio is given by:

$$D_t = T_t^{1+\theta_T}\omega_t^{1+\theta_\omega} \quad \text{with } d\omega_t \quad = \upsilon(\overline{\omega} - \omega_t)dt + \sigma_t^\omega dW_t^\omega, \tag{5.8}$$

where ω_t follows a Vasicek (or Ornstein-Uhlenbeck) process with short-run volatility σ_t^ω, mean reversion υ and long-run mean $\overline{\omega}$ and W_t^ω is a standard Brownian motion (cf. Van den Bremer and Van der Ploeg (2021)). Here θ_T controls the convexity with respect to temperature and θ_ω controls the skew of the shock hitting the damage ratio. Linear (convex) damages in temperature correspond to $\theta_T = 0$ (or > 0). A novel feature of our analysis is that we use the specification:

$$\sigma_t^\omega = \max\left[(1 - t/\bar{t}^\omega)\sigma_0^\omega, 0\right], \tag{5.9}$$

so that volatility starts with σ_0^ω and falls linearly to zero after $\bar{t}^\omega$ years. This captures gradual resolution of damage uncertainty. Volatility is constant if $\bar{t}^\omega \to \infty$. When a temperature cap is implemented, we impose the restriction $T_t \leq T^{cap}$. This is in our setup equivalent to the restriction that only renewable energy must be used once temperature is at its cap, i.e. $u_t = 1$ if $T_t = T^{cap}$.

Finally, we allow for the possibility of an *economic* and a *climatic* tipping point. We assume that the probability of a tipping point increases in global mean temperature. The hazard rate of the *economic* tipping point equals $\lambda_2 T_t$ where λ_2 indicates the rate at which the hazard rate increases with temperature. We assume that when the system tips, a share J_2 of endowment is destroyed. J_2 is a random variable which also follows a power distribution, but with parameter α_2. The main difference between the *economic* tipping point and the disaster process, is that the tipping point can only tip once, while the Barro-style disasters are recurring. We also consider a *climatic* tipping point for which the sensitivity of temperature with respect to cumulative emissions suddenly increases after a tip. More specifically, we assume that before the tip the transient climate response to cumulative emissions is equal to χ_0 and after the tip it jumps to χ_1. The hazard rate for the *climatic* tipping point equals $\lambda_3 T_t$. We show that the two different specifications have very different implications for the optimal carbon price.

5.2.1 Optimal climate policies and implementation in a decentralized economy

We can solve the problem of maximizing expected welfare subject to equations (5.2) to (5.9) using the method of dynamic programming (see Appendix 5.A). The resulting social optimum gives rise to the optimal SCC and can be sustained in a decentralized market economy when, for example, the carbon tax is set to the SCC and the revenue is rebated as lump sums (see Appendix 5.B). The numerical implementation is discussed in Appendix 5.C.

The social cost of carbon (SCC) corresponds to the expected present discounted value of all present and future damages to the economy resulting from emitting one ton of carbon today. It equals the welfare loss of emitting one unit of carbon divided by the instantaneous marginal utility of consumption:

$$SCC_t = \Omega^{i,j}(T_t, \omega_t, X_t, t) C_t^{1/\epsilon} Y_t^{1-1/\epsilon}, \tag{5.10}$$

where $i \in \{0,1\}$, $j \in \{0,1\}$ indicates whether respectively the economic and the climate tipping point have already occurred (cf. equation (5.18)). The second part of equation (5.10) indicates that the optimal SCC is proportional to a weighted geometric average of aggregate consumption and endowment with the weight to consumption equal to 1/EIS. The first part of equation (5.10) indicates that the optimal SCC depends on temperature, shocks to the damage ratio and cumulative learning-by-doing in renewable energy. The SCC corrected for growth of the economy only depends on the first component of (5.10) and is given by $\Omega^{i,j}(T_t, \omega_t, X_t, t)$

We consider two cases for the abatement costs. In the benchmark case abatement costs decline exogenously over time. In the learning-by-doing case abatement costs are endogenous and increase in the stock of accumulated past abatements (i.e. the stock of knowledge). The social benefit of learning corresponds to all the present and future marginal benefits in terms of lower mitigation costs resulting from using one unit of mitigation more today:

$$SBL_t = \Theta^{i,j}(T_t, \omega_t, X_t, t) C_t^{1/\epsilon} Y_t^{1-1/\epsilon} \tag{5.11}$$

(cf. equation (5.19)). Like the SCC, the SBL consists of two components. The second one is proportional to a weighted average of endowment and aggregate consumption and the first one depends on temperature, damage ratio shocks and cumulative learning-by-doing in abatement. In the benchmark case without learning-by-doing, the SBL is simply equal to zero.

When choosing optimal abatement policy, policy makers must recognize that abatement serves two purposes in our set-up: 1) it reduces emissions, which leads to less climate damages in the future and 2) due to learning-by-doing, abatement reduces future abatement costs. But abatement is costly. Policy makers must sacrifice current consumption to make room for abatement if they want to curb global warming and increase (expected) future consumption. Optimal abatement u_t thus follows from the condition that the marginal abatement cost (MAC) must equal the social cost of carbon (SCC) plus the social benefit of learning (SBL):

$$MAC_t = SCC_t + SBL_t \quad \text{where} \quad MAC_t = -\frac{\partial C_t / \partial u_t}{E_t} \tag{5.12}$$

(cf. equation (5.20)). The marginal abatement cost is the cost of abating one more unit of carbon emissions. It increases in the abatement rate u_t since abatement costs are a convex function of the abatement rate. The economy increases abatement until the marginal abatement costs equal the benefits of abatement. If there is no learning-by-doing, the only benefit of abatement is the reduction of climate change damages. In that case the marginal abatement cost is equal to the SCC, which is the expected present discounted value of all current and future damages caused by emitting one more ton of carbon today. The learning-by-doing externality gives an additional incentive to reduce emissions. The marginal abatement cost thus equals the sum of the social cost of carbon and the social benefit of learning. We denote the optimal abatement policy that solves the dynamic programming problem by u_t^*.

When the government implements a carbon tax which is set to $\tau_t = SCC_t$ and a renewable energy subsidy which is set to $s_t = SBL_t$, and the net revenue of these policy instruments are rebated as lump sums, the social optimum can be replicated in a decentralized market economy (see Appendix 5.B). Competitive energy producing firms will then choose the energy mix such that the amount of fossil fuel use equals $F_t = (1 - u_t^*)E_t$ and the amount of renewable energy use equals $R_t = u_t^* E_t$, where E_t is the total amount of energy use in the economy (which we have previously referred to as business-as-usual emissions).

We have adapted the simple but widely used energy model of Nordhaus (2017) and extended it to allow for uncertainty and tipping points in the economy, the climate sensitivity, and damages from global warming. One drawback of this is that in our setting, taxing carbon is equivalent to subsidizing renewable energy since total energy use is not endogenously chosen by the energy producers and since fossil and green energy are perfect substitutes. Optimal policy could thus in such a framework also be replicated by setting a carbon tax equal to $\tau_t = SCC_t + SBL_t$. However, it is important to stress that this is no longer the case in more general models. When fossil fuel and renewable energy use can be optimally chosen separately, replication of the command optimum can only be done by setting $\tau_t = SCC_t$ and $s_t = SBL_t$ (e.g. Rezai and Van der Ploeg (2017a)). Taxing carbon then has different implications than subsidizing green energy. In a more general setting with directed technical change, it can be shown that when green and dirty inputs are sufficiently substitutable, a temporary green energy subsidy is optimal to fight climate change by kickstarting the economy in directions of green technical progress (e.g. Acemoglu, Aghion, Bursztyn, and Hemous (2012)).[24] Although taxing carbon and subsidizing green energy are equivalent in our simple framework, we do interpret the social cost of carbon as the optimal carbon tax and the social benefit of learning as the optimal renewable energy subsidy, to stress that the two are in general not equivalent.

We assume that negative emissions are not possible (or at least not at a competitive

[24]Bovenberg and Smulders (1995, 1996) offer early contributions on climate policy and endogenous growth. It has also been argued that subsidizing green energy technology is not effective to fight climate change, since it leads to higher energy use in total instead of substantially less fossil fuel use (Hassler, Krusell, Olovsson, & Reiter, 2020).

price) and therefore impose an upper bound on the abatement rate of 1. Hence, when it would be optimal to abate more than 100% of the emissions, the optimality condition (5.12) cannot be satisfied anymore. In this case the marginal abatement costs are smaller than the sum of the social cost of carbon and the renewable energy subsidy.

5.2.2 Effects of a temperature cap on optimal abatement and carbon pricing

Optimal policy in presence of a temperature cap still satisfies the first-order condition, but the social cost of carbon now must account for the temperature cap. A temperature cap in our model is equivalent to the restriction that $u_t = 1$ when $T_t = T^{cap}$. We show that in the case of a pure temperature cap (i.e. no effect of climate change on damages to aggregate production), intertemporal optimization implies that the expected growth rate of SCC and of the marginal abatement cost must equal the risk-free interest rate plus the risk premium (for a proof, see Appendix 5.D). Let π_t be the stochastic discount factor. In this case, we thus have that expected growth in the marginal abatement cost and in the optimal carbon price equals:

$$E_t\Big[\frac{dMAC_t}{MAC_t}\Big] = r_t + rp_t, \tag{5.13}$$

where the approximate risk-free rate is given by

$$r_t = E_t\Big[-\frac{d\pi_t}{\pi_t}\Big] = \beta + \frac{\mu_{c,t}}{\epsilon} - \frac{1}{2}(1+1/\epsilon)\gamma\sigma_Y^2 - \lambda_1\Big(\frac{\alpha_1}{\alpha_1-\gamma} - 1 - \frac{\gamma - 1/\epsilon}{\alpha_1+1-\gamma}\Big) \tag{5.14}$$

(cf. equation (5.46)) and the approximate risk premium is given by

$$\begin{aligned} rp_t &= E_t\Big[-\frac{d[\pi_t, MAC_t]}{\pi_t MAC_t}\Big] = E_t\Big[-\frac{d[Y_t^{-\gamma}, Y_t]}{Y_t^{1-\gamma}}\Big] \\ &= \gamma\sigma_Y^2 + \lambda_1\Big(\frac{\alpha_1}{\alpha_1-\gamma} + \frac{\alpha_1}{\alpha_1+1} - \frac{\alpha_1}{\alpha_1+1-\gamma} - 1\Big) \end{aligned} \tag{5.15}$$

(cf. equation (5.48)). In expectation, the growth rate of marginal abatement costs is therefore equal to the risk-free rate plus the risk premium. This result echoes the result derived by Gollier (2020) for a two-period model. It follows from the assumption that temperature is a linear function of cumulative emissions. In that case, we get an equivalent of the celebrated Hotelling rule: the price path assures that temperature does not exceed the cap and achieves intertemporal efficiency. In other words, the risk-adjusted discounted marginal cost of abatement is the same for each period.

5.3 Calibration and benchmark results

We discuss our benchmark calibration and then present and discuss the corresponding optimal time path for respectively the carbon price, the learning-by-doing subsidy, abatement and temperature.

5.3.1 Calibration

In our benchmark calibration, we choose RA = $\gamma = 7$, EIS = $\epsilon = 1.5$ and the rate of impatience $\beta = 2\%$ per year. These are values that are typically used in the asset pricing literature with Epstein-Zin preferences (e.g. Table 1, Cai and Lontzek (2019)) based on empirical evidence. The details of our calibration are reported in table 5.1.

The initial endowment is set to world consumption (using purchasing power parities) of 80 trillion US dollars. We suppose this endowment is subject to normal shocks captured by a geometric Brownian motion with a drift of 2% per year and an annual volatility of 3%. In addition, we have macroeconomic disaster shocks along the lines of Barro (2006, 2009). Here the mean size of the disaster shocks is 8.7% and the mean arrival rate of these shocks is 0.035 per year corresponding to a mean arrival time of 29 years. This calibration yields a real risk-free interest rate of 0.75% and a risk premium of 2.65% if we abstract from the adverse effects of climate change on the economy. Since in the past century climate change has arguably had no effect on interest rates, we can compare these numbers to historical averages.

Dimson et al. (2011) calculate that the global real risk-free rate has been on average 1% and the risk premium 4.5% over the period 1900-2010. We are currently in a low interest environment and in the long run it is questionable whether interest rate will return to their old average levels, which makes 0.75% a reasonable real risk-free interest rate. Our risk premium is lower than the historical average, but our main purpose is not to solve the equity premium puzzle. Furthermore, a risk premium of 2.65% is more realistic compared to most other climate-economy models in which the risk premium is often small or non-existent. These numbers are also close to Gollier (2020) who calibrates the risk-free rate at 1% and the risk premium at 2.5%. This calibration implies that in the case of a temperature cap without damages, the optimal carbon price grows in expectation at a rate equal to the risk-free rate plus the risk premium, i.e. 0.75%+2.65%=3.4%.

Parameters for business-as-usual (BAU) emissions are chosen to match the baseline emissions scenario in Nordhaus (2017) over the first century of the simulation period and afterwards BAU emissions stabilize. The parameters c_0, c_1 and c_2 of the abatement cost function in the benchmark case are taken from the DICE calibration (Nordhaus, 2017). For the learning-by-doing calibration, we take the same value for c_0 (cost of full abatement in initial period) and for c_2 (convexity of abatement costs in u_t). The parameter c_1 now represents the decline in abatement costs when one additional Gt of carbon emissions is abated and is set to $c_1 = 0.375\%$ (cf. Rezai and Van der Ploeg (2017a)). With the learning-by-doing in renewable energy production, future abatement costs depend on cumulative past abatement efforts and thus also depend on the damage calibration. Figure 5.1 compares abatement costs of the benchmark case with the learning-by-doing case, both when damages from global warming are linear and when they are convex.

We take a transient climate response to cumulative emissions (TCRCE) of $1.8^oC/TtC$ (Matthews et al., 2009). The parameters of the uncertain damage shock and of the convexity parameter θ_T are taken from Van den Bremer and Van der Ploeg (2021). For the variant with gradual resolution of damage uncertainty, we assume that the volatility of the damage shock is linearly declining to 0 over a period of 100 years as in equation (5.9).

Table 5.1: *Calibration details.*

Preferences	RA $= \gamma = 7$, EIS $= \epsilon = 1.5$, impatience $= \beta = 2\%$
Economy	Initial endowment $Y_0 = 80$ trillion US dollars *Geometric Brownian motion* Drift in endowment $\mu = 2\%/year$ Volatility of shocks to endowment $\sigma_Y = 3\%/\sqrt{year}$ *Macroeconomic disasters* Arrival rate of disasters $\lambda_1 = 0.035/year$ Mean size of disasters $E[J_1] = 8.7\%$ Shape parameter of power distribution $\alpha_1 = 10.5$
BAU emissions	Initial flow of global emissions in BAU scenario $E_0 = 10GtC/year$ Initial growth of BAU emissions $g_0^E = 1.8\%/year$ Decline of growth rate of BAU emissions $\delta_E = 2.7\%/year$
Abatement costs (Benchmark case)	Initial level of knowledge stock $X_0 = 0$ Initial cost of full decarbonization $c_0 = 7.41\%$ of GDP Rate of technological progress $c_1 = 1.9\%/year$ Convexity parameter cost function $c_2 = 2.6$ Abatement cost volatility $\sigma_X = 1$ Maximum abatement $u \leq 1$
Abatement costs (Learning-by-doing case)	Initial level of knowledge stock $X_0 = 0$ Initial cost of full decarbonization $c_0 = 7.41\%$ of GDP Rate of technological progress $c_1 = 1.9\%$/unit of knowledge Convexity parameter cost function $c_2 = 2.6$ Abatement cost volatility $\sigma_X = 5$ Maximum abatement $u \leq 1$
Temperature	Initial temperature $T_0 = 1^oC$ Transient climate response to cumulative emissions $TCRCE = \chi_0 = 1.8^oC/TtC$ Temperature cap $T^{cap} = 2^oC$ or $T^{cap} = \infty$
Damage ratio	Convexity parameter $\theta_T = 0$ (linear) or $\theta_T = 0.56$ (convex) Skew parameter shocks $\theta_\omega = 2.7$ Mean reversion of shocks $\upsilon = 0.2/year$ Initial and mean steady-state value of shocks $\omega_0 = \overline{\omega} = 0.21$ Constant volatility variant $\sigma_0^\omega = 0.05$, $\bar{t}^\omega = \infty$ Declining volatility variant $\sigma_0^\omega = 0.05$, $\bar{t}^\omega = 100$ years
Economic tipping point	Arrival rate of tipping point $\lambda_2 = 0.01T_t$ Mean tipping damage level $E[J_2] = 2.5\%$ Shape parameter of power distribution $\alpha_2 = 39$
Climatic tipping point	Arrival rate of tipping point $\lambda_3 = 0.006T_t$ $TCRCE$ after tipping $\chi_1 = 2.5^oC/TtC$

Figure 5.1: *Costs of full abatement ($u_t = 1$) in the benchmark and in the learning-by-doing case for two different damage specifications (linear and convex).*

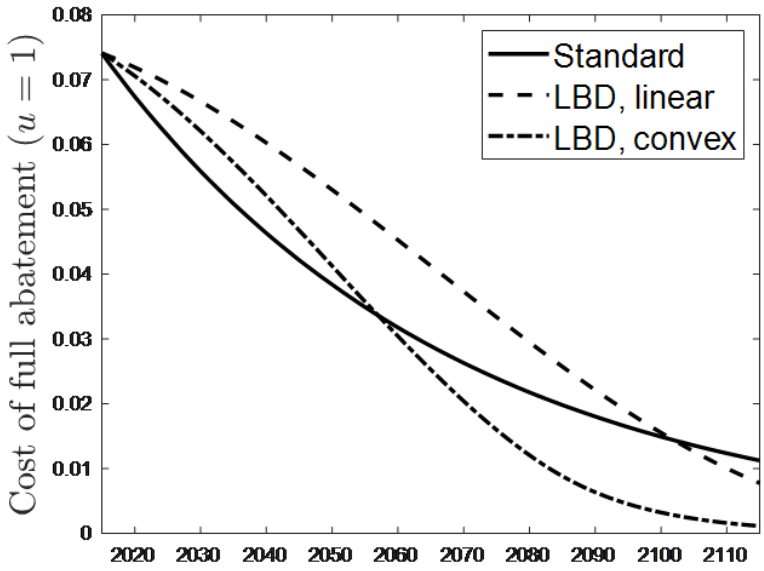

Finally, we assume that initially an economic tipping point tips on average after 100 years. When temperature increases to two (four) degrees Celsius, this becomes on average after 50 (25) years. The size of the damages caused by the tipping disaster is assumed to be on average 2.5%. For the climate tipping point, it takes initially on average 167 years for the climate system to tip. With 2 degrees Celsius warming the average time reduces to 83 years. When the system tips, the TCRCE jumps from $1.8^oC/TtC$ to $2.5^oC/TtC$. Overall, the main message of the two tipping point calibrations is that the probability of tipping in both cases is quite small, but we will show that the impact on optimal carbon prices is nevertheless considerable.

5.3.2 Benchmark optimal carbon prices

With this calibration, the benchmark SCC (with linear damages, no learning-by-doing and no temperature cap) is shown in figure 5.2. The SCC corresponds to the optimal carbon price. The most striking feature of the top two panels is that the ex-ante mean and median paths of the optimal carbon price start at almost 50$/tC and then grow almost in tandem with the growth of the economy.

In fact, there is a modest decline in carbon price corrected for the growth of the economy as can be seen from the top right panel. The median carbon price path lies below the mean carbon price path, and the 5% and 95% bounds become wider for carbon prices that are further in the future as one should expect given that a function of GBM processes is a GBM process itself. As a result of the technological progress in abatement technology, there is a gradual rise in abatement efforts over time. Due to the rise in business-as-usual emissions, temperature rises to around 3 degrees Celsius in the next century but by rather less than in the absence of abatement efforts. The plots also

Figure 5.2: *Benchmark with linear damages, no learning-by-doing, no gradual resolution of uncertainty, no tipping points, and no temperature cap.*

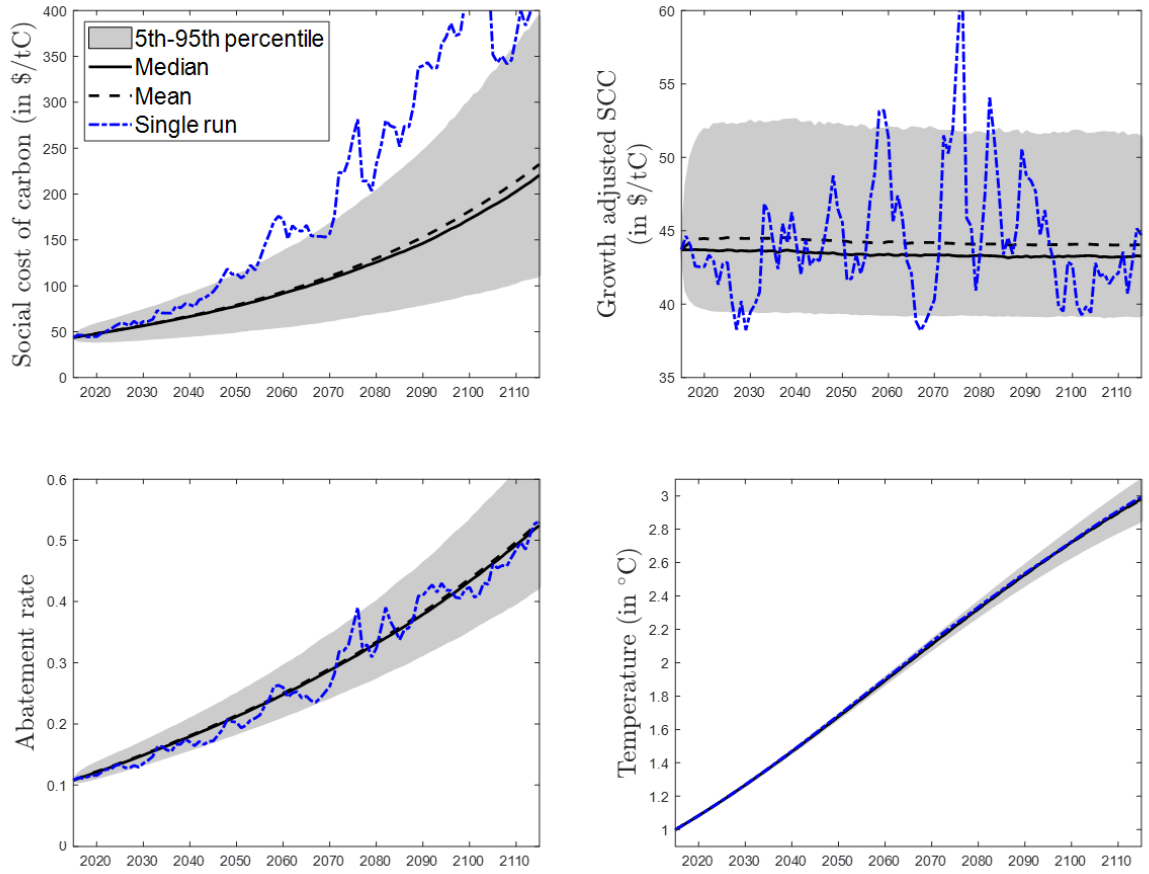

Figure 5.3: *Convex damages.*

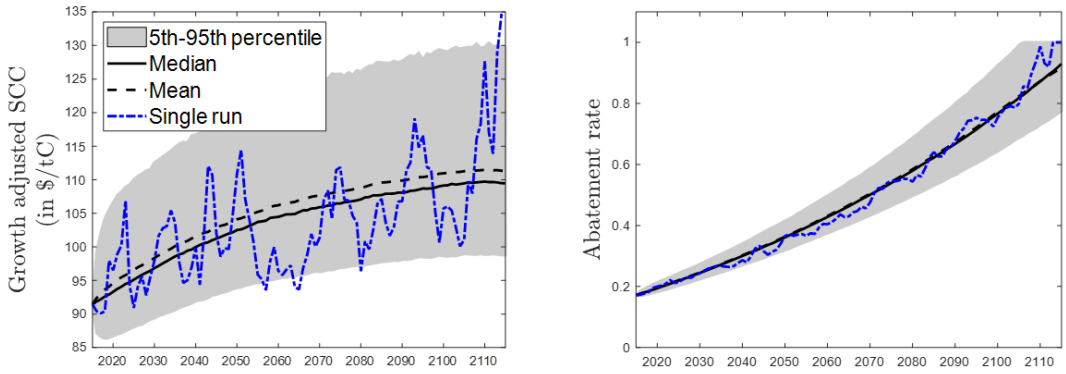

indicate a sample run in blue. This suggests that for individual sample paths of the optimal carbon price there may be substantial volatility, which does not show up in the ex-ante time path for the mean (or median) optimal carbon price. Since we abstracted from stochastic shocks to temperature and abatement efforts are much less volatile, the temperature path itself shows hardly any volatility. When we allow for uncertain tipping points in the sensitivity of temperature to cumulative emissions, this will change.

5.4 Five generalizations of the benchmark

We now discuss five generalizations of the benchmark. For expositional reasons, we discuss these generalizations one by one. In practice, all these generalizations may be relevant at the same time. We discuss first the effects of convex damages, then present the effects of learning-by-doing and a combination of convex damages and learning-by-doing. After that we discuss the implications of gradual resolution of damage uncertainty and then show the differential impacts of climatic and economic tipping points. Finally, we analyse the effects of temperature caps on the time path of carbon prices.

5.4.1 Convex damages

Figure 5.3 presents the effects of convex damages captured by the proportion of output lost due to global warming being a convex rather than a linear function of temperature. Following Van den Bremer and Van der Ploeg (2021), we let this function be proportional to temperature to the power of 1.56. This is slightly less convex than the damage function of Nordhaus (2017) but serves to illustrate the effects of convex damages. The most striking effect of convex damages is that the carbon price starts at a higher level, 91$/tC instead of 44$/tC, and then grows in expectation at a faster pace than in the benchmark. We can see this most strikingly by comparing the top right panel of figure 5.2 with the left panel of figure 5.3. This shows that with convex damages, the path of the optimal carbon price corrected for the growth of the economy rises whilst with linear damages, this path declined mildly. Hence, the abatement efforts are much stronger. The average mitigation rate now rises in a century to 92% instead of 53% in the benchmark. We thus confirm the Monte-Carlo results of Dietz and Stern (2015) in our fully stochastic framework: climate

Figure 5.4: *Learning-by-doing in abating emissions.*

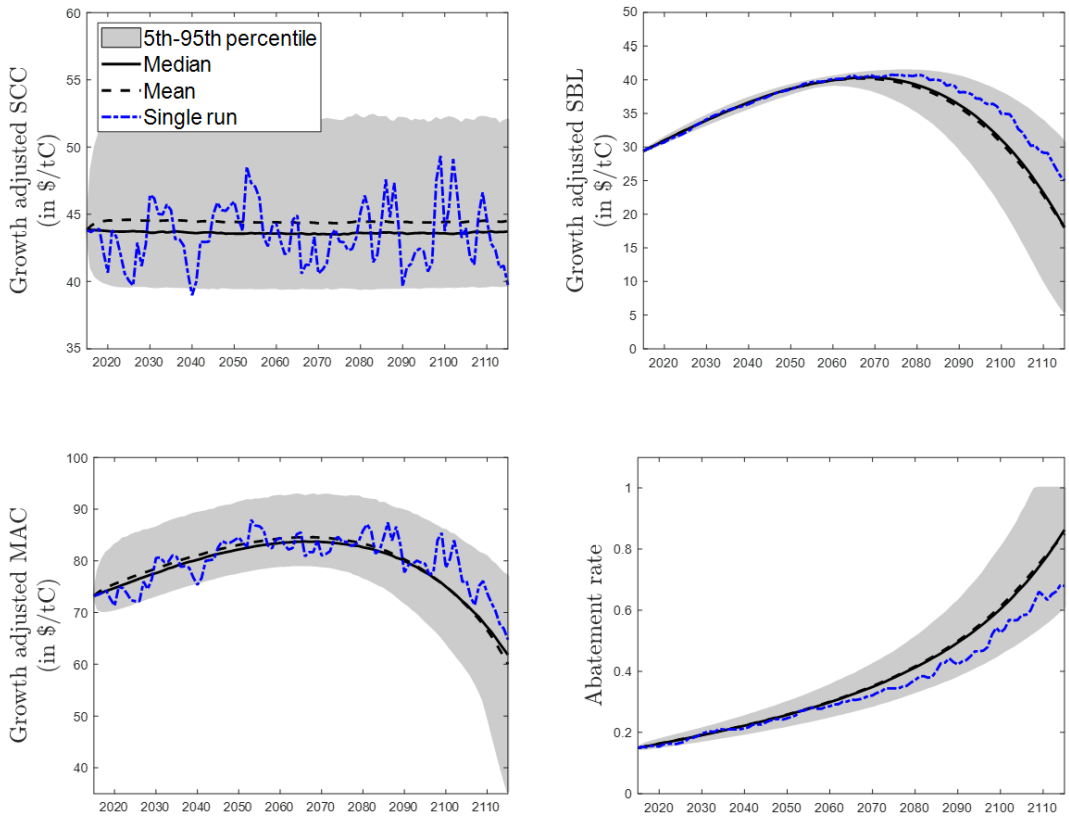

policies get intensified if damages are convex.

5.4.2 Learning-by-doing in abating emissions

Including learning-by-doing into the analysis gives an additional reason for abatement. The marginal abatement cost is now equal to the social cost of carbon plus the social benefit of learning. The social cost of carbon adjusted for economic growth is almost identical to the base situation, so changing the abatement cost structure has no significant effect on optimal carbon prices. Hence, optimal carbon prices still grow in tandem with the economy (see top left panel of figure 5.4).

The social benefit of learning shown in the top right panel of figure 5.4 has a very different shape. It grows faster than the economy in the first 50 years,[25] but after that time abatement costs have been reduced substantially because of learning-by-doing to such an extent that even lower abatement costs do not give much additional benefit anymore. The SBL is therefore sharply declining towards zero at the end of the century. Compared to the benchmark case, the optimal abatement rate is much higher initially. At the end of the century, it is optimal to abate around 85% of emissions, which is much higher than the 53% abatement rate in the benchmark.

[25]Note that the panel displays the growth-adjusted SBL. Hence, an upward-sloping time path of this SBL implies that the SBL grows at a higher rate than the economy.

Figure 5.5: *Convex damages and learning -by-doing in abating emissions.*

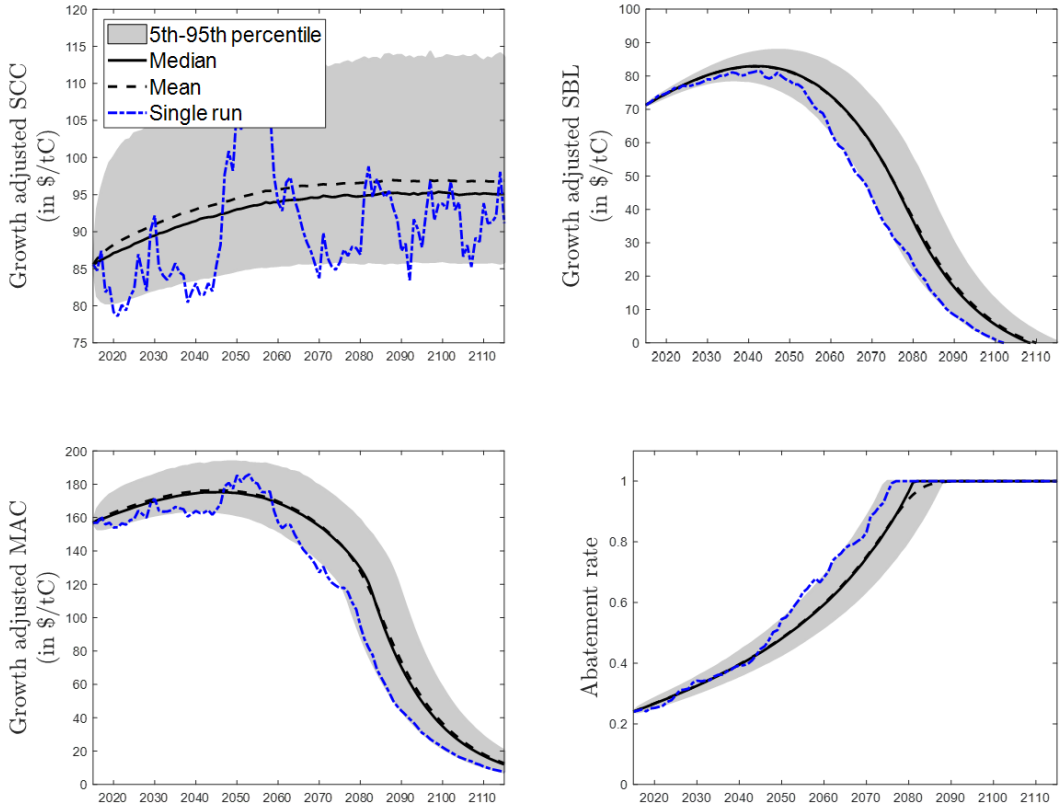

5.4.3 Convex damages and learning-by-doing in abatement

Figure 5.5 shows that combining convex damages and learning-by-doing leads to an even stronger incentive for abating emissions. The optimal carbon price is again very similar to the optimal carbon price without learning-by-doing. The social benefit of learning has a similar shape to the SBL in the linear case. However, it starts much higher and declines towards zero faster. Since damages are more severe, more abatement is optimal and lowering abatement costs by investing in knowledge is even more beneficial, which explains the higher initial level of the SBL. In this scenario it is optimal to fully decarbonize the economy around 2075, much earlier than in the previous scenarios. The main takeaway from the learning-by-doing simulations is that optimal abatement of emissions is understated if learning-by-doing externalities are not internalized.

5.4.4 Gradual resolution of damage uncertainty

Our third generalization is to allow for gradual resolution of damage uncertainty. More precisely, we let the annual volatility of the damage ratio fall to zero linearly in a century. This is a shortcut to capturing slow resolution of uncertainty without delving into the intricacies of learning. The left panel of figure 5.6 indicates that the expected optimal path of carbon prices corrected for growth of the economy now falls over time, much more strongly than the modest decline shown in the benchmark (see top right panel of

Figure 5.6: *Gradual resolution of damage uncertainty.*

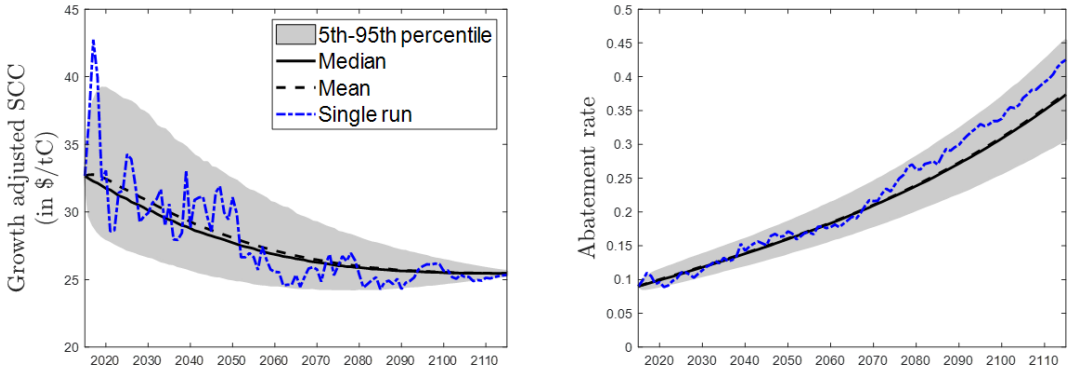

figure 5.2). We find that the carbon price does not only grow much more slowly than the economy, but also starts at only 33$/tC instead of 44$/tC. The fact that there is declining uncertainty about the damage ratio means that policy makers can pursue a less vigorous climate policy than in the benchmark. Declining volatility in the future already has an impact on the optimal carbon price today. This implies that the mitigation rate rises in a century to only 38% compared to 53% in the benchmark. Note that if there is no or very little growth in the economy, the optimal carbon price would decline over time as found by Daniel et al. (2019) for a 7-period model for integrated assessment of economy and the climate. The general point is that gradual resolution of damage uncertainty slows down the rate of growth of the optimal carbon price. In a more formal context of learning and resolution of uncertainty, Gerlagh and Liski (2018) show that this also tends to slow down the rise in optimal carbon prices.

5.4.5 Climatic and economic tipping points

Our fourth generalization is to allow for climatic and economic tipping points. There is a growing literature on the effects of various stochastic tipping points on optimal climate policy (Cai & Lontzek, 2019; Lemoine & Traeger, 2014, 2016; Van der Ploeg & de Zeeuw, 2018). Most of these studies are quite challenging from a numerical point of view. Here we simply present the effects (relative to our benchmark) of two illustrative tipping points.

We first present a single climatic tipping point for which we assume that there is a risk of a regime shift in which the transient temperature response to cumulative emissions suddenly jumps up from $1.8^oC/TtC$ to $2.5^oC/TtC$. Moreover, we assume the arrival rate to be higher at higher temperatures: the initial hazard of this tip at the initial temperature of 1 ^oC is 0.006, which implies an expected arrival time of 167 years, but for every increase in temperature by 1 ^oC we let the hazard rate rise by a further 0.006. This means that at 3 ^oC the hazard is 0.018 and the mean arrival time for the catastrophe is only 56 years. Although these small risks are likely to occur in the very distant future, they have consequences on optimal climate policy now already, as can be seen by comparing figure 5.7 with figure 5.2. The mean optimal carbon price now starts somewhat higher at 48$/tC than in the benchmark and then rises over time. Hence, the mitigation rate ends up higher after a century, at 60% instead of 53%. The blue lines indicate a sample

Figure 5.7: *Risk of a climatic tipping point.*

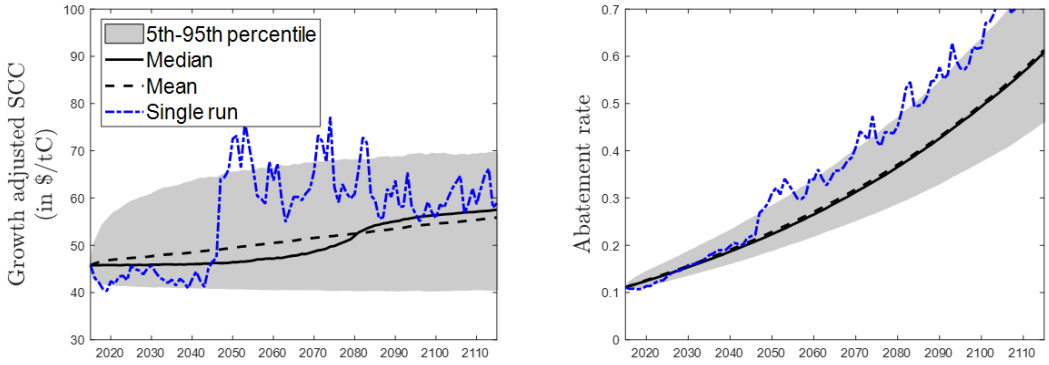

path with the tipping point occurring in 2045. At that time, the carbon price jumps up substantially because of the bigger climate challenge resulting from the increased sensitivity of temperature to cumulative emissions.

Figure 5.8 gives the optimal policy simulations for a different type of tipping point, namely one that leads to a higher effect of global warming on damages instead of increased temperature sensitivity. We assume that the size of the economy drops on average by 2.5% once this tipping point occurs. The initial hazard of this tip at initial temperature is 0.01, which implies an expected arrival time of 100 years. For each increase in temperature by 1 ^oC, the hazard rate is assumed to rise by 0.01. Hence, at 3 ^oC the hazard is 0.03 and the mean arrival time for the tipping point goes down to 33 years. This economic tipping point is thus expected to occur more rapidly than the climate tipping point. The most striking feature is that for this tipping point, the initial carbon price is much higher than in the benchmark, i.e., 78\$/tC instead of 44\$/tC, but that the mean and median paths of the optimal carbon price corrected for growth of the economy fall strongly over time. The blue line indicates a sample run where the tipping point occurs in 2045. At that time, the carbon price drops down instantaneously and, as a result, the mitigation rate drops down at that time too. The intuition behind this drop is obvious: initially, a large fraction of the carbon price is reflecting the urgency of preventing the tipping point. A higher carbon price leads to more mitigation efforts and therefore a lower probability of the tipping. But when despite these additional abatement efforts, the system tips eventually, there are no further tipping points to prevent. Moreover, after the tip has occurred the economy is smaller because of the sudden increase in damages. The social cost of carbon is proportional to output, which is another factor behind the drop in the SCC after the damage catastrophe occurs. The benefit of carbon reduction after the tip is the same as the benefit in the benchmark model without the tipping point for the same level of output.

This is an important point: a tipping point in the climate system that speeds up warming or leads to a slower decay of carbon emissions has very different implications than a tipping point that directly affects the economy. In the former case abatement efforts can be higher before the tip to prevent tipping, but when the system tips eventually abatement efforts jump up even further since one unit of emissions now leads to more global warming. The expected growth adjusted carbon price is therefore growing faster

Figure 5.8: *Risk of an economic tipping point.*

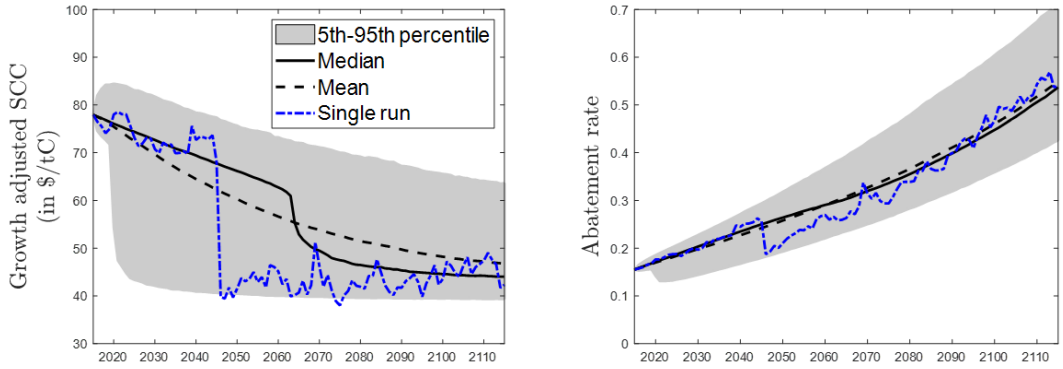

Figure 5.9: *Risk of two tipping points affecting respectively the climate system and the size of the economy.*

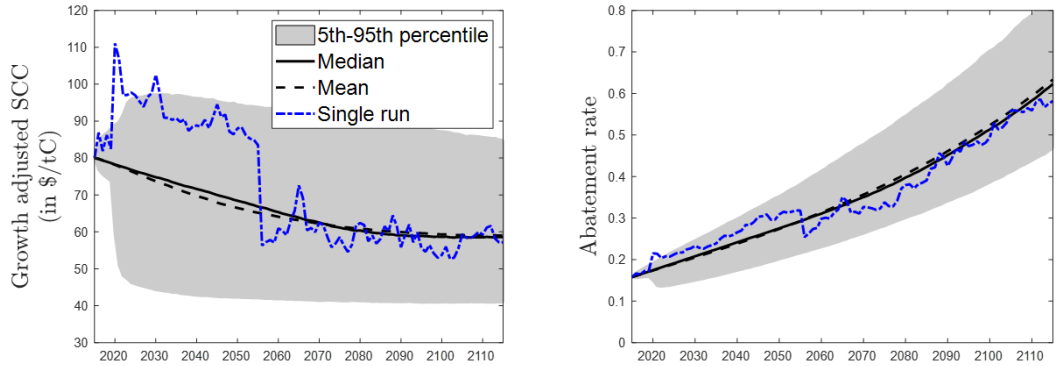

than economic growth. In the latter case of an economic tipping point, abatement efforts before tipping are also higher than in the absence of a tipping point to prevent tipping, but once the damage tipping point has happened, the carbon price jumps down.

We can also combine both types of tipping points in a single simulation. Figure 5.9 shows a sample path in which the climate tipping point tips very early and in which the economic tipping point tips around 2055. The initial carbon price is equal to 80 $/tC. The left panel indicates that the declining effect of the economic tipping point dominates the increasing effect of the climate tipping point. However, the growth-adjusted carbon price or social cost of carbon is now much flatter compared to the left panel of figure 5.8. Abatement efforts are higher when both tipping points are present; the optimal abatement rate is 63% after a century.

Of course, in practice, the impact of a tipping point may take a long time to materialize (Cai & Lontzek, 2019; Van der Ploeg & de Zeeuw, 2018). We have abstracted from this, but protracted effects of tipping points are clearly important in terms of the resulting time path of optimal policy, which will change more gradually. It is also important to allow for cascading tipping points where the onset of one tip might increase the likelihood of another tipping point occurring, by more than implied by the temperature-dependence of

Figure 5.10: *Effects of a 2 degrees Celsius temperature cap without damages.*

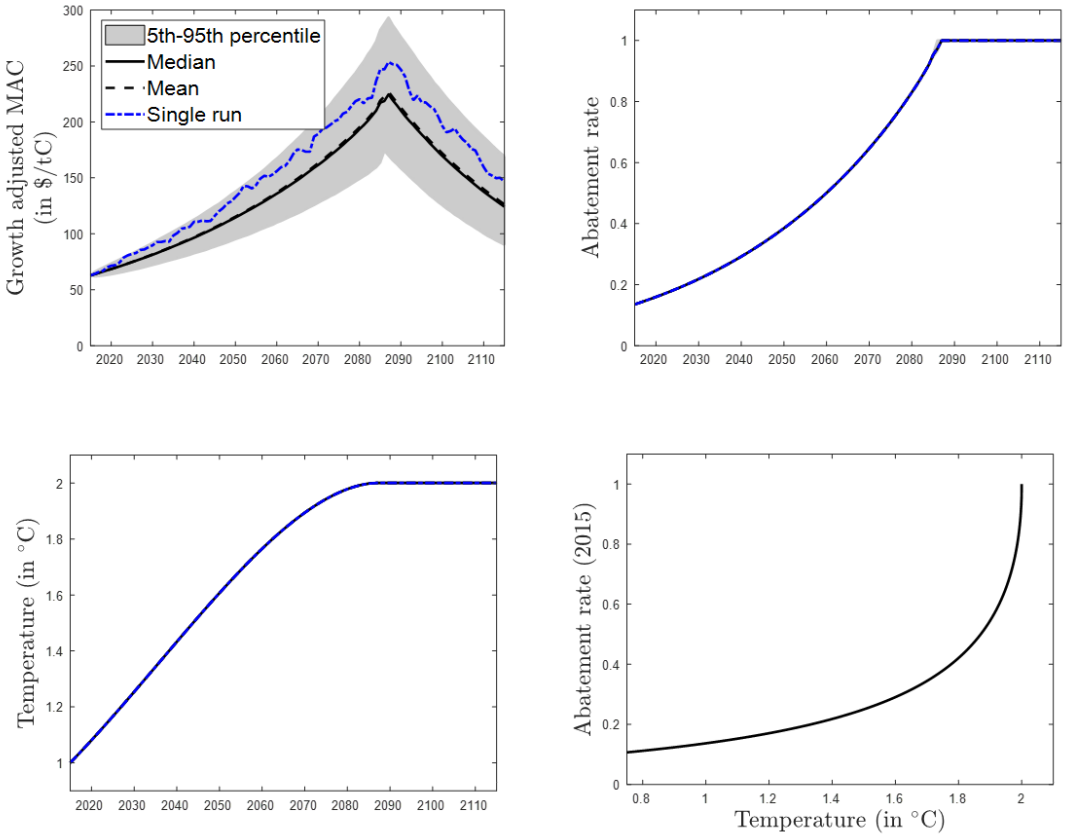

the hazard rate (Cai et al., 2016; Lemoine & Traeger, 2016). In particular, the downward jump after the damage tip occurs will be smaller in that case since there is the remaining incentive to delay future tipping points.

5.4.6 Temperature caps

Although most economists have adopted a welfare-maximizing approach where policy-makers internalize the global warming externalities, many governments (as well as central banks and the Network of Greening the Financial System) have followed the IPCC and have decided that the best way to deal with global warming is to have a ceiling on global mean temperature.

Given that temperature increases with cumulative emissions, the optimal carbon price must then grow at a rate that is equal to the risk-adjusted interest rate which is in our calibration equal to 3.4%. In figure 5.10 we show the optimal climate policies when a cap on global mean temperature of 2 ^oC is implemented and where we abstract from damages to global warming. The top left panel indicates a rapid rise in both the median carbon price and in the median carbon price even when adjusted for growth rate of the economy. The initial carbon price is about a fifth higher than in the benchmark, but the carbon price grows much faster than the growth of the economy. In fact, we numerically confirm our theoretical result that the expected growth rate of the carbon price and the

Figure 5.11: *Effects of a 2 degrees Celsius temperature cap with damages.*

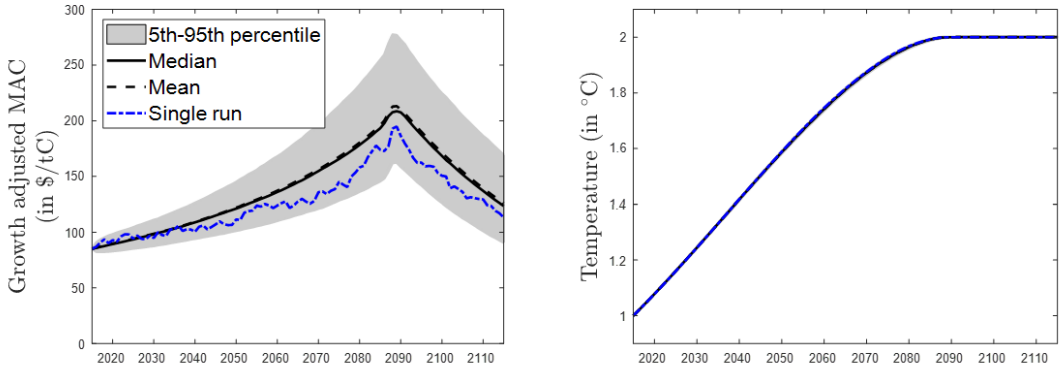

marginal abatement cost indeed equals the risk-free interest rate plus the risk premium. This steep growth in carbon prices ensures a rapid rise in the abatement rate and quick decarbonization of the economy (top right panel). Hence, temperature is much lower in a century: 2 ^oC instead of 3 ^oC (bottom left panel).

Figure 5.11 plots the optimal climate policies under a 2 ^oC cap when there are also linear damages from global warming to aggregate production. We then find that the growth rate of the optimal path of carbon prices is somewhere in between the risk-adjusted rate of interest and the rate of economic growth (cf. Van der Ploeg (2018)). Postponing abatement can be more cost-efficient due to discounting and technological progress in abatement technology, but that also leads to more warming and therefore more damages. The initial price, with both a temperature cap and damages, is therefore higher (90$/tC compared to 60$/tC without damages) and the growth rate lower.

Figure 5.12 shows the optimal policy function at the initial date (2015) for the abatement rate in state space, so as a function of temperature. The solid line shows that the abatement rate increases more and more rapidly in the direction of 100% mitigation as the temperature of cap of 2 degrees Celsius is approached. This very nonlinear feature is necessary to ensure that temperature stays below its cap. One can see that the corresponding optimal policy function for the benchmark case of linear damages is flat. The optimal policy function for the case of convex damages is, of course, much higher and slopes gently upwards as the convexity of damages kicks in. Although the policy function with convex damages starts higher than the one with a temperature cap, it rapidly is overtaken as temperature increases. If we combine linear damages and a temperature cap, the policy function starts slightly higher compared to the case with linear damages only. A similar result emerges for the case with convex damages.

Finally, we calculate the welfare losses relative to the optimal scenario. The welfare loss of business-as-usual relative to the optimum outcome for the benchmark case of linear damages is 0.2%. The welfare loss of enforcing a temperature cap of 2 degrees Celsius relative to the optimal policy setting is also 0.2%. However, with convex damages, the welfare loss of business-as-usual relative to the optimal outcome rises to 0.8%. As a result, the welfare loss of a 2 degrees Celsius temperature cap is only 0.1%. Hence, in the benchmark case with linear damages, the damages are so small that business-as-usual

Figure 5.12: *Optimal policy functions for the abatement rate as function of temperature at the initial date (2015).*

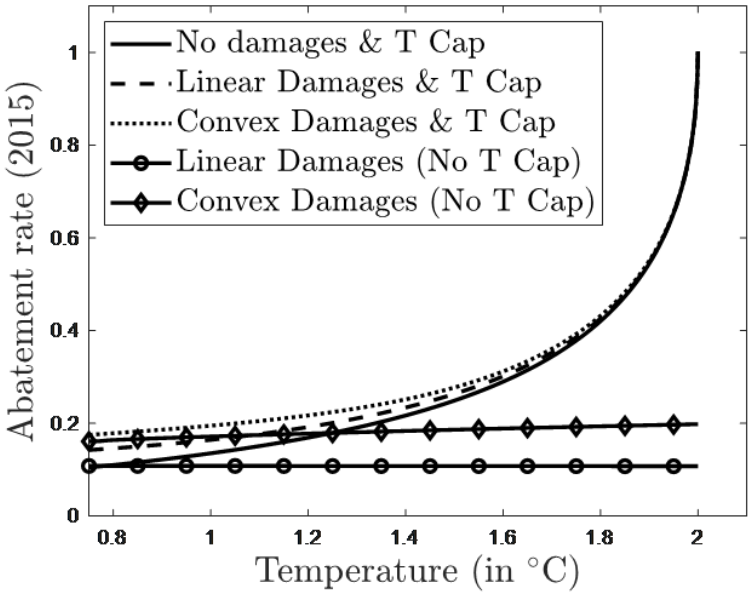

and a temperature cap give roughly the same welfare loss. In the more realistic scenario with convex damages the ambitious climate policy of enforcing a 2 degrees Celsius cap is a lot less costly than doing nothing as under business-as-usual. If we would also take account of tipping points, the difference will be even bigger. Hence, we conclude that it is better to undertake too much climate action than too little or not at all.

5.5 Conclusion

We have shown that convex damages, tipping points and temperature caps all argue in favour of a rising path of carbon prices. Only if there is gradual resolution of uncertainty will there be a declining component in the optimal carbon price, but this effect is dominated by rising components if damages and the economy are growing at empirically plausible rates. Furthermore, convex damages and especially temperature caps require that the carbon prices grow at a faster rate than the economy. Our policy recommendation is therefore that decision makers should start with a significant carbon price and at the same time commit to a rising path of carbon prices. This rising path of carbon prices can, if required by learning-by-doing externalities, be supplemented with a temporary upfront spike in renewable energy subsidies. These two policies give the best guarantee for redirecting investments from carbon-intensive to green technologies.

Only by credibly committing to such a path are corporations going to make the long run and irreversible investments that are needed to transition to the carbon-free economy. Uncertainty about the timing of a transition will cause corporations to hold back investments as carbon-intensive capital stock then acquires an option value in the likely case that capital investment is irreversible so avoiding unnecessary volatility is extremely

important. A practical problem that must be dealt with is that politicians tend to procrastinate and postpone carbon pricing and prefer subsidies to higher carbon prices as they fear of losing office. This can lead to adverse Green Paradox effects, where the anticipation of a stepping up of climate policy induces owners of fossil fuel reserves to extract more quickly and accelerate emissions and global warming rather than slowing it down (Rezai & Van der Ploeg, 2017b; Van der Ploeg & Withagen, 2015). Such political distortions might prevent the path of carbon prices to be not high enough upfront. Credible commitment to a rising path of prices is thus of paramount importance.

5.A Solving for optimal climate policy

Since we include two tipping points each of which can only tip once, we must solve four sub-problems. Define by $V_t^{1,1}$ the value function for the problem where both tipping points have already taken place. $V_t^{1,0}$ is the value function for the problem where the economic (or more precisely the endowment) tipping point has tipped but the climate tipping point has not tipped yet. $V_t^{0,1}$ is defined similarly. Lastly, $V_t^{0,0}$ is the value function before any of the two tipping points have taken place. Each of the four sub-problems satisfies its own Hamilton-Jacobi-Bellman (HJB) equation. The HJB-equation for $V_t^{i,j}$, $i \in \{0,1\}$, $j \in \{0,1\}$ equals:

$$\begin{aligned}
0 = \max_{u_t} \Bigg\{ & f(C_t, V_t^{i,j}) + Z_Y^{i,j}\mu Y_t + \frac{1}{2} Z_{YY}^{i,j}\sigma_Y^2 Y_t^2 + Z_t^{i,j} + Z_T^{i,j}\chi_j(1-u_t)E_t \\
& + Z_\omega^{i,j}\upsilon(\overline{\omega} - \omega_t) + Z_X^{i,j}\mu_X + \frac{1}{2} Z_{\omega\omega}^{i,j}(\sigma_t^\omega)^2 + \frac{1}{2} Z_{XX}^{i,j}\sigma_X^2 \\
& + \lambda_1 E\Big[Z^{i,j}\Big((1-J_1)Y_t, T_t, \omega_t, X_t, t\Big) - Z^{i,j}\Big(Y_t, T_t, \omega_t, X_t, t\Big)\Big] \\
& + \mathbb{I}_{i=0}\lambda_2 T_t E\Big[Z^{i+1,j}\Big((1-J_2)Y_t, T_t, \omega_t, X_t, t\Big) - Z^{i,j}\Big(Y_t, T_t, \omega_t, X_t, t\Big)\Big] \\
& + \mathbb{I}_{j=0}\lambda_3 T_t E\Big[Z^{i,j+1}\Big(Y_t, T_t, \omega_t, X_t, t\Big) - Z^{i,j}\Big(Y_t, T_t, \omega_t, X_t, t\Big)\Big] \Bigg\}
\end{aligned} \tag{5.16}$$

subject to $u_t = 1$ if $T_t = T^{cap}$, where the value function $V_t^{i,j} = Z^{i,j}\Big(Y_t, T_t, \omega_t, X_t, t\Big)$ depends on the three state variables and time and its partial derivatives are denoted by subscripts. The term μ_X is equal to 1 in the benchmark case and equal to $u_t E_t$ if there is learning-by-doing in abatement.

We conjecture and have verified that for each i and j the value function is of the form $V_t^{i,j} = g_t^{i,j}\frac{Y_t^{1-\gamma}}{1-\gamma}$ with $g_t^{i,j} = h^{i,j}\Big(T_t, \omega_t, X_t, t\Big)$ and rewrite equation (5.16) accordingly as:

$$\begin{aligned}
0 = \min_{u_t} \Bigg\{ & \beta\zeta\Big((g_t^{i,j})^{-1/\zeta}\Big(\frac{C_t}{Y_t}\Big)^{1-1/\epsilon} - 1\Big)g_t^{i,j} \\
& + (1-\gamma)\Big(\mu - 1/2\gamma\sigma_Y^2 + \lambda_1\frac{E\Big[(1-J_1)^{1-\gamma}\Big] - 1}{1-\gamma}\Big)g_t^{i,j} + h_t^{i,j} \\
& + h_T^{i,j}\chi_j(1-u_t)E_t + h_\omega^{i,j}\upsilon(\overline{\omega} - \omega_t) + h_X^{i,j}\mu_X + \frac{1}{2}h_{\omega\omega}^{i,j}\sigma_t^2 + \frac{1}{2}h_{XX}^{i,j}\sigma_X^2 \\
& + \mathbb{I}_{i=0}\lambda_2 T_t\Big(E\Big[(1-J_2)^{1-\gamma}\Big]g_t^{i+1,j} - g_t^{i,j}\Big) + \mathbb{I}_{j=0}\lambda_3 T_t\Big(g_t^{i,j+1} - g_t^{i,j}\Big) \Bigg\}
\end{aligned} \tag{5.17}$$

subject to $u_t = 1$ if $T_t = T^{cap}$. We define the social cost of carbon as the welfare loss of emitting one unit of carbon divided by the instantaneous marginal utility of consumption:

$$SCC_t = -\chi\frac{\partial Z_t/\partial T_t}{f_C(C_t, V_t)} = \Omega^{i,j}\Big(T_t, \omega_t, X_t, t\Big)C_t^{1/\epsilon}Y_t^{1-1/\epsilon}, \tag{5.18}$$

where $\Omega^{i,j}\Big(T_t, \omega_t, X_t, t\Big) = -\frac{\chi}{(1-\gamma)\beta}\frac{h_T^{i,j}}{(g_t^{i,j})^{1-1/\zeta}}$. The first part of equation (5.18) indicates that the optimal SCC depends on the shape of the reduced-form value function. The second part indicates that it is proportional to the size of the economy.

The SBL corresponds to all the present and future marginal benefits in terms of lower mitigation costs resulting from using one unit of mitigation more today:

$$SBL_t = \frac{\partial Z_t/\partial X_t}{f_C(C_t, V_t)} = \Theta^{i,j}\Big(T_t, \omega_t, X_t, t\Big) C_t^{1/\epsilon} Y_t^{1-1/\epsilon}, \tag{5.19}$$

where $\Theta^{i,j}\Big(T_t, \omega_t, X_t, t\Big) = \frac{1}{(1-\gamma)\beta}\frac{h_X^{i,j}}{(g_t^{i,j})^{1-1/\zeta}}$.

The optimality of the abatement rate implies that u_t is chosen such that the MAC is equal to the sum of the SCC and the SBL. Abatement on the one hand leads to lower emissions and on the other hand lowers the costs for future abatement, which implies that $SCC_t + SBL_t = MAC_t$, where:

$$MAC_t = -\frac{\partial C_t/\partial u_t}{E_t} = \frac{Y_t/(1+D_t)}{E_t}\frac{\partial A_t}{\partial u_t} = \frac{Y_t/(1+D_t)}{E_t} c_0 e^{-c_1 X_t} c_2 u_t^{c_2-1}. \tag{5.20}$$

The relation $SCC_t + SBL_t = MAC_t$ holds if the restriction $u \leq 1$ is not binding. If $u = 1$, then the sum of the SCC and the SBL will be larger than MAC, but it is not possible to abate more. The single control variable u_t thus tackles both externalities.

The main insight is that in more disaggregated models of energy use two separate policy instruments should be included. In that case carbon emissions should be priced at the SCC whilst mitigation should be subsidized at the SBL. We also refer to the SCC as the optimal carbon price and to the SBL as the optimal mitigation subsidy, while we note that this relation only holds as long as there is an interior solution to optimal abatement. We also report the growth-adjusted quantities of the SCC, SBL and MAC to analyse the determinants of these variables other than economic growth. We define the growth-adjusted social cost of carbon by $SCC_t \frac{C_0^{1/\epsilon} Y_0^{1-1/\epsilon}}{C_t^{1/\epsilon} Y_t^{1-1/\epsilon}}$. This implies that the growth-adjusted social cost of carbon equals the first term of equation (5.18): $-\frac{\chi}{(1-\gamma)\beta}\frac{h_T^{i,j}}{(g_t^{i,j})^{1-1/\zeta}}$, but scaled with $C_0^{1/\epsilon} Y_0^{1-1/\epsilon}$ to make the initial social cost of carbon equal to the actual initial social cost of carbon. The growth adjusted SBL and MAC are defined in the same way.

5.B A decentralized market economy

In the decentralized market economy, we need to consider energy producers, households, and the government separately. We assume that the households own the energy producers. We denote the consumer price for fossil fuel by p_t. Since fossil fuel and renewable energy are perfect substitutes, the consumer price for renewable energy is also equal to p_t. We let τ_t and s_t denote the specific tax on fossil fuel and the subsidy on renewable energy, respectively. Fossil fuel use is denoted by F_t and renewable energy use by R_t, so that the mitigation rate is defined by $u_t = \frac{R_t}{F_t + R_t}$. Total energy use is exogenous and equal to E_t. Profits of and lump-sum rebates to energy producers are denoted by Π_t and S_t,

respectively. Profits of energy firms, the household budget constraint and the government budget constraint are given by

$$\begin{aligned}\Pi_t &= p_t F_t + p_t R_t - \tau_t F_t + s_t R_t - A(u_t, X_t)\frac{Y_t}{1+D_t},\\ C_t &= \frac{Y_t}{1+D_t} + \Pi_t - \tau_t F_t - p_t F_t - p_t R_t,\\ S_t &= \tau_t F_t - s_t R_t.\end{aligned} \tag{5.21}$$

Provided that it is not optimal to fully decarbonize the economy, the first-order optimality conditions for fossil fuel and renewable energy use are

$$\begin{aligned}p_t &= \tau_t - A_u(u_t, X_t)u_t(1-u_t)\frac{Y_t}{F_t(1+D_t)},\\ p_t &= -s_t + A_u(u_t, X_t)u_t(1-u_t)\frac{Y_t}{R_t(1+D_t)}.\end{aligned} \tag{5.22}$$

Now use that $F_t = (1-u_t)E_t$ and $R_t = u_t E_t$ to obtain

$$\begin{aligned}p_t &= \tau_t - A_u(u_t, X_t)u_t\frac{Y_t}{E_t(1+D_t)},\\ p_t &= -s_t + A_u(u_t, X_t)(1-u_t)\frac{Y_t}{E_t(1+D_t)}.\end{aligned} \tag{5.23}$$

Combining these two equations gives:

$$\tau_t + s_t = A_u(u_t, X_t)\frac{Y_t}{E_t(1+D_t)}. \tag{5.24}$$

Note that $MAC_t = A_u(u_t, X_t)\frac{Y_t}{E_t(1+D_t)}$. Imposing a carbon tax and a renewable energy subsidy implies that optimal policy is chosen such that the marginal abatement cost equals the sum of the carbon tax and the renewable energy subsidy. We can therefore replicate optimal policy of the command optimum by setting $\tau_t = SCC_t$ and $s_t = SBL_t$. In our setting, both the learning-by-doing and the climate-change externality are tackled by one policy instrument, i.e. the abatement rate u_t.

5.C Numerical implementation

The HJB-equation is a set of partial differential equations. We solve this system of partial differential equations using a finite-difference method, as described in chapter 3. We can solve the model analytically when there are no climate damages. We use this as our initial guess at time $t_{max} = 500$, and from there solve the system backwards with time step $\delta_t = 1$. The three-dimensional grid is equally spaced with upper boundaries $[T^{max} \;\; \omega^{max} \;\; X^{max}]' = [T^{cap} \;\; 0.7 \;\; 1000]'$ if there is learning-by-doing and $[T^{max} \;\; \omega^{max} \;\; X^{max}]' = [T^{cap} \;\; 0.7 \;\; 200]'$ without learning-by-doing. The lower boundaries are equal to $[T^{min} \;\; \omega^{min} \;\; X^{min}]' = [0.75 \;\; 0 \;\; -25]'$. Without a temperature cap, T^{max} is set to 6 degrees Celsius. Optimal policy is calculated every period by solving for u_t such that the SCC is equal to the

Figure 5.13: *The sparse grid combination method.*

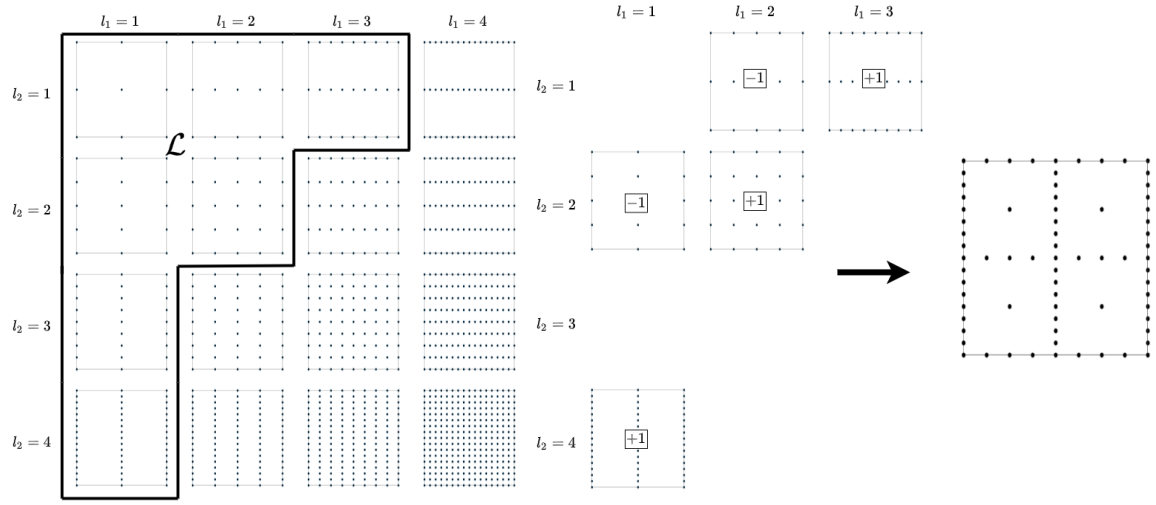

marginal abatement cost. If this requires $u_t > 1$, we set $u_t = 1$. The restriction of the temperature cap is implemented by imposing $u_t = 1$ on the boundary $T_t = T^{max}$. The restriction at the boundary also affects optimal policy at all interior grid points of temperature since it will affect the derivative of the value function with respect to temperature. A temperature cap will thus lead to a higher social cost of carbon and to a higher emissions control rate u_t. More details on the finite-difference method for a more general problem are given in chapter 3.

The sparse-grid combination method that we use in this chapter is slightly different from the implementation in chapter 3. The difference is that we allow for asymmetry in the grids. Define the 'level' of the grid for dimension i by $L_i, i \in \{T, \omega, X\}$. The number of grid points on the edge of the sparse grid in dimension i is equal to $2^{L_i} + 1$. The level therefore controls the amount of grid points and the accuracy in dimension i. When the value function is non-linear in a specific dimension it is possible to have more grid points in that dimension. This is for example useful when we solve the problem with a temperature cap, since in this case the value function becomes quite non-linear in the temperature dimension.

Let $\mathcal{L} = \left\{ l : \frac{l_T - 1}{L_T - 1} + \frac{l_\omega - 1}{L_\omega - 1} + \frac{l_X - 1}{L_X - 1} \leq 1 \right\}$ be the set of all admissible sub-grids where $l = (l_T, l_\omega, l_X)$. The weight of sub-grid l is equal to:

$$w_l = \sum_{i_T=0}^{1} \sum_{i_\omega=0}^{1} \sum_{i_X=0}^{1} (-1)^{i_T + i_\omega + i_X} \mathbb{I}_{(l_T + i_T, l_\omega + i_\omega, l_X + i_X) \in \mathcal{L}}. \tag{5.25}$$

We solve for g on all subgrids that have a non-zero weight w_l. Note that all grids have different grid points. To find the approximation g_l on sub-grid l in a specific point, we use linear interpolation. We then combine the solutions on all sub-grids by summing over the product of the weight and the solutions: $g = \sum_{l \in \mathcal{L}} w_l g_l$.

Figure 5.13 shows an example of the sparse-grid combination method in two dimensions. In the example $L_1 = 3$ and $L_2 = 4$, so the sparse grid will be denser in the second dimension. First, the set L is constructed, which in this example consists of the following

grids: $(1,1),(1,2),(1,3),(1,4),(2,1),(2,2),(3,1)$. Of all grids within this set, the grids $(1,4),(2,2),(3,1)$ all have weight $+1$ and the grids $(1,2),(2,1)$ have weight -1. The other two grids have weight zero and therefore these do not have to be evaluated.

5.D Derivation of the growth rate of marginal abatement costs with a temperature cap and no damages

If climate damages are not taken account of and a temperature cap is in place instead, it does not matter for the time at which the temperature cap is reached whether a unit of emissions is abated today or in some period in the future before that time, at least as long as the relationship between temperature and cumulative emissions is linear. Therefore, along the optimal path, a marginal increase of abatement today combined with a marginal decrease of abatement in the future should not lead to a change in welfare. The cost of a marginal increase of abatement today equals MAC_0, while the benefit of a marginal decrease of abatement in time t equals MAC_t. Optimal behaviour therefore implies that $\pi_0 MAC_0 = E_0[\pi_t MAC_t]$ where $\pi_t = \exp\Big(\int_0^t f_V(C_s,V_s)ds\Big) f_C(C_t,V_t)$ is the stochastic discount factor (Duffie & Epstein, 1992b). We therefore must have that the product $\pi_t MAC_t$ is a martingale. Now calculate:

$$\frac{d\pi_t MAC_t}{\pi_t MAC_t} = \frac{d\pi_t}{\pi_t} + \frac{dMAC_t}{MAC_t} + \frac{d[\pi_t, MAC_t]}{\pi_t MAC_t}. \tag{5.26}$$

Applying the martingale property and rearranging gives:

$$E_t\Big[\frac{dMAC_t}{MAC_t}\Big] = E_t\Big[-\frac{d\pi_t}{\pi_t}\Big] + E_t\Big[-\frac{d[\pi_t, MAC_t]}{\pi_t MAC_t}\Big], \tag{5.27}$$

where $[\pi_t, MAC_t]$ denotes the quadratic covariation for the processes π_t and MAC_t. Note that the first term $E_t\Big[-\frac{d\pi_t}{\pi_t}\Big]$ is exactly equal to the real risk-free interest rate, while the second term is a risk premium related to the correlation between the stochastic discount factor and the marginal abatement costs. Equation (5.27) implies that the optimal carbon price must grow at a rate equal to the sum of the real risk-free interest rate plus a risk premium, similar to Gollier (2020). We now derive the risk-free rate and the risk premium.

5.D.1 Derivation of the risk-free rate and the risk premium

We can work out the stochastic discount factor π_t and the marginal abatement cost function MAC_t. The model without climate damages can be written as follows. The endowment follows from:

$$dY_t = \mu Y_t dt + \sigma_Y Y_t dW_t^Y - J_1 Y_t dN_{1,t}. \tag{5.28}$$

Consumption is equal to endowment minus abatement expenditure: $C_t = (1 - A_t)Y_t$, where the abatement cost function $A_t = c_0 e^{-c_1 X_t} u_t^{c_2}$. Define the consumption-endowment ratio $\xi_t = 1 - A_t = \nu(T_t, X_t, t)$, which depends on the two state variables and time. The two state variables X_t (abatement cost variable) and T_t (temperature) follow from:

$$\begin{aligned} dX_t &= \mu_X dt + \sigma_X dW_t^X, \\ dT_t &= \chi(1 - u_t)E_t dt. \end{aligned} \tag{5.29}$$

The temperature cap adds the restriction $u_t = 1$ if $T_t = T^{cap}$. The HJB-equation corresponding to the value function V_t for this problem is thus given by:

$$\begin{aligned} 0 = \max_{u_t} \Bigg\{ & f(C_t, V_t) + Z_Y \mu Y_t + \frac{1}{2} Z_{YY} \sigma_Y^2 Y_t^2 + Z_t + Z_T \chi (1 - u_t) E_t + Z_X \mu_X \\ & + \frac{1}{2} Z_{XX} \sigma_X^2 + \lambda_1 E\Big[Z\Big((1 - J_1) Y_t, T_t, X_t, t\Big) - Z\Big(Y_t, T_t, X_t, t\Big) \Big] \Bigg\} \end{aligned} \tag{5.30}$$

subject to $u_t = 1$ if $T_t = T^{cap}$, where the value function $V_t = Z(Y_t, T_t, X_t, t)$ depends on two state variables and time and its partial derivatives are denoted by subscripts. We conjecture and have verified that the value function is of the form $V_t = g_t \frac{Y_t^{1-\gamma}}{1-\gamma}$ with $g_t = h(T_t, X_t, t)$ and rewrite equation (5.30) accordingly as:

$$\begin{aligned} 0 = \min_{u_t} \Bigg\{ & \beta \zeta \Big(g_t^{-1/\zeta} \Big(\frac{C_t}{Y_t} \Big)^{1 - 1/\epsilon} - 1 \Big) g_t \\ & + (1 - \gamma) \Big(\mu - \frac{1}{2} \gamma \sigma_Y^2 + \lambda_1 \frac{E[(1 - J_1)^{1-\gamma}] - 1}{1 - \gamma} \Big) g_t \\ & + h_t + h_T \chi (1 - u_t) E_t + h_X \mu_X + \frac{1}{2} h_{XX} \sigma_X^2 \Bigg\} \end{aligned} \tag{5.31}$$

subject to $u_t = 1$ if $T_t = T^{cap}$. The derivatives of instantaneous utility $f(C_t, V_t)$ can be calculated as:

$$\begin{aligned} f_C(C_t, V_t) &= \frac{\beta C_t^{-1/\epsilon}}{\Big((1 - \gamma) V_t \Big)^{1/\zeta - 1}}, \\ f_V(C_t, V_t) &= \beta \zeta \Big((1 - 1/\zeta) C_t^{1 - 1/\epsilon} \Big((1 - \gamma) V_t \Big)^{-1/\zeta} - 1 \Big). \end{aligned} \tag{5.32}$$

Now substitute in $V_t = g_t \frac{Y_t^{1-\gamma}}{1-\gamma}$ and $\xi_t = \frac{C_t}{Y_t}$ to obtain:

$$\begin{aligned} f_C(C_t, V_t) &= \beta \xi_t^{-1/\epsilon} g_t^{1 - 1/\zeta} Y_t^{-\gamma}, \\ f_V(C_t, V_t) &= \beta \zeta \Big((1 - 1/\zeta) \xi_t^{1 - 1/\epsilon} g_t^{-1/\zeta} - 1 \Big). \end{aligned} \tag{5.33}$$

Substituting this into the stochastic discount factor gives:

$$\pi_t = \exp\Big(\int_0^t \beta \zeta \Big((1 - 1/\zeta) \xi_s^{1 - 1/\epsilon} g_s (-1/\zeta - 1) ds \Big) \beta \xi_t^{-1/\epsilon} g_t^{1 - 1/\zeta} Y_t^{-\gamma}. \tag{5.34}$$

Writing π_t as a differential equation gives:

$$\begin{aligned} \frac{d\pi_t}{\pi_t} = & \beta \zeta \Big((1 - 1/\zeta) \xi_t^{1 - 1/\epsilon} g_t^{-1/\zeta} - 1 \Big) dt \\ & + \frac{dY_t^{-\gamma}}{Y_t^{-\gamma}} + \frac{dg_t^{1 - 1/\zeta}}{g_t^{1 - 1/\zeta}} + \frac{d\xi_t^{-1/\epsilon}}{\xi_t^{-1/\epsilon}} + \frac{d[g_t^{1 - 1/\zeta}, \xi_t^{-1/\epsilon}]}{g_t^{1 - 1/\zeta} \xi_t^{-1/\epsilon}}. \end{aligned} \tag{5.35}$$

Applying Itô's lemma to Y_t gives:

$$\frac{dY_t^{-\gamma}}{Y_t^{-\gamma}} = -\gamma\Big(\mu - \frac{1}{2}(\gamma+1)\sigma_Y^2\Big)dt - \gamma\sigma_Y dW_t^Y + \Big((1-J_1)^{-\gamma} - 1\Big)dN_{1,t}. \tag{5.36}$$

Similarly, we apply Itô's lemma to g_t to get:

$$\frac{dg_t}{g_t} = \Big(\frac{h_t}{g_t} + \frac{h_T}{g_t}\chi(1-u_t)E_t + \frac{h_X}{g_t}\mu_X + \frac{1}{2}\frac{h_{XX}}{g_t}\sigma_X^2\Big)dt + \frac{h_X}{g_t}\sigma_X dW_t^X. \tag{5.37}$$

Define $\mu_g = \frac{h_t}{g_t} + \frac{h_T}{g_t}\chi(1-u_t)E_t + \frac{h_X}{g_t}\mu_X + \frac{1}{2}\frac{h_{XX}}{g_t}\sigma_X^2$. Then we can calculate:

$$\frac{dg_t^{1-1/\zeta}}{g_t^{1-1/\zeta}} = (1-1/\zeta)\Big(\mu_g - \frac{1}{2}\frac{1}{\zeta}\frac{h_X^2}{g_t^2}\sigma_X^2\Big)dt + (1-1/\zeta)\frac{h_X}{g_t}\sigma_X dW_t^X. \tag{5.38}$$

Using a similar derivation, we calculate that

$$\frac{d\xi_t^{-1/\epsilon}}{\xi_t^{-1/\epsilon}} = -\frac{1}{\epsilon}\Big(\mu_\xi - \frac{1}{2}(1+1/\epsilon)\frac{\nu_X^2}{\xi_t^2}\sigma_X^2\Big)dt - \frac{1}{\epsilon}\frac{\nu_X}{\xi_t}\sigma_X dW_t^X, \tag{5.39}$$

where $\mu_\xi = \frac{\nu_t}{\xi_t} + \frac{\nu_T}{\xi_t}\chi(1-u_t)E_t + \frac{\nu_X}{\xi_t}\mu_X + \frac{1}{2}\frac{\nu_{XX}}{\xi_t}\sigma_X^2$. The cross terms are equal to:

$$\frac{d[g_t^{1-1/\zeta}, \xi_t^{-1/\epsilon}]}{g_t^{1-1/\zeta}\xi_t^{-1/\epsilon}} = -\frac{1}{\epsilon}(1-1/\zeta)\frac{h_X\nu_X}{g_t\xi_t}\sigma_X^2 dt. \tag{5.40}$$

Putting everything together yields:

$$\begin{aligned}\frac{d\pi_t}{\pi_{t-}} = \Big\{&\beta\zeta\Big((1-1/\zeta)\xi_t^{1-1/\epsilon}g_t^{-1/\zeta} - 1\Big) - \gamma\Big(\mu - \frac{1}{2}(\gamma+1)\sigma_Y^2\Big)\\ &+ (1-1/\zeta)\Big(\mu_g - \frac{1}{2}\frac{1}{\zeta}\frac{h_X^2}{g_t^2}\sigma_X^2\Big) - \frac{1}{\epsilon}\Big(\mu_\xi - \frac{1}{2}(1+1/\epsilon)\frac{\nu_X^2}{\xi_t^2}\sigma_X^2\Big)\\ &- \frac{1}{\epsilon}(1-1/\zeta)\frac{h_X\nu_X}{g_t\xi_t}\sigma_X^2\Big\}dt - \gamma\sigma_Y dW_t^Y + (1-1/\zeta)\frac{h_X}{g_t}\sigma_X dW_t^X\\ &- \frac{1}{\epsilon}\frac{\nu_X}{\xi_t}\sigma_X dW_t^X + \Big((1-J_1)^{-\gamma} - 1\Big)dN_{1,t}.\end{aligned} \tag{5.41}$$

We now substitute this in the HJB-equation. The HJB-equation is equivalent to:

$$\mu_g = -\beta\zeta\Big(g_t^{-1/\zeta}\xi_t^{1-1/\epsilon} - 1\Big) - (1-\gamma)\Big(\mu - \frac{1}{2}\gamma\sigma_Y^2 + \lambda_1\frac{E[(1-J_1)^{1-\gamma}] - 1}{1-\gamma}\Big). \tag{5.42}$$

Substituting this into the stochastic discount factor gives:

$$\begin{aligned}\frac{d\pi_t}{\pi_{t-}} = \Big\{&-\beta - \frac{\mu}{\epsilon} + \frac{1}{2}(1+1/\epsilon)\gamma\sigma_Y^2 + (\gamma - 1/\epsilon)\lambda_1\frac{E[(1-J_1)^{1-\gamma}] - 1}{1-\gamma}\\ &- \frac{1}{\epsilon}\Big(\mu_\xi - \frac{1}{2}(1+1/\epsilon)\frac{\nu_X^2}{\xi_t^2}\sigma_X^2\Big) - \frac{1}{2}\frac{1}{\zeta}(1-1/\zeta)\frac{h_X^2}{g_t^2}\sigma_X^2\\ &- \frac{1}{\epsilon}(1-1/\zeta)\frac{h_X\nu_X}{g_t\xi_t}\sigma_X^2\Big\}dt - \gamma\sigma_Y dW_t^Y + (1-1/\zeta)\frac{h_X}{g_t}\sigma_X dW_t^X\\ &- \frac{1}{\epsilon}\frac{\nu_X}{\xi_t}\sigma_X dW_t^X + \Big((1-J_1)^{-\gamma} - 1\Big)dN_{1,t}.\end{aligned} \tag{5.43}$$

We can thus define μ_π and σ_π such that:

$$\frac{d\pi_t}{\pi_{t-}} = \mu_\pi dt - \gamma\sigma_Y dW_t^Y + \sigma_\pi dW_t^X + \Big((1-J_1)^{-\gamma} - 1\Big)dN_{1,t}. \tag{5.44}$$

We can now first calculate the risk-free rate:

$$\begin{aligned} r_t &= E_t\Big[-\frac{d\pi_t}{\pi_t}\Big] = -\mu_\pi - \lambda_1\Big(E[(1-J_1)-\gamma] - 1\Big) \\ &= \beta + \frac{\mu+\mu_\xi}{\epsilon} - \frac{1}{2}(1+1/\epsilon)\gamma\sigma_Y^2 \\ &- \lambda_1\Big(E[(1-J_1)^{-\gamma}] - 1 + (\gamma - 1/\epsilon)\frac{E[(1-J_1)^{1-\gamma}]-1}{1-\gamma}\Big) \\ &- \frac{1}{2}\frac{1}{\epsilon}(1+1/\epsilon)\frac{\nu_X^2}{\xi_t^2}\sigma_X^2 - 1/2\frac{1}{\zeta}(1/\zeta - 1)\frac{h_X^2}{g_t^2}\sigma_X^2 - 1/\epsilon(1/\zeta-1)\frac{h_X\nu_X}{g_t\xi_t}\sigma_X^2. \end{aligned} \tag{5.45}$$

The effect of abatement uncertainty σ_X on the interest rate is negligible compared to the effect of economic uncertainty σ_Y and jump risk. We can simplify the interest rate if we leave out the terms related to abatement uncertainty. Additionally, we can calculate the expectations of the jump variable J_1, since J_1 follows a power distribution. Lastly, note that the growth rate of consumption, which we call μ_c, is equal to $\mu + \mu_\xi$. The real risk-free rate is thus given by:

$$r_t = \beta + \frac{\mu_c}{\epsilon} - \frac{1}{2}(1+1/\epsilon)\gamma\sigma_Y^2 - \lambda_1\Big(\frac{\alpha_1}{\alpha_1-\gamma} - 1 - \frac{\gamma-1/\epsilon}{\alpha_1+1-\gamma}\Big). \tag{5.46}$$

Marginal abatement costs are given by:

$$MAC_t = -\frac{\partial C_t/\partial u_t}{E_t} = \frac{Y_t}{E_t}\frac{\partial A_t}{\partial u_t} = \frac{Y_t}{E_t}c_0 e^{-c_1 X_t} c_2 u_t^{c_2-1}. \tag{5.47}$$

If we again assume that abatement uncertainty has a negligible effect on the risk premium, we obtain the risk premium:

$$\begin{aligned} rp_t &= E_t\Big[-\frac{d[\pi_t, MAC_t]}{\pi_t MAC_t}\Big] = E_t\Big[-\frac{d[Y_t^{-\gamma}, Y_t]}{Y_t^{1-\gamma}}\Big] \\ &= \gamma\sigma_Y^2 + \lambda_1\Big(E[(1-J_1)^{-\gamma}] + E[1-J_1] - E[(1-J_1)^{1-\gamma}] - 1\Big) \\ &= \gamma\sigma_Y^2 + \lambda_1\Big(\frac{\alpha_1}{\alpha_1-\gamma} + \frac{\alpha_1}{\alpha_1+1} - \frac{\alpha_1}{\alpha_1+1-\gamma} - 1\Big). \end{aligned} \tag{5.48}$$

In expectation, the growth rate of marginal abatement costs is therefore equal to the risk-free rate plus the risk premium.

References

Acemoglu, D., Aghion, P., Bursztyn, L., & Hemous, D. (2012). The environment and directed technical change. *American Economic Review*, *102*(1), 131–66.

Achdou, Y., Han, J., Lasry, J.-M., Lions, P.-L., & Moll, B. (2021). Income and wealth distribution in macroeconomics: A continuous-time approach. *The Review of Economic Studies*.

Aengenheyster, M., Feng, Q. Y., Van der Ploeg, F., & Dijkstra, H. A. (2018). The point of no return for climate action. *Earth System Dynamics*, *9*(3).

Allen, M. R., Frame, D. J., Huntingford, C., Jones, C. D., Lowe, J. A., Meinshausen, M., & Meinshausen, N. (2009). Warming caused by cumulative carbon emissions towards the trillionth tonne. *Nature*, *458*(7242), 1163–1166.

Anderson, E. W., Hansen, L. P., & Sargent, T. J. (2003). A quartet of semigroups for model specification, robustness, prices of risk, and model detection. *Journal of the European Economic Association*, *1*(1), 68–123.

Andreasson, J., & Shevchenko, P. V. (2019). Bias-corrected least-squares Monte Carlo for utility based optimal stochastic control problems. *Macquarie University Working Paper*.

Balata, A., & Palczewski, J. (2017). Regress-later Monte Carlo for optimal control of Markov processes. *University of Leeds*.

Bansal, R., Kiku, D., & Ochoa, M. (2016). Price of long-run temperature shifts in capital markets. *National Bureau of Economic Research*.

Bansal, R., & Yaron, A. (2004). Risks for the long run: A potential resolution of asset pricing puzzles. *The Journal of Finance*, *59*(4), 1481–1509.

Barnett, M., Brock, W., & Hansen, L. P. (2020, 02). Pricing uncertainty induced by climate change. *The Review of Financial Studies*, *33*(3), 1024-1066.

Barro, R. J. (2006). Rare disasters and asset markets in the twentieth century. *The Quarterly Journal of Economics*, *121*(3), 823–866.

Barro, R. J. (2009). Rare disasters, asset prices, and welfare costs. *American Economic Review*, *99*(1), 243–64.

Barro, R. J. (2015). Environmental protection, rare disasters and discount rates. *Economica*, *82*(325), 1–23.

Barro, R. J., & Jin, T. (2011). On the size distribution of macroeconomic disasters. *Econometrica*, *79*(5), 1567–1589.

Bovenberg, A. L., & Smulders, S. (1995). Environmental quality and pollution-augmenting technological change in a two-sector endogenous growth model. *Journal of Public Economics*, *57*(3), 369–391.

Bovenberg, A. L., & Smulders, S. A. (1996). Transitional impacts of environmental policy in an endogenous growth model. *International Economic Review*, 861–893.

Brandt, M. W., Goyal, A., Santa-Clara, P., & Stroud, J. R. (2005). A simulation approach to dynamic portfolio choice with an application to learning about return predictability. *The Review of Financial Studies*, *18*(3), 831–873.

Bretscher, L., & Vinogradova, A. (2018). Escaping Damocles' sword: Endogenous climate shocks in a growing economy. *Economics Working Paper Series*, *18*.

Bretschger, L., & Pattakou, A. (2019). As bad as it gets: How climate damage functions

affect growth and the social cost of carbon. *Environmental and Resource Economics*, *72*(1), 5–26.

Brumm, J., & Scheidegger, S. (2017). Using adaptive sparse grids to solve high-dimensional dynamic models. *Econometrica*, *85*(5), 1575–1612.

Cai, Y., Lenton, T. M., & Lontzek, T. S. (2016). Risk of multiple interacting tipping points should encourage rapid CO_2 emission reduction. *Nature Climate Change*, *6*(5), 520–525.

Cai, Y., & Lontzek, T. S. (2019). The social cost of carbon with economic and climate risks. *Journal of Political Economy*, *127*(6), 2684–2734.

Candler, G. V. (1999). Finite-difference methods for continuous-time dynamic programming. In *Computational methods for the study of dynamic economies.* Oxford University Press.

Chen, Z., & Epstein, L. (2002). Ambiguity, risk, and asset returns in continuous time. *Econometrica*, *70*(4), 1403–1443.

Chichilnisky, G., Hammond, P. J., & Stern, N. (2018). Should we discount the welfare of future generations? Ramsey and Suppes versus Koopmans and Arrow. *Warwick Economics Research Papers Series*.

Coase, R. H. (1960). The problem of social cost. In *Classic papers in natural resource economics* (pp. 87–137). Springer.

Cochrane, J. H. (2009). *Asset pricing: Revised edition*. Princeton university press.

Crost, B., & Traeger, C. P. (2013). Optimal climate policy: Uncertainty versus Monte Carlo. *Economics Letters*, *120*(3), 552–558.

Crost, B., & Traeger, C. P. (2014). Optimal CO_2 mitigation under damage risk valuation. *Nature Climate Change*, *4*(7), 631–636.

Daniel, K. D., Litterman, R. B., & Wagner, G. (2019). Declining CO_2 price paths. *Proceedings of the National Academy of Sciences*, *116*(42), 20886–20891.

Dietz, S. (2011). High impact, low probability? An empirical analysis of risk in the economics of climate change. *Climatic Change*, *108*(3), 519–541.

Dietz, S., & Stern, N. (2015). Endogenous growth, convexity of damage and climate risk: how Nordhaus' framework supports deep cuts in carbon emissions. *The Economic Journal*, *125*(583), 574–620.

Dietz, S., Van der Ploeg, F., Rezai, A., & Venmans, F. (2020). Are economists getting climate dynamics right and does it matter? *CESifo Working Paper*.

Dietz, S., & Venmans, F. (2019). Cumulative carbon emissions and economic policy: In search of general principles. *Journal of Environmental Economics and Management*, *96*, 108–129.

Dimson, E., Marsh, P., & Staunton, M. (2011). Equity premia around the world. *London Business School*.

Dixit, R. K., & Pindyck, R. S. (1994). *Investment under uncertainty*. Princeton university press.

Duffie, D., & Epstein, L. G. (1992a). Asset pricing with stochastic differential utility. *The Review of Financial Studies*, *5*(3), 411–436.

Duffie, D., & Epstein, L. G. (1992b). Stochastic differential utility. *Econometrica*, 353–394.

Ellsberg, D. (1961). Risk, ambiguity, and the savage axioms. *The Quarterly Journal of*

Economics, 643–669.
Epstein, L. G., Farhi, E., & Strzalecki, T. (2014). How much would you pay to resolve long-run risk? *American Economic Review*, *104*(9), 2680–97.
Epstein, L. G., & Schneider, M. (2003). Recursive multiple-priors. *Journal of Economic Theory*, *113*(1), 1–31.
Epstein, L. G., & Zin, S. E. (1989). Substitution, risk aversion, and the temporal behavior of consumption and asset returns: A theoretical framework. *Econometrica*, 937–969.
Epstein, L. G., & Zin, S. E. (1991). Substitution, risk aversion, and the temporal behavior of consumption and asset returns: An empirical analysis. *Journal of Political Economy*, *99*(2), 263–286.
Gerlagh, R., & Liski, M. (2018). Carbon prices for the next hundred years. *The Economic Journal*, *128*(609), 728–757.
Gilboa, I., & Schmeidler, D. (1989). Maxmin expected utility with non-unique prior. *Journal of Mathematical Economics*, *18*(2), 141 - 153.
Gollier, C. (2002a). Discounting an uncertain future. *Journal of Public Economics*, *85*(2), 149–166.
Gollier, C. (2002b). Time horizon and the discount rate. *Journal of Economic Theory*, *107*(2), 463-473.
Gollier, C. (2008). Discounting with fat-tailed economic growth. *Journal of Risk and Uncertainty*, *37*(2), 171–186.
Gollier, C. (2011). On the underestimation of the precautionary effect in discounting. *The Geneva Risk and Insurance Review*, *36*(2), 95–111.
Gollier, C. (2012). *Pricing the planet's future*. Princeton University Press.
Gollier, C. (2020). The cost-efficiency carbon pricing puzzle. *CEPR Working Paper*.
Golosov, M., Hassler, J., Krusell, P., & Tsyvinski, A. (2014). Optimal taxes on fossil fuel in general equilibrium. *Econometrica*, *82*(1), 41–88.
Goosse, H. (2015). *Climate system dynamics and modelling*. Cambridge University Press.
Griebel, M. (1998). Adaptive sparse grid multilevel methods for elliptic PDEs based on finite differences. *Computing*, *61*(2), 151–179.
Griebel, M., Schneider, M., & Zenger, C. (1990). A combination technique for the solution of sparse grid problems. *Technische Universität München*.
Hambel, C., Kraft, H., & Schwartz, E. (2021). Optimal carbon abatement in a stochastic equilibrium model with climate change. *European Economic Review*, *132*, 103642.
Hambel, C., Kraft, H., & Van der Ploeg, F. (2020). Asset diversification versus climate action. *CESifo Working Paper*.
Hansen, L. P., & Sargent, T. J. (2001). Robust control and model uncertainty. *American Economic Review*, *91*(2), 60–66.
Hansen, L. P., & Sargent, T. J. (2008). *Robustness*. Princeton university press.
Hansen, L. P., Sargent, T. J., Turmuhambetova, G., & Williams, N. (2001). Robustness and uncertainty aversion. *Manuscript, University of Chicago*.
Harwood, R. C. (2017). Steady and stable: Numerical investigations of nonlinear partial differential equations. In *A primer for undergraduate research* (pp. 265–303). Springer.
Hassler, J., Krusell, P., Olovsson, C., & Reiter, M. (2020). On the effectiveness of climate policies. *IIES Working Paper*.

Hope, C. (2006). The marginal impact of CO_2 from PAGE2002: An integrated assessment model incorporating the IPCC's five reasons for concern. *Integrated Assessment*, *6*(1).

Hope, C., & Newbery, D. (2007). Calculating the social cost of carbon. *EPRG Working Paper*.

Ikefuji, M., Laeven, R. J., Magnus, J. R., & Muris, C. (2020). Expected utility and catastrophic risk in a stochastic economy–climate model. *Journal of Econometrics*, *214*(1), 110–129.

IPCC. (2013). *Climate change 2013: The physical science basis. contribution of working group 1 to the fifth assessment report of the intergovernmental panel on climate change*. Cambridge, United Kingdom and New York, NY, USA: Cambridge University Press.

IPCC. (2021). *Climate change 2021: The physical science basis. contribution of working group 1 to the sixth assessment report of the intergovernmental panel on climate change*. Cambridge, United Kingdom and New York, NY, USA: Cambridge University Press.

Jain, S., Leitao, Á., & Oosterlee, C. W. (2019). Rolling adjoints: Fast Greeks along Monte Carlo scenarios for early-exercise options. *Journal of Computational Science*, *33*, 95–112.

Jain, S., & Oosterlee, C. W. (2012). Pricing high-dimensional bermudan options using the stochastic grid method. *International Journal of Computer Mathematics*, *89*(9), 1186–1211.

Jain, S., & Oosterlee, C. W. (2015). The stochastic grid bundling method: Efficient pricing of Bermudan options and their Greeks. *Applied Mathematics and Computation*, *269*, 412–431.

Jensen, S., & Traeger, C. P. (2014). Optimal climate change mitigation under long-term growth uncertainty: Stochastic integrated assessment and analytic findings. *European Economic Review*, *69*, 104–125.

Johansson, Å., Guillemette, Y., Murtin, F., Turner, D., Nicoletti, G., de la Maisonneuve, C., ... Spinelli, F. (2012). Looking to 2060: Long-term global growth prospects: A going for growth report. *OECD Economic Policy Papers*.

Joos, F., Roth, R., Fuglestvedt, J. S., Peters, G. P., Enting, I. G., Von Bloh, W., ... Edwards, N. R. (2013). Carbon dioxide and climate impulse response functions for the computation of greenhouse gas metrics: a multi-model analysis. *Atmospheric Chemistry and Physics*, *13*(5), 2793–2825.

Karydas, C., & Xepapadeas, A. (2019). Climate change risks: pricing and portfolio allocation. *CER-ETH-Center of Economic Research (CER-ETH) at ETH Zurich*.

Kelly, D. L., & Kolstad, C. D. (1999). Bayesian learning, growth, and pollution. *Journal of Economic Dynamics and Control*, *23*(4), 491–518.

Kelly, D. L., & Tan, Z. (2015). Learning and climate feedbacks: Optimal climate insurance and fat tails. *Journal of Environmental Economics and Management*, *72*, 98–122.

Klibanoff, P., Marinacci, M., & Mukerji, S. (2005). A smooth model of decision making under ambiguity. *Econometrica*, *73*(6), 1849–1892.

Knight, F. H. (1921). Risk, uncertainty and profit. *New York: Hart, Schaffner and Marx*.

Koijen, R. S., Nijman, T. E., & Werker, B. J. (2010). When can life cycle investors benefit from time-varying bond risk premia? *The Review of Financial Studies*, *23*(2), 741–780.

Kreps, D. M., & Porteus, E. L. (1978). Temporal resolution of uncertainty and dynamic choice theory. *Econometrica*, 185–200.

Lapeyre, B., Sulem, A., & Talay, D. (2005). Simulation of financial models: Mathematical foundations and applications. *To appear*.

Lemoine, D. (2021). The climate risk premium: How uncertainty affects the social cost of carbon. *Journal of the Association of Environmental and Resource Economists*, *8*(1), 27–57.

Lemoine, D., & Rudik, I. (2017). Steering the climate system: using inertia to lower the cost of policy. *American Economic Review*, *107*(10), 2947–57.

Lemoine, D., & Traeger, C. (2014). Watch your step: Optimal policy in a tipping climate. *American Economic Journal: Economic Policy*, *6*(1), 137–66.

Lemoine, D., & Traeger, C. P. (2016). Ambiguous tipping points. *Journal of Economic Behavior & Organization*, *132*, 5–18.

Liu, J., Pan, J., & Wang, T. (2004). An equilibrium model of rare-event premia and its implication for option smirks. *The Review of Financial Studies*, *18*(1), 131–164.

Longstaff, F. A., & Schwartz, E. S. (2001). Valuing American options by simulation: a simple least-squares approach. *The Review of Financial Studies*, *14*(1), 113–147.

Lucas Jr, R. E. (1978). Asset prices in an exchange economy. *Econometrica*, 1429–1445.

Ma, K., & Forsyth, P. (2017). An unconditionally monotone numerical scheme for the two-factor uncertain volatility model. *IMA Journal of Numerical Analysis*, *37*(2), 905–944.

Maenhout, P. J. (2004). Robust portfolio rules and asset pricing. *Review of Financial Studies*, *17*(4), 951–983.

Maenhout, P. J. (2006). Robust portfolio rules and detection-error probabilities for a mean-reverting risk premium. *Journal of Economic Theory*, *128*(1), 136–163.

Martin, I. W., & Pindyck, R. S. (2015). Averting catastrophes: The strange economics of Scylla and Charybdis. *American Economic Review*, *105*(10), 2947–85.

Mattauch, L., Millar, R., Van der Ploeg, F., Rezai, A., Schultes, A., Venmans, F., ... Teytelboym, A. (2019). Steering the climate system: an extended comment. *Centre for Climate Change Economics and Policy Working Paper*.

Matthews, H. D., Gillett, N. P., Stott, P. A., & Zickfeld, K. (2009). The proportionality of global warming to cumulative carbon emissions. *Nature*, *459*(7248), 829–832.

Mehra, R., & Prescott, E. C. (1985). The equity premium: A puzzle. *Journal of Monetary Economics*, *15*(2), 145–161.

Millner, A., Dietz, S., & Heal, G. (2013). Scientific ambiguity and climate policy. *Environmental and Resource Economics*, *55*(1), 21–46.

Munk, C. (2015). *Dynamic asset allocation*. Copenhagen Business School.

Noble, I., Bolin, B., Ravindranath, N., Verardo, D., & Dokken, D. (2000). *Land use, land use change, and forestry*. Cambridge University Press.

Nordhaus, W. D. (1992). The 'DICE' model: Background and structure of a dynamic integrated climate-economy model of the economics of global warming. *Cowles Foundation for Research in Economics, Yale University*.

Nordhaus, W. D. (2014a). Estimates of the social cost of carbon: concepts and results from the DICE-2013R model and alternative approaches. *Journal of the Association of Environmental and Resource Economists*, *1*(1/2), 273–312.

Nordhaus, W. D. (2014b). *A question of balance: Weighing the options on global warming policies*. Yale University Press.

Nordhaus, W. D. (2017). Revisiting the social cost of carbon. *Proceedings of the National Academy of Sciences*, 201609244.

Nordhaus, W. D. (2018). Evolution of modeling of the economics of global warming: Changes in the DICE model, 1992–2017. *Climatic change*, *148*(4), 623–640.

Nordhaus, W. D. (2019, June). Can we control carbon dioxide? (from 1975). *American Economic Review*, *109*(6), 2015-35.

Pathak, P. (2002). Notes on robust portfolio choice. *Harvard University*, *3*, 14.

Pflüger, D. M. (2010). *Spatially adaptive sparse grids for high-dimensional problems* (Unpublished doctoral dissertation). Technische Universität München.

Pigou, A. C. (1920). *The economics of welfare*. London: Macmillan.

Pindyck, R. S. (2017). The use and misuse of models for climate policy. *Review of Environmental Economics and Policy*, *11*(1), 100–114.

Ramsey, F. P. (1928). A mathematical theory of saving. *The Economic Journal*, *38*(152), 543–559.

Rezai, A., & Van der Ploeg, F. (2017a). Abandoning fossil fuel: how fast and how much. *The Manchester School*, *85*, e16–e44.

Rezai, A., & Van der Ploeg, F. (2017b). Second-best renewable subsidies to de-carbonize the economy: Commitment and the green paradox. *Environmental and Resource Economics*, *66*(3), 409–434.

Rietz, T. A. (1988). The equity risk premium: a solution. *Journal of Monetary Economics*, *22*(1), 117–131.

Ruttscheidt, S. (2018). *Adaptive sparse grids for solving continuous time heterogeneous agent models* (Master thesis). Universität Bonn, Bonn.

Shao, A. (2012). *A fast and exact simulation for cir process* (Unpublished doctoral dissertation). University of Florida Gainesville, FL.

Stern, N. (2015). *Why are we waiting?: The logic, urgency, and promise of tackling climate change*. MIT Press.

Stern, N., Peters, S., Bakhshi, V., Bowen, A., Cameron, C., Catovsky, S., ... Edmonson, N. (2006). *Stern review: The economics of climate change* (Vol. 30). HM treasury London.

Strzalecki, T. (2011). Axiomatic foundations of multiplier preferences. *Econometrica*, *79*(1), 47–73.

Thomas, J. W. (2013). *Numerical partial differential equations: finite difference methods*. Springer Science & Business Media.

Tol, R. S. (2002). Estimates of the damage costs of climate change. Part 1: Benchmark estimates. *Environmental and Resource Economics*, *21*(1), 47–73.

Traeger, C. P. (2014). Why uncertainty matters: Discounting under intertemporal risk aversion and ambiguity. *Economic Theory*, *56*(3), 627–664.

Traeger, C. P. (2021). ACE-analytic climate economy. *Universtiy of Oslo*.

Tsai, J., & Wachter, J. A. (2015). Disaster risk and its implications for asset pricing.

Annual Review of Financial Economics, *7*, 219–252.

Tsai, J., & Wachter, J. A. (2018). Pricing long-lived securities in dynamic endowment economies. *Journal of Economic Theory*, *177*, 848–878.

Tsitsiklis, J. N., & Van Roy, B. (2001). Regression methods for pricing complex American-style options. *IEEE Transactions on Neural Networks*, *12*(4), 694–703.

Van Binsbergen, J. H., Fernández-Villaverde, J., Koijen, R. S., & Rubio-Ramírez, J. (2012). The term structure of interest rates in a DSGE model with recursive preferences. *Journal of Monetary Economics*, *59*(7), 634–648.

Van den Bremer, T. S., & Van der Ploeg, F. (2021). The risk-adjusted carbon price. *American Economic Review*, *forthcoming*.

Van der Ploeg, F. (2018). The safe carbon budget. *Climatic Change*, *147*(1), 47–59.

Van der Ploeg, F., & de Zeeuw, A. (2018). Climate tipping and economic growth: precautionary capital and the price of carbon. *Journal of the European Economic Association*, *16*(5), 1577–1617.

Van der Ploeg, F., & Withagen, C. (2015). Global warming and the green paradox: A review of adverse effects of climate policies. *Review of Environmental Economics and Policy*, *9*(2), 285–303.

Vissing-Jørgensen, A., & Attanasio, O. P. (2003). Stock-market participation, intertemporal substitution, and risk-aversion. *American Economic Review*, *93*(2), 383–391.

Wachter, J. A. (2013). Can time-varying risk of rare disasters explain aggregate stock market volatility? *The Journal of Finance*, *68*(3), 987–1035.

Weitzman, M. L. (1998). Why the far-distant future should be discounted at its lowest possible rate. *Journal of Environmental Economics and Management*, *36*(3), 201–208.

Weitzman, M. L. (2007). A review of the stern review on the economics of climate change. *Journal of Economic Literature*, *45*(3), 703–724.

Weitzman, M. L. (2009). Additive damages, fat-tailed climate dynamics, and uncertain discounting. *Economics: The Open-Access, Open-Assessment E-Journal*, *3*.

Weitzman, M. L. (2011). Fat-tailed uncertainty in the economics of catastrophic climate change. *Review of Environmental Economics and Policy*, *5*(2), 275–292.

Weitzman, M. L. (2012). GHG targets as insurance against catastrophic climate damages. *Journal of Public Economic Theory*, *14*(2), 221–244.

Zumbusch, G. W. (2000). A sparse grid PDE solver; discretization, adaptivity, software design and parallelization. In *Advances in software tools for scientific computing* (pp. 133–177). Springer.

6 Policy recommendations

Climate change is one of the main risks that the economy will face in the upcoming decades. Climate scientists have improved our knowledge about climate change, but it remains hard to accurately estimate the impact of the increased carbon concentration on global temperature levels. We know that man-made emissions increase global temperature, but it is still uncertain by which exact amount. And it is even harder to estimate damages resulting from this temperature increase, due to the lack of data and the complex nature of the problem. Furthermore, tipping points and other feedback effects make it hard to predict impacts. Summarizing, we have learned a lot about climate change and its impact, and we are still learning. But there is also much uncertain about future impacts.

This thesis has focused on estimating the social cost of carbon, which is the discounted value of all future damages caused by emitting one unit of carbon emissions today taking into account this uncertainty. It is necessary to estimate the negative value of these uncertain future damages, since mitigation policies to stop climate change must be implemented today. Uncertainty about future impacts of climate change matters a lot for the social cost of carbon. In chapter 2 we introduce an economic model with climate disaster risk. We include both standard risk and ambiguity into the model. In the case of risk, all possible realizations are known and the probability of each realization is known, but the exact outcome is random. Additionally, we add a deeper layer of uncertainty called ambiguity. Ambiguity implies that even the probability distributions are unknown. We find that the social cost of carbon in our model is between 25% and 50% larger if we take into account risk and ambiguity of future climate impacts.

The policy implication is that the large amount of uncertainty around future climate damages should lead to more stringent carbon abatement policy. We should not only focus on the expected impacts of climate change, but also on limiting the probability of a large irreversible impact. Carbon abatement policy can from this point of view also be seen as buying insurance against tipping points and possible large impacts of climate change. The recommendation is thus to start as soon as possible with more carbon abatement at a global scale, which can be implemented using a substantial global carbon tax equal to the social cost of carbon.

The previous discussion mainly focused on the estimate of the current social cost of carbon. It is however not wise to implement a constant carbon price. Chapter 5 investigates the growth rate of the optimal carbon price in several scenarios. The economy is growing over time and a larger economy also implies that more damage can be done to the economy. A common assumption is to assume that climate damages are proportional to the size of the economy. The optimal carbon price in this case grows as the economy grows. Additionally, if climate damages are convex, the social cost of carbon is an increasing function of the temperature anomaly. These two common assumptions (damages proportional to the economy, convex damages) automatically imply that the social cost of carbon should grow in expectation at a rate that is faster than the growth rate of the economy. The growth rate of the economy can thus be used as a lower bound for the growth rate of carbon prices.

On the other hand, we can consider the extreme case in which a temperature cap is implemented and damages are ignored in the objective function. This is the approach

taken in the Paris agreement. This results in a modified Hoteling-rule in which the carbon price grows at the risk-adjusted rate of interest. This rate is above the growth rate of the economy and can be seen as an upper bound for the growth rate of the carbon price. As a rule of the thumb, the carbon price should therefore be growing in between the growth rate of the economy and the risk-adjusted interest rate.

Optimal policy implies that the carbon tax follows all shocks in the climate system and the economy. Within the economic framework it is thus optimal for the price to drop in recessions and jump in booms. And new information about the climate system and damages should be incorporated in the carbon price. This results in a volatile optimal carbon price. However, there is a trade-off for policymakers. Firms and investors that have to make investments want to know future carbon prices. If carbon prices are volatile, this might postpone investments. Also, in terms of transparency and political support volatile carbon prices are not preferred. Policymakers thus face a trade-off between a predictable future carbon price and staying close to the optimal value. This would be an interesting topic for future research.

Summing up, the social cost of carbon is sensitive to assumptions about preferences, discounting and damage specifications. But some general conclusions do emerge. First, taking into account risk and ambiguity about the climate system and climate damages leads to a substantially higher estimate of the social cost of carbon. Second, average carbon prices in the world are currently still close to zero and much lower than optimal. The majority of emissions in the world is still not priced. Several countries have started with carbon pricing but prices are often low or only a small part of total emissions is covered by the pricing systems. Third, not only the initial price should be higher, but prices should also be growing over time. With plausible assumptions the growth rate of the optimal carbon price is larger than the growth rate of the economy.

7 Summary in English

Anthropogenic carbon emissions are the main cause of climate change. It is thus clear that in order to tackle climate change, carbon emissions must be rapidly reduced. This thesis focuses on the question: what is the present value of all damages caused by emitting one unit of carbon today, which is called the social cost of carbon. It is an important input for policy decisions, since it represents the benefit of carbon abatement. The social cost of carbon is estimated using an integrated assessment model, in which a climate model is integrated within an economic framework. Estimating the social cost of carbon requires specifying a model for the climate system, a damage function, an economic model and a utility function. This thesis analyzes how uncertainty and utility specifications affect the social cost of carbon.

Chapter 2 introduces an integrated assessment model with climate disaster risk. The model captures two types of uncertainty. The first type of uncertainty is risk, in which the exact timing and size of climate disasters are unknown, but the probability distribution is known. With risk, all possible realizations are known and the probability of each realization is known, but the exact outcome is random. Additionally, we add a deeper layer of uncertainty called ambiguity. With climate damages, it is realistic to assume that even the probability distributions are unknown. It is taken into account that the best-estimate probability distribution is not the right one. People are averse to both risk and ambiguity, and the model shows that risk and ambiguity have quite different implications for the social cost of carbon. Overall, uncertainty increases the social cost of carbon by a substantial amount. Due to some specific assumptions, the model could be solved largely analytically. These analytic results make the model very transparent. It is then very clear how different parameters affect the social cost of carbon.

Due to some specific assumptions, the model in chapter 2 could be solved without advanced numerical techniques. When these assumptions are relaxed, solving integrated assessment models becomes more challenging due to the 'curse of dimensionality'. Chapter 3 develops and compares two methods to numerically solve integrated assessment models with uncertainty in continuous-time. Integrated assessment models generally have multiple state variables, since the model contains both economic and climate variables. Both methods that are introduced are suitable to solve high-dimensional problems. The first method applies a finite difference method on sparse grids using the combination method. The combination method combines several smaller sub-problems, which makes the algorithm very suitable for parallel computing. The second method relies on stochastic grid points and function approximation using a regression with basis functions. Both methods are applied to a high-dimensional climate-economy model with uncertainty. In the example problem, the stochastic grid method outperforms the finite difference method.

Chapter 4 applies the stochastic grid method to a climate-economy model with a fully stochastic climate model. This chapter investigates the dependence of the social cost of carbon on the policy scenario. Since the social cost of carbon is forward-looking, future carbon abatement policy already affects the social cost of carbon today. While the social cost of carbon using the optimal policy scenario equals the optimal carbon tax, the current policy scenario better captures the welfare loss of carbon emissions. The current policy scenario should thus be used in cost-benefit analysis. Both policy scenarios are used in

the literature to calculate the welfare loss of carbon emissions. We show that if damages are a convex function of temperature, the social cost of carbon is substantially higher in the current policy scenario. It is additionally shown that the delay of climate policy is costly when damages are convex.

Finally, chapter 5 investigates the time path of optimal carbon prices. The focus is often on the initial optimal carbon price. However, the time path of carbon prices is just as important. Investment decisions about carbon abatement have to be taken today while the value of this investment depends on future carbon prices. We start with a very simple setting in which temperature is a linear function of cumulative emissions, damages are proportional to output and damages are a linear function of temperature. In this simple setting, the carbon price grows in expectation at the same rate as the economy. We then investigate the effects of several extensions on the optimal carbon price path: convex damages, learning-by-doing, resolution of uncertainty, tipping points and temperature caps. In the end it is concluded that the optimal carbon price should grow at a rate that is between the growth rate of the economy and the risk-adjusted interest rate.

8 Summary in Dutch

Antropogene CO_2 emissies zijn de voornaamste oorzaak van klimaatverandering. Het is dus duidelijk dat de CO_2 uitstoot snel verminderd moet worden om klimaatverandering tegen te gaan. Dit proefschrift focust op de volgende vraag: wat is de contante waarde van alle schade die veroorzaakt wordt door de uitstoot van een eenheid CO_2. Dit getal wordt de social cost of carbon genoemd. De social cost of carbon is een belangrijk gegeven voor beleidsmakers, omdat het de baten van CO_2 reductie vertegenwoordigt. Dit getal wordt geschat met een zogenoemd geïntegreerd model, waarin een klimaatmodel en een economisch model worden gecombineerd. De social cost of carbon is een functie van het klimaatsysteem, de schadefunctie, het economische systeem en de nutsfunctie. Dit proefschrift analyseert hoe onzekerheid en verschillende nutsfuncties de social cost of carbon beïnvloeden.

Hoofdstuk 2 introduceert een geïntegreerd klimaat-economie model met risico op klimaatrampen. Het model neemt twee types onzekerheid mee. Het eerste type onzekerheid is risico, waarbij de timing en de grootte van een klimaatramp onzeker zijn, maar de kansverdelingen wel bekend zijn. In het geval van risico zijn de mogelijke uitkomsten en de kansverdelingen van deze uitkomsten bekend, maar de uiteindelijke uitkomst is van tevoren onbekend. Naast risico bekijken we ook een diepere onzekerheid genaamd ambiguïteit. Met klimaatrampen is het realistisch om aan te nemen dat zelfs de kansverdelingen onbekend zijn. Het model neemt de mogelijkheid mee dat de beste schatting van de kansverdeling niet de juiste kansverdeling is. Mensen mijden het liefst zowel risico als ambiguïteit. Deze verschillende soorten onzekerheid hebben duidelijke andere effecten op de social cost of carbon. Uiteindelijk kan geconcludeerd worden dat het meenemen van onzekerheid zorgt voor een significant hogere social cost of carbon. Door een aantal specifieke aannames is het mogelijk om het model bijna volledig analytisch op te lossen. Dit zorgt voor een transparante uitkomst, waarbij het erg duidelijk is hoe verschillende parameters de uitkomsten beïnvloeden.

Door bepaalde aannames te maken kon het model in hoofdstuk 2 opgelost worden zonder ingewikkelde numerieke methodes. Zonder specifieke aannames is het niet mogelijk om analytische oplossingen te krijgen, en is het een stuk ingewikkelder om geïntegreerde modellen op te lossen vanwege de 'vloek van de dimensionaliteit'. Hoofdstuk 3 ontwikkelt en vergelijkt twee methodes waarmee geïntegreerde modellen met onzekerheid in continue tijd opgelost kunnen worden. Geïntegreerde modellen hebben vaak meerdere variabelen, omdat het model zowel economische als klimaatgerelateerde variabelen bevat. Beide methodes zijn geschikt om problemen met een hoge dimensie aan variabelen op te lossen. De eerste methode is een finite difference methode waarbij gebruik wordt gemaakt van de combinatiemethode. De combinatiemethode lost verschillende kleinere sub-problemen op en combineert deze resultaten, waardoor het probleem makkelijk in parallel opgelost kan worden. De tweede methode is gebaseerd op stochastische grid punten en een functie approximatie methode gebruikmakend van een regressie met basisfuncties. Beide methodes worden toegepast op een klimaat-economie model met onzekerheid. In het voorbeeldprobleem presteert de stochastische grid methode het beste.

Hoofdstuk 4 past de stochastische grid methode toe op een klimaat-economie model met een volledig stochastisch klimaatmodel. Dit hoofdstuk onderzoekt hoe de social cost of

carbon afhangt van het klimaatbeleid scenario. Toekomstig klimaatbeleid heeft namelijk een effect op toekomstige klimaatschade en dus ook op de social cost of carbon. De social cost of carbon in het geval van een optimaal klimaatbeleid scenario is gelijk aan de optimale CO_2 heffing. Wanneer wordt aangenomen dat het huidig beleid wordt doorgezet kan de social cost of carbon worden geïnterperteert als het huidige welvaartsverlies door CO_2 uitstoot. Voor een kosten-baten analyse is het dus beter om uit te gaan van het huidige beleidsscenario. Beide beleidsscenarios worden in de literatuur gebruikt om de social cost of carbon te berekenen. We laten zien dat als klimaatschade een convexe functie is van temperatuur, dat de social cost of carbon dan substantieel hoger is in het huidige beleidsscenario ten opzichte van het optimale beleidsscenario. Daarnaast laten we in dit hoofdstuk zien dat uitstel van klimaatbeleid duur is als de schade een convexe functie is van temperatuur.

Tenslotte onderzoekt hoofdstuk 5 het tijdspad van optimale CO_2 prijzen. De focus ligt vaak op de initiële optimale CO_2 prijs. Het tijdspad van CO_2 prijzen is echter net zo belangrijk. Investeringskeuzes over CO_2 reductie moet op dit moment gemaakt worden, terwijl de waarde van deze investering afhangt van toekomstige CO_2 prijzen. We beginnen met een simpele setting waarin temperatuur een lineaire functie is van cumulatieve CO_2 uitstoot, klimaatschade een lineaire functie van temperatuur en waarin klimaatschade proportioneel is aan de economie. In deze simpele setting groeit de optimale CO_2 prijs in verwachting met dezelfde groeivoet als de economie. Daarna bekijken we de effecten van verschillende uitbreidingen op het tijdspad van CO_2 prijzen: convexe klimaatschade, leren door te doen, afname van onzekerheid, tipping points en temperatuurlimieten. Uiteindelijk kan geconcludeerd worden dat de optimale CO_2 prijs zou moeten groeien met een groeivoet die tussen de groeivoet van de economie en de risicogecorrigeerde rente ligt.

The Tinbergen Institute is the Institute for Economic Research, which was founded in 1987 by the Faculties of Economics an Econometrics of the Erasmus University Rotterdam, University of Amsterdam and VU University Amsterdam. The Institute is named after the late Professor Jan Tinbergen, Dutch Nobel Prize laureate in economics in 1969. The Tinbergen Institute is located in Amsterdam and Rotterdam. The following books recently appeared in the Tinbergen Institute Research Series:

741. Y.M. KUTLUAY, *The Value of (Avoiding) Malaria*
742. A. BOROWSKA, *Methods for Accurate and Efficient Bayesian Analysis of Time Series*
743. B. HU, *The Amazon Business Model, the Platform Economy and Executive Compensation: Three Essays in Search Theory*
744. R.C. SPERNA WEILAND, *Essays on Macro-Financial Risks*
745. P.M. GOLEC, *Essays in Financial Economics*
746. M.N. SOUVERIJN, *Incentives at work*
747. M.H. COVENEY, *Modern Imperatives: Essays on Education and Health Policy*
748. P. VAN BRUGGEN, *On Measuring Preferences*
749. M.H.C. NIENTKER, *On the Stability of Stochastic Dynamic Systems and their use in Econometrics*
750. S. GARCIA-MANDICÓ, *Social Insurance, Labor Supply and Intra-Household spillovers*
751. Y. SUN, *Consumer Search and Quality*
752. I. KERKEMEZOS, *On the Dynamics of (Anti)Competitive Behaviour in the Airline Industry*
753. G.W. GOY, *Modern Challenges to Monetary Policy*
754. A.C. VAN VLODROP, *Essays on Modeling Time-Varying Parameters*
755. J. SUN, *Tell Me How To Vote: Understanding the Role of Media in Modern Elections*
756. J.H. THIEL, *Competition, Dynamic Pricing and Advice in Frictional Markets: Theory and Evidence from the Dutch Market for Mortgages*
757. A. NEGRIU, *On the Economics of Institutions and Technology: a Computational Approach*
758. F. GRESNIGT, *Identifying and Predicting Financial Earthquakes using Hawkes Processes*
759. A. EMIRMAHMUTOGLU, *Misperceptions of Uncertainty and Their Applications to Prevention*
760. A. RUSU, *Essays in Public Economics*
761. M.A. COTOFAN, *Essays in Applied Microeconomics: Non-Monetary Incentives, Skill Formation, and Work Preferences*
762. B.P.J. ANDRÉE, *Theory and Application of Dynamic Spatial Time Series Models*
763. P. PELZL, *Macro Questions, Micro Data: The Effects of External Shocks on Firms*
764. D.M. KUNST, *Essays on Technological Change, Skill Premia and Development*
765. A.J. Hummel, *Tax Policy in Imperfect Labor Markets*

766. T. Klein, *Essays in Competition Economics*
767. M. VIGH, *Climbing the Socioeconomic Ladder: Essays on Sanitation and Schooling*
768. Y. XU, *Eliciting Preferences and Private Information: Telle Me What You Like and What You Think*
769. S. RELLSTAB, *Balancing Paid Work and Unpaid Care over the Life-Cycle*
770. Z. DENG, *Empirical Studies in Health and Development Economics*
771. L. KONG, *Identification Robust Testing in Linear Factor Models*
772. I. NEAMŢU, *Unintended Consequences of Post-Crisis Banking Reforms*
773. B. KLEIN TEESELINK, *From Mice to Men: Field Studies in Behavioral Economics*
774. B. TEREICK, *Making Crowds Wiser: the Role of Incentives, Individual Biases, and Improved Aggregation*
775. A. CASTELEIN, *Models for Individual Responses*
776. D. KOLESNYK, *Consumer Disclosures on Social Media Platforms: A Global Investigation*
777. M.A. ROLA-JANICKA, *Essays on Financial Instability and Political Economy of Regulation*
778. J.J. KLINGEN, *Natural Experiments in Environmental and Transport Economics*
779. E.M. ARTMANN, *Educational Choices and Family Outcomes*
780. F.J. OSTERMEIJER, *Economic Analyses of Cars in the City*
781. T. ÖZDEN, *Adaptive Learning and Monetary Policy in DSGE Models*
782. D. WANG, *Empirical Studies in Financial Stability and Natural Capital*
783. L.S. STEPHAN, *Estimating Diffusion and Adoption Parameters in Networks: New Estimation Approaches for the Latent-Diffusion-Observed-Adoption Model*
784. S.R. MAYER, *Essays in Financial Economics*
785. A.R.S. WOERNER, *Behavioral and Financial Change – Essays in Market Design*
786. M. WIEGAND, *Essays in Development Economics*
787. L.M. TREUREN, *Essays in Industrial Economics - Labor market imperfections, cartel stability, and public interest cartels*
788. D.K. BRANDS, *Economic Policies and Mobility Behaviour*
789. H.T.T. NGUYEN, *Words Matter? Gender Disparities in Speeches, Evaluation and Competitive Performance*
790. C.A.P BURIK, *The Genetic Lottery. Essays on Genetics, Income, and Inequality*